The Role of Retinoic Acid in Cartilage Mechanoflammation

Pragash Kamalathevan

St Hugh's College, University of Oxford

Supervisors:

Professor Tonia Vincent

Professor Dominic Furniss

Kennedy Institute of Rheumatology

Nuffield Department of Orthopaedics, Rheumatology and Musculoskeletal Sciences

University of Oxford

Thesis submitted to the University of Oxford for the degree of Doctor of Philosophy (DPhil) in Musculoskeletal Sciences

Trinity Term 2022

TABLE OF CONTENTS

ABSTRACT

Osteoarthritis (OA) is a highly prevalent condition that affects more than 40% of individuals over the course of their lifetime. There are currently no disease-modifying OA drug (DMOAD) licensed for the treatment of this disease. An Icelandic genome wide association study (GWAS) study identified common polymorphic variants in ALDH1A2, the gene which encodes the enzyme involved in the synthesis of all-trans retinoic acid (atRA), with severe hand OA. Subsequent data from our lab showed that atRA-responsive genes are downregulated on cartilage injury. Mechanical injury is one of the principal risk factors in the development of OA. Cartilage injury is known to activate downstream inflammatory signalling that is driven in a transforming growth factor activated-beta 1 (TAK1) dependent manner and thereby increase inflammatory gene regulation, in a process known as mechanoflammation. Talarozole (TLZ), a CYP26 inhibitor, which prevents the breakdown of atRA, suppresses the upregulation of inflammatory genes on cartilage injury. My project sought to identify the mechanism by which atRA-responsive genes were downregulated and determine how atRA suppressed mechanoflammation on cartilage injury. The downregulation of atRA-responsive genes on cartilage injury was mediated in both cytosolic phospholipase A2 (cPLA2) - and reactive oxygen species (ROS)-sensitive manner. TAK1 phosphorylation on cartilage injury was partially mediated in a nicotinamide adenine dinucleotide phosphate oxidase (NOX)-sensitive manner, whereas TAK1 was responsible for the partial phosphorylation of cPLA2 on cartilage injury. Apoptosis signal regulating kinase 1 (ASK1) was the key driver of mitogen activated protein kinases (MAPKs) (Jun N terminal kinase (JNK) and extracellular signal regulated kinase (ERK)) on cartilage injury and downstream inflammatory gene regulation. atRA suppressed mechanoflammation in a peroxisome proliferator activated receptor gamma (PPARG)-sensitive manner. These findings suggest that both boosting atRA level and ASK1 inhibition can suppress

mechanoflammation in articular cartilage and identifies each pathway as targets for potential disease modifying drugs in the treatment of OA.

ACKNOWLEDGEMENTS

My journey throughout my PhD has taught me invaluable lessons in time-management, organisational skills and above all, perseverance. The first 18 months of my DPhil was a real struggle for various reasons. Above all, I was finding it difficult to become accustomed to the life of a lab scientist having come from a clinical background. The repeated early experimental failures were deeply demotivating given the hours that I had spent to optimise the work. I later became more experienced in the lab and just prior to the pandemic things began falling into place. However, I then spent 4 months away of my DPhil between March 2020 to June 2020, whilst the Kennedy Institute was closed, to help on the NHS frontline. This period helped me reflect on my project and how best to move forward when I went back. Throughout the entire process both my supervisors, Professor Tonia Vincent and Professor Dominic Furniss, have been a bedrock. Professor Vincent has been an indispensable guide for me. She has mentored me on both a scientific and personal basis and helped me to overcome many obstacles throughout my studies. I was grateful to have matured in her lab as a clinician-scientist with access to people and resources at the very forefront of cartilage biology. Professor Furniss has likewise been integral in providing me with emotional support and scientific advice about how best to direct my project. I loved my face-to-face meetings with him where I felt I had the freedom to talk about things that were also non-project related without any fear.

I would like to further thank the support given to me by Dr Hayat Muhammad. I built both a strong friendship and working relationship with him after I re-entered lab-work post the COVID19 pandemic. Whenever I was demotivated or reached an experimental block, Hayat would always be the first one to offer me potential solutions to keep me going. This was invaluable and made going into lab more enjoyable. I would also like to thank others who

have helped me to shape my initial project including Dr. Linyi Zhu and Dr. Stuart Keppie. From both, I learnt core skills and techniques that I utilised throughout my DPhil, thank you.

Finally I wanted to thank my family who have been with me throughout from start to finish. My brother in particular offered moments of emotional support when I thought I was failing. My parents have equally given me words of advice and direction throughout my DPhil. They both struggled early on in their lives themselves so that they could build a strong foundation for their children. I hope that achieving this DPhil makes them both proud and celebratory over the risks they undertook to now have jumped leaps and bounds. The single most important person in my progress throughout my DPhil was my partner and fiancé, Fran. There were many moments when I felt like giving up and periods I thought I would never be able to overcome. However, she believed in me throughout and motivated me to keep progressing. She would selflessly accompany me on my travels to lab, made sure I ate at lunch and generally kept sane. She was always the first to remind me that my physical and mental wellbeing came before medicine, science or the prestige of an Oxford DPhil. I am proud and joyous to soon call her my wife and very much owe a lot of this work to her. Lastly and surely my late grandmother has been an ever present and shining guide in my life and I am sure helped me through this journey too.

LIST OF FIGURES

LIST OF TABLES

LIST OF ABBREVIATIONS

ADAMTS4	A distintegrin and metalloproteinase with thrombospondin motif 4
ADAMTS5	A distintegrin and metalloproteinase with thrombospondin motif 5
ADH	Alcohol dehydrogenases
Akt	serine/threonine kinase 1
ALDH1A2	Aldehyde dehydrogenase 1A2
AP-1	Activator protein 1
ARE	Antioxidant response element
ARE	adenosine/uridine rich elements
ASK1	Apoptosis signal regulating kinase 1
ATP	Adenosine triphosphate
atRA	all-trans-retinoic acid
atRAL	all-trans-retinal
atROL	all-trans-retinol
BMP	Bone morphogenetic protein
bp	base pairs
CAT	Catalase
CCL2	C-C motif chemoligand 2
CDKN1A	Cyclin dependent kinase inhibitor 1A
cDNA	complementary cDNA
ChIP	Chromatin Immunoprecipitation
CIA	Collagen-induced arthritis
COL2	Collagen type II
COMP	Cartilage oligomeric matrix protein
CoQ10	Coenzyme Q10
COX2	Cycloxygenase 2
cPLA2	cytosolic phospholipase A2
CRABP	Cellular retinoic acid binding protein
CTGF	Connective tissue growth factor
CYP26	Cytochrome P450 26
DMEM	Dulbecco's modified eagle's medium
DMM	Destabilisation of medial mensicus
DMOADs	Disease modifying osteoarthritis drugs
DMSO	Dimethyl sulfoxide
DNA	Dioxyribonucleic acid
DPT	Dermatopontin
DUSP	Dual specificity phosphatase
ECM	Extracellular matrix
ER	Oestrogen receptor
ERK	Extracellular signal regulated kinase
FABP	Fatty acid binding protein
FAD	Flavin adenine dinucleotide
FBS	Fetal bovine serum
FGF	Fibroblast growth factor

FSH	Follicle stimulating hormone
GAG	Glycosaminoglycans
GDF	Growth/differentiation factor
GPx	Glutathione peroxidase
GSH	Glutathione
GWAS	Genome wide association study
H2O2	Hydrogen peroxide
HDGF	Hepatoma derived growth factor
HETE	Hydroxyeicosatetraenoic acid
HIF-1α	Hypoxia inducible factor 1 alpha
HpETE	Hydroperoxyeicosatetraenoic acid
Hylauranan	HA
IGFBP7	Insulin like growth factor binding protein 7
IκBα	Inhibitor of kappa light chain gene enhancer in B cells
IKK-β	Inhibitor of nuclear factor kappa-B kinase subunit beta
IL	Interleukin
iNOS	inducible nitric oxide synthase
iPLA2	Calcium independent phospholipase A2
JNK	c-Jun N-terminal kinase
KLF2	Kruppel like factor 2
KO	Knock out
LH	Luteinising hormone
LOX	Lipoxygenase
LRP1	Low density lipoprotein receptor-related protein 1
LRTA	Lecithin retinol acetyl transferase
LTZ	Letrozole
MAPK	Mitogen activated protein kinase
MAPKK	Mitogen activated protein kinase kinase
MAPKKK	Mitogen activated protein kinase kinase kinase
MCF2L	MCF.2 cell line derived transforming sequence-like protein
MCP	metacarpophalangeal
Mins	Minutes
MLI	Meniscal ligamentous injury
MMP	Matrix metalloproteinase
mRNA	messenger RNA
MS	Mass Spectroscopy
MYd88	Myeloid differentiation primary response 88
NAC	N-acetyl cysteine
NAD	Nicotinamide adenine dinucleotide
NADP	Nicotinamide adenine dinucleotide phosphate
NADPH	Nicotinamide adenine dinucleotide phosphate
NF-κB	Nuclear factor kappa-light-chain enhancer of activated B cells
NGF	Nerve growth factor
NOX	Nicotinamide adenine dinucleotide phosphate oxidases
NRF2	Nuclear factor erythroid 2-related factor 2
NSAID	Non-steroidal anti-inflammatory drugs

PBS	Phosphate buffered solution
PCM	Pericellular matrix
PCR	polymerase chain reaction
PGE2	Prostaglandin E2
PMSF	phenylmethylsulfonyl
PPAR	Peroxisome proliferator activated receptor
PPRE	Peroxisome proliferator activated receptor reponse element
PRDX	Peroxiredoxin
PUFA	Polyunsaturated fatty acids
PVDF	poly (vinylidene)
RALDH	Retinaldehyde dehydrogenase
RAR	Retinoic acid receptor
RARE	Retinic acid response element
RBP	Retinol binding protein
RCT	Randomised controlled trials
RDH	Retinol dehydrogenase
RIPA	Radioimmunoprecipitation assay
RNA	Ribonucleic acid
ROS	Reactive oxygen species
RXR	Retinoid X receptor
SDS-PAGE	Sodium dodecyl sulphate polyacrylamide gel
siRNA	small inhibitory RNA
SMAD	Suppressor of mothers against decapentaplegic
SNP	Single nucleotide polymorphisms
SOD	Superoxide dismutase
sPLA2	secreted phospholipase A2
STRA6	stimulated by retinoic acid 6 gene
TAK1	Transforming growth factor beta activated kinase 1
TBST	Tris-buffered saline with 0.1% Tween 20 detergent
TGF-β	Tranforming growth factor beta
TIMP	Tissue inhibitor of metalloproteinases
TLR4	Toll like receptor 4
TLZ	Talarozole
TNFα	Tumour necrosis factor alpha
TRAF6	TNF recepetor-associated factor 6
TRPV4	Transient receptor potential vanilloid 4
TTP	Tristetraprolin
Wnt	Wingless/integrated pathway
4-HNE	4-hydroxynoneal
5Z-7	5Z-7 Oxozeanol

1 CHAPTER 1: INTRODUCTION

1.1 Osteoarthritis

Osteoarthritis (OA) is a degenerative joint disease that is highly prevalent amongst the elderly population and results in significant pain and disability. Other than age, the disease is characterised by a culmination of aetiological factors including trauma, obesity and genetic predisposition [1]. OA has been conventionally described as a disease of 'wear and tear' and the end result of increased attrition on any one particular joint. This traditional paradigm was originally based on the observation that chondrocytes (residing cell type in cartilage) have very low metabolism and impaired repair capabilities compared to other tissue like skin. The avascular and aneural environment in which chondrocytes reside was thought to not be favourable towards a regenerative phenotype. However, progress in molecular biology since the 1990s have now regarded the 'wear and tear' description of OA to be a 'misnomer', as the disease is not simply caused by attrition. Instead, research over the past two decades has shown that OA is driven by abnormal remodelling of cartilage that in turn is driven by a host of inflammatory signalling in response to mechanical injury (termed as mechanoflammation) [2]. The activation of such mechano-sensitive pathways drive degradative proteases, which results in the destruction and loss of articular cartilage [2]. In addition, OA is characterised by a lack of repair promoting responses towards injurious stimuli conducted through the matrix [3]. The disease is now thought to be characterised by a shift in the cartilage phenotype from one that is pro-regenerative to degenerative, where the cartilage loses its capabilities to repair and to suppress the chronic inflammation in response to mechanical and biochemical stress (known as mechanoflammation). The imbalance between pro-degenerative and pro-repair pathways, thickening to subchondral bone, formation of osteophytes (bony spurs) and chronic low-

grade inflammation are thought to characterise the current definition of OA. Moreover, although initially considered to be cartilage driven, OA is now widely regarded to be a multifaceted tissue disease with inflammatory mediators released by cartilage, bone and synovium [4]. Despite these recent advances in gaining a deeper molecular insight into OA, there is still an unmet need for a disease-modifying agent in this field. OA as a disease has a significant economic impact that can be categorised into both direct and indirect costs [5]. Direct costs include hospitalisation and non-curative treatment, including surgical management whereas indirect costs include absence from work and decreased productivity secondary to debilitating symptoms, including pain and loss of joint function. Given the societal impact, understanding, identifying and subsequently targeting molecular pathways that drive disease in OA is imperative to help us repurpose or develop a putative drug to either halt or reverse disease progression.

1.2 Cartilage biology

During embryology, cartilage is formed from the mesoderm germ layer in a process known as chondrogenesis [6]. During development, mesenchyme differentiates into chondroblasts which secrete extracellular matrix (ECM) composed of collagen type II (COL2), aggrecan and proteoglycan [6]. Embedded within this ECM is the sole cell type found in cartilage: chondrocyte. There are three main types of cartilage (hyaline cartilage, elastic cartilage and fibrocartilage) found within the human body, and their structure and function depend on this variation. Hyaline cartilage is the most widespread and found in structures including the trachea, nose and ventral segments of the ribs. Hyaline cartilage has relatively few fibres and provides a smooth surface to resist compressive forces at bone articulation sites. Elastic cartilage contains an abundance of elastic fibres in its ECM and is the most cellular of the three types of cartilage. Elastic cartilage is found in the external ear, epiglottis and apices of the arrytenoids. The high elastic content enables elastic cartilage to provide structural integrity whilst maintaining flexibility. Finally, fibrocartilage contains the most collagen and has no perichondrium enabling it to resist high degrees of tension and resistive forces. For such reasons, fibrocartilage is found in intervertebral discs and tendons.

1.2.1 Articular cartilage

Articular cartilage has been typically classified into four morphological zones depending on its depth from the articular surface: the superficial zone, the transitional zone, the deep zone and the calcified layer (Figure 1.1). The superficial zone is comprised of an elongated layer of chondrocytes organised parallel to the articulating surface [7]. A thin layer of synovial fluid, called lubricin, covers the superficial zone, allowing to function as the gliding surface of the joint [8]. The transitional zone contains a denser network of collagen fibrils organised

in a columnar fashion with fewer cells, compared to the superficial zone, organised in a spherical manner [9]. The deep zone comprises of chondrocytes that are organised in a perpendicular fashion relative to the subchondral bone [9]. This layer contains the largest diameter of collagen fibrils, the highest proteoglycan content and the fewest amount of chondrocytes [9]. The deepest, the calcified layer, separates the softer cartilage above from subchondral bone below. Chondrocytes from the deep zone bore into the calcified region and act a means of connection between the articular surface and subchondral bone [10].

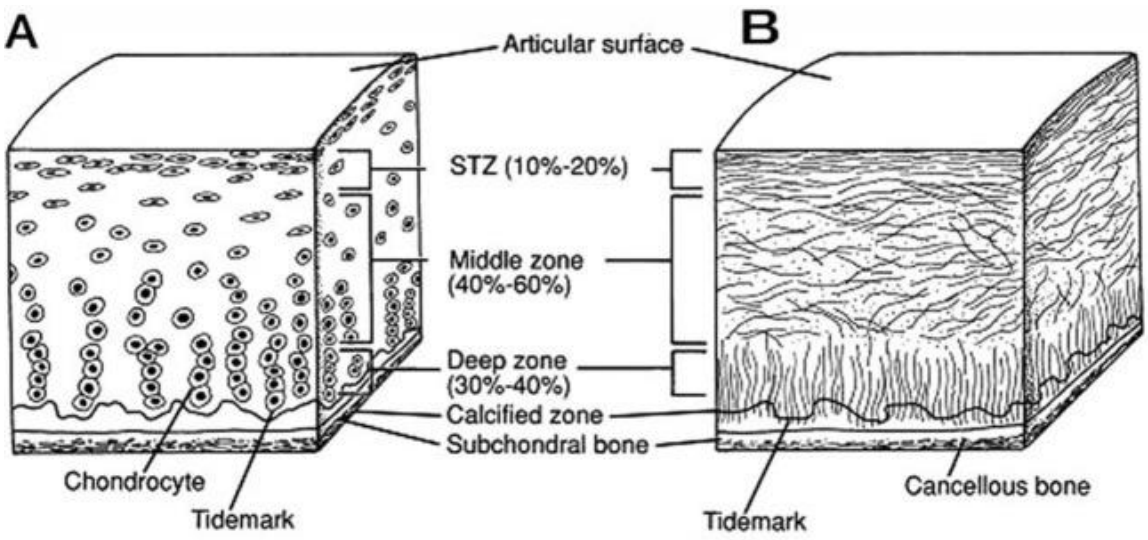

Figure 1.1: Schematic representation of a cross section of healthy articular cartilage.

A, cellular organization in the zones of articular cartilage; B, collagen fibre architecture. STZ – superficial zone. Adapted from Sophia Fox et al. (2009).

1.2.2 Articular cartilage composition

Articular cartilage is composed of hyaline cartilage and is both avascular and aneural. The superficial zone of articular cartilage is composed of primarily COL2 and type IX collagen [9]. COL2 is the predominant collagen and accounts for 90%–95% of the collagen found in the ECM of articular cartilage [9]. Although there are five different genetic subtypes of

collagen, only three are specific to cartilage: type II, IX and X. On the one hand, a minor collagenous component, collagen type IX, covalently cross-links with collagen type II (COL2) to stabilise the collagen fibril network [11]. On the other hand, type X collagen is a short-chain, non-fibril-forming collagen synthesised primarily by hypertrophic chondrocytes [12]. Collectively, the other collagen types, although present as a minority, help to form and stabilise the COL2 fibril network.

In addition to COL2, type VI collagen is a major structural element of the matrix that immediately surrounds a chondrocyte, also known as the pericellular matrix (PCM) (Figure 1.2). Type VI collagen forms a close network with COL2 and aggrecan in the PCM helping to anchor the chondrocyte within the matrix [13]. The PCM also acts as a repository for growth factors which can be activated, released and transported [14]. In fact, the PCM is regarded as a site of mechano-transduction, transmitting injurious signals from the articular surface to bound growth factors such as fibroblast growth factor (FGF), hepatoma-derived growth factor (HDGF) and connective tissue growth factor (CTGF) [14-16].

Proteoglycan is another constituent of the ECM of cartilage and accounts for approximately 10% to 15% of the wet weight [17]. Articular cartilage contains a variety of different proteoglycans each serving a different function. The subtypes of proteoglycans include aggrecan, decorin, biglycan and fibromodulin. Each of these is composed of glycosaminoglycans (GAGs) of which there is chondroitin sulphate, keratan sulphate, heparin sulphate and dermatan sulphate [18].

The largest and most abundant proteoglycan is aggrecan, which is able to form links with hylauran (HA) to form proteoglycan aggregates. Aggrecan is critical in providing the ECM with osmotic properties allowing for water retention in articular cartilage which provides the cartilage with its resilience against compressive forces [19]. The other proteoglycans

(decorin, bigyclan and fibromodulin), although lower in abundance, provide a critical function in stabilising the PCM and binding onto key growth factors, namely, FGF, HDGF and CTGF [13].

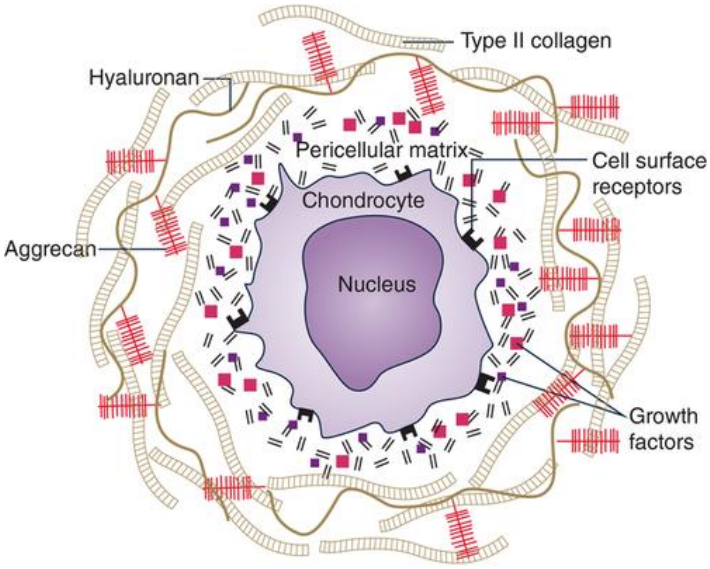

Figure 1.2: Schematic diagram of a chondrocyte and the surrounding environment.

The chondrocyte is surrounded by the pericellular matrix (PCM), together known as the chondron. The PCM acts as a repository for growth factors but lacks fibrillary collagens and aggrecan. (Adapted from Vincent & Wann et al. 2018).

1.2.3 Homeostasis of ECM

Articular cartilage has a unique biochemical composition allowing it to successfully dissipate forces evenly across the joint surface. The unique spatial distribution of proteoglycans within the collagen fibrillary network not only provides the ECM with the capability to withstand mechanical forces [20] but also perceives them as biochemical signals and transduces these to underlying chondrocytes in the PCM [21]. The bidirectional characteristic of the ECM enables it to not only act as a sensor of mechanical load but also to transduce these signals onto chondrocytes, initiating a biochemical response [13]. This

process of mechanoadaptation enables the ECM to be better composited for future mechanical loading.

The structure of the PCM is vital in providing the articular cartilage with its biochemical function. In-vivo experiments provide evidence for the PCM to facilitate the transduction of biochemical and biomechanical signals to residing chondrocytes [21]. The presence of type IV collagen in the PCM facilitates its function as a regulator of mechanotransduction by anchoring the chondrocyte to the surrounding ECM through cross-linking with COL2 and aggrecan [22]. Further cell-matrix interactions are facilitated by the binding of type IV collagen to integrin receptors on the cell surface membrane of chondrocytes and the presence of perlecan in the PCM [23]. Perlecan acts as a repository for growth factors (FGF2, HDGF and CTGF) which are released upon compressive forces on the ECM, enabling the activation of downstream mechanoadaptive responses [14, 15]. In perlecan knockout (KO) mice, this mechanotransduction response is disrupted resulting in an ECM matrix that is less mechano-adapted with reduced stiffness [24].

1.2.4 Factors that determine ECM turnover

1.2.4.1 Mechanical load

Mechanical stress is one of the principal factors that influence ECM homeostasis [2]. There are different types of mechanical forces that a joint can be subjected to: tensile, compressive and shear force. In healthy cartilage, the composition of the ECM is such that it enables a lifetime of mechanical resistance to consistent cyclic loading deformation. It has been documented that cartilage responds to physiological magnitudes of mechanical strain (between 10% and 20%) with increased synthesis of proteoglycan, aggrecan and cartilage

oligomeric matrix protein (COMP) [25]. A certain transmembrane ion channel, transient receptor potential vanilloid 4 (TRPV4), is a key mechanosensor and is responsible for enhanced matrix synthesis under moderate loading [26]. In human chondrocytes, it has been shown that mechanical loading results in the activation of similar stress-induced ion-channels and integrins resulting in the release of interleukin 4 (IL4) [27]. This has been shown to increase aggrecan expression and decrease matrix metalloproteases (MMP)-3 [27].

The more recently discovered PIEZO ion channels have been shown to transduce biomechanical signals through the assembly of focal adhesion molecules and scaffolding proteins resulting in the reorganisation of the cytoskeleton [28, 29]. The latter acts as a funnel between the ECM and the chondrocyte nucleus and, by doing so, orchestrates gene expression and matrix synthesis responses to mechanical loading [30]. The reorganisation of the cytoskeleton also activates downstream mitogen activated protein kinases (MAPKs) [31] and Rho GTPases [32]. These, in conjunction with other signalling cascades, converge onto the chondrocyte cell nucleus to further influence transcriptional changes and tissue homeostasis.

1.2.4.2 Oxygen Tension

Alongside mechanical loading, oxygen tension is another critical regulator of ECM homeostasis in cartilage [33]. Cartilage is naturally maintained in a hypoxic environment (2%–4%) compared to other vascularised tissue [34]. Chondrocytes therefore rely predominantly on glycolytic metabolism for cellular energy [34]. Coyle et al. showed that exposure of bovine chondrocytes to hypoxic conditions resulted in the expression of key matrix synthesis genes [35]. A supporting study showed that sustained hypoxia resulted in an increase in GAG deposition and enhanced COL2 [36]. The nuclear transcription factor,

hypoxia-inducible factor – 1 alpha (HIF-1α), is a major regulator of cellular adaptations to hypoxia. Under low oxygen tension (oxygen tensions <4%), HIF-1α is important in directing cellular metabolism towards glycolysis whilst also maintaining cellular homeostasis [37]. HIF-1α has been shown to translocate to the nuclei of chondrocytes under hypoxic conditions whilst the HIF-1α protein is significantly degraded in oxygen tensions >4% [38]. Although HIF-1α nuclear translocation and increased collagen production have been associated with hypoxic conditions, neither have been causatively linked with one another. In fact, there have been contrasting findings regarding the effect of oxygen tension on matrix synthesis. One study showed hypoxic environments to increase the messenger ribonucleic acid (mRNA) expression of aggrecan but decrease *COL2A1* expression [39]. The varying results might be explained by the different methods used to maintain a hypoxic environment. Despite this, it remains inconclusive how varying oxygen tension influences cartilage homeostasis.

1.2.5 ECM turnover in OA

OA pathology is characterised by changes in the composition and structure of the ECM. In healthy tissue, the ECM is composed mostly of COL2 providing tensile strength in conjunction with the negatively charged aggrecan, which provides compressive resistance through its osmotic properties. In OA, the changes to ECM composition predispose the cartilage to mechanical instability and thereby initiating a pathological process headed towards joint pain and disability [40].

Aggrecan degradation (by aggrecanses) is an important hallmark of OA. Members of the disintegrin and metalloproteinase with thrombospondin motif (ADAMTS) family of proteins have been shown to cleave aggrecan at the aggrecanase site [41, 42]. Of the

ADAMTS proteins, ADAMTS4 and ADAMTS5 are the two most principal proteins implicated in aggrecan degradation in OA [43]. Although *ADAMTS4* gene is inducible in primary chondrocytes through IL1 stimulation [44] deletion of *ADAMTS4* in murine models of OA does not provide protection by preventing aggrecan loss [45]. On the other hand, ADAMTS5 KO has a marked protective role in preventing aggrecan degradation in murine OA model [46].

Nonetheless, aggrecan degradation alters the permeability and mechanical compliance of the matrix [47]. The change in the compressive modulus of the ECM exposes the cartilage to greater strains for a given mechanical stimulus.

In conjunction with ADAMTSs, another family of zinc-dependent endopeptidases, MMPs, are responsible for the cleavage of collagen [48]. MMPs are subcategorised depending on their substrate specificity and include collagenases, gelatinases, stromelysins. matrilysins, membrane-type MMPs and other nonclassified MMPs [49]. Multiple MMPs play a role in the degradation of aggrecan and collagen of which MMP1, -8 and -13 are regarded as classical collagenases [50]. MMP1 is located in the superficial zone of articular cartilage but also produced by activated osteoblasts located in the subchondral cysts in OA patients [51]. MMP8 is mainly produced by chondrocytes in the superficial zones and together with MMP1 is responsible for the cleavage of interstitial COL2 [52]. MMP13 is considered to be the most important MMP responsible for the cleavage of collagen in articular cartilage. This is secondary to the abundance of MMP13 in osteoarthritic cartilage and its preference to cleave COL2 over other subtypes [53] although it is important to note that MMP13 is almost undetectable in healthy, disease-free cartilage [54]. L. A. Neuhold et al. showed that MMP13 activity resulted in increased cartilage degradation in the joints of transgenic mice [55]. Wang et al. reinforced these findings and showed that MMP13 KO mice displayed increased COL2 and aggrecan after OA induction through meniscal ligamentous injury

(MLI) [56]. Similarly, disease progression is mildly halted in a destabilisation of medial meniscus (DMM) model of OA in MMP13 KO mice [57]. Given that MMP13 is the major collagenase in OA and confers the highest specificity towards COL2, it was unsurprising that the use of an MMP13 inhibitor decelerated MLI-induced OA progression [56].

MMP2 and MMP9 (gelatinases) have been shown to be enhanced in OA cartilage [58]. Together, both MMP2 and MMP9 are capable of cleaving type I, IV, V, VII and X collagens; laminin; elastin; fibronectin and proteoglycans [58]. MMP3 (stromelysin 1) has been shown to be elevated in the superficial zones of mechanically loaded cartilage, and it predominantly degrades proteoglycan [59]. A category of molecules, TIMPs, are tissue-specific, endogenous inhibitors of MMPs. Four homologous members of the TIMP family have been reported: TIMP1, TIMP2, TIMP3 and TIMP4. MMP activity is tightly controlled by TIMPs [60]. Of the inhibitors, TIMP1 displays the highest affinity for MMPs 1, 3, 9 and 13 [61]. TIMP1 serum levels are elevated and are a good predictor of a patient's development of hip OA [62]. A more recent study showed that TIMP3 overexpression proved to be protective against cartilage destruction during late-stage OA [63].

Collectively, the two most significant enzymes driving cartilage turnover in OA are ADAMTS5 and MMP13. Yamamoto et al. showed that both ADAMTS5 and MMP13 are constitutively produced in adult human chondrocytes [54]. However, in healthy adults, MMP13 is rapidly co-endocytosed with ADAMTS5 via low density lipoprotein receptor-related protein 1 (LRP1) receptors [54]. The same group showed in 2017 that OA progression is typified by increased shedding of the LRP-1 receptor attributed to local sheddases such as ADAM17 and MMP14 [64].

Taken together, the breakdown of proteoglycan and COL2 in OA undermines the integrity of the ECM network. The changes in the structure and the composition of the ECM

significantly affect the mechanical properties of the cartilage rendering it unable to withstand and dissipate mechanical strain.

There are several changes that occur to collagen in OA. In-vivo studies in rabbit have shown that collagen content in early OA is increased [65]. This is associated with a change in the subtype of collagen from type II to type I [65]. COL2 fibrils form an endoskeleton and contain interfibrillar sites which associates with proteoglycan in the ECM. Therefore, the resultant change in phenotype to collagen type I in progressive OA alters the integrity of the collagen-proteoglycan network, thereby decreasing the elasticity of the ECM [40].

1.2.6 Changes in biomechanical environment in OA

OA is considered a multifactorial disease being a common end result of culmination of factors (age, obesity and trauma) initiating a multitude of pathways, resulting in an altered biomechanical joint. This is evidenced by observations that the aetiology of hip OA can be a result of minor developmental deformities that were previously unrecognised [66]. Further evidence emphasising the importance of altered biomechanics in the aetiology of OA has been provided by the observation that joint distraction, by alleviating the mechanical forces subjected through the joint, protects from the development of OA [67-69].

In late OA, the mechanical microenvironment changes because of a significant loss of aggrecan and water, which reduces the mechanical compliance of cartilage [9, 70]. Recent evidence has also shown that collagen fibrils thicken in OA cartilage further impairing mechanical integrity [71]. Through a positive feedback cycle, the manner by which the ECM responds to further mechanical stress is not only dependent on the tissue's morphology but also on the changing biomechanical properties of the diseased cartilage. This is evidenced by studies showing altered loading due to joint instability (i.e. secondary to ligament

transection or meninsectomy) to be a significant risk factor for the onset and progression of OA [72, 73]. Repeated mechanical stress on injured joints not only impairs the integrity of the ECM but also results in remodelling of the subchondral bone [74]. These changes result in decreased tissue stiffness in tension, compression and shear stresses. Ultimately, these changes in the mechanical properties of the joint and secondary alterations in ECM homeostasis set an ever-deteriorating biomechanical environment. Such changes intensify the progression of OA, leading to the formation of fibrocartilaginous tissue and osteophyte formation replacing the degraded cartilage [75].

1.2.7 Impairment of mechanotransduction in OA

Mechanosensors in the joint are responsible for sensing mechanotransduction signals and transferring them from physical stimuli to biochemical signalling. This can be in the form of inflammatory responses, metabolic changes and protein phosphorylation.

The PCM is one of the most critical mechanotransducers and mechanosensors in the cartilage [22]. Khoshgoftar et al. demonstrated that the PCM can change stress magnitudes on the chondrocytes [76]. This is further evidenced by in-situ imaging of chondrocyte deformation showing the PCM to regulate local stress [77]. Interestingly, the PCM can also act as a nonlinear mechanical adaptor by either dampening high-intensity strain transmitting to the superficial zone or amplifying lower-intensity mechanical strain from the middle to the deep zone [78]. The PCM not only modulates the stress-strain, but by regulating the osmotic and fluid-flow environment, it functions as a regulator of mechanotransduction in the chondrocyte [78].

In a diseased state, this regulatory function of the PCM is impaired and thereby affects chondrocyte activity. Seminal studies have shown changes in the PCM composition in OA.

Preliminary studies on canine and human chondron morphology showed chondrocyte proliferation to be preceded by changes to the proteoglycan and collagen composition in the PCM [79, 80]. Subsequent studies showed enlarged chondrons with cell cluster formation and loose organisation of the PCM [81, 82]. A more recent study showed a change in the collagen phenotype in the PCM from type II to type I [83]. The resultant loss of composition of the PCM renders it incapable to act as a reliable mechanosensor for the residing chondrocyte, primarily because of the impairment of outreaching primary cilium on the chondrocyte's membrane.

The primary cilium is recognised as a key mechanosensor in chondrocytes [84]. The primary cilium has now been identified as having several ion-gated channels, such as the transient receptor potential vanilloid 4 (TRPV4) [30]. In conjunction with matrix protein receptors, such as integrin, the primary cilium interacts with the matrix proteins to act as a key mechanotransducer [85]. The TRPV4 receptor in particular is capable of initiating intracellular Ca2+-signalling in response to mechanical stimuli [86]. In osteoarthritic cartilage, the length of the primary cilium is increased, impairing its ability to act as a competent mechanical transducer [87].

As discussed earlier, the PCM acts as a repository for a variety of growth factors [14, 16]. In diseased cartilage, the regulatory proteins are released in response to injury. Namely, FGF2, which is sequestered on perlecan, is released secondary to injury or cyclic compression [16]. The physiological role of FGF2 as a mechanosensor is thought to be beneficial, with FGF2 KO mice developing accelerated OA after DMM [88]. However, there is an open consensus on the role of different variants of the FGF receptors (FGFR) in disease. FGFR3 KO mice are characterised by accelerated OA [89] whereas FGFR1 ligation causes chondro-degradation [90]. This suggests that pathological states might be driven by selective receptor-ligation compared to the mechano-environment in healthy cartilage. There is also

evidence of impaired FGF2 signalling in diseased cartilage secondary to decreased ligand affinity to the matrix, attributable to sulphotransferase enzyme, which is capable of modifying heparin sulphate motifs on aggrecan [91].

One study showed that there is a probable mobile pool of available ligand capable of binding to cell surface receptors [92]. Tracking the movement of FGF2 through the use of gold-nanoparticle-labelled FGF2 molecules showed that whilst some molecules are fixed within the matrix, others are characterised by dynamic movement [92]. This suggested that in diseased articular cartilage, direct mechanical overload can reduce the overall volume of the matrix and thereby affect the available biological pool of FGF2 ligands.

Seminal studies have shown that another PCM growth factor, transforming growth factor β (TGF-β), is mechanosensitive. TGF-β-dependent genes are shown to be induced in bovine chondrocytes subjected to cyclic loading [93, 94]. TGF-β is secreted extracellularly, where it binds onto larger latent TGF-β binding proteins to form a larger complex, which in turn binds onto fibrillin and fibulin [94]. Deletion of TGF-β receptor 2 (TGF-βR2) in mice results in an accelerated OA phenotype [95] whilst young mice with truncated TGF-βR2 developed OA-like joints [96]. Canonical TGF-β signalling involves the phosphorylation of downstream suppressor of mothers against decapentaplegic (SMAD) proteins which translocate to the nucleus to activate or repress gene expression [97]. The implication of TGF-β as a critical mechanosensor is further evidenced by the observation that knockdown of SMAD3 not only resulted in the early development of OA but also caused chondrocyte hypertrophy [98].

1.2.8 Modelling cartilage injury

Our group has used direct cartilage injury as a model to investigate the signalling pathways which are activated on injury [16, 99]. There are two variations to this model depending on the species. In the porcine model, trotter joints are dissected open and cartilage explanted and cut into smaller pieces. In the mouse model, injury is defined by avulsion of the hip. Both these procedures have been demonstrated to activate catabolic pathways that lead onto inflammation, release of aggrecanases and MMPs and consequent cartilage breakdown (mechanoflammation) whilst also initiating cartilage repair pathways illustrated by the release of growth factors such TFG-β and FGF2 (chondroprotection) [14, 16, 94]. A common in-vivo model that is used to study mechano-inflammatory and chondroprotective pathways activated by cartilage injury is the DMM model. However, the type of mechanical loading has been shown to be important in favouring either mechanoflammation or chondroprotection. Burleigh et al. demonstrated using an in-vivo DMM mice model that mechanoflammation is induced by shear stress whereas compressive loading on the joint is responsible for initiating chondroprotective response, involving the release of growth factors [100]. These models are therefore constantly used by our lab to either further delineate known pathways or discover new signalling pathways that are mechanosensitive. Doing so helps us understand the pathological processes that underpin OA and thereby facilitate the discovery of new drug targets.

1.2.9 Mechanoflammation after cartilage injury

Inflammation plays an important role in governing the structural integrity of the ECM of articular cartilage. Mechanical damage–induced inflammation is not only restricted to the cartilage but also involves the surrounding synovial membrane in conjunction with the

underlying subchondral bone [101]. Our lab has extensively looked at inflammatory processes following cartilage injury, a process that we have termed mechanoflammation [2]. Mechanoflammation can be categorised into either the inflammatory signalling response or inflammatory gene response that follows cartilage injury [2]. Various intracellular signalling pathways have been shown to be activated on cartilage injury including the mitogen activated protein kinase (MAPK)/extracellular signal regulated kinase (ERK) pathway, the nuclear factor kappa light chain enhancer of activated B cells (NF-κB) pathway, the wingless/integrated (Wnt) pathway, the TGF-β pathway and the Hippo-YAP pathway [16, 94, 99, 102].

1.2.9.1 TAK1 activation

Transforming growth factor-beta activated kinase 1 (TAK1) is a member of the MAPK kinase kinase family. TAK1 is known to have a diverse set of roles in the regulation of physiological and pathological processes involving inflammatory responses, cell proliferation, metabolic regulation and tissue remodelling [103]. TAK1 was originally discovered in the late 1990s as a downstream mediator of TGF-β signalling [104]. Accumulating evidence has since revealed that TAK1 is activated by a host of stimuli such as TNFα, IL1β and lipopolysaccharide (LPS) [105]. Upon activation, TAK1 phosphorylates downstream targets such as the MAPK family (ERK, c-jun N-terminal kinase (JNK), p38) and NF-κB family of proteins [103]. The activation of TAK1 depends on TAK1-binding proteins (TAB) 1, 2 and 3 [103]. TAB1 has been shown to play a more dominant role in the activation of TAK1 whereas TAB2 and TAB3 have more redundant roles [103]. Binding of the TAB1-TAK1 complex to K63-polyubiquitination chain facilitates the auto-phosphorylation of TAK1 and its activation [103]. The TAK1-TAB1 complex is responsible for the subsequent phosphorylation of inhibitor of nuclear factor kappa-B kinase subunit

beta (IKK-β) at key serine residues within its activation loop, resulting in IKK-β activation and the eventual activation of NF-κB signalling [106]. In addition, the TAK1-TAB complex also phosphorylates members of the mitogen activated protein kinase kinase (MAPKK) family, which in turn phosphorylates JNK and p38 kinases [103]. I go into further detail about MAPK and NF-κB signalling below.

Accumulating studies have defined TAK1 as a driver of inflammation and ECM destruction in cartilage [107]. Conditional, cartilage-specific deletion of TAK1 in mice resulted in impairment in the morphology and maintenance of cartilage homeostasis [107]. In addition, silencing TAK1 in human chondrocytes by using small inhibitory RNA (siRNA) resulted in the downregulation of cyclooxygenase 2 (*COX2*), *MMP1* and *MMP13* whilst also reducing the release of prostaglandin E 2 (PGE2) [108]. A more recent study demonstrated that the use of small molecule inhibitor to TAK1, 5Z-7 oxozenaol (5Z-7) protected against cartilage degradation by downregulating a series of inflammatory genes through inhibiting MAPK and NF-κB signalling [109]. 5Z-7 also prevented ECM degradation in OA cartilage explants [109]. Our lab has also provided further evidence for the role of TAK1 in cartilage injury [99]. TAK1 is rapidly activated by 30 seconds following porcine cartilage injury [99]. Ismail et al. demonstrated that inhibiting TAK1 not only prevented JNK phosphorylation and inhibited the kappa light chain gene enhancer in B cells (IκBα) degradation but also inhibited the upregulation of injury-induced inflammatory genes (mechanoflammation) [99]. In mice, the group further demonstrated that MAPK and NF-κB signalling pathways (and subsequent upregulation of inflammatory genes) are reduced in hip avulsion samples collected from cartilage-specific TAK1 null mice compared to wild-type mice [99]. Ismail et al. further attempted to investigate the upstream mediators activating TAK1 on cartilage injury. The group used a TNF receptor-associated factor 6 (TRAF6) KO mice to investigate whether the activation of TAK1 was mediated through this specific E3 ligase. However, TRAF6 KO

showed JNK activation suggesting TAK1 phosphorylation on cartilage was not TRAF6-dependent. In addition, myeloid differentiation primary response 88 (MyD88)-KO mice also displayed injurious signalling suggestive of the fact that upstream toll-like receptors (TLRs) and interleukin 1 receptor (IL1R) have no major role in injury-induced TAK1 activation [99]. Up until now, the upstream mediator of TAK1 activation on cartilage injury remains unknown (Figure 1.3). However, it is believed that the upstream mediator to TAK1 is neither soluble nor secreted on injury [2].

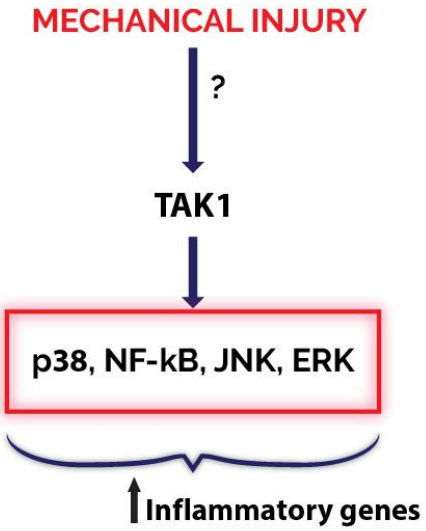

Figure 1.3: Schematic representation of the activation transforming growth factor beta activated kinase (TAK)-1 and downstream pathways on cartilage injury.

Mechanical injury activates transforming growth factor beta-activated kinase 1 (TAK1). TAK1 activates downstream mitogen activated protein kinases (MAPKs) that include extracellular signal kinase (ERK) c-Jun N-terminal kinase 2 (JNK 2) and p38. TAK1 also activates nuclear factor kappa-light-chain-enhancer of activated B cells (NF-κB) signalling. The activation of MAPKs and NF-κB results in the increased expression of pro-inflammatory genes, causing the release of key cartilage degrading proteases. The upstream mediator to TAK1 remains unknown.

1.2.9.2 MAPK/ERK pathway

Cartilage injury has been shown to cause rapid activation in the mitogen activated protein kinase (MAPK) pathway [16, 99] (Figure 1.3). MAPKs belong to the CMGC group of protein kinases which also include glycogen synthase kinases (GSK), cyclin-dependent kinases (CDKs) and CDK-like kinases [110]. MAPKs phosphorylate their own dual serine or threonine residues in a process known as auto-phosphorylation [110]. Alternatively, they phosphorylate downstream substrates on serine and threonine motifs [110]. MAPKs are downstream of a three-tiered kinase cascade system: MAPK, MAPK kinase (MAPKK) and MAPK kinase kinase (MAPKKK) [110]. Phosphorylation and activation of MAPKs by MAPKKs occurs by phosphorylation of a conserved Thr-X-Tyr motif [110]. Through integration within this signalling module, MAPKs are involved in the signal transduction of various extracellular stimuli into coordinated, adaptive cellular and nuclear responses [111]. By doing so, MAPKs are responsible for controlling multiple cellular functions including cell differentiation, cell death, nuclear transcription and protein biosynthesis [110]. Several cytokines have been shown to signal through the MAPK pathway, including tumour necrosis factor (TNF)-alpha (α), interleukin (IL) 1, IL2 and IL6 [112-115].

Although there are 20 different serine/threonine kinases that are classified under the MAPK family, the best characterised MAPKs in the context of cartilage injury include extracellular signal-regulated kinase (ERK), JNK and the p38 MAPK.

Studies have shown rapid activation of ERK1/2 on cartilage injury [16, 99] (Figure 1.3). ERK1 and 2 are activated by MAPKK1 and MAPKK2, respectively (both MAPK kinases) [110]. In a model of dog OA, the use of ligand to voltage gated Ca2+ channels reduced the phosphorylation of ERK1/2 and the development of OA lesions [116]. A further study used a rabbit OA model to show that a MEK 1/2 inhibitor not only prevented the activation of

ERK but also suppressed the progression of OA [65]. Furthermore, Starkman et al. showed that ERK might be a negative regulator of proteoglycan synthesis in OA [117].

JNK is another member of the MAPK family and is encoded by three genes (JNK1, JNK2 and JNK3). Phosphorylation of JNK results in the activation of various transcription factors that attach onto activator protein -1 (AP-1) binding sites including Jun proteins (c-Jun, JunB and JunD), Fos proteins (c-Fos, FosB, Fra-1 and Fra-2) and activation transcription factor 2 (ATF2) [118]. The activation of JNK itself is mediated by two dual-specificity protein kinase, namely, MAPKK4 and MAPKK7 [118]. The latter two are substrates of MAPKKK (TAK1). Various studies have implicated the involvement of JNK activation in the progression of OA. In 2016, Yang et al. showed that two important synovial fluid pro-inflammatory cytokines, CCCL8 and CXCL5, worsened disease progression in OA secondary to the upstream activation of JNK [119]. Chondrocyte proliferation and apoptosis were further induced by the activation of JNK in this study [119]. A later study showed that the activation of proteolytic enzyme and subsequent aggrecan degradation was JNK-dependent [120]. Other groups investigated the role of JNK activation in the context of OA through the use of inhibitor targeted at the JNK signalling pathway. The use of a JNK inhibitor, SP600125, decreased the expression of the apoptotic factors p53, caspase 3 and Bcl-2 induced by TNFα [121]. Other studies have further reinforced that inhibiting JNK suppresses the production of inflammatory mediators and decreases the expression and activity of MMP1, MMP3 and MMP13 [122]. Our group has specifically shown that JNK is phosphorylated by two minutes (mins) following porcine cartilage injury in a TAK1-sensitive manner [99] (Figure 1.3). Further to this, JNK2 knockout (KO) mice are partially protected from the development of OA [123]. This is proposed to be through the suppression of inflammatory genes *IL6*, *ADAMTS4*, *IL18*, *IL1A* and nerve growth factor (*NGF*) in JNK2

KO mice compared to wild-type mice and significantly reduced aggrecan fragments in JNK2 KO mice [123].

P38 is another member of the MAPK family with reported significance in OA disease progression. P38 upregulated pro-inflammatory cytokines through different mechanisms. These include either the phosphorylation of downstream transcription factor AP-1 or through the stabilisation of inflammatory gene mRNAs containing 3' untranslated region adenosine/uridine-rich elements (AREs) [124] [125]. He-Yan Sun et al. showed that inhibition of the p38-MAPK signalling pathway dampened inflammation-induced cell loss and mitigated chondrocyte apoptosis [126]. This was consistent with an earlier study where the use of SB203580 and VX-745 attenuated both cartilage degeneration and pain in rat model of OA [127]. Other studies further demonstrated small-molecule p38 inhibitors to suppress the regulation of inflammatory genes and MMPs [128, 129]. The activation of p38 is directed by upstream MAPKK kinases such as MEK1 and MEK2 [130]. One particular group inhibited MEK1/2 and demonstrated that a significant reduction in ECM destruction and formation of osteophytes in a rabbit model of OA secondary to the transection of the anterior cruciate ligament [131].

1.2.9.3 NF-κB pathway

NF-κB is a nuclear transcription factor which regulates numerous innate and adaptive immune responses [132]. NF-κB is part of a family of five structurally related members; these include NF-κB1, NF-κB2, RelA, RelB and c-Rel. Each of these transcription factors activate or repress target genes by binding to specific DNA-motifs [133]. IκB belongs to a family of inhibitory proteins which normally sequesters NF-κB proteins in the cytoplasm. The best-studied IκB family member is IκBα [133].

The activation of NF-κB involves the activation of either canonical or noncanonical signalling pathways. The canonical signalling pathway responds to a wide array of stimuli including pro-inflammatory cytokines, pattern associated molecular patterns (PAMPs), damage associated molecular patterns (DAMPs) and the TNF receptor (TNFR) superfamily members [132]. The primary mechanism of action for the canonical pathway involves the degradation of IκBα through site-specific phosphorylation at serine residues [133]. Phosphorylation of IκBα is induced by IKK, composed of two catalytic subunits (IKKα and IKKβ) and a regulatory domain named NEMO. Once activated, IKK is responsible for the phosphorylation of IκBα, resulting in the degradation of IκBα in a ubiquitin-dependent manner [132]. This initiates the nuclear translocation of NF-κB transcription factors, predominantly as RelA/p50 and c-Rel/p50 heterodimers. These then bind onto the specific DNA element, kB enhancer, to influence gene transcription.

The non-canonical NF-κB signalling pathway responds to a much narrower range of stimuli, most notably to pathogens. Non-canonical NF-κB signalling is not dependent on IκBα degradation, but is instead characterised by the phosphorylation of p100, a NF-κB2 precursor protein [132]. The initiating step in this pathway involves the activation of IKKα by NF-κB-inducing kinase (NIK), which results in the phosphorylation of p100, thereby inducing p100 ubiquitination and its degradation. This results in the release of mature NF-κB2 which in turn induces the nuclear translocation of the p52/RelB non-canonical, heterodimeric complex [133].

NF-κB is very well categorised as a mediator of pro-inflammatory genes in cells [132]. Dysregulation of the NF-κB signalling pathway has been shown in cancer, autoimmune and fibrotic diseases [132]. Early studies in the 2000s first identified the NF-κB signalling pathway as being pro-inflammatory in OA pathology. Such studies showed that IL1-β-

induced inflammatory gene expression in cultured chondrocytes was abrogated by the use of NF-κB inhibitors [134]. These findings were further reinforced by subsequent loss-of-function studies that demonstrated the knockdown of p65 resulting in protection from disease progression in injured cartilage lesions [135, 136]. An inhibitor study to the upstream mediator in the canonical NF-κB signalling pathway revealed that intraarticular injection of an inhibitor to IKKα/β suppresses the induction of *ADAMTS5* and *MMP13* in a surgically induced OA model [137].

Further studies have shown that NF-κB is capable of inducing inflammatory gene expression such as *MMP1*, *MMM9*, *COX2*, inducible nitric oxide synthase (*INOS)* and *PGE2*, involved in the degradation of the cartilage ECM matrix [135]. NF-κB is also capable of upregulating other transcription factors involved in driving disease in OA including hypoxia inducible factor 1α (HIF-1α), E74-liks factor 3 (ELF3) [135]. HIF-1α is directly responsible for the induction of catabolic factors, such as *MMP13*, in chondrocytes [135]. It has also been shown to enhance *FAS* gene expression and, by doing so, mediate chondrocyte apoptosis [138]. Moreover, chondrocyte-specific deletion of ELF3, and downstream target of NF-κB, resulted in decreased levels of DMM-induced *MMP13* and *INOS* [139].

There are many factors that have been reported to activate NF-κB signalling in OA. Arguably one of the most important factors inducing NF-κB signalling is mechanical overloading. As discussed TAK1 is a key driver in the intracellular signalling response to cartilage injury. Intraarticular injection of a TAK1 inhibitor (5Z-7) resulted in the suppression of NF-κB signalling and ameliorated OA in a rat DMM model [109]. The dynamism between TAK1 and NF-κB signalling following OA induction was shown by Ismail et al. [99]. Cartilage injury resulted in the phosphorylation of IκB and caused subsequent degradation of IκB to start by 30 seconds reaching a maximum of 5 mins

following injury. These responses were correlated with increased nuclear translocation of the NF-κB transcription factor, p65, into the middle and deep zones of cartilage [99]. Moreover, the use of 5Z-7 abolished IκB degradation, and this was correlated with a reduction in the expression of injury-induced inflammatory genes. These studies underpinned the importance of cartilage injury and mechanical loading on the activation of TAK1 and subsequent activation of NF-κB signalling (Figure 1.3).

Other activators of NF-κB include extracellular secreted factors such as leptin, ghrelin, osteopontin and periostin. Osteopontin itself has been shown to be higher in the synovial fluid of patients with OA. Furthermore, osteopontin resulted in the increased expression of MMP13 through the activation of NF-κB signalling [140]. Despite this, there have been conflicting findings about the role of osteopontin in OA. A recent study demonstrated that osteopontin in fact inhibited OA progression through the OPN/CD44/PI3K axis [141].

Lastly, inflammatory cytokines produced from damaged OA cartilage have also been shown to be activators of the NF-κB signalling pathway. Several cytokines belonging to the interleukin family are known activators of NF-κB including IL1β and IL36α [132]. The latter, IL36α, has been recently shown to not only be expressed higher in diseased joint but also to exert a catabolic effect through NF-κB signalling [142].

Collectively, evidence suggests that various injury-induced signalling pathways in OA are interconnected with NF-κB signalling underpinning the significance of the NF-κB pathway in OA pathology.

1.2.10 Chondroprotection after cartilage injury

1.2.10.1 FGF2 signalling

FGF2 has an important role in regulating the growth and development of chondrocytes and synovial cells [143]. During development, dysregulated FGF2 signalling results in chondroplasia whereas postnatally aberrant FGF2 signalling causes the degeneration of articular cartilage [144]. Historical data from our lab has revealed that FGF2 is highly mechanosensitive and released on cartilage injury [16]. However, there are conflicting findings about the role of FGF2 in articular chondrocytes. FGF2 has been shown to upregulate the transcription of *MMP1* and *MMP13* in human articular chondrocytes [145]. Another study showed FGF2 to upregulate the expression of *ADAMTS5* [146]. Other studies have demonstrated that FGF2 is chondroprotective by inducing the expression of tissue inhibitor of metalloproteinase 1 (*TIMP1*) and suppressing the IL1-induced upregulation of *ADAMTS4* and *ADAMTS5* [88, 147]. In addition, exogenous FGF2 induced mitogenic effects to induce articular cartilage repair in-vivo [148]. The opposing findings focusing on FGF2 in cartilage homeostasis appear to be determined by the receptor through which it signals. The catabolic effects of FGF2 are now agreed to be mediated through FGF1 ligation whereas the pro-regenerative effects of FGF2 are mediated via FGFR3 [143]. This is further supported by the finding that FGF18, which has been shown to increase proteoglycan synthesis, selectively activates FGFR3 [149]. FGF2 is released from the PCM on cartilage injury, and it has been shown to suppress the expression of FGFR3 [143]. Injury may therefore change the expression of FGFR subtypes and thereby shift the phenotype towards a catabolic state. This is supported by the fact that there is reduced expression of FGFR3 in human osteoarthritic cartilage compared to normal disease-free cartilage [143].

Taken together, the expression of FGFR3 in the cartilage plays a central role in maintaining a pro-anabolic phenotype.

1.2.10.2 TGF-β signalling

TGF family comprises of 35 members of proteins and function in cell differentiation, proliferation and homeostasis in multiple tissues [150]. TGF-β has also proven to be central in ECM homeostasis and cartilage degradation. TGF-β is released from cells in a small latent complex (SLC), which consists of a covalent dimer of active TGF-β in a covalent association with two latency-associated peptides (LAPs) [150]. The SLC covalently binds to latent TGF-β binding proteins (LTBPs) to form a large latent complex (LLC). Van der Kraan et al. demonstrated that either deficient or aberrant TGF-β signalling results in accelerated OA in an aging mice model [151]. Moreover, inhibition of TGF-β resulted in increased cartilage damage [151]. Besides being a key factor in promoting a pro-regenerative state, TGF-β has also been purported to suppress IL1-mediated upregulation of *MMP13* and *MMP14* [152]. Collectively, these studies demonstrate that not only can TGF-β stimulated ECM production, but it might also suppress mechanoflammation.

Our group has further demonstrated that other protective molecules include connective tissue growth factor (CTGF) which is covalently bound to latent TGF-β in the PCM [94]. On cartilage injury, the latent TGF-β -CTGF complex is released resulting in the activation of the TGF-β complex in a CTGF-dependent manner [94]. Once activated TGF-β phosphorylates SMAD2/3 resulting in activation and subsequent nuclear translocation of SMAD4. The phosphorylation of SMAD2 downstream of active TGF-β was associated with thicker cartilage that was more resistant to degradation [94].

Taken together, the latent TGF-β -CTGF pathway is integral in maintaining the cartilage in a pro-anabolic state and compensates for the loss of ECM associated with mechanical injury. Ultimately, how the balance between pro-degenerative (mechanoflammation) and pro-regenerative (chondroprotective) pathways are regulated after cartilage injury remains unknown. However, suppression of mechanoflammation in OA may inhibit matrix turnover and promote intrinsic repair responses to favour chondroprotection [2].

1.3 Current therapeutics in OA

Current treatment in the field of OA is largely limited to nonsteroidal anti-inflammatory drugs (NSAIDs) or steroidal intra-articular injections to treat inflammation and pain. These treatment options only serve to provide symptomatic relief from pain in OA but are not classified as disease modifying. There is still a pressing need for disease modifying OA drugs (DMOADs) in the field of OA. DMOADs are intended to modify the pathophysiology of OA and thereby halt or reverse the progression of OA. Such drugs are led by targeting emerging molecular mechanisms orchestrating disease in OA, such as those described above. DMOADs can be classified into either those targeting the signalling pathways that activate pro-inflammatory cytokines (namely TAK1, MAPK pathway and NF-κB) or targeting chondroprotective pathways that offset the loss of the ECM (namely FGF2, TGF-β). As discussed, both pro-degenerative and pro-regenerative pathways are responsive to mechanical forces through the joint, either physiological loading or pathological overloading of the joint. Successful DMOADs are therefore intended to suppress mechanoflammation and/or promote a regenerative response in the cartilage.

1.3.1 Targeting pro-inflammatory signalling pathways

Over the last decade, a number of human clinical trials have been conducted to test the efficacy of drugs intended to suppress mechanoflammation. IL1 has long been an attractive target, as it has been shown to promote cartilage degradation by stimulating the release of MMP13 and ADAMTS5 [153]. However, these findings were in conflict with numerous in-vivo models of OA in which IL1 was either deleted or knocked out. Clements et al. demonstrated that IL1 KO mice were not protected from OA induced by partial

menisectomy [154]. These findings were reinforced by a later study that showed no protection from OA disease progression in IL1α /IL1β double KO mice [155]. Despite these unfavourable results, there was a pressing drive towards human studies in the form of randomised controlled trials (RCTs) in OA targeting IL1. Two separate RCTs that utilised a dual antibody against IL1α and IL1β in hand OA [156] and knee OA [157], respectively, both failed to reach their primary outcome and provide clinical efficacy. Another RCT that involved 160 individuals with knee OA injected with intra-articular injections of anakinra failed to demonstrate clinical efficacy at three months [158].

IL6 has also been implicated in disease progression in OA. Several studies have demonstrated higher levels of IL6 in OA synovial fluid compared with healthy individuals whilst further work showed IL6 to induce *MMP3*, *MMP13* and *ADAMTS* [159-161]. These studies formed the basis to validate a randomised, double-blind, placebo-controlled study using tocilizumab, an antibody against the IL6 receptor, in patients with hand OA (ClinicalTrials.gov Identifier: NCT02477059). In the study, a total of 45 and 46 patients were randomly assigned to receive tocilizumab or placebo, respectively. The authors concluded that overall, tocilizumab did not alleviate pain or improve hand function compared to placebo control.

The use of anti-TNFα therapies proved to be efficacious in relieving pathological symptoms in patients with RA [162]. However, clinical trials involving anti-TNFα therapies in patients with OA have yielded negative, disappointing results. The use of adalimumab (a human monoclonal antibody that prevents the binding of TNFα to its receptor) was shown to be ineffective at reducing disease activity and pain in both hand [163] and knee OA [164].

Hydroxychloroquine was another agent nominated to be a potential disease-modifying drug after anecdotal evidences revealed that it was effective in patients with ‘inflammatory’ hand

OA [165]. Hydroxychloroquine had already been well established with clinical trials for RA with good safety profiles [166, 167]. However, the use of hydroxychloroquine in a RCTs with hand OA patients proved to be futile [168]. The authors demonstrated that at six months, hydroxychloroquine was no more effective than placebo for pain relief in patients with moderate to severe hand pain with radiographic OA [168].

Another drug used in a clinical trial with the hope to improve pain and disability in patients with OA was doxycycline. Besides its function as an antimicrobial agent, doxycycline has been shown to inhibit MMPs and thereby prevent the degradation of collagen type IX [169, 170]. However, extension of doxycycline into human studies has provided less than promising results. One study conducted by Brandt et al. in 2005 demonstrated that doxycycline suppressed the progression of radiographic knee OA [171]. However, the authors did not find any clinically relevant correlates with this observation. In other words, doxycycline was not found to reduce pain or improve daily function of the joint any more so than placebo [171]. The clinical inefficacy of doxycycline was confirmed by a later RCT conducted in 2011 by Snijders et al. [172]. In this study, doxycycline was confirmed to not be effective in reducing pain, stiffness or function in patients with knee OA over a 24-week study period [172]. Moreover, compared to the placebo group, significantly more participants who were taking doxycycline withdrew from the study because of a higher incidence of adverse effects.

Taken together, the development of a new effective pharmacological agent to target mechanoflammation has proven to be futile. Although in the last decade, studies centred on joint biology have identified various molecular treatment targets, in the hope of alleviating joint pain, inflammation and disability, none of these to date have either modified disease process or relieved pain in patients with OA.

1.3.2 Targeting repair signalling pathways

Targeting signalling pathways that promote a reparative response in cartilage also serve as a potential development on towards a DMOAD. As discussed, FGF2 is not only highly expressed in the synovial fluid of OA patients, but it is also released rapidly from within the PCM on cartilage injury to activate extracellular-signal-regulated-kinase signalling pathway [16]. FGF2 exerts a chondroprotective effect and has been shown to inhibit proteoglycan degradation through the suppression of *ADAMTS5*, *MMP1* and *MMP13* [88]. Despite this, there have been conflicting findings from FGF2 blockade. In human OA chondrocytes, the use of FGF receptor antagonists actually increases the expression of matrix-degrading enzymes [145]. Whereas in a murine model of surgically induced OA, FGF2 KO accelerated the progression of disease which was rescued by the administration of recombinant FGF2 treatment [173]. These contrasting findings might reflect a differing role for FGF2 between species. Recently, there has been a focus on FGF18, which has been reported to exert a significant role in cartilage repair [174, 175]. Intraarticular injections of FGF18 in a surgical rat OA model was associated with increased cartilage thickness and decreased ECM degradation in a dose-dependent manner [174]. A subsequent study confirmed these findings with intraarticular injection of human recombinant FGF18 [176]. Due to the success of these in-vivo studies, there is currently an ongoing clinical trial with the use of recombinant FGF18 protein in OA patients (NCT01919164). The initial phase I study showed that sprifermin had a good safety profile but also significantly reduced cartilage degradation in knee OA patients [177]. The phase II trial is currently ongoing and requires further evaluation to mark FGF18 treatment as a novel DMOAD.

Treatment targeting catabolic signalling pathways might be beneficial in slowing down the rate of disease progression but would not be effective in reconstructing degenerated cartilaginous tissue. Typically, regeneration is demarked by chondrogenic differentiation of stem cells into mature chondrocytes which deposit ECM. Compared to other tissues like skin or liver, cartilage relatively possesses poor regenerative capacity [178]. This is compounded by factors such as poor integration of regenerated cartilage with existing cartilage and subchondral bone, reorganisation of regenerated cartilage into fibrocartilginous tissue and the degree of cartilage defect [179]. Despite this, recent studies have shown articular cartilage to possess some stem-like properties. For example, certain studies have shown that chondrocytes isolated from the superficial layer of bovine articular cartilage not only express mesenchymal stem cell markers but are also capable of acquiring a chondrogenic phenotype over a certain number of passages [180, 181]. TGF-β has been proposed as a playing a key role in the differentiation of progenitor stem cells into chondrocytes [182]. In in-vitro studies, TGF-β has not only enhanced the gene expression of *COL2A1* and aggrecan from chondrocytes isolated from the superficial layer, but it also expressed chondrogenic characteristics [182, 183]. However other in-vivo studies have shown that overactivation of TGF-β signalling resulted in abnormal chondrogenesis and excess matrix turnover [184]. The potential of regenerative agents in cartilage biology have been recently translated into patients via clinical trials. Kartogenin 34 (KA34) is a small bioactive molecule that promotes cartilage regeneration through stem cell differentiation. KA34 was utilised in a phase I clinical study in patients with knee OA; however, definite results have not yet been reported. Another class of drug, LNA043, directed as an agonist towards novel angiopoietin like protein 3 (ANGPTL3), has been introduced in patients with knee cartilage defects. ANGPTL3 itself is responsible for regulating lipid metabolism and angiogenesis. Two separate clinical trials have shown favourable safety profile and effective

drug delivery into cartilage in patients with knee OA [185]. Patients are currently being recruited in a phase II clinical study utilising LNA043.

Another emerging approach is the use of stem cells as a means of regenerative medicine in OA. At present, some evidence suggested beneficial effects of autologous mesenchymal stem cell and adipose-derived stem cell (ASC) transplantation as a therapeutic option for knee OA [186, 187]. However, the majority of trials are stagnant at phase I with issues arising around dosing and successful grafting.

Despite a growing abundance of knowledge into the molecular mechanisms of OA, it has proven challenging to find clinically successful DMOADs. The navigation towards this goal is ongoing, but recent advances in genetic and molecular biology are allowing research to better direct the path towards this overarching objective.

1.4 Molecular discovery in OA

Molecular analysis may identify pathways that modulate disease by enhancing or interfering with injury pathways. Two principal approaches are most commonly used to investigate molecular pathogenesis: RNA transcriptomic analysis, by microarray or RNA sequencing (RNA-seq), and genetic analysis by genome wide association studies (GWASs). These tools have the potential to identify candidate pathways orchestrating disease, as each are broad and agnostic in their approach i.e. do not bias analysis towards particular pathways. Instead, they offer the ability to identify novel pathways and test the strength of preidentified ones. RNA-seq is able to measure the expression of multiple coding and noncoding genes with a high signal-to-noise ratio and reliability. RNA-seq studies have been used to examine pathways active in disease by comparing more- and less-affected regions of articular cartilage taken at time of joint replacement. Recently RNA-seq studies have helped to identify *LINC00167* as a potential early biomarker for OA by exploration of RNA-seq in peripheral blood leukocytes from OA and control patients [188]. Another study used RNA-seq and employed an integrated approach to discover an OA miRNA interactome and related pathways [189]. RNA-seq has also been used to perform single-cell analysis from chondrocytes isolated by enzymatic digestion from OA cartilage [190]. Quanbo et al. used single-cell RNA-seq (scRNA-seq) to identify seven different subpopulations of chondrocytes in human OA cartilage, each defined by a different phenotype and function [191]. The group further delineated different gene expression profiles at different stages of OA using single-cell resolution [191]. Such results provide new insights about how to effectively manipulate human OA cartilage to modify disease progression.

Transcriptomic analysis is another method that is used in the hopeful discovery of potentially new modifiable pathways in OA progression. Whilst allowing molecular studies to be carried out without bias, transcriptomic analyses are limited by having to specify the tissue

for analysis and typically being restricted to tissue taken at the time of surgical joint replacement i.e. at end-stage disease where a normal comparator is often missing. Nonetheless, in 2018, transcriptomic analysis of chondrocytes in hip OA identified 888 upregulated and 732 downregulated genes in hip OA chondrocytes compared to non-OA chondrocytes [192]. Amongst these newly discovered, overexpressed genes were dermatopontin (*DPT*), insulin like growth factor binding protein 7 (*IGFBP7*) and kruppel like factor 2 (*KLF2*). Such work enables future groups to interrogate identified genes in the context of OA disease progression. For example, a subsequent functional study demonstrated that *KLF2* protected against OA by suppressing oxidative stress via the nuclear factor erythroid 2-related factor 2 (NRF2)/ antioxidant response element (ARE) signalling pathway [193]. A recent transcriptomic study in 2019 conducted by H. Li et al. unveiled another set of newly recognised genes, noncoding RNAs, which could be further interrogated as diagnostic biomarkers or therapeutic targets in OA [194]. The groups discovered a total of 739 mRNAs and 1152 noncoding RNAs to be differentially expressed in OA cartilage tissue. These included genes associated with ECM-receptor interaction, TGF-β signalling pathway, osteoclast differentiation and insulin-signalling pathway [194].

In the last decade, genome-wide association studies (GWAS) have provided researchers with molecular insights by identifying polymorphic variants in genes associated with disease risk. A GWAS study is typically reported by depicting blocks of correlated single nucleotide polymorphisms (SNPs) that show a statistically significant association with disease. The workflow of a GWAS involves data collection (DNA and phenotypic data from individuals), genotyping, data processing (involves the imputation of untyped variants using haplotype phasing and quality control), association testing (genetic association tests are run for each genetic variant), meta-analysis (results from smaller cohorts are combined), replication

(results are replicated in an independent cohort) and finally interpreting the results by conducting multiple post-GWAS analyses [195].

GWAS studies help to identify common and rare variants associated with a particular trait or disease. Identifying a variant as such is population-specific, with common variants being those with an allelic frequency above 10% in the population [195]. However, as the sample population size grows, this threshold can be as low as 1%. Therefore, GWAS studies require large population sizes (>10,000) to reduce bias and increase the reliability and reproducibility of genetic associations [195]. The output from a GWAS study consists of a list of p values, effect sizes and directionality (either positive or negative correlation) of all tested polymorphic variants with the trait of interest. Further analyses using post-hoc GWAS are then conducted to determine the most likely causal variants together with their functional consequence in convergence with biological pathways. GWAS studies help to therefore give us a mechanistic insight into the biological pathways responsible for a disease, further enabling us to focus research and future drug development.

Within the last decade, a multitude of GWAS studies have been conducted to identify a number of genetic variants associated with OA progression within individual populations that have exceeded genome-wide significance ($p<5\times10-8$); arcOGEN was the first GWAS in OA to identify candidate polymorphic variants that reached genome wide significance levels (p-value of <5×10^-8) [196]. In this study of 7410 individuals with severe hip or knee OA, 9 variants were identified that approached or reached genome-wide significance [196]. Subsequent GWASs in OA have increased in size, and this has increased the number of identified disease risk variants. In 2011, Valdes et al. discovered a variant in the growth/differentiation (GDF) 5 gene to reach genome-wide significance for knee OA [197], whilst in the same year, another group showed that a variant in MCF.2 Cell Line Derived Transforming Sequence-like protein (*MCF2L*) was associated with high risk of OA [198].

The same group demonstrated that MCF2L regulates NGF, and treatment against NGF with monoclonal antibodies reduced pain and improved function in patients with knee OA [199].

The GWAS of interest which built the foundation for my DPhil was conducted in 2014 within an Icelandic population [200]. This study identified polymorphic variants in the aldehyde dehydrogenase 1A2 (*ALDH1A2*) gene with high risk of hand OA and large joint OA [200].

1.4.1 Functional discovery of risk variants of ALDH1A2

The first GWAS study to identify *ALDH1A2* was performed in hand OA in the Icelandic population in 2014 [200]. Several allelic variants (in linkage disequilibrium) in *ALDH1A2* were found to be significantly associated with severe hand OA (odds ratio around 1.5 for each locus). The at-risk variants predicted low levels of *ALDH1A2* expression, and this was confirmed in functional studies which also showed that there was significant allelic imbalance in diseased tissues [200, 201]. The group further showed allelic imbalance of the risk variant in heterozygotes when studying expression levels in OA joint tissues, especially when articular cartilage was considered in isolation [201]. The overall expression of *ALDH1A2*, in both diseased and nondiseased samples, was highest in cartilage compared to synovium, bone and fatpad [201]. This study further went on to look at the effect of knockdown of *ALDH1A2* on gene expression in isolated primary human chondrocytes. The knockdown of *ALDH1A2* resulted in a significant reduction in the expression of several all-trans-retinoic acid (atRA)-responsive genes including retinoic acid receptor alpha (*RARA*), retinoic acid receptor beta (*RARB*), retinoic acid receptor gamma (*RARG*) and cytochrome P450 26B1 (*CYP26B1*) [201]. This implied that ALDH1A2 is a key functional regulator of atRA-metabolism in cartilage. Another study looking at the possible functional

consequences of ALDH1A2 noted that in human articular chondrocytes ALDH activity was strongly associated with the expression of chondrogenic markers: *COL2A1* and *SOX9* [202]. The isotypes *ALDH1A2* and *ALDH1A3* were most likely responsible for the overall ALDH activity – thereby suggesting *ALDH1A2* and *ALDH1A3* to be markers of active chondrocytes producing active collagen, alluding to a mechanism by which ALDH1A2 maybe protective in OA [202]. A different study conducted by Steinberg et al. investigated the differential expression of genes and molecular pathways in primary human chondrocytes isolated and characterised between osteophytic and low-grade inflammatory articular cartilage [203]. *ALDH1A2* expression was shown to be significantly reduced in osteophytic tissue compared to low-grade articular cartilage across all three omic levels including genome-wide DNA methylation, gene expression and protein levels [203]. This adds further compelling evidence of the association between severely affected osteoarthritic cartilage, albeit hip in this study, and the involvement of *ALDH1A2* in the pathogenesis of OA. *ALDH1A2* has also been implicated in knee OA [204, 205].

1.5 atRA

1.5.1 atRA biosynthetic pathway

All-trans-retinoic acid (atRA) is progressively derived in a stepwise manner from the lipid-soluble vitamin A or *all-trans-retinol* (atROL) (Figure 1.4). *Retinoids* is a hypernym that includes all structurally related compounds to vitamin A including those that show biological atROL activity. After ingestion, atROL is first hydrolysed in the intestinal mucosa before absorption via the small intestinal enterocyte in its fat soluble form [206]. In the plasma, atROL is bound to retinol binding protein 4 (holo-RBP 4) for transport and cellular uptake. atROL target cells express an RBP receptor encoded by the *STRA6* (stimulated by retinoic acid 6) gene. Cellular uptake of atROL from holo-RBP requires functional coupling between STRA6 and intracellular lecithin retinol acetyl transferase (LRTA) [206].

Vitamin A and its esters are converted to retinoic acid and related active compounds via a two-step oxidation process. The enzymes that catalyse the first, reversible oxidisation step of atROL to all-trans-retinal (atRAL) belong to one of two classes, the cytosolic alcohol dehydrogenase (ADHs) belonging to the medium chain dehydrogenases and the retinol dehydrogenases belonging to the microsomal short chain dehydrogenases (RDHs) [206].

Null mouse mutants for *ADH5* show early growth defects and reduced viability although these phenotypic changes are prevented when supplemented with dietary retinol [207]. Interestingly, when *ADH1* -/- mutants are treated with retinol they are more sensitive to embryological vitamin A toxicity [207]. This suggests that ADH1 may have a role in clearing excess retinoids rather than be involved in atRA synthesis.

The retinol dehydrogenases have well established roles in the visual cycle. *RDH5* -/- mice are embryologically viable but have a delay in dark photoadaptation, consistent with its role in regenerating 11 cis retinaldehyde after photo-bleaching [208].

RDH10 uses nicotinamide adenine dinucleotide (NAD+) or nicotinamide adenine dinucleotide phosphate (NADP+) as a cofactor to synthesise atRAL from atROL (Figure 1.4). Deletion of *RDH10* results in disruption of atRA synthesis and leads to the loss of atRA signalling in craniofacial tissues and trunk mesoderm [209]. The reduced levels of atRA ultimately causes embryological lethality because of orofacial, limb and organ deformities [209]. RDH12 uses a reduced form of nicotinamide adenine dinucleotide phosphate (NADPH) as a cofactor for the reduction of atRAL into atROL, thereby decreasing the synthesis of cellular atRA (Figure 1.4). Deletion of *RDH12* results in slowed kinetics of atRAL reduction and delayed dark adaption in retinal pigment epithelial cells [210]. A dynamic balance between RDH10 and RDH12 is essential to control cellular atRA levels within the nanomolar range.

The final step in atRA synthesis is the irreversible oxidation of atRAL to atRA (Figure 1.4). This is carried out by three retinaldehyde dehydrogenases (RALDHs): RALDH1, RALDH2 and RALDH3. Of the three, RALDH2 protein, encoded by the *ALDH1A2* gene, is the earliest to be expressed in development occurring in the primitive streak and mesodermal cells, later being found in the lateral mesoderm, posterior heart tube and rostral forebrain [211]. *ALDH1A2* -/- knockout mice die before mid-gestation from heart dysmorphogenesis [212]. In relation to cartilage, hypomorphic variants from the gene coding for this enzyme, *ALDH1A2*, was shown to be associated with severe hand OA; this was replicated consistently in other European cohorts [213].

Studies have shown that knockout of the *ALDH1A2* gene in mice during development resulted in chondrocytic dysmorphogensis [212, 214]. Mice null for *ALDH1A2* showed limb-bud patterning abnormalities with hypoplastic or absent forelimb buds. Many of these null mice died before mid-gestation [214]. Taking the above together with data from the GWAS study puts ALDH1A2 at the forefront as a key orchestrator in atRA signalling and in particular its potential role in the pathogenesis of OA. If we are able to better understand the molecular orchestration between ALDH1A2 and other metabolic components in the atRA pathway, we may be able to manipulate the progression of OA.

The other RALDHs, RALDH1 and RALDH3, are primarily required for eye and nasal morphogenesis during embryonic development [214]. They do not seem to have such an integral role in cartilage as RALDH2.

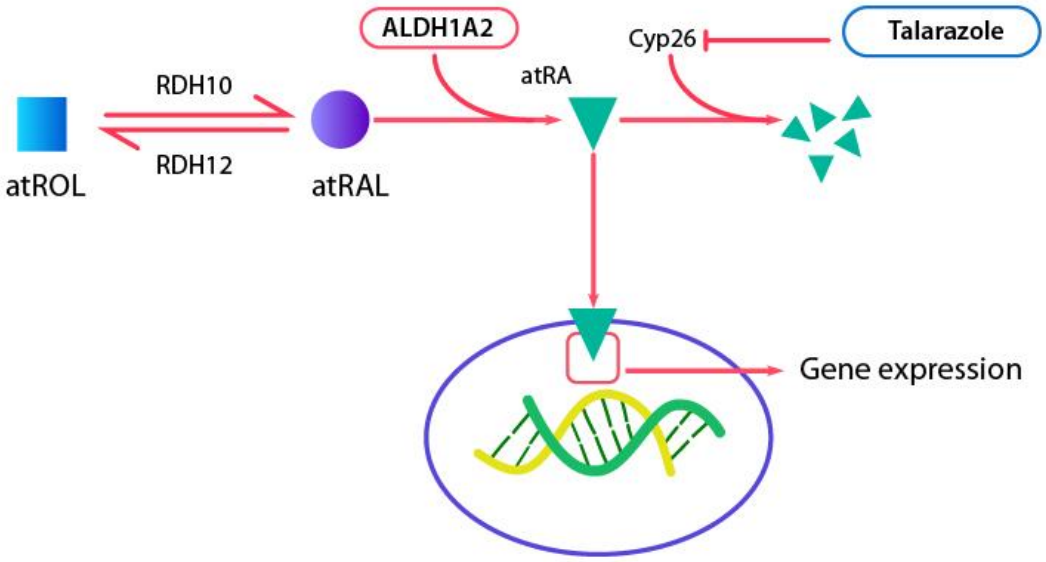

Figure 1.4: Schematic representation of the all-trans-retinoic acid (atRA) biosynthetic pathway.

All-trans-retinol (atROL) is oxidised by retinol dehydrogenase 10 (RDH 10) into all-trans-retinal (atRAL). Retinol dehydrogenase 12 (RDH12) catalyses the reverse reaction from atRAL to atROL. atRAL can be further oxidised irreversibly into all-trans retinoic acid (atRA) by aldehyde dehydrogenase 1 family, member A2 (ALDH1A2) enzyme. atRA translocated into the nucleus bound to cellular retinoic acid binding protein 2 (CRABP2). In the nucleus atRA binds onto the promoter regions of atRA-responsive genes to either activate or repress gene expression. atRA can also be metabolised into inactive polar metabolites by cytochrome P450 family 26 (CYP26) enzymes. Talarozole is a CYP26 enzyme inhibitor, which prevents the breakdown of atRA.

1.5.2 Transport of atRA within the cells

Cellular retinoic acid binding proteins (CRABPs) transport atRA within cells to either its nuclear receptors or to the degrading enzymes (Cyp26s). CRABPs bind atRA with high affinity and transport atRA intracellularly. The two cellular retinoic acid binding proteins, CRABP1 and CRABP2, are highly conserved and belong to a family of cytosolic lipid binding proteins [206]. CRABP1 protects cells from excess atRA by binding it within the cytosol and prevents transport to its nuclear receptors. Instead, CRABP1 is responsible for facilitating the degradation of atRA by Cyp26 enzymes [215]. On the other hand, CRABP2 is responsible for binding atRA and translocating it into the nucleus onto the heterodimeric

nuclear receptors Retinoic Acid Receptor (RAR) – Retinoid X Receptor (RXR), thereby increasing atRA-responsive gene regulation [215]. Despite this, adult mice with deletion in both *CRABP1* and *CRABP2* have supernumerary digits on the forelimb at low penetrance, but they are both viable [216]. This suggests that the function of CRABPs in atRA signalling is redundant, and other proteins can compensate for their roles.

Another binding protein, fatty acid binding protein 5 (FABP5), is responsible for binding atRA and transporting it to the nucleus to activate the nuclear receptor peroxisome proliferator-activated receptor beta/delta (PPAR β/δ) [217]. Collectively, CRABP2, CRABP2 and FABP5 shepherd the fine balance between cellular atRA signalling and degradation.

1.5.3 atRA nuclear signalling

Once delivered to the nucleus, atRA can bind to one its nuclear receptors to influence gene transcription. There are two families of nuclear receptor proteins actively involved in atRA mediated transcription: Retinoic Acid Receptor (RAR) and Retinoid X Receptor (RXR). Both of these receptor proteins are members of the nuclear transcription family of steroid/thyroid retinoid nuclear receptors [218]. RAR and RXR each have three identified isotypes, designated as alpha, beta and gamma subtypes. The gene sequence for each of the RAR isotypes differs significantly from each other, but the gene sequence for each isotype is highly conserved in both humans and mice, which raises the speculation that each RAR isotype has a specific function [218]. In addition to the three isotypes, each RAR and RXR domains exist as multiple isoforms. These result from the alternative splicing of a primary transcript or differential promoter usage [218]. Both RAR and RXR are not active in their monomeric forms. Instead, RAR forms a heterodimeric complex with RXR: (RAR:RXR).

The RAR:RXR receptor complex is the predominant protein complex for atRA signalling and is bound onto specific retinoic acid response element (RARE)-motifs on the promoter regions of target genes [218]. The RARE domain consists of a direct repeat of a hexameric sequence of 5′-(A/G)G(G/T)TCA-3′[219]. The RAR:RXR complex can bind onto the RARE domain, even in the absence of a ligand and maintain target gene repression, through recruiting co-repressor complexes [219] (Figure 1.5A). Therefore, in the absence of atRA, co-repressors of the nuclear receptor co-repressor (NCOR) family bind to RAR and recruit repressive factors such as polycomb repressive complex 2 (PRC2) and histone deacetylase (HDAC) preventing gene transcription [218]. Upon ligand atRA binding, the co-repressors are released and allow co-activators of the nuclear receptor co-activator (NCOA) family to bind to RAR and recruit activating factors such as Trithorax and histone acetylase (HAT) [218]. This results in chromatin remodelling and facilitates the assembly of the preinitiation transcription complex. RXR can not only form heterodimers with RAR, but it can also heterodimerise with another receptor protein called peroxisome proliferator activated receptor (PPAR) [220] (Figure 1.5B). The RXR-PPAR (β/δ) is bound onto the peroxisome proliferator activated receptor response element (PPRE) domain found on the promoter regions of target genes. Collectively, RARE and PPRE-target genes are either activated or repressed in the presence of ligand (Figure 1.5). RARE domains are better established in the literature and have been described as conserved sequences found in the promoter region of genes regulated directly by atRA [221, 222]. The list of genes that are atRA-responsive has become extensive in the last decade [223]. Many of the genes encoding the intermediate components and enzymes in the biosynthesis of atRA are themselves atRA-responsive including *RDH10*, *CYP26A1*, *CRABP1*, *CRABP2*, *RARA*, *RARB* and *RARG* [224-226]. Consequently, the mRNA fold change of these atRA-responsive genes are a surrogate

measure of the level of endogenous atRA in cells. Direct measurement of cellular atRA is possible but is extremely challenging because free atRA is highly unstable in light.

A few studies have also shown that the RAR nuclear receptor is also capable of forming a heterodimeric complex with the oestrogen receptor (ER). Ross-innes et al. showed on a genome-wide scale that RARA and ER can co-occupy regulatory regions together with chromatin [227]. Therefore, under the presence of oestrogen, there is induction of the RARA-ER complex. These findings, together with other supporting studies [228, 229], demonstrated RARA to be an essential component of the ER complex. Perhaps this is particularly important in the context of hand OA, which is extremely prevalent around the perimenopausal age when there are fluctuations in the follicle stimulating hormone (FSH): luteinising hormone (LH) levels and reduced circulating oestrogen [230]. Oestrogen itself is synthesised by the enzyme aromatase, or CYP19A, from testosterone. Interestingly, *CYP19A* is an established atRA-responsive gene [231].

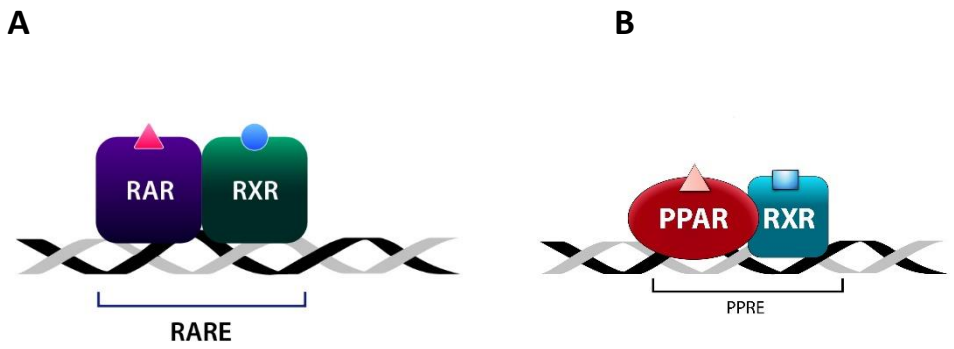

Figure 1.5: Schematic representation of all-trans-retinoic acid (atRA) nuclear signalling.

All-trans-retinoic acid (atRA) binds onto Cellular Retinoic Acid Binding Protein 2 (CRABP2) which delivers atRA into the nucleus to bind onto the heterodimers of Retinoic acid Receptors (RAR) or Retinoic X Receptors (RXR). The heterodimeric RAR-RXR complex binds onto specific Retinoic Acid Response Elements (RAREs) present on the promoter regions of at-RA responsive genes (A). Alternatively, fatty acid binding protein 5 (FABP5) delivers atRA into the nucleus to binds onto the RXR-PPAR heterodimeric complex present on peroxisome proliferator response elements (PPREs) (B). atRA can either activate or repress target genes that contain RAREs or PPREs.

1.5.4 atRA degradation

The cytochrome P450 enzymes, namely CYP26, is known to be involved in the biodegradation of atRA into inactive polar metabolites [232-235] (Figure 1.4). CYP26 is an atRA-hydroxylase that is inducible by atRA-responsive gene regulation [235]. Three isomers have been identified in humans: CYP26A1 [233, 234, 236], CYP26B1 [237] and CYP26C1 [238]. Published data suggest CYP26B1 is more ubiquitously expressed in humans than CYP26A1 and CYP26C1 [239], with the latter predominantly expressed in the liver [240, 241]. Functionally, CYP26A1 is proposed to be the most important enzyme in the clearance of atRA in humans [239, 240]. In terms of substrate specificity, atRA is the primary substrate metabolised by CYP26A1 and CYP26B1 [239] although at microM concentrations, 9-cis-RA and 13-cis-RA are also substrates of CYP26s [242]. The primary metabolite formed by the degradation of atRA by CYP26A1 and CYP26B1 is 4-oxo-RA [241]. The CYP enzymes can be targeted pharmacologically to boost intracellular atRA levels.

1.5.5 atRA in skeletal development

atRA has been implicated in a wide range of morphogenic functions during development [243-245] and has a critical role in skeletal development [245-247]. Temporospatial patterning of atRA controls the ability to form a forelimb bud as well as controlling the proximal-distal patterning of the forelimb [248-252]. Gene deletion of *ALDH1A2* in mice causes a failure to initiate forelimb sprouting [248, 253, 254], and *RDH10*$^{-/-}$ mice exhibit decreased cartilage condensations and near-complete agenesis of the ulnar and radius [209, 255]. They also have interdigital webbing. Seminal studies have demonstrated that compound mutant embryos not only showed severe defects in the developing skeleton but

also resulted in developmental failure in multiple organs. Lohnes et al. showed that *RARA*/*RARG*-null mouse embryos had severe defects in craniofacial and axial skeletal development [245]. Other significant malformations included sternal defects and rib fusion. Moreover, the authors identified homeotic transformation of vertebrae, which was determined to be under the control of *HOX* genes, which were themselves direct atRA-responsive genes [245]. Subsequent studies discovered variable endogenous atRA concentrations along the dorsal embryonic trunk [256, 257]. Higher concentrations were noted in the mid-region and lower levels in the cranial and caudal regions [257]. This two-tailed concentration gradient of atRA was tightly regulated by variable levels of CYP26A1 enzymes responsible for the degradation of atRA.

The same authors also noted that *RARA*/*RARG*-null mouse embryos depicted severe defects in forelimb development and more so than hindlimb [211]. These defects included, digit fusion, polydactyly, reduction in limb length and decreased ossification in the radius [211]. Zhao et al. later demonstrated that these complex forelimb changes might be due to reduced ALDH1A2 enzyme synthesised in the digit mesenchyme, shown by using RARE-LacZ reporter mice [258].

Another study investigated compound mutations in *RARB*/*RARG*. Here, the authors demonstrated that mice showed growth retardation by three weeks postnatal [246]. Moreover, the growth plates had significantly lower amounts of aggrecan. Further examination of the growth plates showed that they had significantly lower amounts endogeneous atRA [259]. Collectively, these studies demonstrated that absence of *RAR* genes and altered atRA signalling resulted in deranged skeletal growth and digit fusion.

atRA has also been reported to have a role in early embryo chondrogenesis. It was demonstrated in RARE-LacA-reported mice that atRA signalling was undetectable within

limb mesenchymal condensations undergoing chondrogenesis but was strongly expressed in nonchondrogenic regions [260]. This suggested that the initiation of chondrogenesis required a steep drop in atRA concentrations. This idea is further supported by the fact that atRA appeared to be present in the form of an anterior–posterior concentration gradient in the developing limb buds [261].

1.5.6 atRA in postnatal tissue

atRA has been used as a catabolic agent in vitro [262-265]. This degradative effect, much like that induced by IL1, is reported to be mediated through specific proteinases such as MMP13 [266, 267] and the aggrecanases, ADAMTS4 and ADAMTS5 [268-270]. In bovine-isolated chondrocytes, atRA shifts chondrocytes towards a hypertrophic phenotype associated with proteoglycan loss [266, 271]. The concentration of atRA used in these studies is at supra-physiological concentrations (micromolar range), which is orders of magnitude higher than endogenous serum or cellular levels (3–13 nM in human plasma [272]). The catabolic actions described in vitro are at odds with the described anti-inflammatory role of atRA and probably do not reflect the endogenous biological role of atRA within cartilage. Zeng et al. was one of the first studies to allude to an anti-inflammatory role for atRA in cartilage [273]. The authors demonstrated that in a collagen-induced arthritis model, atRA inhibited the secretion of pro-inflammatory mediators. TNFα, IL17α and IL10 and thereby inhibited the inflammatory response and progression of arthritis in collagen-induced arthritis (CIA) rats. The authors concluded that the anti-inflammatory mechanism of atRA might be secondary to the correction of Th1/Th2 and Th17/Treg imbalances [273]. A number of other studies have reported the anti-inflammatory actions of atRA in renal tubular cells, alveolar epithelium and in rheumatoid arthritis [274, 275].

1.6 ROS

Reactive oxygen species (ROS) are oxygen-containing free radical species. The sequential reduction of oxygen with concomitant addition of electrons results in the formation of ROS which includes hydroxyl radical, hydrogen peroxide, superoxide anion, nitric oxide and hypochlorite anion [276]. The presence of unpaired electrons on ROS makes them highly reactive, unstable, electrophilic species capable of damaging cellular protein and nuclear material. There are three main sites through which ROS is produced including the mitochondria, nonmitochondrial membrane-bound nicotinamide adenine dinucleotide phosphate (NADPH) oxidase (NOX) and xanthine oxidase (XO) [276]. Under physiological states, cellular ROS levels are maintained in a stable yet dynamic equilibrium between factors that produce and eliminate ROS [276].

1.6.1 Sites of ROS production

1.6.1.1 Mitochondrial ROS

Jensen in 1961 was the first to describe the generation of ROS from the mitochondria [277]. This was drawn based on observations that a fraction of the oxygen consumption by the mitochondria was converted to hydrogen peroxide (H_2O_2) by (inner mitochondrial membrane complexes catalysing NADH). It is now well established that mitochondrial ROS production takes place at the inner mitochondrial membrane during oxidative phosphorylation [277]. Complex I (also known as NADH-ubiquinone oxidoreductase) is the main contributor of ROS in the mitochondria. In fact, 40% of all mitochondrial disorders are associated with mutations in complex I subunits [277]. Complex I produces dominantly the superoxide anion through two main mechanisms. One is determined by a high NADH/NAD+ ratio resulting in reduced flavin mononucleotide (FMN) sites on complex I.

FMN is a small molecule bound onto mitochondrial complex I, responsible for oxidising NADH and generating electrons to be reduced by ubiquinone. The second mechanism by which complex I produces superoxide anion is by donating electrons to a Coenzyme Q (CoQ10) pool that is coupled with a high protonmotive force. Although the CoQ10 pool is a protective pool in the mitochondria acting as a neutralising repository to hold electrons, when this becomes saturated and the flow of electrons through the mitochondrial complexes is high, a combination of these two events results in a high amount of reverse electron transfer and the generation of superoxide anion [277].

1.6.1.2 NADPH Oxidase

NADPH oxidases (NOXs) are integral membrane-bound complexes that produce ROS. NOXs have been reported to produce either superoxide anions or hydrogen peroxide in a NADPH-dependent manner [278]. There are seven members that contribute towards the NOX family, all of which have a similar catalytic core but different regulatory domains. The different enzyme isoforms are not ubiquitous but are instead expressed differentially between tissues. The catalytic core of NOXs composed of a dehydrogenase and transmembrane domain. Electrons are sequentially transferred from the noncovalently bound flavin adenine dinucleotide (FAD) (harboured in the dehydrogenase domain) to the heme groups in the transmembrane domain and finally to the oxygen located on the outer membrane to produce superoxide or hydrogen peroxide [278]. The ROS produced from NOXs have established role in host defences (respiratory burst response) but also have the potential to exert a pathological effect when dysregulated. High NOX-dependent ROS production has been associated with hyper-proliferation, DNA damage and cell death [278].

1.6.2 Antioxidant systems in cells

Antioxidants are responsible for neutralising free radical species. Endogenous antioxidants can be broadly categorised into either enzymatic or nonenzymatic antioxidants. Enzymatic antioxidants include superoxide dismutase (SOD), catalase (CAT), glutathione peroxidase (GPx) and thioredoxin (Trx) system [279]. SOD catalyse superoxide into oxygen and hydrogen peroxide whereas CAT is responsible for further catalysing the hydrogen peroxide into molecular oxygen and water. GPx belong to a family of three evolutionary groups and use GSH as a reductant to reduce hydrogen peroxide into water. The thioredoxin system is composed of NADPH, thioredoxin reductase (TrxR) and thioredoxin (Trx). Trx and TrxR form a dimer which harbours an FAD-containing enzyme that catalyses the NADPH reduction of the oxidised catalytic site in Trx to a reduced form [279].

Nonenzymatic antioxidants include vitamin A (retinol), vitamin C, vitamin E and coenzyme Q10 (CoQ10). Vitamin A and carotenoids are capable of quenching singlet oxygen, neutralising thiyl radicals and stabilising peroxyl radicals. Vitamin C has a broader range of effects and can also scavenge superoxide radicals and hydroxyl radicals. The antioxidant effects of vitamin E is mediated through preventing a process known as lipid peroxidation, a process by which free radicals attack phospholipids containing carbon–carbon double bonds [279]. CoQ10 is a critical lipid-soluble component of the inner mitochondrial membrane responsible for the transport of electrons from complexes I and II to complex III, resulting in the eventual production of adenosine triphosphate (ATP). In its reduced form, CoQ10 serves as a lipid-soluble antioxidant protecting cellular and mitochondrial membranes from oxidation [280]. The protective action of CoQ10 as an electron transporter relies upon the availability of NADPH oxidoreductases reducing oxidised CoQ10 back to its reduced form [280].

The best established and well-known commercial antioxidant is N-acetyl cysteine (NAC). NAC is reported to exert its antioxidant effects through one of three mechanisms. First is through a direct antioxidant effect by scavenging certain oxidant species. Secondly, NAC acts as the precursor for cysteine which is the rate-limiting amino acid for the synthesis of glutathione (GSH). GSH is a powerful antioxidant whilst also acting as a reducing substrate for various antioxidant enzymes. Lastly, NAC is capable of breaking the disulphide bridges on high molecular weight glycoproteins to restore the thiol pool and, by doing so, regulates the cellular redox state [281]. In clinical therapy, NAC is used in patients for acetaminophen poisoning by replenishing hepatic glutathione (GSH) which in turn neutralises harmful and electrophilic molecules (such as acetaminophen) [282].

1.6.3 ROS signalling and function

Under physiological conditions, ROS are produced in majority of cell types to act as important cellular messengers in signal transduction pathways regulating a host of functions including adaptations to hypoxia, immunity, differentiation and autophagy [276]. For example, amongst immune cells, autophagy is characterised by a process known as the 'respiratory burst'. In this process, ROS production is stimulated by phagocytes, catalysed by NADPH oxidase, and serves to provide protection against invading pathogens [276]. ROS is thought to exert its biological functions via one of three different methods: interaction with transition metal elements, binding to reactive cysteine thiols and thereby regulating intracellular signalling pathways and finally through the formation of lipid peroxidation products [276].

Many enzymes that are regulated by ROS contain iron (Fe), copper (Cu) or zinc (Zn). For example, NO activated both heme-containing cyclic guanylate cyclase and copper-

containing cytochrome p450 enzymes [283]. Both these events induce either an intracellular signalling cascade (through cGMP as a second messenger) or result in the reduction of the electron transport chain [283].

Through binding to reactive cysteine thiols, ROS can form S-nitrosothiols. The latter is an important physiological (and pathological) regulator of signalling pathways and transcription factors including NF-κB, JNK, AP-1 and p21 kinase. Under physiological conditions, s-nitrosothiols provide protections against exaggerated oxidative stress [284].

ROS can also exert a biological function by modifying target phospholipids, in a process known as lipid peroxidation [276].

1.6.4 ROS production in chondrocytes

Levels of lipid peroxidation product and nitrated products are higher in the cartilage and synovial fluid of patients with OA [285]. Conversely, antioxidative capabilities in OA cartilage is much reduced, with a number of studies having shown reduced levels of key antioxidant function including; SOD, CAT and GPx in diseased cartilage [286-288]. There are three principal sources of ROS in chondrocytes: NADPH oxidase, nitric oxide synthase and the mitochondria. The majority of ROS production in chondrocytes is derived from NADPH oxidase [288]. Studies have shown an imbalance in the redox state of cartilage from patients with OA. It has been shown that porcine articular chondrocytes are capable of producing superoxide ROS via the NADPH oxidase complex [288]. Moreover, several studies have associated increased NADPH oxidase activity as the driver for ROS production and consequent cartilage degradation in OA [288].

Nitric oxide synthase (NOS) is another major contributor of ROS in articular chondrocytes. Chondrocytes in the superficial zone overproduce inducible NOS (iNOS), which has also been shown to be mostly produced in human OA chondrocytes [289]. Studies have demonstrated that selective inhibition of iNOS halts the progression of experimental OA [289].

The mitochondrion is another key source of ROS in OA chondrocytes. Mitochondrial dysregulation has been shown to impair the respiratory chain complexes and result in electron transfer chain regulation [290]. Cillero et al. demonstrated such an impairment in mitochondrial metabolism is associated with increased *COX2* expression and PGE_2 synthesis inducing MMPs and decreasing ATP production [291]. Another study demonstrated that the depletion of SOD2, the major antioxidant in mitochondria, occurs in early cartilage degradation and further perpetuates the production of ROS in OA [292]. Moreover, hypercholesterolemia animal models have been associated with increased mitochondrial-derived oxidative stress leading to cartilage degeneration and chondrocyte hypertrophy [293]. This underpins the importance of dietary components in the regulation of mitochondrial metabolism and the pathology of OA.

1.6.5 ROS function in articular cartilage

ROS have been implicated in disturbing the structural integrity of the ECM. Endogenously produced superoxide anion inhibited the production of proteoglycan in human articular chondrocytes [285]. It has been reported that hydrogen peroxide inhibits matrix synthesis through dysregulation of mitochondrial metabolism and reduced production of ATP [292]. Moreover, nitric oxide free radical is demonstrated to be involved in the IL1-dependent inhibition of COL2 synthesis [294]. COL2 synthesis was suppressed by NO- at a post-

translation level by inhibiting prolyl hydroxylase, an enzyme involved the post translational processing of COL2 [294].

ROS has also been implicated in the activation of intracellular signalling cascades; *INOS* has been demonstrated to be activated by NF-κB and MAPK signalling in various studies [295]. J. Martel-Pelletier et al. showed that the IL17 stimulated *INOS* gene expression and subsequent NO production via MAPK, p38 and NF-κB signalling pathways [296]. Furthermore, in bovine articular chondrocytes, the superoxide free radical mediated the IL1-dependent activation of NF-κB signalling [288]. Dysregulation of NF-κB signalling secondary to changes in the redox milieu of the chondrocytes led to induction of *INOS* and *COX2* gene expression [288]. Other studies have demonstrated that increased ROS inhibit the PI3 kinase (PI3K)/ serine/threonine kinase 1 (Akt) pathway whilst activating the MAPK pathway driving the inflammation and disease in OA models [288]. Y.Y. Lo et al. further showed that ROS acts as an intermediate signalling molecule in the activation of JNK by IL1 and TNFα [297]. ROS is also induced by growth factors in the PCM. Basic FGF (bFGF) induced ROS production in bovine chondrocytes via the activation of NADPH oxidase resulting in increased expression of c-fos [298].

1.6.6 Mechanical stress and ROS

ROS have been shown to be sensitive to mechanical stress in various cells including cardio myocytes and endothelial cells [299]. Wolff et al. first demonstrated that similarly mechanical loading resulted in ATP stimulation through the release of mitochondrial ROS in bovine osteochondral explants [300]. The use of an electron transport inhibitor, rotenone, significantly suppressed mechanically induced ROS production [300].

Further studies have shown that application of mechanical force to articular cartilage stimulates the production of ROS, including superoxide, nitric oxide, hydrogen peroxide and peroxynitrite [285]. Mechanically induced ROS production was shown to cause chondrocyte death, increased inflammatory gene expression and changes in the structural integrity of the ECM network [285].

1.6.7 Role of endogenous antioxidants in OA

The natural antioxidant system in chondrocytes is disturbed in patients with OA [288]. SOD2 is the main antioxidant defence system in cartilage, and this is significantly reduced in patients with OA [288]. One particular study showed that the presence of NO competes with SOD for O2- resulting in the formation of ONOO- in osteoarthritic cartilage and thereby dysregulating the redox state [301]. It has been further shown from in-vivo work that the dysregulation of SOD occurs prior to the development of OA lesions, suggesting the imbalance in the antioxidant capability of the cartilage to be an early indicator in the development of OA [288].

Recently, studies have demonstrated dysregulation in the peroxiredoxin (PRDX) system in OA. Loss-of-function studies showed that either suppression or knockdown of *PRDX5* gene resulted in an increase in ROS in OA chondrocytes and subsequent chondrocyte apoptosis [302].

Lastly, nuclear factor erythroid factor 2-related factor 2 (NRF2), a transcription factor which regulates antioxidant enzyme, is chondro-protective in the progression of OA. Knockout of *NRF2* gene resulted in the upregulation of MMP and severe damage to articular cartilage. NRF2 is proposed to exert its antioxidant effects by influencing antioxidant response

elements in its target genes such as haemeoxygenase 1 and NADPH quinine oxidoreductase 1 [303].

1.7 Lipid peroxidation

As discussed above, lipids within the cell can undergo nonenzymatic oxidation by ROS in a process known as lipid peroxidation. In this process, free radicals oxidise an unsaturated lipid chain to form a hyperoxidised lipid (lipid peroxidation product) and a hydroxyl radical [288]. One of the most potent lipid peroxidation products is 4-hydroxynoneal (4-HNE) derived from ω−6 polyunsaturated fatty acids (PUFAs) such as linoleic acid and arachidonic acid (Figure 1.6). At supraphysiological levels, 4-HNE has been reported to act as a potent second messenger regulating a number of intracellular signalling pathways to influence chondrocyte apoptosis, inflammation and modify functional proteins [288]. Below, I focused on the mechanism by which 4-HNE is produced from the lipid bilayer secondary to the action of PLA2 enzymes.

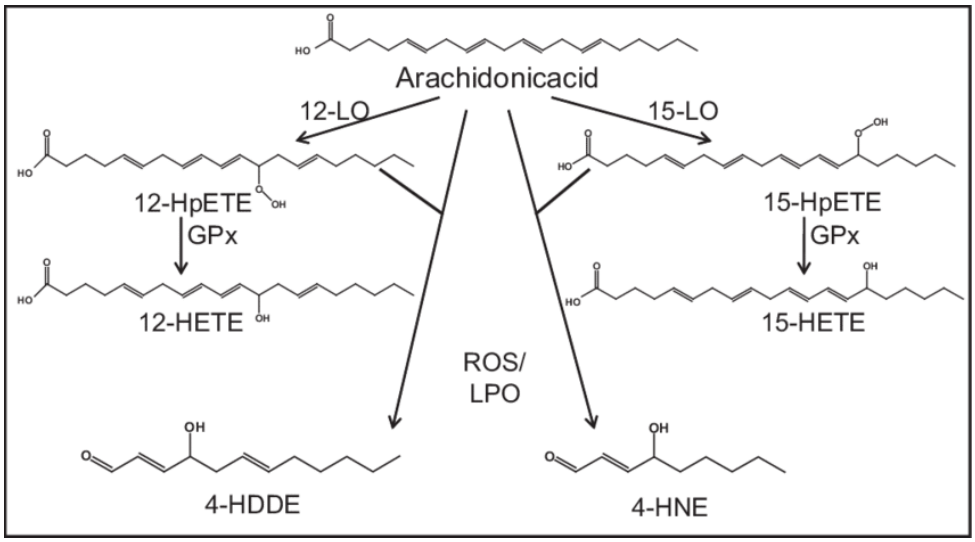

Figure 1.6: Schematic representation of the generation of 4-hydroxynoneal (4-HNE) from arachidonic acid.

Phospholipase A2 (PLA2) enzymes metabolise polyunsaturated fats in the lipid membrane to generate arachidonic acid. Arachidonic acid is further metabolised by 12-lipoxygenase (12-LO) and 15-lipoxygense (15-LO) into 12- hydroperoxyeicosatetraenoic acid (HpETE) and 15-HpETE, respectively. Reactive oxygen species (ROS) induced inactivation of reduced glutathione (GPx) diverts 15-HpETE to the peroxidation pathway (LPO) to generate 4-hydroxynoneal (4-HNE). Adapted from Anne Negre-Salvayre et al. (2010).

1.7.1 PLA2 enzymes

4-HNE is produced downstream of arachidonic acid, a PUFA that is released from the lipid bilayer membrane by the action of phospholipase A2. The PLA2 family of enzyme can be classified into three main categories: cytosolic PLA2 (cPLA2), secreted PLA2 (sPLA2) and Ca2+-independent PLA2 (iPLA2) [304].

cPLA2 is a calcium-dependent enzyme that metabolises PUFAs in the lipid bilayer. The C2 domain of cPLA2 binds the enzyme by hydrophobic intracellular portion of the lipid bilayer. sPLA2 is secreted extracellularly whilst iPLA2 is involved in stimulus-induced arachidonic acid within the cell but its presence and action is highly dependent on the cell type and stimulus [304]. Of all the isoforms, cPLA2 is the one that is most ubiquitously expressed in human and mice tissue but also highly conserved across species (95% amino acid homology) [304]. cPLA2 is regulated at both translational and post-translational levels. Although it is expressed at basal levels in most cells, it has been demonstrated to be induced by various intracellular signalling pathways involving TAK1, Ras and MAPKs [305, 306]. The catalytic activity of cPLA2 is enhanced by phosphorylation of serine 505 whereas phosphorylation at serine 727 blocks the binding of cPLA2 to an inhibitory complex in the cytoplasm which consists of p11/annexin A2 [307]. Other studies have also shown that cPLA2 expression is induced by transcriptional factors including NF-κB, hypoxia-inducible factor and c-Jun [308, 309]. The ability of cPLA2 to release arachidonic acid is Ca2+-dependent and requires the phosphorylation of the catalytic residues and interaction of these with polyphosphoinositides in the membrane. cPLA2 has fundamental roles in normal physiological processes including lipid homeostasis, gastrointestinal and renal function [307]. Similarly, cPLA2 has been implicated in disease processes such as post ischaemic brain injury, spinal cord damage and also various lung diseases including fibrotic lung disease and cancer [310].

1.7.2 Metabolism of arachidonic acid

cPLA2 activation by transient elevations of intracellular Ca2+, phosphorylation of serine 505 within the catalytic domain results in the hydrolysis of the sn-2 position of PUFAs in the cellular membrane and the release of AA [307]. AA is then further metabolised by COXs, lipoxygenases (LOXs) and CYP enzymes to a spectrum of lipid mediators that includes prostanoids, leukotrienes, epoxyeicosatrienoic acids and lipoxins.

COXs were the first enzymes to have been discovered that metabolise arachidonic acid. COX are known to generate prostanoids such as prostaglandins (PGs) and thromboxane A2 (TXA2) [311]. There are two distinct isoforms of COXs; COX1 and COX2, each of which is expressed ubiquitously across most cells although COX2 is known to have a more prominent role in inflammation, including OA [312]. NSAIDs such as aspirin and ibuprofen are inhibitors of COX enzymes.

The second metabolising pathway is the cytochrome p450 pathway. Although there are numerous subclasses of CYP enzymes, the most important in the context of AA metabolism are omega hydroxylase and epoxygenase [311]. Omega hydroxylase converts AA into hydroxyeicosatetraenoic acids (HETES) whereas epoxygenase activity generates epoxides and epoxyeicosatrienoic acids (EETs). The latter function as mainly autocrine and paracrine effectors in the cardiovascular system and kidney [311]. EETs can be further metabolised by epoxide hydroxylase into dihydroxyeicosatrienoic acids (DHET).

Lastly, the LOX pathway generates leukotrienes. 5-LOX metabolises AA into 5-hydroperoxyeicosatetraenoic acid (HpETE) which is further metabolised into leukotriene A4 (LTA4). Depending on the cellular milieu, LTA4 can be further metabolised into LTB4 or LTC4. LTC4 is further metabolised into LTD4 or LTE4. Leukotrienes are particularly important in the pathology of allergic diseases mediating inflammation [313]. Arachidonate

5-LOX and leukotriene receptor antagonists have been developed for the treatment of asthma and seasonal allergies [314], while 12 and 15-LOX enzymes are responsible for metabolising arachidonic acid into 12-HpETE and 15-HpETE, respectively. Under reduced cellular milieu, glutathione peroxidase (GPx) is responsible for the reduction of 12 and 15-HpETE into 12 and 15-hydroxyeicosatetraenoic acid (HETE). However, under states of oxidative stress with reduced pools of NADPH, GPx remains in an oxidised state. This diverts 12- and 15-HpETE to the peroxidation pathway leading to the formation of 4-hydoxdodecadineal (4-HDDE) and 4-hydroxynoneal (4-HNE) [288].

1.7.3 Effect of 4-HNE on cartilage

Incubation of cartilage explants with 4-HNE has been reported to increase the amount of cleaved COL2 fragments in a dose-dependent manner [315]. Moreover, the inhibition of COL2 expression by 4-HNE was shown to be secondary to the activation of specific transcription factors such as specificity protein (Sp) transcription factor [315]. The concentration of 4-HNE in the cartilage seems to be an important factor in determining its underlying role. Another study reported an increase in the gene expression of *MMP13* in 4-HNE treated human OA chondrocytes [316]. Supporting studies have reported the 4-HNE mediated upregulation of *MMP13* gene to be mediated through p38 MAPK and ERK1/2 phosphorylation [130, 317]. Additionally, this increase in *MMP13* was associated with an inhibition of TIMP1 production [318]. Inflammatory genes, including *COX2* and *INOS*, have also been shown to be induced in chondrocytes by 4-HNE [319].

4-HNE is also capable of regulating cell proliferation and apoptosis in human OA chondrocytes [320]. At high concentrations, 4-HNE significantly increased cell death and chromatin condensation [320]. Further interrogation into apoptotic signalling pathways

revealed that 4-HNE suppressed Akt activity [321]. Supportive studies demonstrated that 4-HNE caused activation of various other pro-apoptotic factors and these effects were reversed by the action of antioxidants, such as NAC [322]. El-Bikai et al. reported a different mechanism of 4-HNE-induced cell apoptosis where the authors reported 4-HNE bound onto COL2 and modulated the adhesion molecules intercellular adhesion molecule (ICAM)-1 and a1b1 integrins [323]. The reduction in the adhesion molecules was associated with increased caspase 3 activation and cell death [323].

1.7.4 4-HNE modulation of atRA metabolism

There is some evidence in the literature for the interaction between atRA metabolism and lipid peroxidation products. In particular, Kedishvilli et al. demonstrated that RDH12, the enzyme responsible for the synthesis of atRAL from atROL, was inhibited by nonanal at high concentrations in retinal pigment epithelial cells (a lipid peroxidation product) [324]. However, 4-HNE did not inhibit the RDH12 retinaldehyde reductase activity. Instead, the authors demonstrated that 4-HNE inhibited the activities of lecithin:retinol acyl transferase and aldehyde dehydrogenase which resulted in decreased levels of retinyl esters and atRA levels within RPE cells [324]. In other studies, it also been reported that ALDH enzymes provide protection against lipid peroxidation and thereby regulate the redox state of the cell [325]. Many lipid products serve as substrates to ALDH enzymes. One particular study showed that in states of increased lipid peroxidation, ALDH enzymes become saturated and can be diverted away from atRA synthesis [326].

1.8 Historical work that led up to my DPhil

Dr Linyi Zhu, a postdoctoral scientist at the Vincent Lab, was integral in conducting the historical work that led up to my project. First, Zhu demonstrated that atRA-responsive genes were highly mechanosensitive. She showed that cartilage injury in the porcine model rapidly downregulated atRA-responsive genes by four hours post injury (Fig 1.7B). This was paralleled by an increase in inflammatory gene regulation (Fig 1.7C) (mechanoflammation). The preinjection of the trotter joints with a CYP26 inhibitor, talarozole (TLZ), prior to injury, prevented the downregulation of atRA-responsive genes. Moreover, the downregulation of atRA-responsive genes on cartilage injury was also TAK1-sensitive (Fig. 1.8). Importantly, TLZ suppressed the upregulation of key inflammatory genes on injury (Fig 1.7C).

Zhu therefore identified atRA to be a key anti-inflammatory agent in the joint with the potential to suppress mechanoflammation. Therefore, if we are able to identify the mechanisms by which atRA fell on cartilage injury and how it suppressed inflammatory gene regulation, then we would be able to identify further pharmacological targets with which mechanoflammation might be prevented. Such methods would have the potential to translate in the future into new therapeutic interventions in the treatment of OA.

Therefore, following this work, the aims of my DPhil were twofold:

1. To determine the mechanism by which atRA-responsive genes were downregulated on cartilage injury.
2. To determine the mechanism by which atRA suppressed the upregulation of inflammatory genes on cartilage injury.

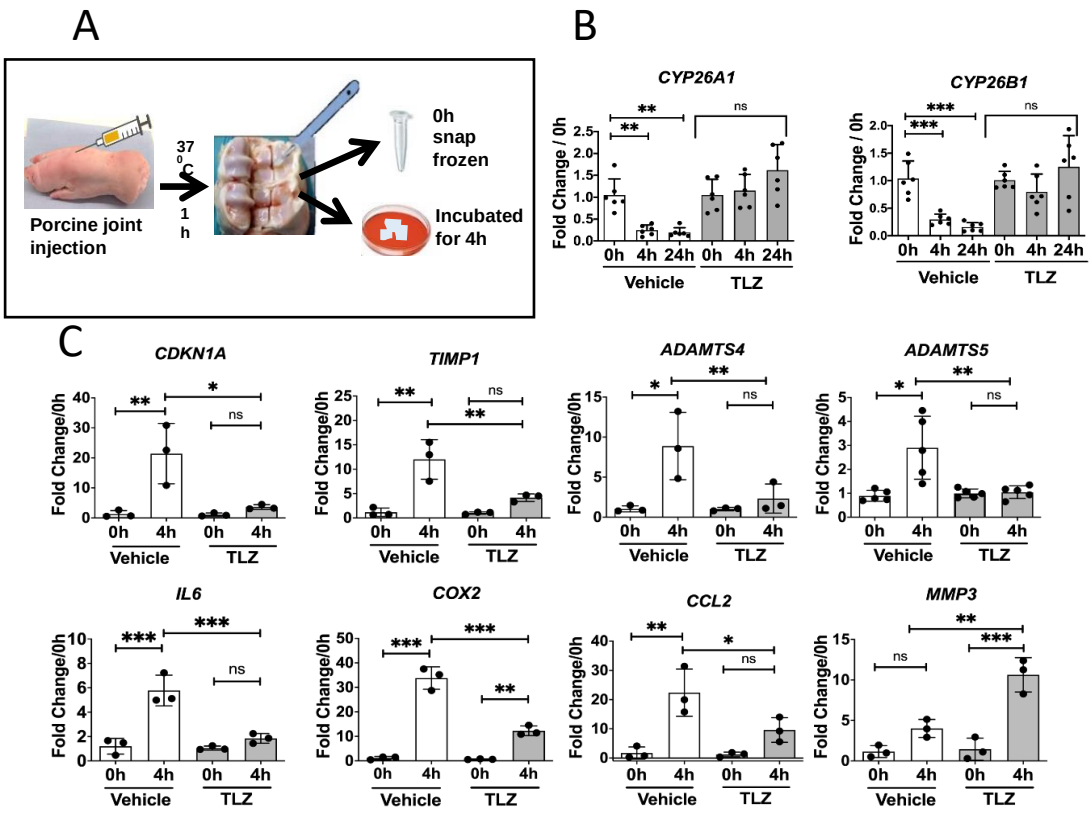

Figure 1.7: Talarozole prevents the drop of atRA-responsive genes after injury and suppresses injury-induced inflammatory genes. (Figure from Dr. Linyi Zhu).

(A) Schematic showing the protocol for porcine MCP joint inhibitor injection. Porcine MCP joints were injected with 5 µM talarozole (TLZ) or vehicle. After 1h at 37 °C, cartilage was explanted and either snap frozen (0h) or cultured in the presence of inhibitor or vehicle for 4h. Total RNA was extracted and gene expression levels for atRA-responsive genes (B) and inflammatory genes (C), measured by quantitative PCR. n = 3-6 (as shown) for each group. Statistical analysis was performed using one-way ANOVA with Tukey's post hoc analysis. Bars represent the mean ± SEM, ns = not significant, *p < 0.05, **p < 0.01, and ***p < 0.001.

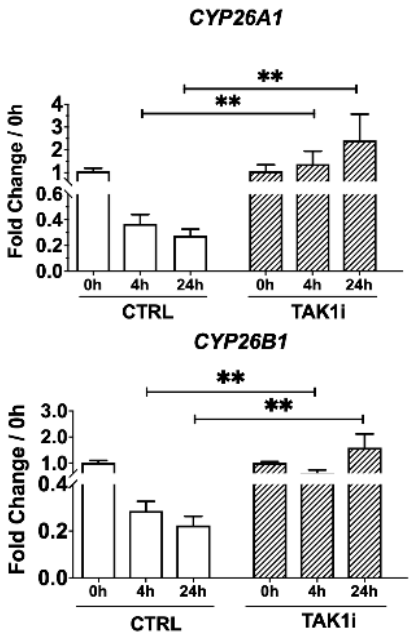

Figure 1. 8: TAK1 inhibition prevents the downregulation of atRA-responsive genes. (Figure from Dr. Linyi Zhu).

Trotter MCP joints were pre-injected with 5 µM TAK1 inhibitor prior to cartilage explantation. Cartilage explants were either snap frozen or incubated for 4 hours in serum free DMEM containing either TAK1 inhibitor (TAK1i) or vehicle. RNA was extracted, converted to cDNA and RT-PCR was performed to measure expression for CYP26A1 and CYP26B1 genes (data from Linyi Zhu). Bars show the mean ± SEM of 3 independent experiments. $*$ = $P < 0.05$; $**$ = $P < 0.01$, ns= not significant.

2 CHAPTER 2: MATERIALS AND METHODS

2.1 Cell Culture

Porcine metacarpophalangeal (MCP) joints were decontaminated in 2% Virkon for 20 mins before being equilibrated at 37°C, 5% CO_2 for 1 hour. The MCP joints were opened and cartilage explanted and further cut into smaller pieces. Explanted cartilage was incubated with collagenase (1mg per ml per 1g of cartilage) (ThermoFisher Scientific, Inc (Massachusetts, USA) (Table 2.1) overnight at 37°C. Collagenase digest was centrifuged at 10,000X RPM for 5 mins. Pellets were washed and suspended in Dulbecco's modified Eagle's medium (DMEM) containing 4.5 g/l of glucose and L-Glutamine (Lonza, Verviers, Belgium) and were supplemented with 10 % fetal bovine serum (FBS) (ThermoFisher Scientific, Massachusetts, USA), 25mmol Hepes and 1 % penicillin, streptomycin and amphotericin (Gibco, NY, USA). Cell were plated at a density of 1 million per well in DMEM with 10% FBS and 25 mmol of Hepes, 1% penicillin/streptomycin and amphotericin for 24 hours. Cells were serum starved by incubating for 24 hours in serum-free DMEM and then stimulated for 4 hours with serum free medium containing either drug (4-HNE or TLZ) (Table 2.2) or vehicle.

Table 2.1: List of materials and reagents used.

Name	Provider	Catalogue Number
Collagenase	ThermoFisher Scientific, Inc (Massachusetts, USA)	17101015
Dulbecco's modified Eagle's Medium (DMEM)	Lonza (Verviers, Belgium)	BE12-604F
Gibco™ Fetal Bovine Serum	ThermoFisher Scientific, Inc (Massachusetts, USA)	11533387
Hepes, Pencillin and Streptomycin	ThermoFisher Scientific, Inc (Massachusetts, USA)	15140148
10X RIPA Buffer	Abcam (Cambridge Biomedical Campus (CBC) in Cambridge, UK)	ab156034
Phenylmethylsulfonyl fluoride (PMSF)	ThermoFisher Scientific, Inc (Massachusetts, USA)	36978
Sodium Orthovandate	Sigma-Aldrich (St. Louis, Missouri, USA)	s6508
Protease Inhibitor Cocktail	Abcam (Cambridge Biomedical Campus (CBC) in Cambridge, UK)	ab271306
Polyvinylidene difluoride (PVDF) Membrane	ThermoFisher Scientific, Inc (Massachusetts, USA)	88518
β-Mercaptoethanol	Sigma-Aldrich (St. Louis, Missouri, USA)	60-24-2
RNeasy Micro Kit (50)	Qiagen (Hilden, Germany)	74004
Rnase-Free DNase set	Qiagen (Hilden, Germany)	79254
TRIzol™ Reagent	ThermoFisher Scientific, Inc (Massachusetts, USA)	15596026
High-Capacity RNA-to-cDNA™ Kit	ThermoFisher Scientific, Inc (Massachusetts, USA)	4387406
Rnase Inhibitor	ThermoFisher Scientific, Inc (Massachusetts, USA)	N8080119
SYBR™ Green PCR Master Mix	ThermoFisher Scientific, Inc (Massachusetts, USA)	4309155
Amersham Hyperfilm ECL	Cytiva (Malborough, USA)	28906835
ECL™ Western Blotting Reagents	Sigma-Aldrich (St. Louis, Missouri, USA)	GERPN2106
10X ReBlot Plus Strong Antibody Stripping Solution	Merck (New Jersey, USA)	2502

2.2 Trotter injury model

Freshly slaughtered 3-6 month old porcine forelimbs were ordered from the local abattoir. Upon arrival to the Institute, porcine metacarpophalangeal (MCP) joints were decontaminated in 2% Virkon for 20 mins before being equilibrated at 37 °C, 5% CO_2 for 1 hour. MCP joints were injected with either inhibitor or vehicle control and incubated for another 1 hour at 37 °C. The MCP joints were opened and cartilage was rapidly explanted and cut into smaller pieces. Explanted cartilage was either immediately snap frozen in liquid nitrogen (zero hour time point) or cultured in serum free DMEM (containing 4.5 g/l of glucose and L-Glutamine and supplemented with 25mmol Hepes and 1 % Penicillin, Streptomycin and amphotericin) with or without inhibitor (Table 2.2) for 4 hours at 37 °C, 5% CO_2 before being snap frozen.

Table 2.2: List of drugs used for in-vitro and ex-vivo trotter injection work.

Drug Name	Provider	Catalogue Number
Talarozole (TLZ)	MedChem Express (Monmouth Junction, USA)	HY-14531-10
4-hydroxoxynoneal (4HNE)	Sigma-Aldrich (St. Louis, Missouri, USA)	75899-68-2
5Z-7-Oxozeaenol (5Z-7)	Tocris Bioscience (Bristol, UK)	253863-19-3
PPARG inhibitor (GW9662)	Sigma-Aldrich (St. Louis, Missouri, USA)	22978-25-2
cPLA2 inhibitor (PACOCF3)	Abcam (Cambridge Biomedical Campus (CBC) in Cambridge, UK)	ab141761
12/15 LOX inhibitor (ML351)	Tocris Bioscience (Bristol, UK)	6448
Selonsertib	MedChem Express (Monmouth Junction, USA)	GS-4997
Apocynin	Tocris Bioscience (Bristol, UK)	498-02-2

2.2.1 Trotter injury in hypoxic chamber

To investigate the effect of variable oxygen tension on mechanoflammation the trotter injury assay was conducted under normoxic (21% O_2) or hypoxic conditions (2% O_2) using a hypoxic chamber located in an adjacent research facility (Target Discovery Institute, Oxford). Porcine trotters were equilibrated for 1 hour at 37°C, 5% CO_2, in a hypoxic chamber (2% O_2) (in the Target Discovery Institute, Oxford) or under normoxic conditions (21% O_2) on the same day in The Kennedy Institute. In both instances, all tissue reagents were also equilibrated to their respective oxygen tension. The trotter MCP joints were then dissected open and cartilage explanted under hypoxic or normoxic conditions. Explanted cartilage was cultured in serum free DMEM, at their respective oxygen tension, for various time periods before being snap frozen.

2.2.2 Trotter injury under yellow light conditions

In order to investigate the effect of variable light conditions on mechanoflammation, I conducted the trotter injury assay under ambient light or yellow light conditions. Porcine MCP joints were carefully opened and cartilage explanted, either in ambient light or yellow light. Explanted cartilage under yellow light was either snap frozen in liquid nitrogen (zero hour time point) or cultured for 4 hours in serum free DMEM at 37 °C, 5% CO_2 within bijou tubes that were covered with opaque aluminium foil. Explanted cartilage under ambient light conditions were cultured for 4 hours in transparent bijou tubes containing serum free DMEM at 37 °C, 5% CO_2.

2.3 Western blot analysis

1 X radioimmunoprecipitation assay (RIPA) buffer, was prepared from stock 10X RIPA Buffer (Abcam, Cambridge, UK) (Table 2.1). 1X RIPA buffer was supplemented with phenylmethylsulfonyl fluoride (PMSF) (ThermoFisher Scientific, Massachusetts, USA), sodium orthovandate (Sigma-Aldrich, St. Louis, Missouri, USA) and protease inhibitor cocktail (Abcam, Cambridge, UK). Porcine metacarpophalangeal (MCP) joints were decontaminated in 2% Virkon for 20 mins before being equilibrated at 37°C, 5% CO_2 for 1 hour. MCP joints were injected with either inhibitor or vehicle control and incubated for another 1 hour at 37 °C. The MCP joints were opened and cartilage was rapidly explanted, as described in Materials and Methods. Explanted cartilage was either immediately cooled in ice-cold 1X RIPA Buffer (zero hour time point) or cultured in serum free DMEM with or without inhibitor for various periods of time (5 mins, 10 mins and 30 mins) at 37 °C, 5% CO_2 before being transferred to ice cold, 1X RIPA buffer. Explants with 1X RIPA buffer, were mildly shaken for 45 mins at 4°C. Lysates were run on hand-made 10% Sodium Dodecyl Sulphate-Polyacrylamide Gel (SDS-PAGE) and transferred to poly (vinylidene) (PVDF) membrane (ThermoFisher Scientific, Massachusetts, USA). PVDF membrane was blocked in 5% milk for 1 hour at room temperature, incubated overnight in 1:1000 primary antibody (Table 2.3), washed 3 times (3X 10 mins) for a total of 30 mins in 1X tris-buffered saline with 0.1% Tween 20 detergent (TBST) and incubated for a further hour in 1:2000 secondary antibody. The PVDF membrane was further washed 3 times (3X 10 mins) for a total of 30 mins in 1X TBST. Signal was enhanced by use of chemiluminescence ECL reagent (Sigma-Aldrich, St. Louis, Missouri, USA) and subsequently visualised using autoradiography films (Cytiva, Malborough, USA). The blot was stripped using 1X ReBlot stripping solution (Merck, New Jersey, USA), re-blocked in 5% milk and finally re-probed for total ERK (tERK) as the loading control. The quantification of three separate

experiments was performed using FIJI-App, ImageJ-win64 Gel Analysis software and normalised to tERK.

Table 2.3: List of primary antibodies used for western blot work.

Antibody	Species	Dilution	Provider	Catalogue Number
Anti-Total ERK (tERK)	Rabbit	1:1000	Cell Signalling Technology (Massachusetts, USA)	sc-94
Anti-Phospho-SAPK/JNK (pJNK)	Rabbit	1:1000	Cell Signalling Technology (Massachusetts, USA)	9251
Anti-Phospho-p44/42 MAPK (ERK1/2)	Rabbit	1:1000	Cell Signalling Technology (Massachusetts, USA)	9101
Anti-Phospho-TAK1 (Thr187)	Rabbit	1:1000	Cell Signalling Technology (Massachusetts, USA)	4536
Anti-Phospho-cPLA2 (Ser505)	Rabbit	1:500	Cell Signalling Technology (Massachusetts, USA)	2831

2.4 RNA extraction

2.4.1 RNA extraction of cartilage samples

RNA extraction was performed using the RNeasy Micro Kit (50) purchased from Qiagen (Hilden, Germany). Cartilage was pulverised into fine powder using a pestle and mortar with liquid nitrogen. Pulverised tissue was then suspended in Buffer RLT with 1:100 β-mercaptoethanol and stored at -80 °C. Defrosted samples were centrifuged at 13,000X RPM for 30 seconds at 4 °C Celsius so that the cartilage homogenate collected at the bottom of the Eppendorf tube. 590 µl of RNase-free water and 10 µl of Qiagen proteinase K solution was added and mixed thoroughly before being left to incubate at 55 °C for 10 mins. The samples were centrifuged further for 3 mins at 13,000X RPM at room temperature to form a pellet. The supernatant was transferred into a tube and 50% volumes of 100% ethanol was added to the clear lysate and mixed well by pipetting. The whole sample, including any precipitate, was then transferred to an RNeasy MinElute spin column placed in a 2mL collection tube (supplied with the kit) before being centrifuged for 15 seconds at 13,000X RPM. The flow through was discarded, 350 µl of Buffer RW1 added and then centrifuged again for 15 seconds at 13,000X RPM. Flow through was discarded and DNAase I solution was added directly to the RNeasy MinElute spin column membrane and incubated at room temperature for 15 mins. 350 µl of Buffer RW1 was added to the RNeasy MinElute spin columns and centrifuged for 15 seconds at 13,000X RPM. The RNeasy MiElute spin columns were placed in a new 2mL collection tube and 500 µl of Buffer RPE was added before being centrifuged for a further 15 seconds at 13,000X RPM. 500 µl of 80% ethanol was added to the spin columns and centrifuged for 2 mins at 13,000X RPM. The lids of the spin columns were opened and centrifuged further at full speed for 5 mins. The spin columns were placed in new 1.5ml Eppendorf's. 14 µl of RNase-free water was directly added to the

centre of the membrane and left to incubate at room temperature for 10 mins before being centrifuged for 1 minute at full speed to elute the RNA. RNA concentration was estimated using a nanodrop machine with an expected concentration over 100ng/µl and a 260/280 ratio around 2.00.

2.4.2 RNA extraction of cells

After cell incubation with drug or vehicle, media was aspirated and cell were washed once with ice-cold phosphate buffered solution (PBS) (1-2ml). PBS was then aspirated and 1ml of TRIzol (ThermoFisher Scientific, Massachusetts, USA) was added. The plate was scraped gently and was left at 4 °C for 5 mins. The TRIzol/cell lysate mixture was then transferred into a 1.5 ml Eppendorf tube and centrifuged for 5 mins at 13,000X RPM. Supernatant was collected and transferred into cleaned Eppendorf tube. 100 µl 1-Bromo-3-choloropropane (Sigma-Aldrich, Dorset, England) was added and gently vortexed, incubated for 5 mins at room temperature and then phase separated by centrifugation at 13,000X RPM for 10 mins at 4 °C. Further steps were carried out as per the manufacturer instructions (RNeasy Mini-Kit, Qiagen, Hilden, Germany).

2.5 cDNA Synthesis

Complementary DNA (cDNA) was synthesized from the DNase treated RNA using a high capacity reverse transcription kit (ThermoFisher Scientific, Massachusetts, USA) following the manufacturer's guidelines (in a total of a 20 µl reaction, 100 ng – 500 ng RNA were added to 13.2 µl RNase free water (X µl RNA + X µl water = 13.2 µl). A 1X master mix solution contained 2 µl of 10X RT buffer, 0.8 µl 10 mM deoxyribonucleotides (dNTPs), 2 µl of random primer, 1 µl RNase inhibitor (20 U) and 1 µl reverse transcriptase (50 U) per reaction) using a C1000 touch thermocycler (BioRad, Hertfordshire, UK). A reverse transcribing programme was set as: 25 ℃ for 10 mins, 37 ℃ for 120 mins and finally 85 ℃ for 5 mins. cDNA was diluted in RNAse free water according to their initial concentration (100 ng 1:5, 500 ng 1:25)

2.6 qPCR (quantitative polymerase chain reaction) analysis

A total of 10 µl of reaction mixture containing 1 µl cDNA template, 1 µl of each forward and reverse primer (Table 2.4), 5 µl of SYBR™ Green PCR Master Mix (ThermoFisher Scientific, Massachusetts, USA) and 2 µl of nuclease-free water was added to each well of a 384 well plate. Each reaction was run in a triplet. The plate was sealed and centrifuged for 1 min at 10,000X RPM. Real Time-qPCR was carried out on a ViiA™ 7 Real-Time PCR System (Applied Biosystems) under the following conditions; 1X stage 1: 95 °C for 10 mins; 40X stage 2: 95 °C for 15 s; 60 °C for 1 min. Relative gene expression or fold change value were calculated by applying $2^{-\Delta\Delta Ct}$ Formula. 18S served as house keeping control gene.

Table 2.4: Primers used for quantitative PCR (qPCR).

Gene	Forward Strand Sequence (5' to 3')	Reverse Strand Sequence (5' to 3')
18S	TGCAGAATCCTCGCCAATACA	AGTCGCTCCAAGTCTTCACG
CYP26A1	GCACGGCAGATCCTACAGA	CTTCAGCTCCTCTCGCACT
CYP26B1	GCACGGCAGATCCTACAGA	TGTCCAGAGCATCCGAGTAG
RARA	CGGAACAAGAAGAAGAAGGAGG	CCAGAGGTCAATGTCCAGAGA
RARB	CCGACCTTGTGTTCACCTTC	CCGTCTCTGTGTCATCCATC
RARG	GTCCTCTGGCTACCACTACG	CACAGCTTCCTTGGACATGC
IL6	ATGCTTCCAATCTGGGTTCAA	CACAAGACCGGTGGTGATTCT
COX2	CCGACAGCCAAAGACACTCA	CGGAGGTGTTCAGGAGTGTGA
ADAMTS4	ACACGCCTCCGATACAGCTT	GTAGAACGTGGCGTTGAAGGA
CCL2	TGTGCCTGCTGCTCACTG	GCAGCAGGTGACTGGAGAAT
TIMP1	GAGCCCCAGAGTTCAACCAGAC	GGCGGGGGCGTAGATGA
MMP3	GGAGTTCCTGATGTTGGTTACTTC	CAAAACTTTTCCAGGTCCGTCAAA
CDKN1A	CTCCCAGGGCAGGAAACG	TTGTTTCCAGCAGGACAAGG
NGF	CACTGGAACTCGTATTGTACCACAA	GCCTGCTTGCCGTCCAT

2.7 Promoter searching

The RARE-motif was identified from the literature as a direct repeat of the consensus sequence separate by 1, 2 or 5 nucleotides. Eight different consensus sequence or atRA binding sites have been identified in the literature. The presence of RARE-motifs on the promoter regions of genes were identified by using the Ensemble genome browser database. All genes searched were within species sus scrofa (porcine). The export configuration for the forward and reverse strands were set to FASTA sequence, 2000 kilobases (kb) upstream of the 5' region. The 5' flanking sequence that was generated was subjected into Clustal Omega, an online multiple alignment software (Clustal Omega < Multiple Sequence Alignment < EMBL-EBI) and aligned against the different sequences of potential RARE-motifs.

2.8 Statistical analysis

Statistical analysis was performed using Prism 8 software (GraphPad Software Inc., USA). The degree of significance was calculated and reported as; p-value ≤ 0.05: significant (*) or p-value ≤ 0.01: highly significant (**). P-value greater than 0.05 were defined as non-significant (n.s.). The comparison of two sets of measurements were performed using an unpaired t-test. Experiments that included three or more groups were analysed for statistical differences using either a one-way or two-way ANOVA. A two-way ANOVA was utilised when the outcome was determined by two factors. Following a one-way or two-way ANOVA, multiple comparisons analyses was conducted using a Tukey's test which compared the means of each distinct treatment group.

3 CHAPTER 3: CHARACTERISATION OF THE DROP IN ALL-TRANS-RETINOIC ACID (atRA)

3.1 Introduction

Mechanical stress has been shown to induce inflammation in articular cartilage by a process known as mechanoflammation [2]. This is characterised by the activation of inflammatory signalling and upregulation of inflammatory response genes [16, 99, 327]. The latter include interleukin 6 (*IL6*), cyclooxygenase 2 (*COX2*), a disintegrin and metalloproteinase with thrombospondin motifs 4 (*ADAMTS4*), C–C motif chemokine ligand 2 (*CCL2*), tissue inhibitor of metalloproteinase 1 (*TIMP1*), matrix metalloproteinase 3 (*MMP3*), cyclin dependent kinase inhibitor 1A (*CDKN1A*) and nerve growth factor (*NGF*) [99, 328]. Cartilage has been shown to be highly mechanosensitive in experimental models of OA [46, 329, 330]. Moreover, inflammatory gene regulation is abrogated upon joint immobilisation after OA induction [100]. The role of inflammatory signalling in OA is suggested by reduction in disease in JNK2 KO mice [123]. Gaining a comprehensive insight into mechanoflammation and how it might be suppressed would help to identify disease modifying treatment options in OA.

All joints are subjected to compressive and shear stress forces throughout a person's lifetime, including nonweight-bearing joints, such as the hands. Severe hand OA has been associated with single nucleotide polymorphic (SNP) variants in the *ALDH1A2* gene, first identified in an Icelandic population [200]. The two main risk variants rs3204689 and rs4238326 were associated with odds ratios of 1.44 and 1.46, respectively, for severe hand OA and are present at high allele frequency in the population at 52% and 41%, respectively.

The *ALDH1A2* gene encodes for the enzyme which synthesises atRA in a rate-limiting step. atRA is transported into the nucleus to induce gene transcription or broken down into inactive polar metabolites. In the nucleus, atRA can bind onto one of three retinoic acid receptors (RARα, RARβ and RARγ) or one of two peroxisome proliferator activated receptors (PPAR) (PPARβ/δ). Once bound by atRA, each of these nuclear receptors forms a heterodimeric complex with retinoic acid X receptors (RXRα, RXRβ and RXRγ). The RAR-RXR forms a heterodimeric complex on RARE-motifs whereas the PPAR-RXR heterodimeric complex is present on PPRE-motifs [331]. Each of these motifs are present on the promoter regions of atRA-responsive genes which can either activate or repress target genes [211]. Alternatively, atRA can be metabolised by CYP26 enzymes (CYP26A1, CYP26B1, CYP26C1) into inactive metabolites [211]. Selective groups of drugs known as retinoic acid metabolising agents (RAMBAs) can inhibit the CYP26 enzymes thereby increasing the levels of atRA [332, 333]. TLZ is the most specific and selective RAMBA, which is currently already in commercial use in the treatment of psoriasis and acne [334].

Since atRA is extremely light sensitive, it is difficult to directly measure the levels of atRA in cells [335]. Instead, upregulated atRA-responsive genes can be used as a surrogate marker for the levels of atRA. *CYP26* and *RAR* genes are such atRA-responsive genes, as these contain RARE-motifs in their promoter regions. Our lab has shown that atRA is highly mechanosensitive, and atRA-responsive genes are rapidly downregulated on cartilage injury (data currently in review). TLZ maintains levels of atRA and has a marked anti-inflammatory effect in the cartilage, suppressing mechano-inflammatory genes. This highlights that maintaining or indeed increasing atRA levels in cartilage is a key objective in therapeutic OA. As such, it is important to not only characterise the fall in atRA on cartilage injury but also determine the factors that might be driving this fall.

3.2 Results

3.2.1 atRA-responsive genes are downregulated on cartilage injury

In order to validate results previously obtained in the lab, I wanted to show that atRA-responsive genes were downregulated on cartilage injury. As previously mentioned, atRA is challenging to measure directly, so I used the atRA-responsive genes (*CYP26A1*, *CYP26B1*, *RARA, RARB* and *RARG*) as surrogate makers for the level of atRA in cartilage [336-338]. Freshly slaughtered 3- to 6-month-old porcine forelimb joints were equilibrated to 37°C. Cartilage was explanted and then rapidly cut into smaller pieces, each approximately 1–2 mm^2 and either snap-frozen in liquid nitrogen (zero hour time point) or cultured in serum-free Dulbecco's Modified Eagle Medium (DMEM) solution for 4 hours at 37°C, 5% CO_2. RNA was extracted, converted to complementary DNA (cDNA) and real-time PCR (RT-PCR) conducted to measure gene expression. Each atRA-responsive gene expression was normalised to *18S* and expressed relative to its normalised zero hour time points (n = 3 separate trotters). *CYP26A1*, *CYP26B1*, *RARA*, *RARB* and *RARG* were all significantly downregulated on porcine cartilage injury at 4 hours (p value, by unpaired t-test < 0.05) compared to zero hour time points (Fig 3.1).

Next, I characterised the temporal pattern of this mechanosensitive response of atRA-responsive genes on injury. Porcine MCP joints were opened, cartilage explanted, rapidly cut into smaller pieces and either snap-frozen (zero time point) or cultured for various periods of time (5 mins, 30 mins, 1 hour, 2 hours, 4 hours or 24 hours) in serum-free medium (n = 3 separate trotters).

RNA was extracted, cDNA synthesised and RT-PCR run on a panel of atRA-responsive genes (*CYP26A1*, *CYP26B1*, *RARA*, *RARB* and *RARG*). Statistical significance of

comparison between time points was conducted using a one-way ANOVA, with post hoc multiple comparisons corrected using Tukey's tests.

The drop in atRA-responsive genes occurred in a broadly linear fashion around 1 hour (Fig 3.2A) and persisted for 24 hours (Fig 3.2B). *CYP26A1* (Fig 3.2A) expression showed gradual downward trend over time from zero hour to 4 hours but was only downregulated to a statistically significant level at 4 and 24 hours (Fig 3.2B) ($p < 0.01$). *CYP26B1* showed an extremely similar downward trend (Fig 3.2A) and dropped by 39% (SD ± 0.126) at 2 hours post injury reaching statistical significance at 4 hour and 24 hours ($p < 0.01$) (Fig 3.2B). *RARA* markedly fell to 52% at 4 hours to 48% at 24 hours (SD ± 0.097) ($p < 0.01$) (Fig 3.2). *RARB* fell to less than 50% (SD ± 0.140) on injury reaching statistical significance by 1 hour, and this was maintained at 4 hours (Fig 3.2A) and 24 hours ($p < 0.01$) (Fig 3.2B). The expression of *RARG* showed a stepwise downward trend reaching a statistical significant drop of 45% (SD ± 0.087) at 1 hour ($p < 0.01$) and to more than a 50% drop by 4 hours (Fig 3.2A) and 24 hours ($p < 0.01$) (Fig 3.2B).

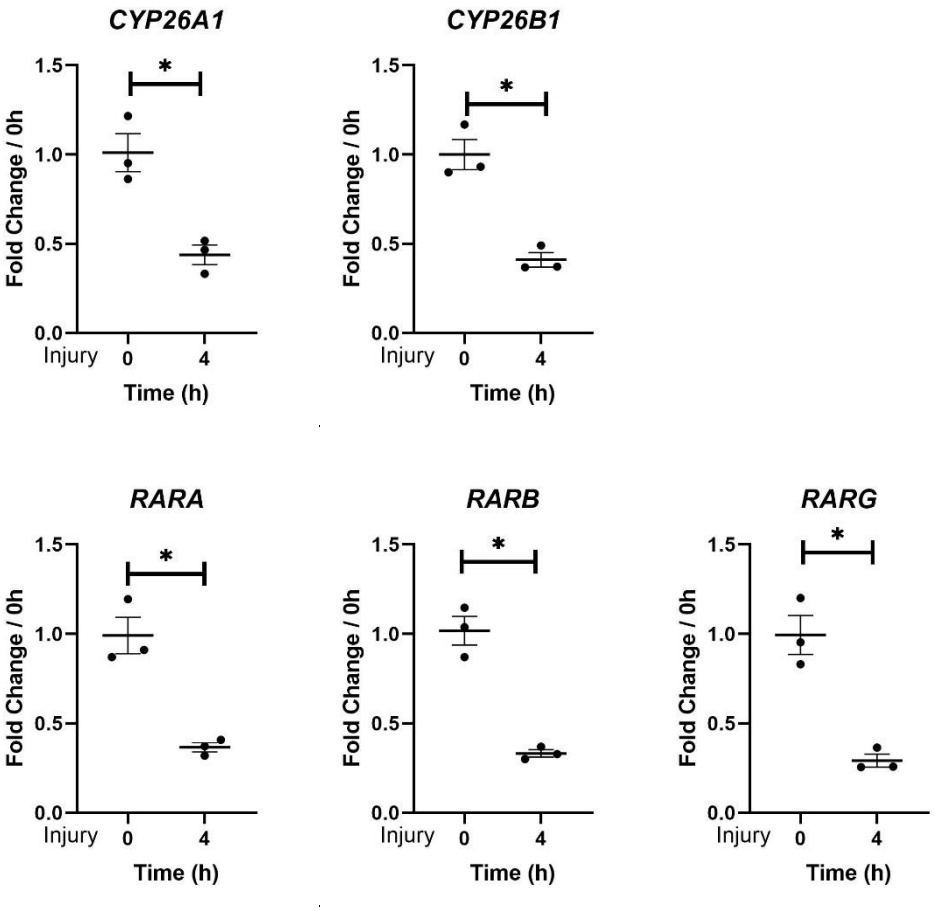

Figure 3.1: atRA-responsive genes are downregulated on porcine cartilage injury.

Porcine metacarpophalangeal joints (MCP) were decontaminated in 2% Virkon for 20 minutes before being equilibrated at 37 °C, 5% CO_2 for 1 hour. The MCP joints were then opened and cartilage explanted off the articular surface as described in Materials and Methods. Explanted cartilage was either immediately snap frozen in liquid nitrogen (zero hour time point) or cultured in serum free DMEM for 4 hours at 37 °C before being snap frozen. RNA was subsequently extracted from the tissue and used in quantitative reverse transcriptase-polymerase chain reaction (RT-PCR) to measure a panel of atRA-responsive genes (*CYP26A1*, *CYP26B1*, *RARA*, *RARB* and *RARG*). Statistical significance of comparison between zero hour and 4 hour time points was measured using an unpaired t-test. Bars shows the mean ±SEM of 3 independent experiments (separate trotter joints). * = $P < 0.05$; ** = $P < 0.01$, by unpaired t-test. CYP26A1 = Cytochrome P450 Family 26 Subfamily A Member 1, CYP26B1 = Cytochrome P450 Family 26 Subfamily B Member 1, RARA = Retinoic Acid Receptor Alpha, RARB = = Retinoic Acid Receptor Beta, RARG = = Retinoic Acid Receptor Gamma.

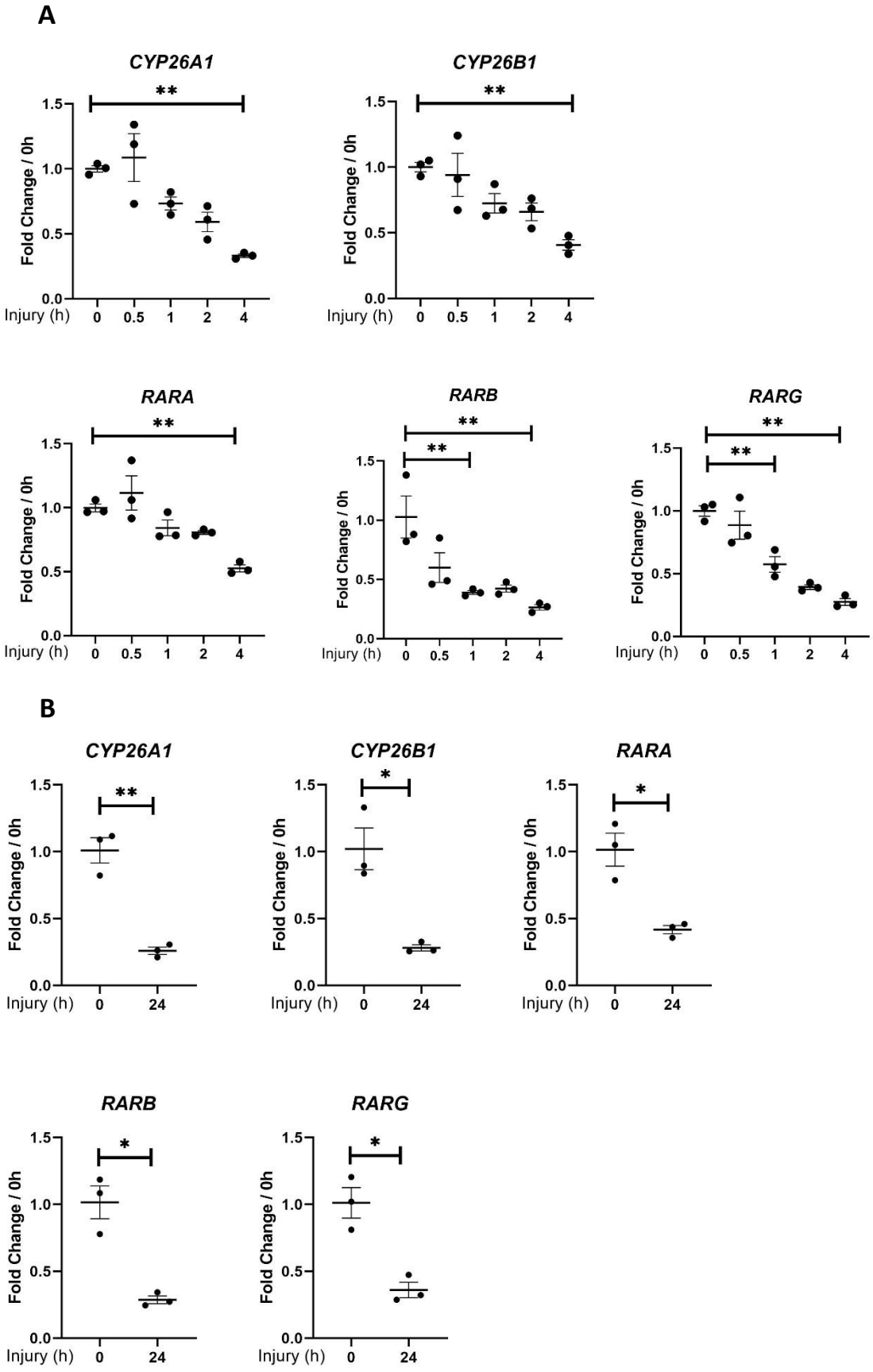
A
CYP26A1
CYP26B1
RARA
RARB
RARG
Fold Change / 0h
Injury (h)
0
0.5
1
2
4
**
*
B
CYP26A1
CYP26B1
RARA
RARB
RARG
Fold Change / 0h
Injury (h)
0
24
*
**

Figure 3.2: atRA-responsive genes are rapidly downregulated on cartilage injury and lasts up to 24-hours.

Porcine metacarpophalangeal (MCP) joints were decontaminated in 2% Virkon for 20 minutes before being equilibrated at 37°C, 5% CO_2 for 1 hour. The MCP joints were opened and cartilage was rapidly explanted, as described in Materials and Methods. Explanted cartilage was either immediately snap frozen in liquid nitrogen (zero hour time point) or cultured in serum free DMEM for varying amounts of time (either up to 4 hours, A; or up to 24 hours, B) at 37°C, 5% CO_2 before being snap frozen. RNA was subsequently extracted from the tissue and used in quantitative reverse transcriptase-polymerase chain reaction to measure a panel of atRA-responsive genes. Statistical significance of comparison between time points was conducted using a one-way ANOVA, with multiple comparisons corrected using Tukey's tests. Bars shows the mean ±SEM of 3 independent experiments (separate trotter joints). ns= not significant, * = P < 0.05; ** = P < 0.01, by one-way ANOVA. CYP26A1 = Cytochrome P450 Family 26 Subfamily A Member 1, CYP26B1 = Cytochrome P450 Family 26 Subfamily B Member 1, RARA = Retinoic Acid Receptor Alpha, RARB = = Retinoic Acid Receptor Beta, RARG = = Retinoic Acid Receptor Gamma.

3.2.2 Inflammatory genes are upregulated on cartilage injury

Mechanical injury has been previously shown by our group to activate inflammatory signalling and induce a panel of inflammatory genes in articular cartilage by a process known as mechanoflammation [99]. In order to validate the observation of inflammatory gene upregulation on mechanical injury to cartilage, I conducted a further series of trotter injury experiments and measured inflammatory gene regulation.

Each inflammatory gene expression was normalised to *18S* and expressed relative to its normalised zero hour time points (n = 3 separate trotters). Statistical significance of comparison between zero hour and 4 hour time points was conducted using an unpaired t-test. All inflammatory genes tested were upregulated on cartilage injury. *COX2* was the most strongly upregulated gene on cartilage injury whereas *CCL2* was the least regulated gene on cartilage injury (*COX2* 40.3-fold ± 3.636 SD $p < 0.01$, *IL6* 9.1-fold ± 0.808 SD $p < 0.05$, *ADAMTS4* 4.6-fold ± 0.3919 SD $p < 0.05$, *MMP3* 15.1-fold ± 1.897 SD $p < 0.05$, *CCL2* 3.6-fold ± 0.3524 SD $p < 0.05$, *TIMP1* 3.2-fold ± 0.2648 SD $p < 0.05$, *CDKN1A* 4.1-fold ± 0.2648 SD $p < 0.05$ and *NGF* 17.6-fold ± 2.261 SD $p < 0.05$).

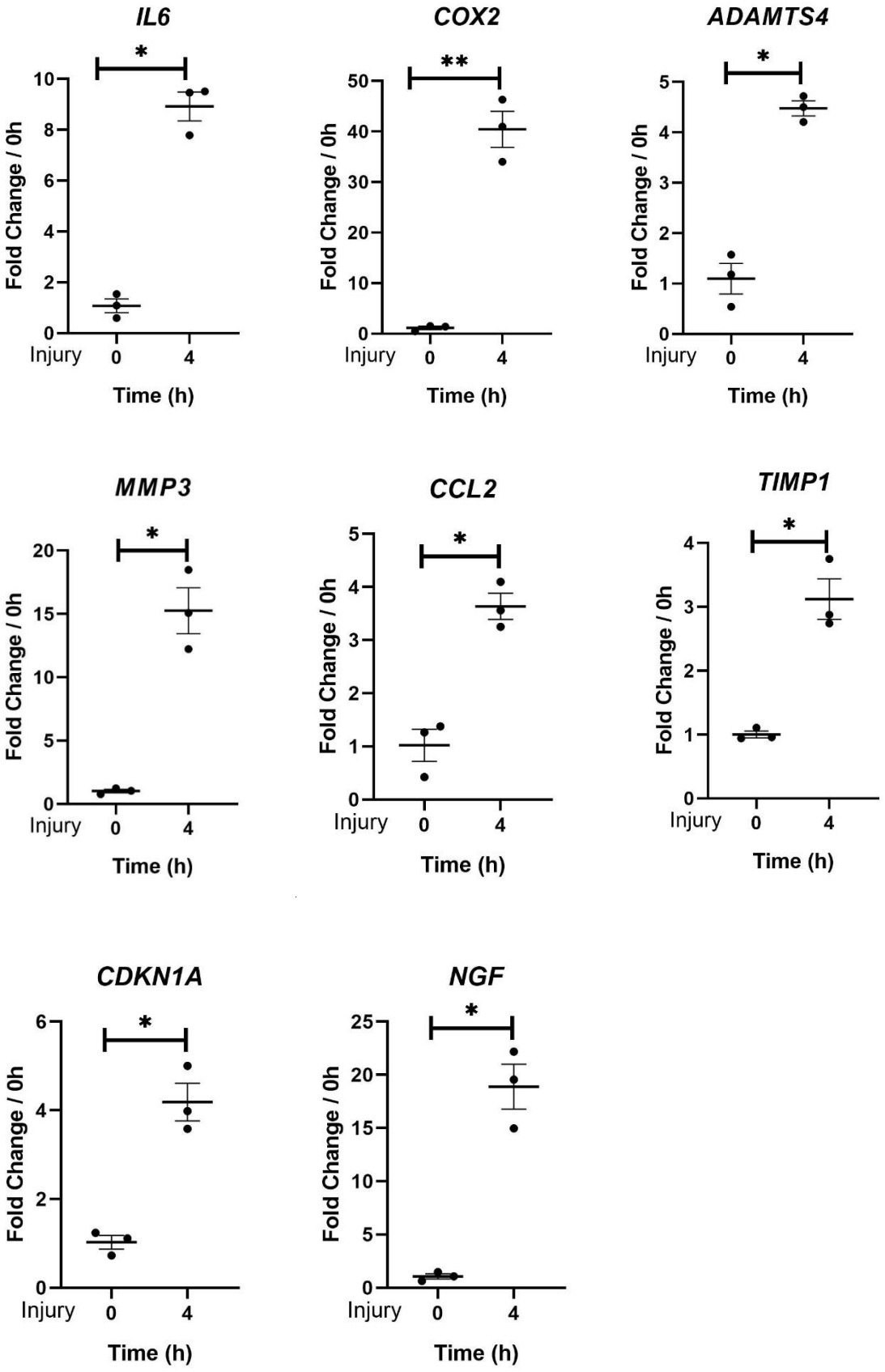
IL6
COX2
ADAMTS4
MMP3
CCL2
TIMP1
CDKN1A
NGF
Fold Change / 0h
Injury
0
4
Time (h)
*
**

Figure 3.3: Inflammatory genes are upregulated on porcine cartilage injury.

Porcine metacarpophalangeal (MCP) joints were decontaminated in 2% Virkon for 20 minutes before being equilibrated at 37 °C, 5% CO_2 for 1 hour. The MCP joints were opened and cartilage was rapidly explanted as described in Materials and Methods. Explanted cartilage was either immediately snap frozen in liquid nitrogen (zero hour time point) or cultured in serum free DMEM for 4 hours at 37 °C, 5% CO_2 before being snap frozen. RNA was subsequently extracted from the tissue and used in quantitative reverse transcriptase-polymerase chain reaction to measure a panel of inflammatory genes. Statistical significance of comparison between zero hour and 4 hour time points was conducted using an unpaired t-test. Bars shows the mean ± SEM of 3 independent experiments (separate trotters). * = $P < 0.05$; ** = $P < 0.01$, by unpaired t-test. IL6 = Interleukin 6, COX2= Cyclooxygenase-2, ADAMTS4 = ADAM Metallopeptidase With Thrombospondin Type 1 Motif 4, MMP3= Matrix metalloproteinase-3, CCL2= C-C Motif Chemokine Ligand 2, TIMP1= TIMP metallopeptidase inhibitor 1, CDKN1A= Cyclin Dependent Kinase Inhibitor 1A, NGF= Nerve growth factor.

3.2.3 Downregulation of atRA-responsive genes on cartilage injury is talarozole-sensitive

Having shown that the drop in atRA-responsive genes on cartilage injury was mirrored by an increase in inflammatory gene expression, I determined whether this response could be suppressed by restoring atRA levels in the cartilage. To achieve this, I used a highly selective CYP26 inhibitor called TLZ. By inhibiting CYP26, TLZ inhibits the breakdown of atRA and thereby increases cellular atRA concentration.

Trotter MCP joints were injected with 1 ml of serum-free DMEM with inhibitor (5 μM TLZ) or dimethyl sulfoxide (DMSO) (vehicle) and equilibrated at 37°C, 5% CO_2 for a further 1 hour. Cartilage was explanted and either snap-frozen or cultured for 4 hours into serum-free DMEM with 5 μM TLZ or vehicle. RT-PCR was performed and gene expression normalised to 18S and expressed relative to its zero hour time points. Three independent experiments were performed, in which each experiment was performed on nine individual trotter joints (n = 9 separate trotters). Statistical significance between treatment groups was conducted using a two-way ANOVA, with post hoc multiple comparisons corrected using Tukey's test.

TLZ prevented the downregulation of *CYP26A1* by 81% (SD ± 0.099) and completely prevented the downregulation of *CYP26B1* (100%, SD ± 0.097) and *RARB* (100%, SD ± 0.095) on cartilage injury. The downregulation in *RARA* and *RARG* was suppressed by TLZ by 77% (SD ± 0.096) and 90% (SD ± 0.067), respectively (Fig 3.4).

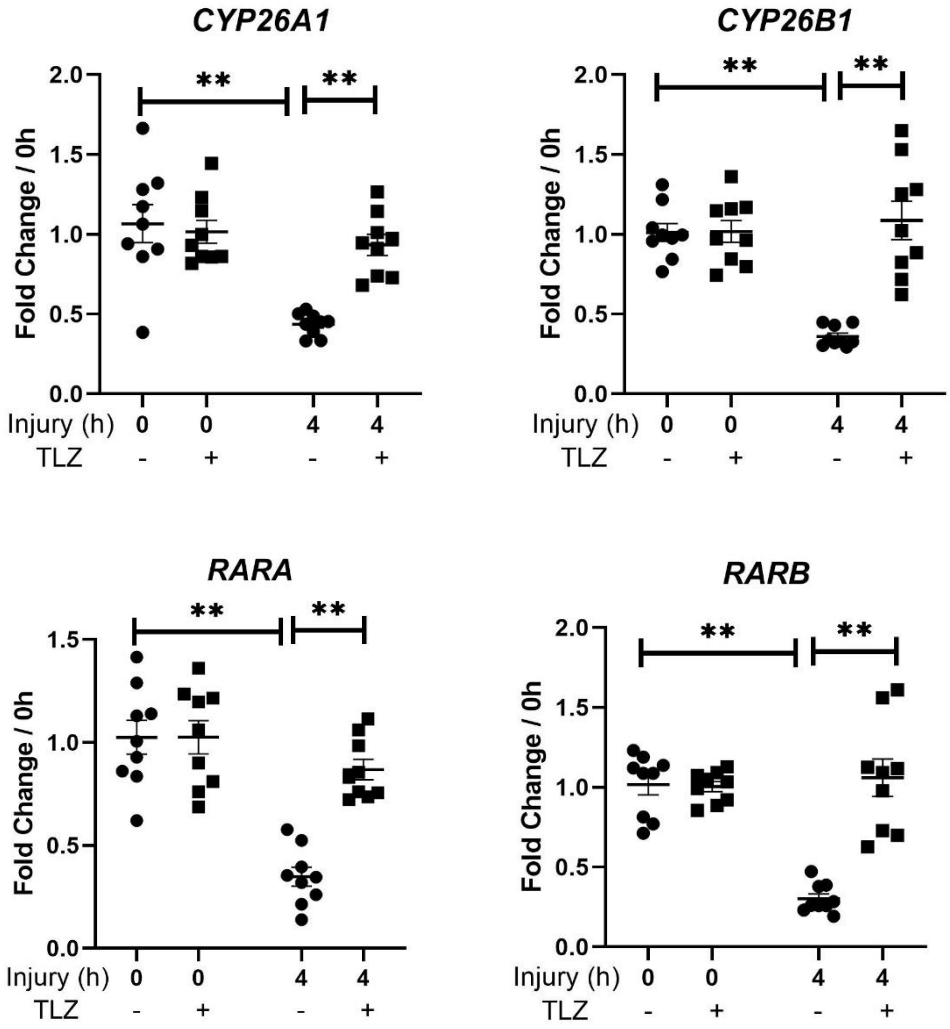

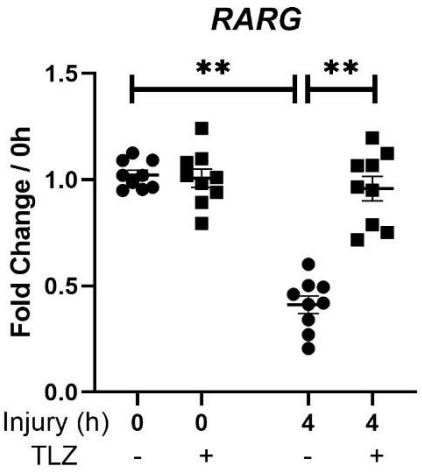

Figure 3.4: Talarozole prevents the downregulation of atRA-responsive genes on cartilage injury.

Porcine metacarpophalangeal (MCP) joints were decontaminated in 2% Virkon for 20 minutes before being equilibrated at 37 °C, 5% CO_2 for 1 hour. MCP joints were injected with either talarozole (TLZ) or vehicle control and incubated for another 1 hour at 37 °C. The MCP joints were opened and cartilage was rapidly explanted. Explanted cartilage was either immediately snap frozen in liquid nitrogen (zero hour time point) or cultured in serum free DMEM for 4 hours at 37 °C, 5% CO_2 before being snap frozen. RNA was subsequently extracted from the tissue and used in quantitative reverse transcriptase-polymerase chain reaction to measure a panel of atRA-responsive genes. Statistical significance of comparison between treatment groups was conducted using a two-way ANOVA, with post-hoc multiple comparisons corrected using Tukey's tests. Bars shows the mean ± SEM of 3 independent experiments in which each experiment was performed on 3 individual trotter joints (n= 9 separate trotters). * = $P < 0.05$; ** = $P < 0.01$, by two-way ANOVA. CYP26A1 = Cytochrome P450 Family 26 Subfamily A Member 1, CYP26B1 = Cytochrome P450 Family 26 Subfamily B Member 1, RARA = Retinoic Acid Receptor Alpha, RARB = = Retinoic Acid Receptor Beta, RARG = = Retinoic Acid Receptor Gamma.

3.2.4 Upregulation of inflammatory genes on cartilage injury is talarozole-sensitive

Having observed that TLZ prevented the downregulation of atRA-responsive genes on cartilage injury, I next explored whether the maintenance of endogenous atRA by TLZ was able to supress the upregulation of inflammatory genes on cartilage injury.

In order to test this, I used the cDNA from the experiment conducted in section 3.2.3 and examined the expression of the defined panel of inflammatory genes. Statistical significance between groups was conducted using a two-way ANOVA, with post hoc multiple

comparisons corrected using Tukey's test. TLZ completely suppressed the upregulation of *ADAMTS4* (100%, SD ± 1.66) whereas it suppressed the upregulation of *IL6*, *COX2*, *CCL2* and *TIMP1* by 84% (SD ± 1.98), 61% (SD ± 2.48), 51.6% (SD ± 1.21) and 55.4% (SD ± 1.35), respectively (Fig 3.5). On the other hand, *MMP3* gene expression was induced further by 1.8-fold (SD ± 0.457) on injury compared with the injured, vehicle control ($p < 0.01$) (Fig 3.4). *NGF* was upregulated 21.4-fold (SD ± 3.08) on cartilage injury but was unaffected by TLZ (Fig 3.5).

From these sets of experiments, I was able to confirm previously observed results from the lab. First is that atRA-responsive genes are rapidly downregulated on cartilage injury, and this is associated with an upregulation of inflammatory genes (by mechanoflammation).

Secondly, both can be reversed by TLZ, a compound that inhibits atRA catabolism. One important consideration to consider was whether the drop in atRA on injury was due to an environmental artefact (i.e., due to exposure to light or high oxygen tensions). Therefore, I explored how the drop in atRA on injury was influenced by varying levels of ambient light or oxygen tension.

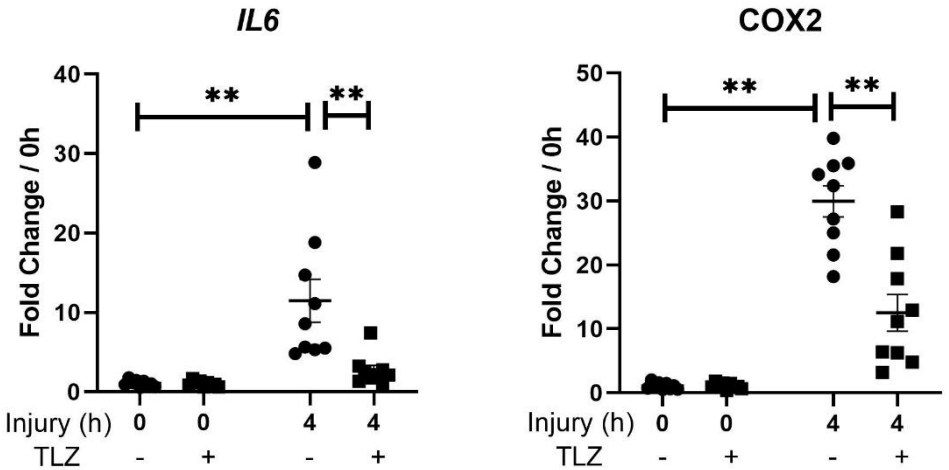

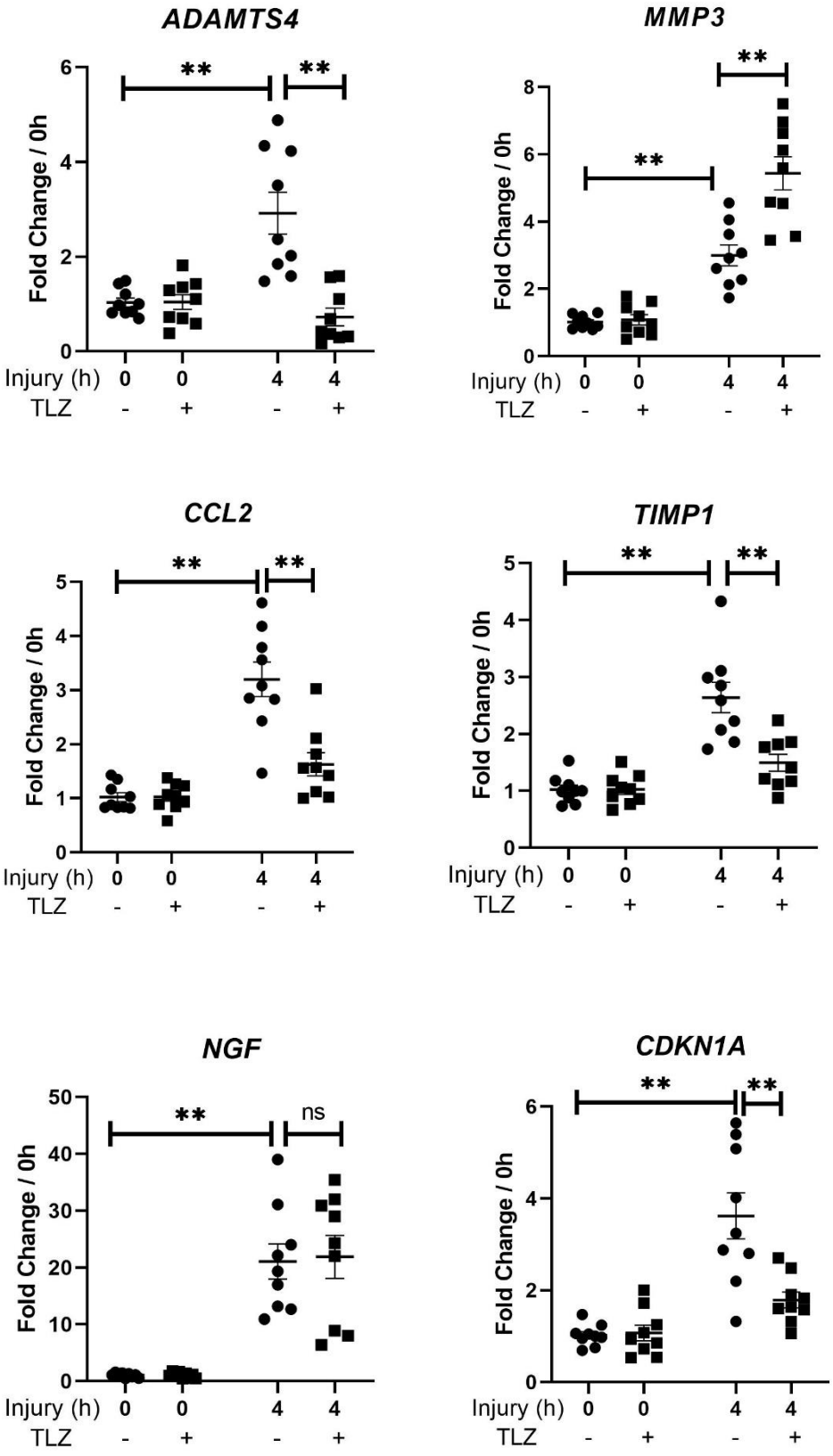
ADAMTS4
MMP3
CCL2
TIMP1
NGF
CDKN1A
Fold Change / 0h
Injury (h)
TLZ
**
ns

Figure 3.5: Talarozole suppresses the upregulation of inflammatory genes on cartilage injury.

Porcine metacarpophalangeal (MCP) joints were decontaminated in 2% Virkon for 20 minutes before being equilibrated at 37 °C, 5% CO_2 for 1 hour. MCP joints were injected with either talarozole (TLZ) or vehicle control and incubated for another 1 hour at 37 °C. The MCP joints were opened and cartilage was rapidly explanted. Explanted cartilage was either immediately snap frozen in liquid nitrogen (zero hour time point) or cultured in serum free DMEM with or without TLZ for 4 hours at 37 °C, 5% CO_2 before being snap frozen. RNA was subsequently extracted from the tissue and used in quantitative reverse transcriptase-polymerase chain reaction to measure a panel of atRA-responsive genes. Statistical significance of comparison between treatment groups was conducted using a two-way ANOVA, with post-hoc multiple comparisons corrected using Tukey's tests. Bars shows the mean ± SEM of 3 independent experiments in which each experiment was performed on 3 individual trotter joints (n= 9 separate trotters). * = $P < 0.05$; ** = $P < 0.01$, ns= by two-way ANOVA. IL6 = Interleukin 6, COX2= Cyclooxygenase-2, ADAMTS4 = ADAM Metallopeptidase With Thrombospondin Type 1 Motif 4, MMP3= Matrix metalloproteinase-3, CCL2= C-C Motif Chemokine Ligand 2, TIMP1= TIMP metallopeptidase inhibitor 1, CDKN1A= Cyclin Dependent Kinase Inhibitor 1A, NGF= Nerve growth factor.

3.2.5 Varying light intensity does not affect the downregulation of atRA-responsive genes on cartilage injury

atRA is the biologically active product synthesised from Vitamin A or all-trans-retinol (atROL) [339]. Both atROL and atRA are extremely susceptible to oxidative stress [340]. Studies have reported significant loss or isomerisation of atRA or atROL in cell cultures grown in variable light conditions [340, 341]. On exposure to high light intensity, atRA undergoes photodecomposition into inactive polar metabolites which renders it biologically inert [335].

As we have shown that atRA-responsive genes fall on cartilage injury, it was important to determine whether this was a direct consequence of injury and not due to exposure of the joint to high ambient light intensity and/or high oxygen tension. Therefore, I first conducted the experiment described in 3.2.1 under yellow light conditions (dark conditions).

Porcine MCP joints were carefully opened and cartilage explanted, either in ambient light or under yellow light conditions. Those cartilage explants derived from MCP joints in yellow

conditions were cultured in bijou tubes wrapped completely in opaque aluminium foil prior to transportation to the incubator. RNA was extracted from cartilage explants for RT-PCR.

All atRA-responsive genes (*CYP26A1*, *CYP26B1*, *RARA*, *RARB* and *RARG*) were significantly downregulated on cartilage injury under both yellow and ambient light conditions ($p < 0.01$) (Fig 3.6). For each atRA-responsive gene, there was no significant difference between the four-hour cartilage injury time points under yellow light or ambient light conditions (Fig 3.6).

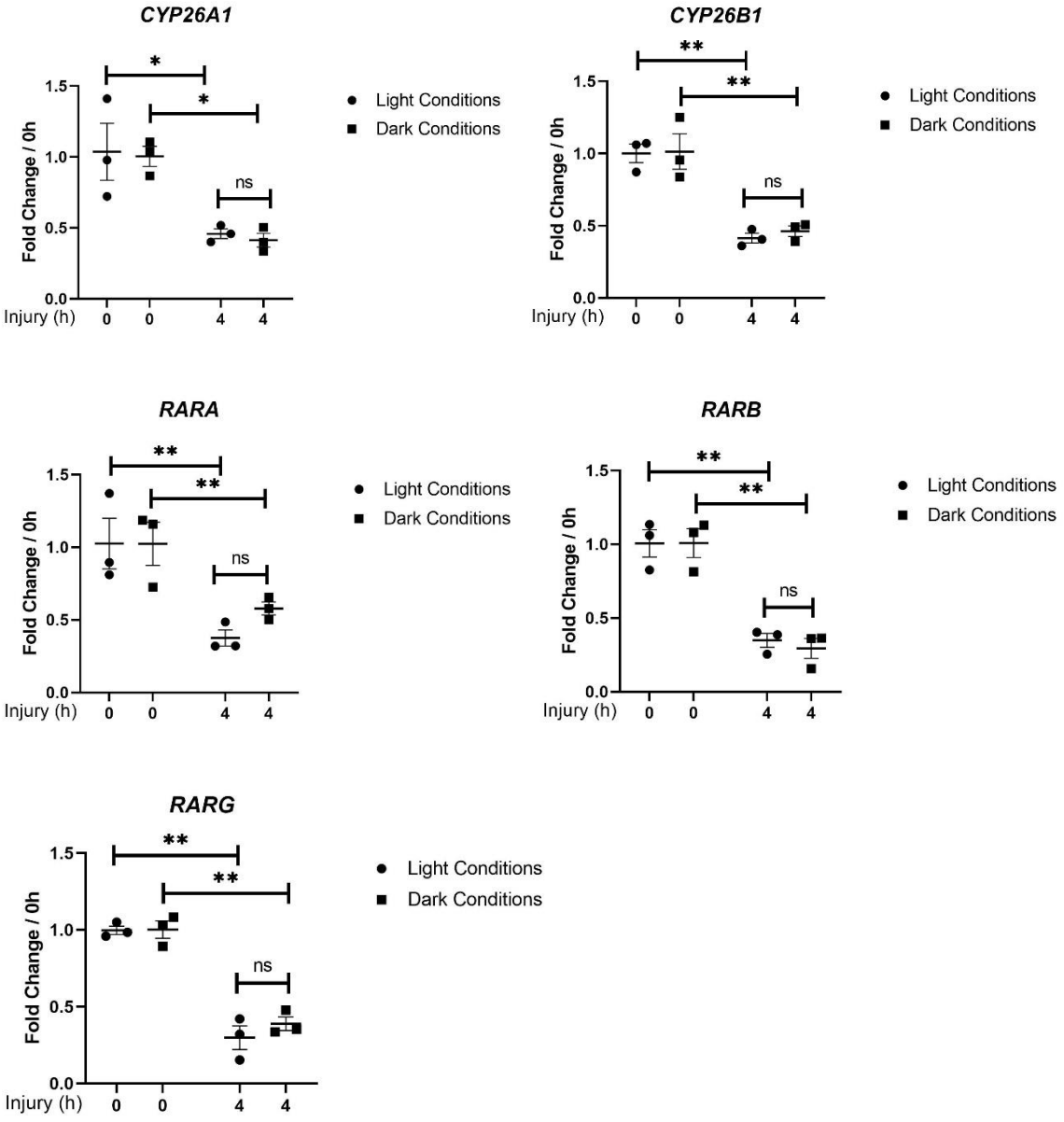

Figure 3.6: all-trans-retinoic (atRA)-responsive genes are downregulated on cartilage injury in both light and dark conditions.

Porcine metacarpophalangeal (MCP) joints were decontaminated in 2% Virkon for 20 minutes before being equilibrated at 37°C, 5% CO_2 for 1 hour. The MCP joints were opened either in light or dark (under yellow light) conditions. Cartilage was rapidly explanted, in either of these varying light conditions. Explanted cartilage was either immediately snap frozen in liquid nitrogen (zero hour time point) or cultured in serum free DMEM for 4 hours at 37°C, 5% CO_2 before being snap frozen. RNA was subsequently extracted from the tissue and used in quantitative reverse transcriptase-polymerase chain reaction to measure a panel of atRA-responsive genes. Statistical significance of comparison between groups were conducted using a two-way ANOVA, with multiple comparisons corrected using Tukey's tests. Bars shows the mean ± SEM of 3 independent experiments (n= 3 separate trotters). ns= not significant, * = $P < 0.05$; ** = $P < 0.01$, by two-way ANOVA. CYP26A1 = Cytochrome P450 Family 26 Subfamily A Member 1, CYP26B1 = Cytochrome P450 Family 26 Subfamily B Member 1, RARA = Retinoic Acid Receptor Alpha, RARB = = Retinoic Acid Receptor Beta, RARG = = Retinoic Acid Receptor Gamma.

3.2.6 Oxygen tension does not affect the downregulation of atRA-responsive genes on cartilage injury

Having shown that varying light intensity does not affect the downregulation of atRA-responsive genes on cartilage injury, I next tested the role of varying oxygen tension during the injury response. The oxygen tension in cartilage is usually maintained between 2%–4%, significantly lower compared with other highly vascularised tissues, like skin or neural tissue [34, 342]. It was therefore important to ascertain that the downregulation of atRA-responsive genes seen on cartilage injury was not triggered by exposure of the cartilage to atmospheric oxygen tension (21%).

I conducted the cartilage injury assay under normoxic (21% O_2) or hypoxic conditions (2% O_2) using a hypoxic chamber located in an adjacent research facility. Four porcine trotters were equilibrated for 1 hour at 37°C, 5% CO_2, in the hypoxic chamber (2% O_2). An additional four trotters were equilibrated under normoxic conditions (21% O_2) on the same day in the Kennedy Institute. In both instances, an additional procedure was carried out ensuring that all tissue reagents were also equilibrated to their respective oxygen tension and

that culture conditions were also controlled. RNA was extracted from cartilage explants as previously described, converted to cDNA and gene analysis conducted using RT-PCR.

CYP26A1, *CYP26B1*, *RARA*, *RARB* and *RARG* gene expression fell by more than 50% on cartilage injury at four hours under both normoxic and hypoxic conditions compared to its respective zero hour values ($p < 0.01$) (Table 1.6). There was no statistically significant difference in the expression of *CYP26* genes and *RAR* genes at four hours between hypoxic and normoxic conditions (Fig 3.7).

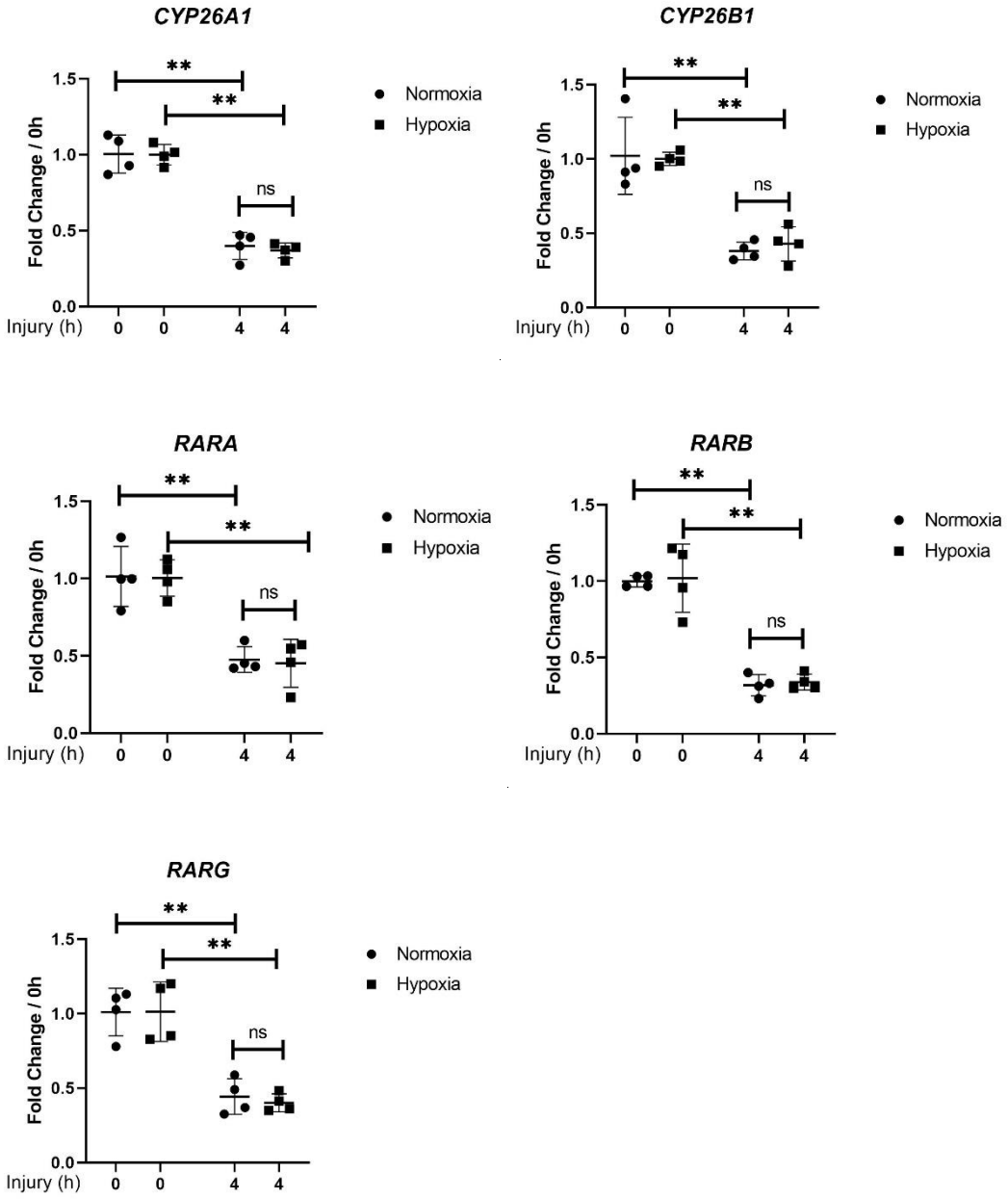

Figure 3.7: The downregulation of atRA-responsive genes on cartilage injury is unaffected by oxygen tension.

Porcine metacarpophalangeal (MCP) joints were decontaminated in 2% Virkon for 20 minutes before being equilibrated at 37°C, 5% CO_2 for 1 hour in either normoxic (21% O_2) or hypoxic (2% O_2) conditions. The MCP joints were then opened in either normoxic or hypoxic conditions and cartilage was rapidly explanted. Explanted cartilage was either immediately snap frozen in liquid nitrogen (zero hour time point) or cultured in serum free DMEM for 4 hours at 37°C, 5% CO_2, in either normoxic or hypoxic conditions before being snap frozen. RNA was subsequently extracted from the tissue and used in quantitative reverse transcriptase-polymerase chain reaction to measure a panel of atRA-responsive genes. Statistical significance of comparison between treatment groups was conducted using a two-way ANOVA, with multiple comparisons corrected using Tukey's tests. Bars shows the mean ±SEM of 4 independent experiments. ns= not significant, * = P < 0.05; ** = P < 0.01, by two-way ANOVA. CYP26A1 = Cytochrome P450 Family 26 Subfamily A Member 1, CYP26B1 = Cytochrome P450 Family 26 Subfamily B Member 1, RARA = Retinoic Acid Receptor Alpha, RARB = = Retinoic Acid Receptor Beta, RARG = = Retinoic Acid Receptor Gamma.

3.2.7 Oxygen tension does not affect the upregulation of inflammatory genes on cartilage injury

Next, I determined whether ambient oxygen level effected the inflammatory gene response on injury. I used the same cDNA samples from the trotter injury assay conducted in section 3.2.6 and measured the expression of inflammatory genes.

There was no significant difference in the upregulation of inflammatory genes on cartilage injury between normoxic and hypoxic environment. Collectively, these results indicated that the mechanosensitive response of atRA-responsive genes and inflammatory genes on cartilage injury were secondary to a true biological response to injury and not affected by environmental factors or artefact such as varying light intensity or artefact.

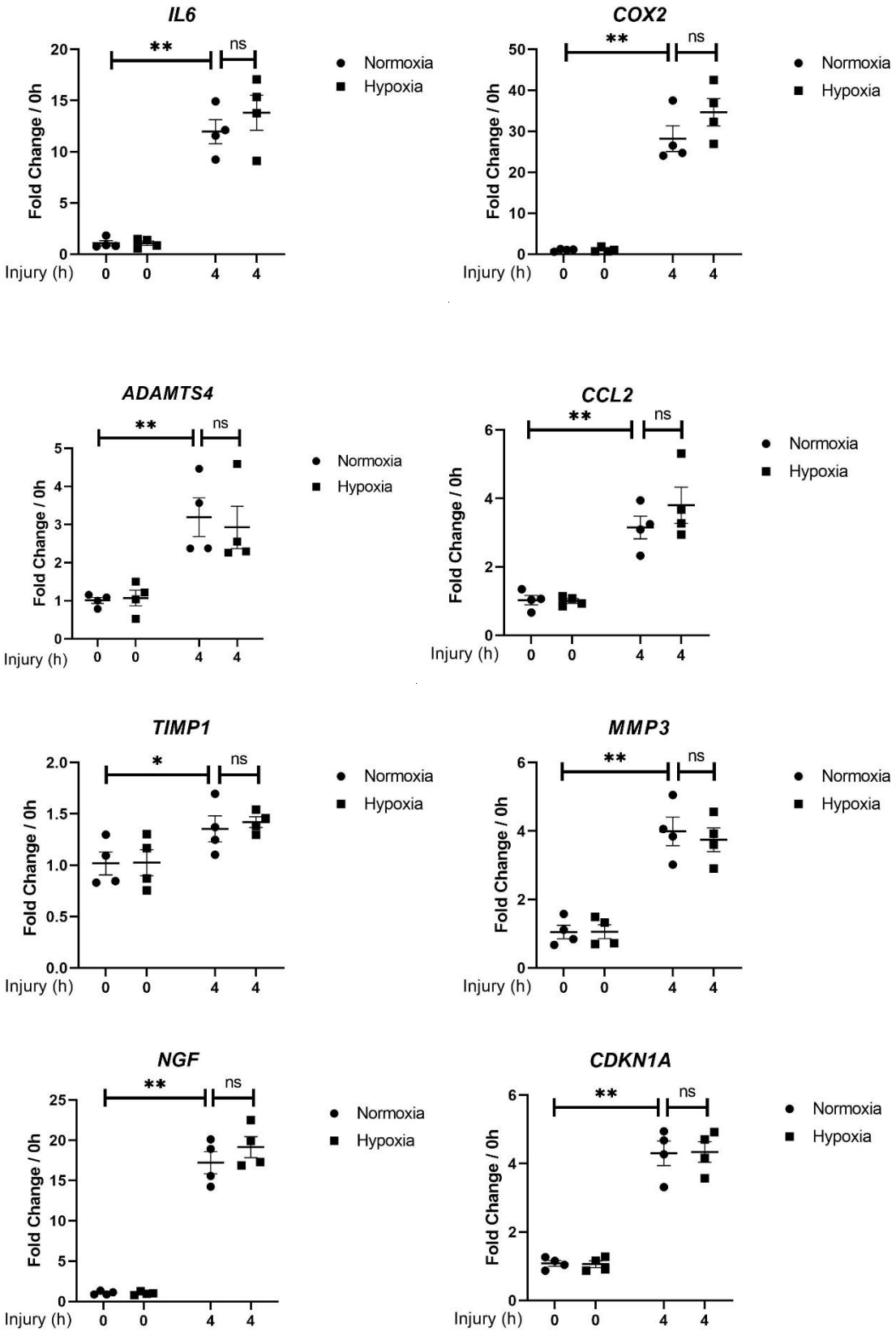
IL6
COX2
ADAMTS4
CCL2
TIMP1
MMP3
NGF
CDKN1A
Fold Change / 0h
Injury (h)
0 0 4 4
Normoxia
Hypoxia
**
*
ns

Figure 3.8: The upregulation of inflammatory genes on cartilage injury is unaffected by oxygen tension.

Porcine metacarpophalangeal (MCP) joints were decontaminated in 2% Virkon for 20 minutes before being equilibrated at 37°C, 5% CO_2 for 1 hour in either normoxic (21% O_2) or hypoxic (2% O_2) conditions. The MCP joints were then opened in either normoxic or hypoxic conditions and cartilage was rapidly explanted. Explanted cartilage was either immediately snap frozen in liquid nitrogen (zero hour time point) or cultured in serum free DMEM for 4 hours at 37°C, 5% CO_2, in either normoxic or hypoxic conditions before being snap frozen. RNA was subsequently extracted from the tissue and used in quantitative reverse transcriptase-polymerase chain reaction to measure a panel of atRA- responsive genes. Statistical significance of comparison between treatment groups was conducted using a two-way ANOVA, with multiple comparisons corrected using Tukey's tests. Bars shows the mean ±SEM of 4 independent experiments. ns= not significant, * = $P < 0.05$; ** = $P < 0.01$, by two-way ANOVA. IL6 = Interleukin 6, COX2= Cyclooxygenase-2, ADAMTS4 = ADAM Metallopeptidase With Thrombospondin Type 1 Motif 4, MMP3= Matrix metalloproteinase-3, CCL2= C-C Motif Chemokine Ligand 2, TIMP1= TIMP metallopeptidase inhibitor 1, CDKN1A= Cyclin Dependent Kinase Inhibitor 1A, NGF= Nerve growth factor.

3.3 Discussion

3.3.1 atRA-responsive genes are mechanosensitive

Mechanical injury is one of the biggest risk factors in the development of OA [2]. In recent years, various intracellular signalling pathways and transcription factors have been shown to be mechanosensitive (regulated by cartilage injury) [15, 16, 99]. A number of these were subsequently shown to have a functional role in the pathology of OA [14, 99]. I confirmed previous findings from the lab that atRA-responsive genes were equally sensitive to cartilage injury. atRA-responsive genes were consistently downregulated by four hours post cartilage injury. The key premise to this work was the identification of hypomorphic variants in the *ALDH1A2* gene as conferring a higher risk of developing hand OA [200, 201]. These studies showed that lower mRNA transcripts of *ALDH1A2* increased the risk of OA [200, 201]. The downregulation of atRA-responsive genes observed on cartilage injury was therefore congruous with these genetic studies. The results suggested that basal levels of atRA remained high in uninjured cartilage, but concentrations fall rapidly following cartilage injury. Either atRA biosynthesis was reduced, or it was degraded rapidly following injury; I investigated the mechanism by which atRA-responsive genes fall in the next chapter. atRA-responsive gene regulation was sustained to low levels for up to 24 hours following cartilage injury. This suggested that low levels of atRA in injured cartilage might not only have biological relevance, in the acute phase of injury, but also throughout the chronicity of disease. Although I did not investigate longer time courses, it would be interesting to investigate whether atRA-responsive genes recover fully after cartilage injury at longer time periods (more than 48 hours post cartilage injury).

The downregulation of atRA-responsive genes on cartilage injury was unaffected by variable light intensities or oxygen tension. Light exposure results in the photodegradation

of atRA into inactive polar metabolites, 13RA and 9RA, or even non-retinoid products [340, 341]. atRA has been commonly used in dermatological preparations, and it has been observed that atRA degradation is most rapid at 420nm wavelength of light [341]. Another study reported that the UVA portion of solar light is the major contributor of atRA photodegradation (420nm) [335]. Exposure of the trotter MCP joints to ambient light during experimentation could therefore be a key confounding factor in the downregulation of atRA-responsive genes on injury. However, given that atRA-responsive genes were downregulated equally in both ambient light and yellow light conditions, it is unlikely that higher light intensities were confounding the downregulation of atRA-responsive genes on cartilage injury. There may be another reason as to why atRA did not degrade in a light sensitive manner in these experiments. Inclusion of atRA in liposomes has been demonstrated to protect against photodegradation across a spectrum of wavelengths [343]. It is also possible that in my experiments cellular atRA was protected by the density of the extracellular matrix. It was also demonstrated that the downregulation of atRA-responsive genes on cartilage injury was unaffected by variable oxygen tension. atRA is known to react rapidly with molecular oxygen, where it undergoes auto-oxidation involving free radical chain reactions [344]. However, one study showed that radical-induced inactivation of atRA was only initiated at extremely high partial pressures of oxygen and not at levels that represent ambient conditions [345]. The consistent downregulation of atRA-responsive genes in both yellow light and low oxygen tension suggested that this was a true biological response to injury and not driven by an environmental artefact.

3.3.2 Mechanoinflammatory genes

I demonstrated that mechanical injury, induced by explanting porcine cartilage from an intact joint, caused an upregulation of inflammatory genes including *IL6*, *COX2*, *ADAMTS4*, *MMP3*, *CCL2*, *TIMP1*, *NGF* and *CDKN1A*. This injury-induced upregulation of inflammatory genes was demonstrated in other studies from our lab in both murine and porcine tissue [99, 123]. Inflammatory genes are thought to be induced by the activation of inflammatory signalling pathways: NF-κB, JNK and p38. This is driven by the upstream MAPKKK, TAK1 [99] (Figure 3.9). The use of a TAK1 inhibitor prevents NF-κB and JNK activation post injury and also suppresses the inflammatory gene response to injury [99]. The inflammatory gene response that occurs secondary to the activation of the inflammatory signalling pathways has been coined as "mechanoflammation" [2]. A number of these inflammatory genes have been investigated in in-vitro, in vivo and in clinical trials to establish their roles on OA pathogenesis. With the exception of NGF, very few of them have demonstrated to be good therapeutic target in OA, although many of them have support for a role in OA degradation in in-vitro.

COX2, *NGF* and *IL6* were three of the strongest upregulated genes on cartilage injury. *COX2* is a TAK1- sensitive gene and contains a number of NF-κB binding motifs in its promoter region [346]. *COX2* is the enzyme to catalyse the production of PGE_2 from arachidonic acid metabolism which increases the release of matrix degrading enzymes and inhibits proteoglycan synthesis [311], although there has been no direct in-vivo evidence that it is involved in OA pathogenesis [155]. I*L6* is another TAK1-sensitive gene [99]. IL6 cytokine binds to the IL6 receptor to activate downstream canonical signalling via JAK/STAT and non-canonical signalling via the MAPK and PI3 kinase cascade [347]. Higher IL6 concentrations in the serum and synovial fluid of OA patients have been correlated with

increased severity of disease [348]. Despite this, IL6 has been reported to exert both catabolic and protective roles in cartilage. Additional studies showed IL6 promoted proteoglycan synthesis in human OA chondrocytes, perhaps through stimulation of TIMPs [349]. However, more recent studies demonstrated that IL6 induces matrix-degrading enzymes MMP3, MMP13 and ADAMTSs which mediate cartilage degradation [160, 161]. Despite these in-vitro studies suggesting a role for IL6 in cartilage degradation, a large randomised control clinical trial which used an antagonist against the IL6 receptor failed to improve disease progression or OA-related symptoms in patients with hand OA (ClinicalTrials.gov Identifier: NCT02477059).

My studies also showed an upregulation of *MMP3* and *ADAMTS4* expression with injury. MMP3 protein is involved cartilage degradation with a broad substrate specificity for collagen II, III and IV [350]. It is also capable of degrading laminin, proteoglycans and fibronectin [350]. ADAMTS4 protein is elevated in early stages of OA [351]. ADAMTS4 is an aggrecan degrading enzyme; neutralising antibodies to ADAMTS4 in porcine cartilage and immunoprecipitation with anti-ADAMTS4 in bovine cartilage prevented cartilage ECM degradation following IL1 stimulation [352, 353]. Despite these findings, ADAMTS4 KO mice were not protected from developing OA [45] whereas ADAMTS5 KO mice demonstrated OA protection [46]. *ADAMTS5*, known to be regulated post translationally rather than the transcriptional level, is not strongly regulated at the transcriptional level on cartilage injury (unpublished data from our lab). This is consistent with very modest regulation on cartilage injury (data not shown). All metalloproteases are synthesised as zymogens; production of the active enzyme is achieved by cleavage of the prodomains by proprotein convertases [43]. Therefore, the biological function of active enzyme is determined by more than just an increase in the mRNA transcript of the gene.

CDKN1A was also upregulated on porcine cartilage injury. *CDKN1A* encodes a cyclin dependent kinase inhibitor and functions as a cell cycle regulator at G1. Although I saw an increase in *CDKN1A* expression on injury, one study demonstrated that *CDKN1A*-deficient mice were actually more susceptible to OA progression, implying *CDKN1A* provided protection in OA [354]. Being a cell cycle regulator, CDKN1A arrests cell in G1 inducing cell senescence. In cancer cells, CDKN1A prevents p53-induced cell apoptosis [355]. Therefore, the acute increase of *CDKN1A* gene expression on cartilage injury might illustrate a protective response by the injured chondrocytes to avoid cell death and obtain a senescent phenotype. However, achieving cell senescence might not confer benefit, as it can counteract the proliferative capability of injured chondrocytes and as such its ability to repair. In keeping with this, Leon et al. showed that the clearance of senescent cells attenuated the development of post-traumatic OA and increased the expression of cartilage tissue ECM proteins in an in-vivo mouse model [356].

Similar to *CDKN1A*, *TIMP1* gene was upregulated on porcine cartilage injury; however, it has been reported to have a protective role by regulating ECM homeostasis through inhibiting cartilage degrading MMPs [357]. An imbalance between TIMPs and MMPs is thought to contribute towards OA progression. The increase in *TIMP1* regulation in acute cartilage injury might therefore represent a protective mechanism by shifting the balance towards an anticatabolic state.

CCL2 gene increased modestly on cartilage injury. Raghu et al. in 2017 demonstrated that CCL2 and its receptor, CCR2, was increased in a mouse model of OA [358]. CCL2 is a primarily a chemoattractant to traffic CCR2-expressing monocytes to the site of injured cartilage. Although higher circulating levels of CCL2 were found in patients with OA, deletion of CCL2 or CCR2 do not alter cartilage degradation scores in murine OA but may alter pain responses [359]. *NGF* was upregulated by 20-fold on injury. Of all the

inflammatory genes I tested, only *NGF* has been established to have a role in OA pathology in both in-vitro, in-vivo and clinical studies [360, 361]. I discuss these in greater detail in the discussion section 3.3.3.

3.3.3 Manipulation of atRA levels and mechanoflammation in cartilage by talarozole

I explored the regulation of atRA-responsive genes (as a surrogate for atRA levels) after cartilage injury. Explantation of porcine articular cartilage or avulsion of murine femoral head cartilage caused rapid downregulation of atRA-responsive genes (*CYP26A1*, *CYP26B1* and retinoic acid receptors: *RARA*, *RARB* and *RARG* (data in review)). The drop in atRA post cartilage injury (40%–80%) occurred within the first 2–4 hours after injury and was sustained for at least 24 hours. Inhibition of injury-induced inflammatory signalling pathway after TAK1 inhibition prevented the drop in atRA-responsive genes on injury (Fig. 3.8) indicating that the effect of injury on atRA levels is dependent on intracellular inflammatory signalling.

As atRA is purported to be anti-inflammatory, I tested whether preventing the drop in atRA at the time of injury might suppress inflammatory gene regulation. An efficient way to increase endogenous atRA is to inhibit its metabolism using retinoic acid metabolism blocking agents (RAMBAs) that inhibit CYP26 activity. Preinjection of the porcine joint with the RAMBA TLZ prior to injury, maintained atRA levels. Moreover, TLZ prevented the upregulation of inflammatory gene regulation. In particular, TLZ prevented the upregulation of *IL6*, *COX2*, *ADAMTS4*, *CCL2*, *TIMP1* and *CDKN1A*. The suppressive action of TLZ on *IL6*, *COX2* and *ADAMTS4* regulation suggested that maintaining atRA levels might prevent putative degradative pathways and protect cartilage after injury. Conversely, TLZ also prevented the upregulation of *TIMP1* on injury, which is known to

inhibit *MMPs* and counteract cartilage degradation [61]. The TLZ-sensitive suppression of *CDKN1A* expression on cartilage injury suggests a role for atRA in chondrocyte senescence. Chondrocytes are known to possess poor proliferative capabilities compared to other cell types like vascular cells or hepatocytes. Therefore, the ability of atRA to suppress *CDKN1A* might enable chondrocytes to maintain a more proliferative phenotype capable of initiating repair.

Interestingly, TLZ further enhanced the upregulation of *MMP3* on cartilage injury. [49]. The finding that raised atRA levels in the cartilage increased *MMP3* expression conflicts the anti-inflammatory effects atRA has on the other inflammatory genes measured. The reasons for this was explored in Chapter 7.

NGF gene expression was not suppressed by the action of TLZ. Anti-NGF therapy has been demonstrated to improve pain in patients with hip and knee OA in a phase III study [198]. A supportive in-vivo study by our group showed that active immunisation against NGF attenuated chronic pain behaviour in murine OA [361]. In addition, intra-articular injection of NGF induces sensitisation and knee hyperalgesia in mice [362]. The maintenance of atRA levels did not suppress *NGF*, suggesting that although atRA exerts an anti-inflammatory effect in the joint it does not influence all inflammatory genes such as *NGF*. Therefore, if TLZ is to be used therapeutically in OA, it might not actually target all OA-related symptoms, like pain.

3.3.4 RAMBAs as a new therapeutic target in OA

atRA itself has been used as an agent in the treatment of a number of conditions including acne, psoriasis, Kaposi's sarcoma and acute promyelocytic leukaemia [363]. However, its

use is limited by stability of the molecule and route of administration. Both topical and oral administration of atRA causes the auto-induction of endogenous CYP26 enzymes, leading to degradation of endogenous atRA [363]. Inappropriate metabolism of endogenous retinoids by CYP26 enzymes can promote retinoid deficiency resulting in skin desquamation and hyperkeratinisation [363]. The use of RAMBAs as medicinal agents is a more tractable approach, as it increases endogenous atRA by circumventing the auto-induction process. RAMBAs share CYP26 inhibitory activity through active azole structures and include a number of agents in clinical use [363]. Ketoconazole, (currently used as an antifungal agent), was the first identified RAMBA after being shown to inhibit CYP-mediated degradation of atRA in rat liver microsomes [364]. A more selective RAMBA in atRA metabolism, liarozole was then identified and successfully used in phase III trials for prostate cancer [365] and psoriasis [366]. Liarozole inhibits CYP26 with an IC50 value between 2.2 and 6.0 uM [365]. In rats, liarozole was shown to decrease the elimination of plasma atRA post IV administration [242]. Despite early successes in clinical trials, subsequent use was suspended because of severe adverse effects, mostly secondary to the nonspecific effects on other CYP isozymes, including CYP17 and CYP19 (also known as aromatase).

The nonselective inhibitory action of liarozole and ketoconazole on CYP-enzymes created a demand for an agent that better targeted atRA degradation without off-target actions, especially upon androgen metabolism. This led to a third-generation RAMBA, TLZ, which conferred high specificity [334]. TLZ inhibits atRA degradation in the nanomolar concentration (IC50 value = 4 nM). Within this therapeutic range, TLZ only exerts minimal effects on the inhibition of the CYP-dependent enzymes involved in steroid biosynthesis. TLZ has been used successfully in phase II clinical trials in the treatment of psoriasis and acne [334]. Interestingly, in many of the patients who participated in the clinical trials with TLZ, the plasma level of atRA did not rise beyond physiological levels [334]. In addition,

the adverse effects reported were restricted to mild skin changes in comparison to the other RAMBAs. Our lab has shown that administration of TLZ, via osmotic mini-pumps, modified disease progression and reduced osteophyte size in a murine OA model (Zhu, Kamalathevan, et al. manuscript in revision). These data suggest that RAMBAs, either through suppression of mechanoflammation or through an alternative mechanism could be repurposed in clinical trials of OA patients to study structural changes, joint function and pain.

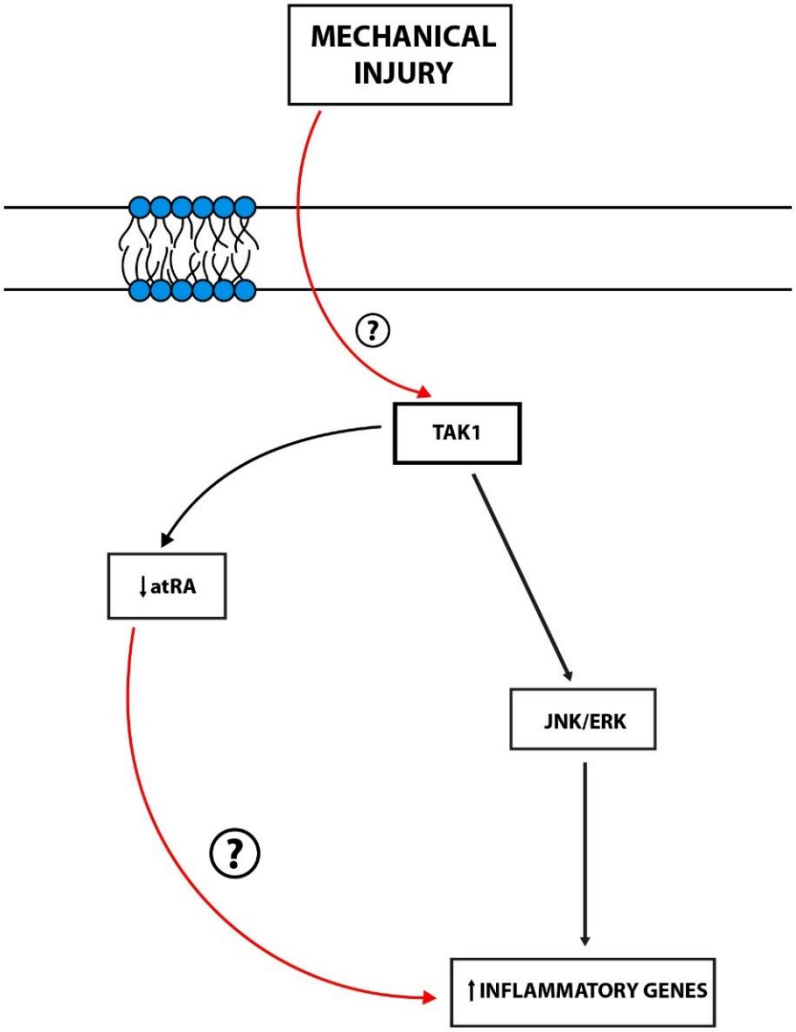

Figure 3.9: Schematic representing working hypothesis achieved at the end of Chapter 3

Mechanical injury phosphorylates transforming growth factor beta-activated kinase 1 (TAK1) which phosphorylates downstream Jun N-terminal kinase (JNK) and extracellular signal-regulated kinase (ERK) (possible also involving NF-κB) resulting in an upregulation of inflammatory genes. All-trans-retinoic acid (atRA)-responsive genes are downregulated on cartilage injury in a TAK-1 sensitive manner but p38- and ERK-independent, manner The mechanism by which atRA-responsive genes are downregulated and how atRA suppresses inflammatory gene regulation on cartilage injury were addressed next. Red line = undetermined; black line = full activation; black dotted line = partial activation.

4 CHAPTER 4: DETERMINING THE CAUSE FOR THE DROP IN atRA-RESPONSIVE GENES ON CARTILAGE INJURY.

4.1 Introduction

In Chapter 3 I showed that atRA-responsive genes are rapidly downregulated on cartilage injury and that maintaining endogenous levels of atRA in the cartilage, by the use of a RAMBA, has a marked anti-inflammatory effect by suppressing mechano-inflammatory genes. Historical data from our lab has revealed that the downregulation of atRA-responsive genes is also TAK1-sensitive (unpublished) (Fig 1.8). Furthermore, inhibiting TAK1, strongly suppresses some key injury induced inflammatory genes such as *IL6*, *COX2* and *ADAMTS4* [99].

Thorough search of the literature revealed that the general redox state of the cell can also influence intracellular atRA concentrations [324]. In particular, cPLA2-generated 4-HNE has been implicated in decreasing atRA levels in retinal pigment epithelial cells by inhibiting the ALDH1A2 enzyme [367]. cPLA2 is an enzyme involved in the generation of arachidonic acid from PUFAs in the lipid bilayer membrane [311]. Arachidonic acid is further metabolised by 12/15 LOX enzymes into various lipid metabolites, such 12-HETE and 15-HETE. The generation of 4-HNE is highly dependent on ROS, which depletes intracellular GPx and thereby diverts 12- and 15-HETE into lipid peroxidation forming 4-HNE [288]. 4-HNE, itself has been demonstrated to have catabolic effects on cartilage within in-vitro studies [316, 322].

ROS has been long associated with chronic diseases and investigated in the OA research domain extensively [276, 285]. There are two main sites for ROS generation in the cartilage: one is via the mitochondria (60%), and the other is through a membrane protein complex called NADPH oxidase. Antioxidants are reducing agents which either sequester ROS

globally in cells (e.g. NAC) or specifically target mitochondrial ROS generation (e.g. Co-enzyme Q10) and NOX (NOX inhibitors).

In this chapter, I investigated the factors that determined the fall in atRA-responsive genes on cartilage injury. In particular, I studied whether the downregulation of atRA-responsive genes was dependent on cPLA2 and ROS-mediated pathways.

4.2 Results

4.2.1 4-HNE downregulates atRA-responsive genes in-vitro

Having determined that the drop in atRA-responsive genes on cartilage injury was likely due to a true biological response to injury and having characterised the pattern of this drop, I next investigated the factors that led to this drop.

A thorough search of the literature drew my attention to the cytosolic phospholipase A2 (cPLA2) pathway and the generation of 4-hydroxynonenal (4-HNE) as a potential mechanism by which atRA-responsive genes are downregulated [324]. cPLA2 is a peripheral membrane protein that liberates arachidonic acid from membrane phospholipids. Arachidonic acid is further metabolised by downstream enzymes 12- and 15-lipoxygenase (12- and 15-LOX) to the corresponding hydroperoxyeicosatetraenoic acids (12- and 15-HpETE) which are further oxidised, in the presence of reactive oxygen species (ROS), to the lipid peroxidation product 4-hydroxynoneal (4-HNE) [368]. 4-HNE is considered to be the most toxic α,β-unsaturated aldehyde formed from ω-6 polyunsaturated fats [369].

On this premise, I tested whether exogenous 4-HNE regulated atRA-responsive genes in primary chondrocytes. Primary porcine chondrocytes were isolated from trotter MCP joints and stimulated with 10 µM 4-HNE, 20 µM 4-HNE, 0.5 µM TLZ or DMSO (vehicle). These concentrations are in keeping with reported physiological ranges [369].

Treatment of primary porcine chondrocytes with TLZ resulted in a significant upregulation of atRA-responsive genes (*CYP26A1*, *CYP26B1*, *RARA* and *RARG*, $p < 0.01$; *RARB*, $p < 0.05$, by one-way ANOVA with multiple comparisons corrected using Tukey's tests), *CYP26A1* (2.5-fold, $p < 0.01$), *CYP26B1* (1.8-fold, $p < 0.01$), *RARA* (1.6-fold, $p < 0.01$), *RARB* (1.6-fold, $p < 0.05$) and *RARG* (2.2-fold, $p < 0.01$). Treatment with 20 µM 4-HNE

significantly downregulated *CYP26A1* ($p < 0.01$) and *RARA* ($p < 0.05$). The expression of *CYP26A1* and *RARA* with 20µM 4-HNE dropped by more than 50% compared to vehicle. A lower concentration of 10 µM 4-HNE resulted in a downward trend in the expression of *CYP26A1* and *RARA*, but this did not reach statistical significance. Although *CYP26B1* and *RARB* expression revealed a downward trend when treated with low and high concentrations of 4-HNE, neither reached statistical significance. 10 µM of 4-HNE downregulated *RARG* by more than 50% to reach statistical significance, and this was also the case when treated with 20 µM 4-HNE ($p < 0.01$) (Fig 4.1).

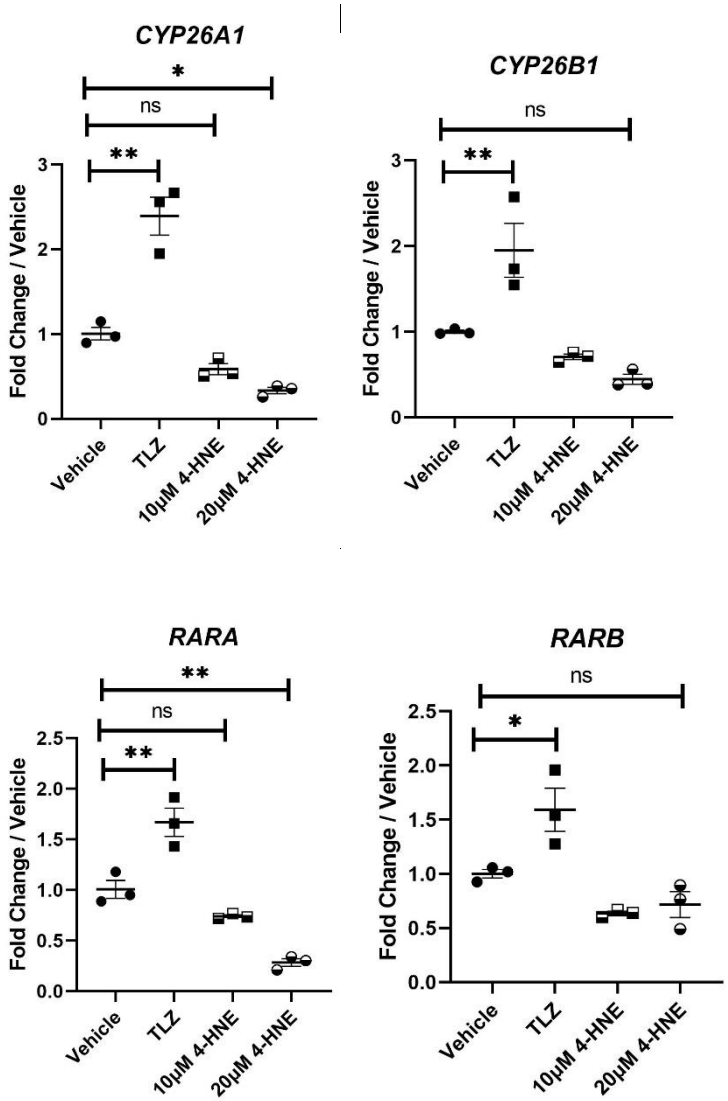

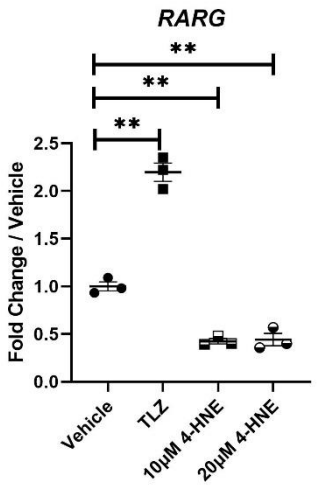

Figure 4.1: 4-HNE downregulates atRA-responsive genes in isolated porcine chondrocytes.

Porcine metacarpophalangeal (MCP) joints were decontaminated in 2% Virkon for 20 minutes before being equilibrated at 37°C, 5% CO_2 for 1 hour. The MCP joints were opened and cartilage explanted. Explanted cartilage was incubated with collagenase (1mg per ml per 1g of cartilage) for 6 hours at 37. Collagenase digest was centrifuged at 500X g for 5minutes. Pellets were washed and suspended in 10% fetal bovine serum (FBS). Cell were plated at a density of 1 million per well in DMEM with 10% FBS and 25 mmol of Hepes, penicillin/streptomycin and amphotericin for 24 hours. Cells were incubated for a further 24 hours in serum-free DMEM and then stimulated for 4 hours with either 0.5 µM talarozole (TLZ), 10 µM 4-hydroxynoneal (4-HNE), 20 µM 4-HNE or vehicle control. RNA was subsequently extracted from the tissue, converted to cDNA and used in quantitative reverse transcriptase-polymerase chain reaction (RT-PCR) to measure a panel of atRA-responsive genes. Statistical significance of comparison between groups was conducted using a two-way ANOVA, with multiple comparisons corrected using Tukey's tests. Bars shows the mean ±SEM of 3 independent experiments (separate trotters). ns= not significant, * = $P < 0.05$; ** = $P < 0.01$, by two-way ANOVA. CYP26A1 = Cytochrome P450 Family 26 Subfamily A Member 1, CYP26B1 = Cytochrome P450 Family 26 Subfamily B Member 1, RARA = Retinoic Acid Receptor Alpha, RARB = = Retinoic Acid Receptor Beta, RARG = = Retinoic Acid Receptor Gamma.

4.2.2 cPLA2 is phosphorylated on cartilage injury

Having observed that atRA-responsive genes are downregulated by 4-HNE treatment of primary porcine chondrocytes, I next explored whether the upstream membrane-bound protein, cPLA2, was activated on cartilage injury. As discussed, 4-HNE is generated downstream of arachidonic acid metabolism, which itself is liberated from the phospholipid membrane by the enzymatic action of cPLA2 [370].

It is important to note that the activation of cPLA2 is dependent on its phosphorylation. Therefore, I investigated the phosphorylation of cPLA2 by western blot analysis at short time points following cartilage injury (0 hours, 5 mins, 10 mins and 30 mins).

Porcine cartilage explants were cultured for various periods of time mentioned above in serum-free media, and tissue lysates were extracted for western blotting. Lysates were run on 10% SDS PAGE gel and immunoblotted for cPLA2 (Fig 4.2A). The signal was enhanced by use of chemiluminescence and subsequently visualised using autoradiography. The membrane was stripped and reprobed for total-ERK (tERK) used as a loading control (Fig 4.2B).

In the ex-vivo tissue (zero hour), I demonstrated no basal phosphorylation of cPLA2. The time-course experiments demonstrated phosphorylation at 10 mins which was sustained at 30 mins.

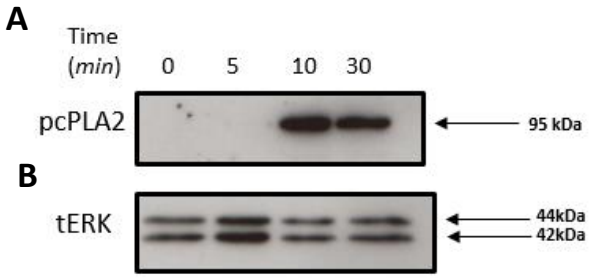

Figure 4.2: cPLA2 is phosphorylated on porcine cartilage injury.

Porcine metacarpophalangeal (MCP) joints were decontaminated in 2% Virkon for 20 minutes before being equilibrated at 37°C, 5% CO_2 for 1 hour. The MCP joints were opened and cartilage was rapidly explanted, as described in Materials and Methods. Explanted cartilage was either immediately cooled in ice-cold 1X RIPA Buffer or cultured for various periods of time after explanation (5min, 10min and 30min) in serum free DMEM at 37°C, 5% CO_2 before being transferred to ice cold, 1X RIPA buffer. Explants with 1X RIPA buffer, were mildly shaken for 45 minutes at 4°C. Lysates were run on 10% Sodium Dodecyl Sulphate-Polyacrylamide Gel (SDS PAGE) and transferred to poly (vinylidene) (PVDF) membrane. PVDF membrane was blocked in 5% milk for 1 hour at room temperature, incubated overnight in 1:1000 primary antibody (pcPLA2), washed 3 times in 1X TBST and incubated for a further hour in 1:2000 secondary antibody. pcPLA2 signal was enhanced by use of chemiluminescence (A Upper) and subsequently visualised using autoradiography. The blot was stripped and re-probed for total ERK (B Lower).

4.2.3 cPLA2 inhibition suppresses the phosphorylation of cPLA2 on cartilage injury

Having shown that cPLA2 was phosphorylated on cartilage injury, I further validated these findings. To do so, I used a commercial inhibitor to cPLA2 (palmityl trifluoromethyl ketone, PACOCF3, Sigma Aldrich). The catalytic activity of cPLA2 is enhanced by phosphorylation at Ser505 [307]. PACOCF3 has an IC50 value of 3.8 μM and blocks the Ser505 phosphorylation site on cPLA2, thereby decreasing its enzymatic activity. Inhibition of cPLA2 by PACOCF3 has been previously reported in neurites in the context of neuronal death response [371].

To see whether PACOCF3 inhibits the phosphorylation of cPLA2 on cartilage injury, trotter MCP joints were injected with 1 ml of DMEM with 10 μM cPLA2 inhibitor (PACOCF3) or vehicle. The joints were then left for a further 1 hour to equilibrate at 37°C before being opened and the cartilage rapidly explanted. Explanted cartilage was either immediately transferred into cold 1X lysis buffer (zero hour time point) or cultured for various amounts of time (5 mins, 10 mins and 30 mins). Porcine tissue lysates were resolved by 10% SDS PAGE and immunoblotted for pcPLA2 as described above. Quantification of three separate experiments (three separate trotters) was performed using FIJI-App, ImageJ-win64 Gel Analysis software. Results were normalised to tERK and statistical significance of comparison between groups analysed by a two-way ANOVA, with post hoc multiple comparisons corrected using Tukey's tests.

The phosphorylation of cPLA2 was reduced by prior injection with PACOCF3 compared to vehicle control (Fig 4.3A). tERK was measured in both cPLA2i-injected and vehicle-injected samples as the loading control (Fig 4.3B). Quantification of three separate experiments (n = 3) (Fig 4.3C) showed that pcPLA2 (normalised to tERK) was significantly increased between 5 mins and 10 mins in control samples. There was a marked reduction in the phosphorylation of cPLA2 by 71.5% (SD ±1.21) at 30 mins in those samples treated with PACOCF3 compared to vehicle control.

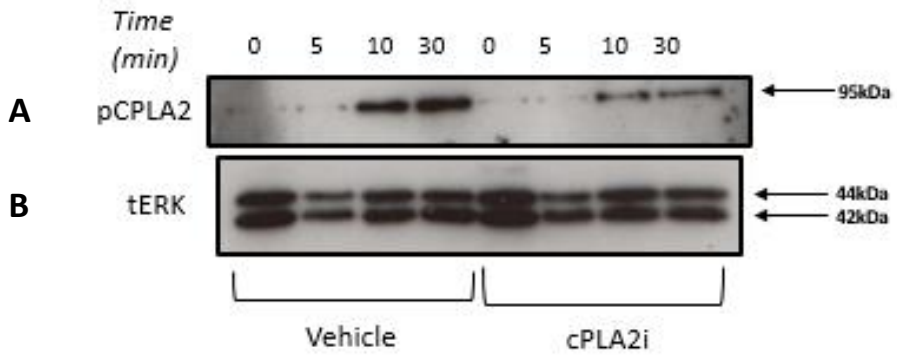

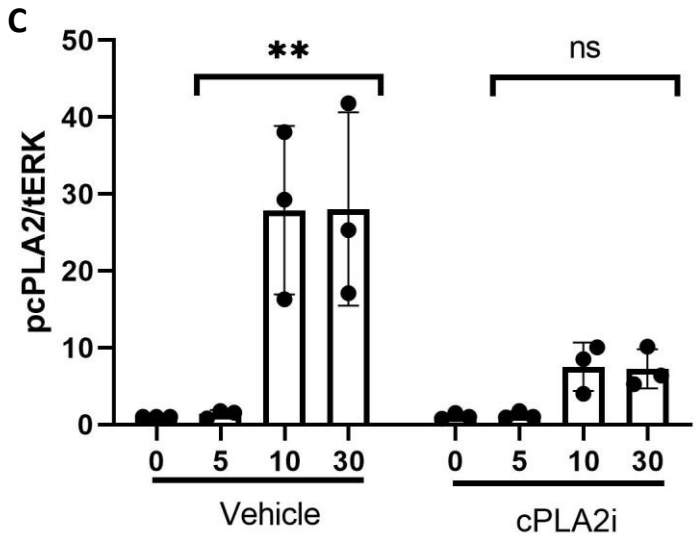

Figure 4.3: cPLA2 inhibition suppresses the phosphorylation of cPLA2 on cartilage injury.

Porcine metacarpophalangeal (MCP) joints were decontaminated in 2% Virkon for 20 minutes before being equilibrated at 37°C, 5% CO_2 for 1 hour. MCP joints were injected with either 10 µM cPLA2 inhibitor (cPLA2i) or vehicle control and incubated for another 1 hour at 37 °C. The MCP joints were opened and cartilage was rapidly explanted, as described in Materials and Methods. Explanted cartilage was either immediately cooled in ice-cold 1X RIPA Buffer nitrogen (zero hour time point) or cultured in serum free DMEM with or without cPLA2i for various periods of time (5min, 10min and 30min) at 37 °C, 5% CO_2 before being transferred to ice cold, 1X RIPA buffer. Explants with 1X RIPA buffer, were mildly shaken for 45 minutes at 4°C. Lysates were run on 10% Sodium Dodecyl Sulphate-Polyacrylamide Gel (SDS PAGE) and transferred to poly (vinylidene) (PVDF) membrane. PVDF membrane was blocked in 5% milk for 1 hour at room temperature, incubated overnight in 1:1000 primary antibody (pcPLA2), washed 3 times in 1X TBST and incubated for a further hour in 1:2000 secondary antibody. pcPLA2 signal was enhanced by use of chemiluiminescence (A Upper) and subsequently visualised using autoradiography. A representative blot of three separate experiments is shown (A). The blot was stripped and re-probed for total ERK (B Lower). The quantification of three separate experiments testing pcPLA2 was performed using FIJI-App, ImageJ-win64 Gel Analysis software and normalised to total ERK (C).

4.2.4 Downregulation of atRA-responsive genes on cartilage injury is cPLA2-sensitive

Having showed that cPLA2 was activated at 10 and 30 mins post cartilage injury and that this signal was suppressed by the use of a commercial inhibitor to cPLA2 (PACOCF3), I next explored whether the downregulation of atRA-responsive genes on cartilage injury was

prevented by the use of PACOCF3. At this point, I hypothesised that blocking cPLA2 phosphorylation would prevent the downregulation of atRA-responsive genes on injury.

Trotter MCP joints were left to equilibrate for 1 hour at 37°C prior to being injected with 1 ml of serum-free media with inhibitor (PACOCF3 (cPLA2i) (10 μM) or vehicle control (DMSO). I subsequently conducted the trotter injury assay; RNA was extracted and converted to cDNA, and RT-PCR was conducted to investigate the expression of a panel of atRA-responsive genes. Each atRA-responsive gene expression was normalised to *18S* and expressed relative to its normalised zero hour time points (n = 9 separate trotters). Statistical significance of comparison between treatment groups was performed using a two-way ANOVA, with multiple comparisons corrected using post hoc Tukey's tests.

PACOCF3 reversed the downregulation of *CYP26A1* by 100% (SD ± 0.138) on cartilage injury, where it was able to prevent the injury-induced downregulation of *CYP26B1*, *RARA* and *RARG* by 72% (SD ± 0.093), 84% (SD ± 0.119) and 54% (SD ± 0.052), respectively (Fig 4.4).

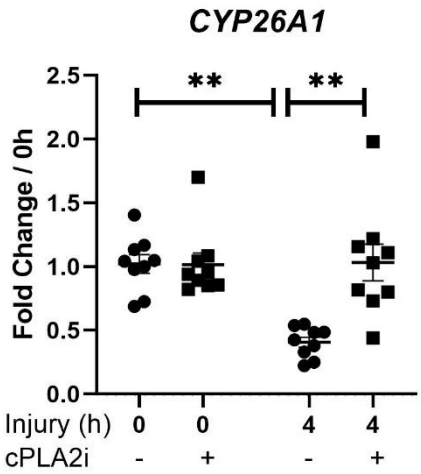
CYP26A1
**
**
Fold Change / 0h
2.5
2.0
1.5
1.0
0.5
0.0
Injury (h) 0 0 4 4
cPLA2i - + - +

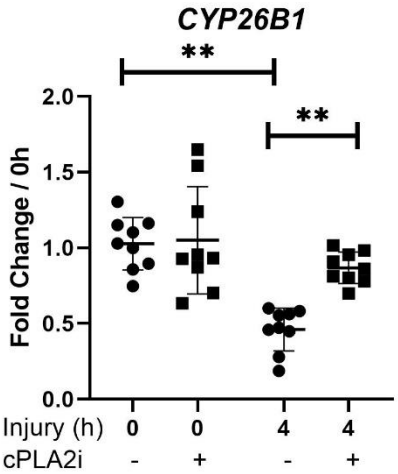
CYP26B1
**
**
Fold Change / 0h
2.0
1.5
1.0
0.5
0.0
Injury (h) 0 0 4 4
cPLA2i - + - +

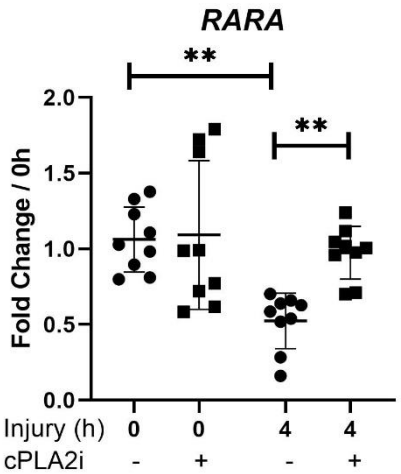
RARA
**
**
Fold Change / 0h
2.0
1.5
1.0
0.5
0.0
Injury (h) 0 0 4 4
cPLA2i - + - +

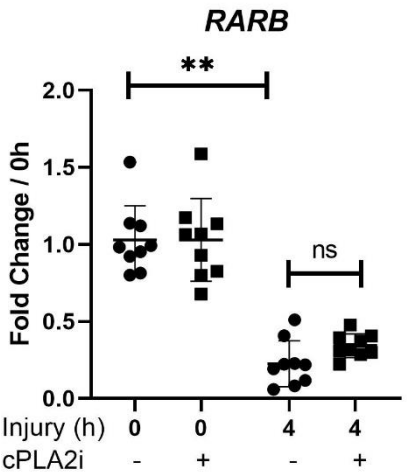
RARB
**
ns
Fold Change / 0h
2.0
1.5
1.0
0.5
0.0
Injury (h) 0 0 4 4
cPLA2i - + - +

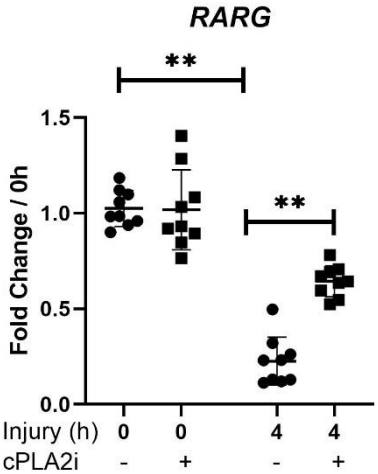
RARG
**
**
Fold Change / 0h
1.5
1.0
0.5
0.0
Injury (h) 0 0 4 4
cPLA2i - + - +

Figure 4.4: cPLA2 inhibition prevents the downregulation of atRA-responsive genes on cartilage injury.

Porcine metacarpophalangeal (MCP) joints were decontaminated in 2% Virkon for 20 minutes before being equilibrated at 37 °C, 5% CO_2 for 1 hour. MCP joints were injected with either 10 µM cPLA2 inhibitor (cPLA2i) or vehicle control and incubated for another 1 hour at 37 °C. The MCP joints were opened and cartilage was rapidly explanted. Explanted cartilage was either immediately snap frozen in liquid nitrogen (zero hour time point) or cultured in serum free DMEM with or without cPLA2i for 4 hours at 37 °C, 5% CO_2 before being snap frozen. RNA was subsequently extracted from the tissue and used in quantitative reverse transcriptase-polymerase chain reaction to measure a panel of atRA-responsive genes. Statistical significance of comparison between treatment groups was conducted using a two-way ANOVA, with post-hoc multiple comparisons corrected using Tukey's tests. Bars shows the mean ± SEM of 3 independent experiments in which each experiment was performed on 3 individual trotter joints (n= 9 separate trotters). ns = not significant, * = $P < 0.05$; ** = $P < 0.01$, by two-way ANOVA. CYP26A1 = Cytochrome P450 Family 26 Subfamily A Member 1, CYP26B1 = Cytochrome P450 Family 26 Subfamily B Member 1, RARA = Retinoic Acid Receptor Alpha, RARB = = Retinoic Acid Receptor Beta, RARG = = Retinoic Acid Receptor Gamma.

4.2.5 Upregulation of inflammatory genes on cartilage injury is cPLA2-sensitive

Having determined that the downregulation of atRA-responsive genes on cartilage injury was cPLA2-sensitive, I wanted to determine whether the use of a cPLA2 inhibitor (PACOCF3) suppressed the injury-induced upregulation of inflammatory genes in the same experimental samples generated from section 4.2.4. Multiple PLA2 isoforms have already been shown to be expressed and stimulated by pro-inflammatory stimuli in OA chondrocytes [372].

I measured the gene expression of a panel of inflammatory genes known to be induced by injury using the cDNA samples collected from the experiment conducted in section 4.2.4.

PACOCF3 suppressed *IL6* and *COX2* upregulation by 75% (SD ± 2.66) and 72% (SD ± 3.14), respectively, whereas it suppressed the upregulation of *ADAMTS4* and *MMP3* by 97% (SD ± 0.319) and 90% (SD ± 0.659), respectively (Fig. 4.5). The induction of *TIMP1* on cartilage injury was also suppressed by PACOCF3 ($p < 0.05$) although to a weaker extent by only 58% (SD ± 0.262).

The use of PACOCF3 had no effect on the upregulation of *CDKN1A*, *CCL2* and *NGF*.

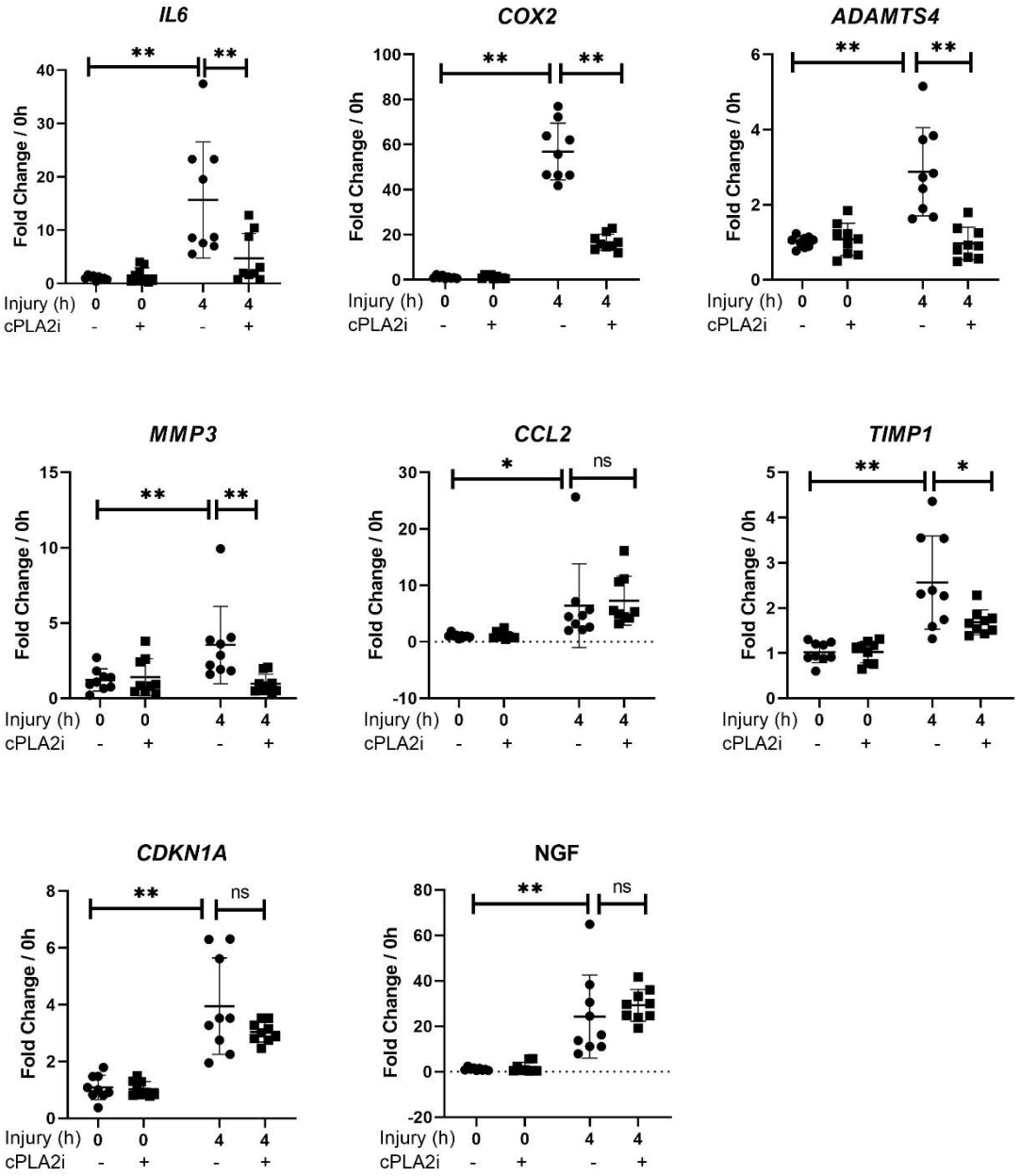

Figure 4.5: cPLA2 inhibition suppresses the upregulation of inflammatory genes on cartilage injury.

Porcine metacarpophalangeal (MCP) joints were decontaminated in 2% Virkon for 20 minutes before being equilibrated at 37 °C, 5% CO_2 for 1 hour. MCP joints were injected with either 10 µM cPLA2 inhibitor (cPLA2i) or vehicle control and incubated for another 1 hour at 37 °C. The MCP joints were opened and cartilage was rapidly explanted as described in Materials and Methods. Explanted cartilage was either immediately snap frozen in liquid nitrogen (zero hour time-point) or cultured in serum free DMEM with or without cPLA2i for 4 hours at 37 °C, 5% CO_2 before being snap frozen. RNA was subsequently extracted from the tissue and used in quantitative reverse transcriptase-polymerase chain reaction to measure a panel of inflammatory genes. Statistical significance of comparison between treatment groups was conducted using a two-way ANOVA, with post-hoc multiple comparisons corrected using Tukey's tests. Bars shows the mean ± SEM of 3 independent experiments in which each experiment was performed on 3 individual trotter joints (n= 9 separate trotters). ns = not significant, * = $P < 0.05$; ** = $P < 0.01$, by two-way ANOVA. IL6 = Interleukin 6, COX2= Cyclooxygenase-2, ADAMTS4 = ADAM Metallopeptidase With Thrombospondin Type 1 Motif 4, MMP3= Matrix metalloproteinase-3, CCL2= C-C Motif Chemokine Ligand 2, TIMP1= TIMP metallopeptidase inhibitor 1, CDKN1A= Cyclin Dependent Kinase Inhibitor 1A, NGF= Nerve growth factor.

4.2.6 Downregulation of atRA-responsive genes on cartilage injury is 12/15 LOX-sensitive

In order to further interrogate the hypothesis that the downregulation of atRA-responsive genes on cartilage injury was cPLA2-sensitive, I used a commercial inhibitor to the enzymes downstream of cPLA2 but upstream of 4-HNE generation. 12- and 15-lipoxygenases (12/15 LOX) principally act downstream of cPLA2 metabolising PUFAs, catalysing the oxidation of arachidonate resulting in the formation of 12-hydroxyperoxyeicosa-tetraenoic acid (12-HpETE) and 15-hydroxyperoxyeicosa-tetraenoic (15-HpETE), respectively [373]. Free radical–induced inactivation of GPx diverts 12- and 15-HpETE to the peroxidation pathway and results in the formation of lipid peroxidation products, including 4-HNE [374]. Given that cPLA2 inhibition prevented the downregulation of atRA-responsive genes on cartilage injury, I used a combined commercial inhibitor to 12/15LOX and discerned if the effect was similar to inhibiting cPLA2.

I used the 12/15 lipoxygenase inhibitor, ML351, from Sigma Aldrich. ML351 has an IC50 value of 200 nM for both 12-and 15-LOX and I used a concentration of 1 µM in trotter MCP joints and conducted the same porcine injury assay as described above. Explants were collected at zero and four hours post cartilage injury in MCP joints injected with either vehicle or 1 µM of ML351.

Following RNA extraction and cDNA synthesis, RT-PCR was used to measure the expression of a panel of atRA-responsive genes. Both *CYP26* genes and *RAR* gene expression fell by more than 50% on cartilage injury compared to injured vehicle-injected joints by four hours (Fig 4.6). The use of ML351 significantly suppressed the downregulation of *CYP26A1* (100%, SD ± 0.078), *CYP26B1* (100%, SD ± 0.093), *RARB* (35%, SD ± 0.091) and *RARG* (34%, SD ± 0.052) (Fig 4.6). However, ML351 had no effect on the downregulation of *RARA* on cartilage injury.

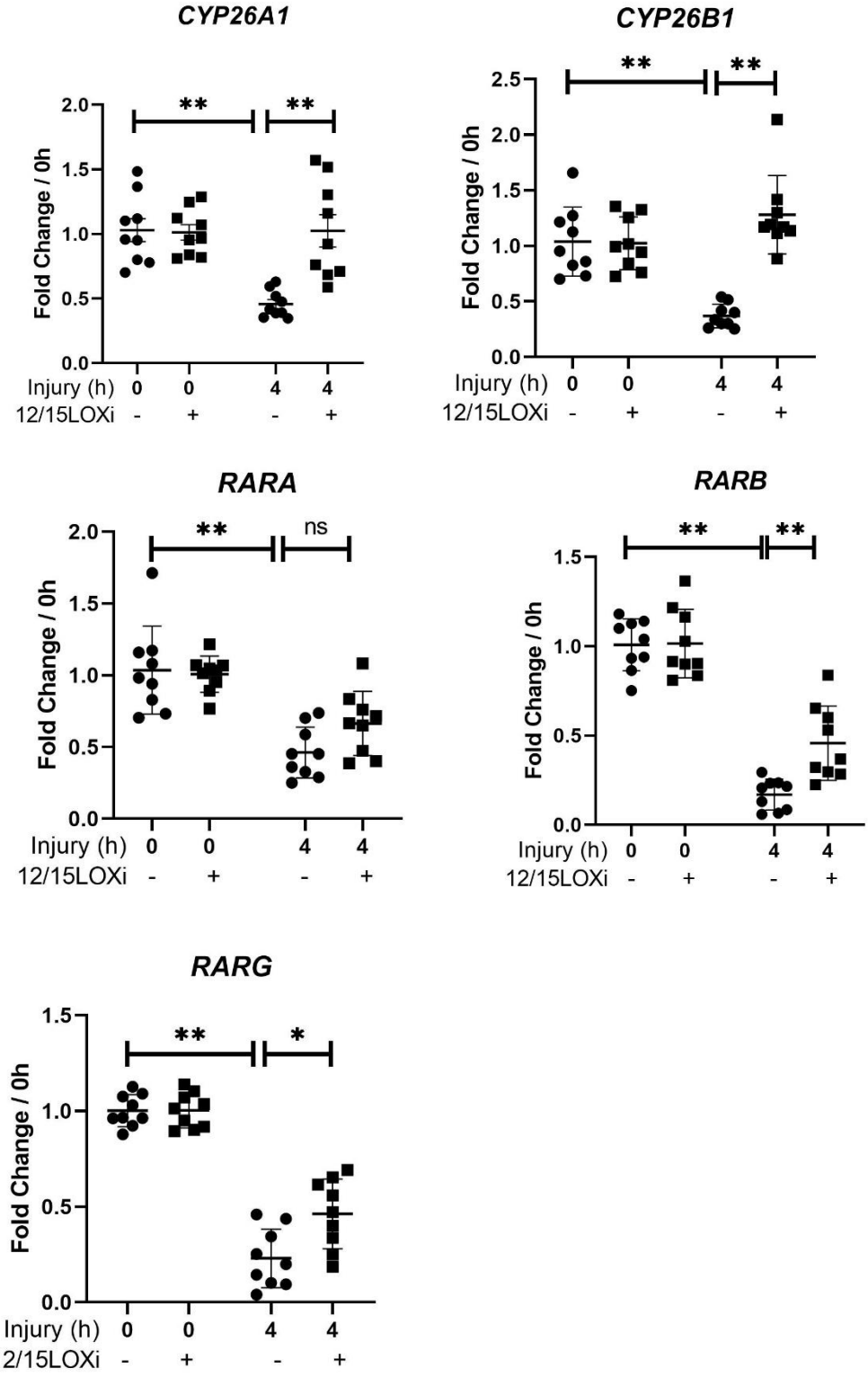
CYP26A1
CYP26B1
RARA
RARB
RARG
Fold Change / 0h
Injury (h)
12/15LOXi
**
ns
*

Figure 4.6: 12/15LOX inhibition prevents the downregulation of atRA-responsive genes on cartilage injury.

Porcine metacarpophalangeal (MCP) joints were decontaminated in 2% Virkon for 20 minutes before being equilibrated at 37 °C, 5% CO_2 for 1 hour. MCP joints were injected with either 1 µM 12/15 lipoxygenase inhibitor (12/15LOXi) or vehicle control and incubated for another 1 hour at 37 °C. The MCP joints were opened and cartilage was rapidly explanted. Explanted cartilage was either immediately snap frozen in liquid nitrogen (zero hour time point) or cultured in serum free DMEM with or without 12/15LOXi for 4 hours at 37 °C, 5% CO_2 before being snap frozen. RNA was subsequently extracted from the tissue and used in quantitative reverse transcriptase-polymerase chain reaction to measure a panel of atRA- responsive genes. Statistical significance of comparison between treatment groups was conducted using a two-way ANOVA, with post-hoc multiple comparisons corrected using Tukey's tests Bars shows the mean ± SEM of 3 independent experiments in which each experiment was performed on 3 individual trotter joints (n= 9 separate trotters). ns = not significant, * = P < 0.05; ** = P < 0.01, by two-way ANOVA. CYP26A1 = Cytochrome P450 Family 26 Subfamily A Member 1, CYP26B1 = Cytochrome P450 Family 26 Subfamily B Member 1, RARA = Retinoic Acid Receptor Alpha, RARB = = Retinoic Acid Receptor Beta, RARG = = Retinoic Acid Receptor Gamma.

4.2.7 Upregulation of inflammatory genes on cartilage injury is 12/15 LOX-sensitive

Having demonstrated that 12/15 LOX inhibition prevented the downregulation of key atRA-responsive genes, I explored whether the use of 12/15 LOXi (ML351) prior to cartilage injury also suppressed the upregulation of inflammatory genes. I hypothesised that inhibition of either cPLA2 or 12/15 LOX would suppress the production of toxic lipid peroxidation products, which in turn would increase cellular atRA and thus suppress inflammatory gene regulation on cartilage injury. I used the cDNA samples from the experiment conducted in Fig 4.2.6 to test a panel of inflammatory genes via RT-PCR.

All inflammatory genes were significantly upregulated on cartilage injury ($p < 0.01$) (Fig 4.7). Pre-injection of the joints with ML351 significantly suppressed the upregulation of *IL6* on cartilage injury by 45.2% (SD ±1.23) compared to injured vehicle control by 4 hours ($p < 0.05$). ML351 also significantly suppressed the upregulation of *COX2* and *MMP3* ($p < 0.01$) by 75.3% (SD ± 5.81) and 50.2% (SD ± 0.726), respectively, on cartilage injury. *ADAMTS4* upregulation on cartilage injury was completely reversed (SD ± 0.322)

by the action of ML351. On the other hand, the upregulation of *CCL2*, *TIMP1*, *NGF* and *CDKN1A* were unaffected by the presence of ML351 in the joint prior to cartilage injury (Fig 4.7).

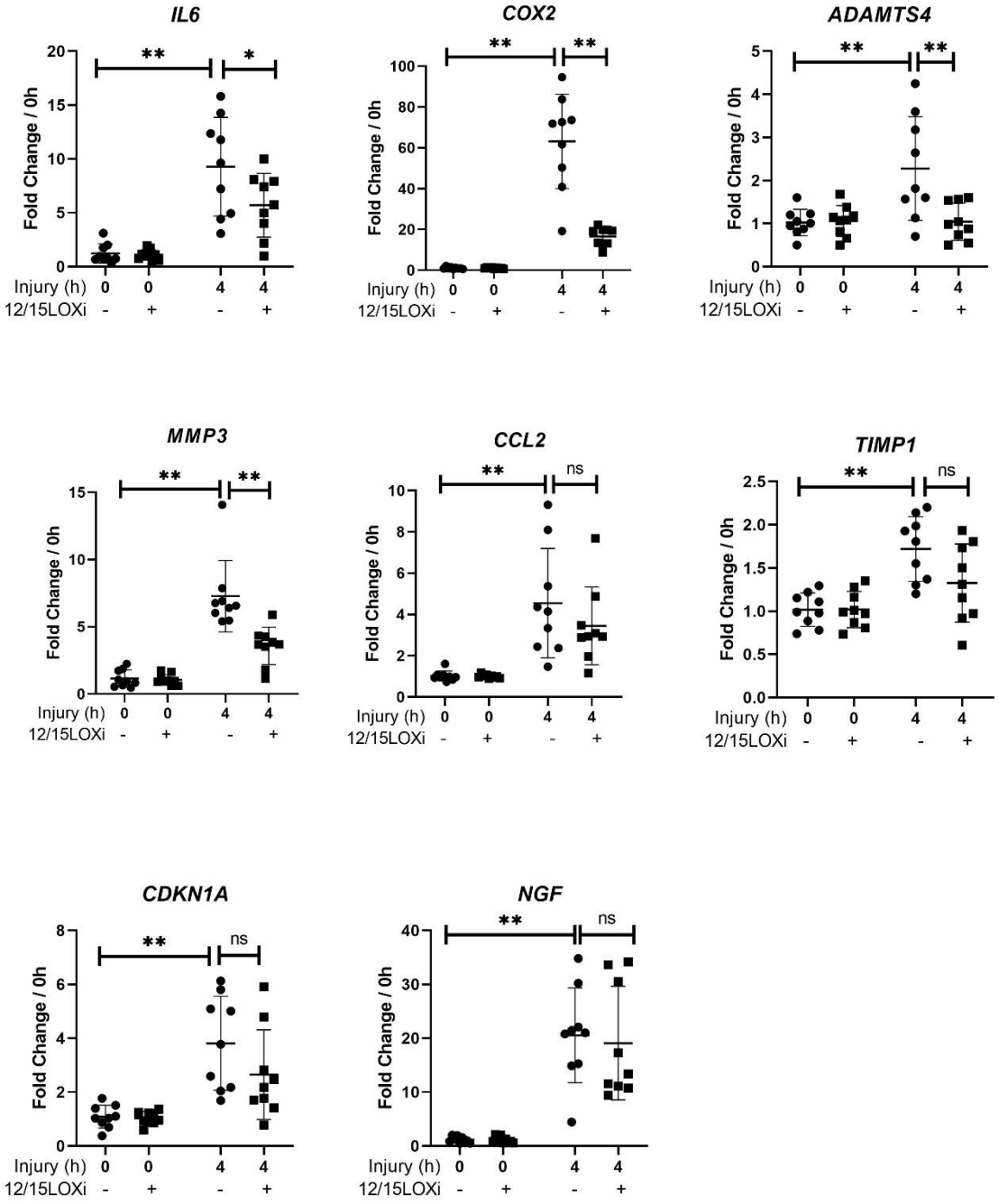

Figure 4.7: 12/15LOX inhibition suppresses the upregulation of inflammatory genes on cartilage injury.

Porcine metacarpophalangeal (MCP) joints were decontaminated in 2% Virkon for 20 minutes before being equilibrated at 37 °C, 5% CO_2 for 1 hour. MCP joints were injected with either 1 µM 12/15 lipoxygenase inhibitor (12/15LOXi) or vehicle control and incubated for another 1 hour at 37 °C. The MCP joints were opened and cartilage was rapidly explanted. Explanted cartilage was either immediately snap frozen in liquid nitrogen (zero hour time point) or cultured in serum free DMEM with or without 12/15LOXi for 4 hours at 37 °C, 5% CO_2 before being snap frozen. RNA was subsequently extracted from the tissue and used in quantitative reverse transcriptase-polymerase chain reaction to measure a panel of inflammatory genes. Statistical significance of comparison between treatment groups was conducted using a two-way ANOVA, with post-hoc multiple comparisons corrected using Tukey's tests. Bars shows the mean ± SEM of 3 independent experiments in which each experiment was performed on 3 individual trotter joints (n= 9 separate trotters). ns = not significant, * = $P < 0.05$; ** = $P < 0.01$, by two-way ANOVA. IL6 = Interleukin 6, COX2= Cyclooxygenase-2, ADAMTS4 = ADAM Metallopeptidase With Thrombospondin Type 1 Motif 4, MMP3= Matrix metalloproteinase-3, CCL2= C-C Motif Chemokine Ligand 2, TIMP1= TIMP metallopeptidase inhibitor 1, CDKN1A= Cyclin Dependent Kinase Inhibitor 1A, NGF= Nerve growth factor.

4.2.8 Downregulation of atRA-responsive genes and upregulation of inflammatory genes on cartilage injury is ROS-sensitive

I next determined whether the downregulation of atRA-responsive genes on cartilage injury was downstream of ROS generation. ROS is required for the generation of 4-HNE downstream of cPLA2 metabolism. Therefore, I tested whether blocking ROS production would dampen the injury response of atRA-responsive genes and inflammatory genes. I targeted the various sources that contribute to ROS production in chondrocytes. These include cytosolic ROS production (which is globally sequestered by NAC), mitochondrial ROS production (inhibited by CoQ10) and NADPH-oxidase dependent ROS production from the cellular membrane (inhibited by the use of a NOX inhibitor).

4.2.8.1 Downregulation of atRA-responsive genes on cartilage injury is NAC-sensitive

First, I used NAC which has been extensively used as an antioxidant agent in multiple systems. NAC works by mopping up cellular free radical species such as superoxide and hydroxyl anions in cells.

I used the same injury trotter assay as described in earlier and preinjected MCP joints with either 20 mM of NAC or vehicle control (DMSO) prior to cartilage injury (n = 9 separate trotters). Dissected cartilage was either snap frozen or cultured for 4 hours in either serum-free media containing 20 mM NAC or vehicle. RNA was extracted, converted to cDNA and RT-PCR conducted to measure the expression of a panel of atRA-responsive genes.

All atRA-responsive genes in those injured MCP joints that were injected with vehicle were significantly downregulated on cartilage injury ($p < 0.01$) (Fig 4.8). NAC reversed the downregulation of *CYP26A1* by 100% (SD ± 0.134) and *CYP26B1* by 100% (SD ± 0.092) whereas it only prevented the downregulation of *RARB* and *RARG* by 21.2% (SD ± 0.062) and 39.8% (SD ± 0.078), respectively. NAC was unable to prevent the downregulation of *RARA* on cartilage injury.

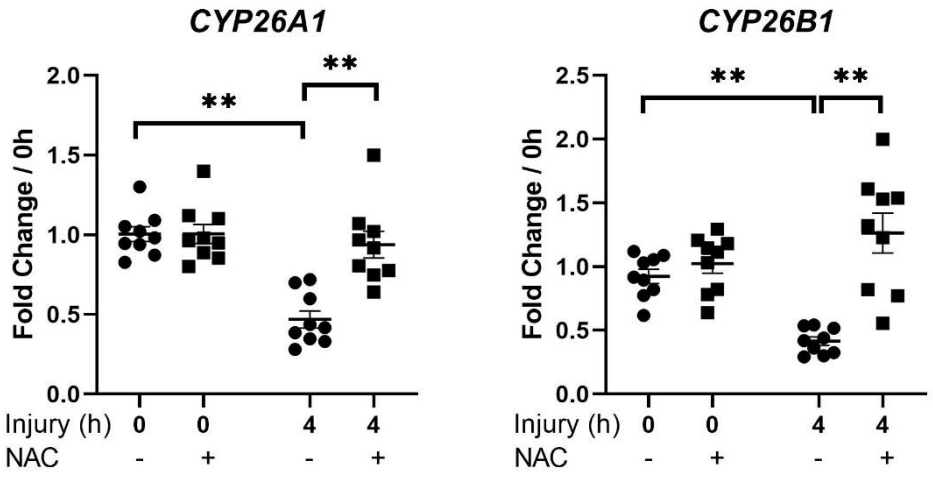

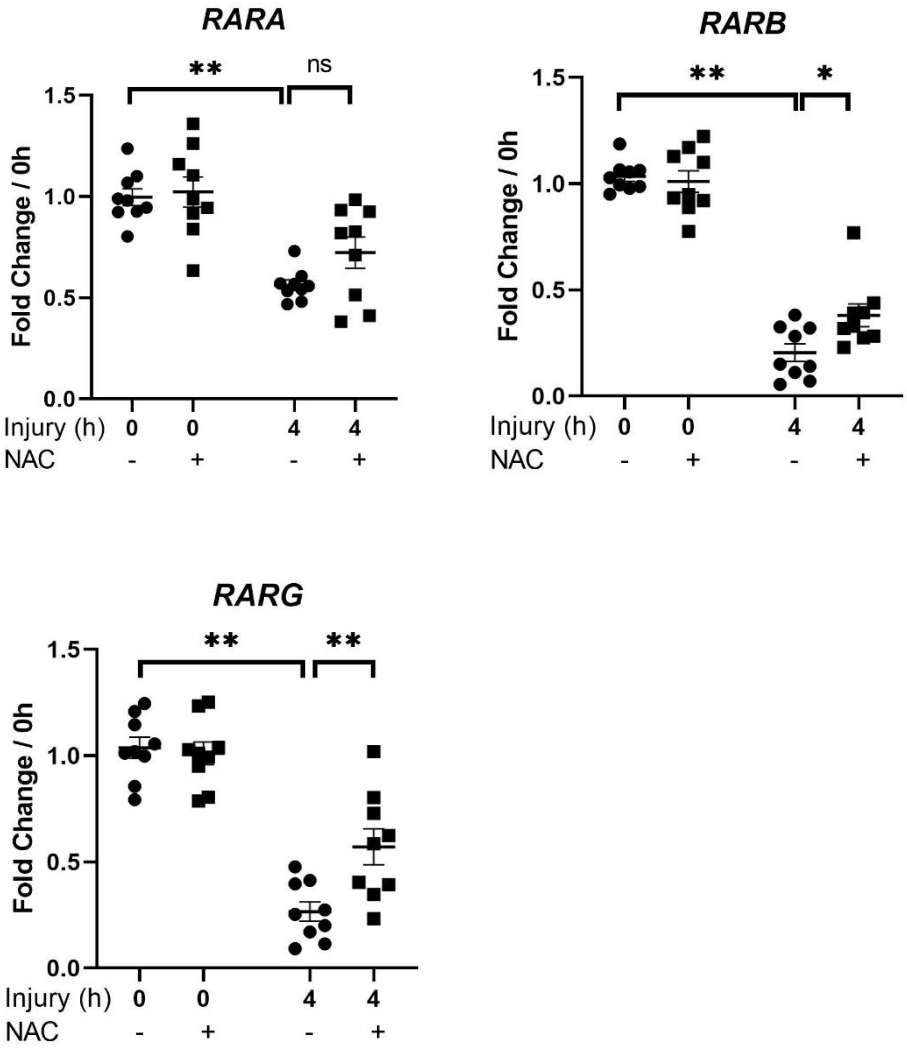

Figure 4.8: NAC prevents the downregulation of atRA-responsive genes on cartilage injury.

Porcine metacarpophalangeal (MCP) joints were decontaminated in 2% Virkon for 20 minutes before being equilibrated at 37 °C, 5% CO_2 for 1 hour. MCP joints were injected with either 20mM NAC or vehicle control and incubated for another 1 hour at 37 °C. The MCP joints were opened and cartilage was rapidly explanted. Explanted cartilage was either immediately snap frozen in liquid nitrogen (zero hour time point) or cultured in serum free DMEM with or without NAC for four hours at 37 °C, 5% CO_2 before being snap frozen. RNA was subsequently extracted from the tissue and used in quantitative reverse transcriptase-polymerase chain reaction to measure a panel of inflammatory genes. Statistical significance of comparison between treatment groups was conducted using a two-way ANOVA, with post-hoc multiple comparisons corrected using Tukey's tests. Bars shows the mean ± SEM of 3 independent experiments in which each experiment was performed on 3 individual trotter joints (n= 9 separate trotters). ns = not significant, * = $P < 0.05$; ** = $P < 0.01$, by two-way ANOVA. CYP26A1 = Cytochrome P450 Family 26 Subfamily A Member 1, CYP26B1 = Cytochrome P450 Family 26 Subfamily B Member 1, RARA = Retinoic Acid Receptor Alpha, RARB = = Retinoic Acid Receptor Beta, RARG = = Retinoic Acid Receptor Gamma.

4.2.8.2 Upregulation of inflammatory genes on cartilage injury is NAC-sensitive

After having showed that NAC prevented the downregulation of *CYP2A1* and *CYP26B1* on cartilage injury, I determined whether it also suppressed the upregulation of inflammatory genes on cartilage injury. NAC has been previously shown to act as anti-inflammatory in multiple systems including OA models [282, 375]. However, the relationship between the use of antioxidants, such as NAC, atRA-signalling and inflammatory gene response in the context of cartilage injury has not been previously reported. I used the cDNA samples from the injury assay conducted in section 4.2.8.1 and measured the expression of a panel of inflammatory genes.

All seven inflammatory genes tested were significantly upregulated on cartilage injury in vehicle-injected MCP joints. NAC suppressed the upregulation of *IL6* by 72.2% (SD ± 3.53) whereas it completely suppressed the upregulation of *ADAMTS4* (100%, SD ± 0.507), *MMP3 (*100%, SD ± 1.28) and *CDKN1A (*100%, SD ± 0.420) on cartilage injury (Fig 4.9). On the other hand, the upregulation of *COX2*, *CCL2*, *TIMP1* and *NGF* on injury was unaffected by the preinjection of trotter MCP joints with NAC (Fig 4.9).

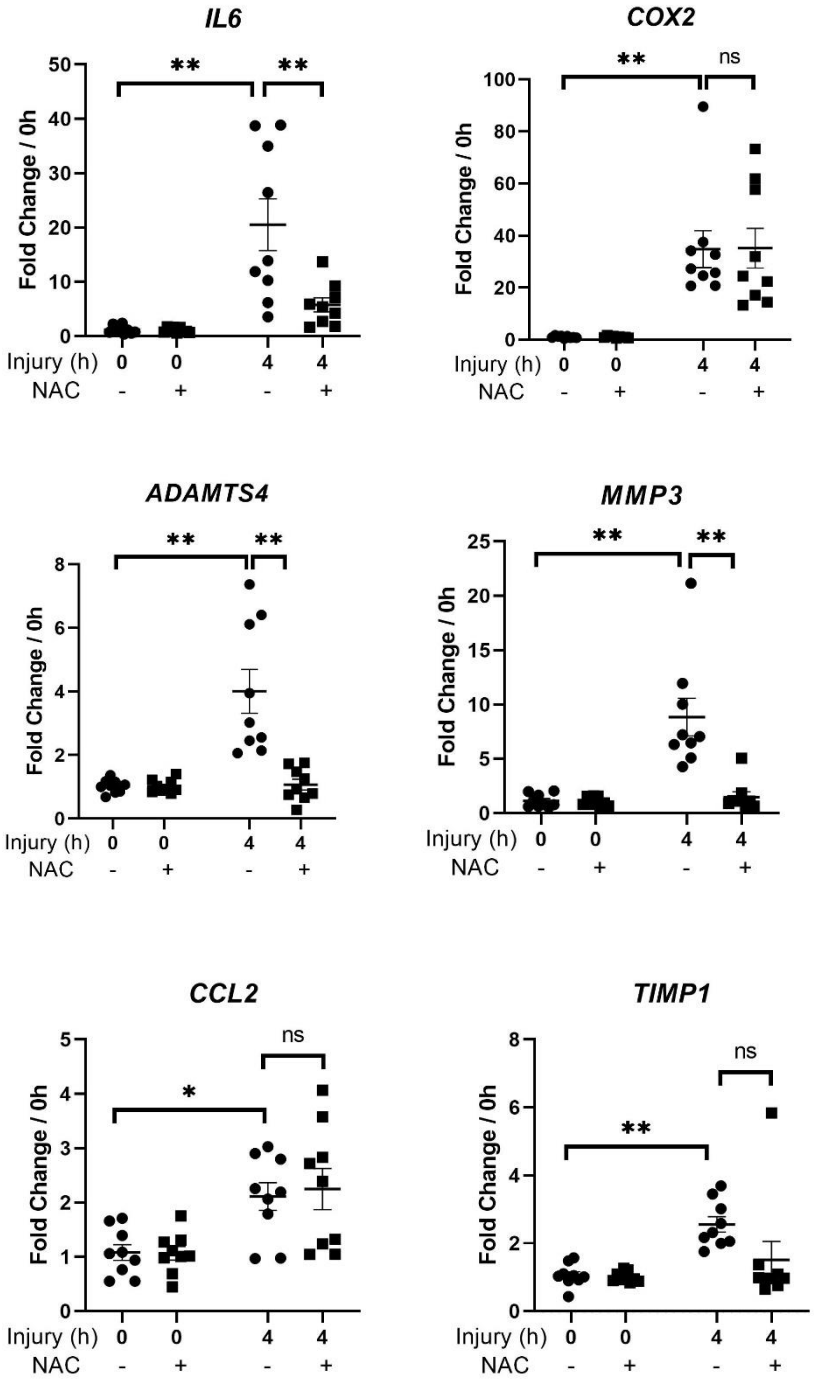
IL6
COX2
ADAMTS4
MMP3
CCL2
TIMP1
Fold Change / 0h
Injury (h) 0 0 4 4
NAC - + - +
**
ns
*

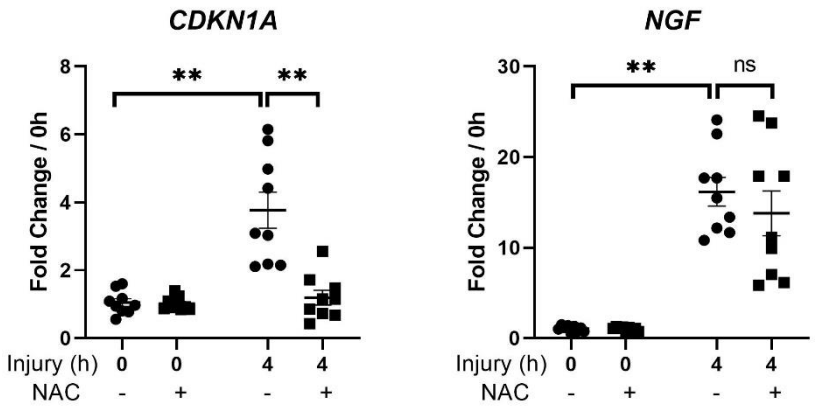

Figure 4.9: NAC suppresses the upregulation of inflammatory genes on cartilage injury

Porcine metacarpophalangeal (MCP) joints were decontaminated in 2% Virkon for 20 minutes before being equilibrated at 37 °C, 5% CO_2 for 1 hour. MCP joints were injected with either 20mM NAC or vehicle control and incubated for another 1 hour at 37 °C. The MCP joints were opened and cartilage was rapidly explanted. Explanted cartilage was either immediately snap frozen in liquid nitrogen (zero hour time point) or cultured in serum free DMEM with or without NAC for 4 hours at 37 °C, 5% CO_2 before being snap frozen. RNA was subsequently extracted from the tissue and used in quantitative reverse transcriptase-polymerase chain reaction to measure a panel of inflammatory genes. Statistical significance of comparison between treatment groups was conducted using a two-way ANOVA, with post-hoc multiple comparisons corrected using Tukey's tests. Bars shows the mean ± SEM of 3 independent experiments in which each experiment was performed on 3 individual trotter joints (n= 9 separate trotters). ns = not significant, * = P < 0.05; ** = P < 0.01, by two-way ANOVA. . IL6 = Interleukin 6, COX2= Cyclooxygenase-2, ADAMTS4 = ADAM Metallopeptidase With Thrombospondin Type 1 Motif 4, MMP3= Matrix metalloproteinase-3, CCL2= C-C Motif Chemokine Ligand 2, TIMP1= TIMP metallopeptidase inhibitor 1, CDKN1A= Cyclin Dependent Kinase Inhibitor 1A, NGF= Nerve growth factor.

4.2.8.3 Downregulation of atRA-responsive genes on cartilage injury is CoQ10-sensitive

I used NAC to sequester ROS in the cartilage in a nonspecific manner as reported in the literature. Having obtained the above results showing NAC to not only prevent the downregulation of *CYP26A1* and *CYP26B1* on cartilage injury but to also suppress mechano-inflammatory genes, I next targeted specific ROS-generation sites in the cell. One of the principal generators of ROS in chondrocytes is the mitochondria. ROS is produced from the mitochondria via the electron transfer chain because of the leakage of electrons between mitochondrial complexes and the subsequent generation of ROS. Co-enzyme Q10

(CoQ10) specifically blocks complex I and IV in the inner mitochondrial membrane and prevents the generation of ROS.

I used CoQ10 in the trotter injury assay and determined whether this prevented the downregulation of atRA-responsive genes on cartilage injury. 150 μM of CoQ10 was preinjected into the joint. Injured cartilage explants were incubated in either serum-free media containing CoQ10 or vehicle. RNA was extracted from explants converted to cDNA and gene expression measured for a panel of atRA-responsive genes.

CYP26 genes and *RAR* genes were rapidly downregulated in injured vehicle-injected MCP joints by 4 hours ($p < 0.01$) (Fig 4.10). Compared to injured vehicle-injected joints, CoQ10-injected joints prevented the downregulation of *CYP26A1*, *CYP26B1* and *RARG* by 81.3% (SD ± 0.089), 60.1% (SD ± 0.062) and 45% (SD ± 0.099), respectively (Fig 4.10). CoQ10 was not able to prevent the downregulation of *RARA* or *RARB* on cartilage injury.

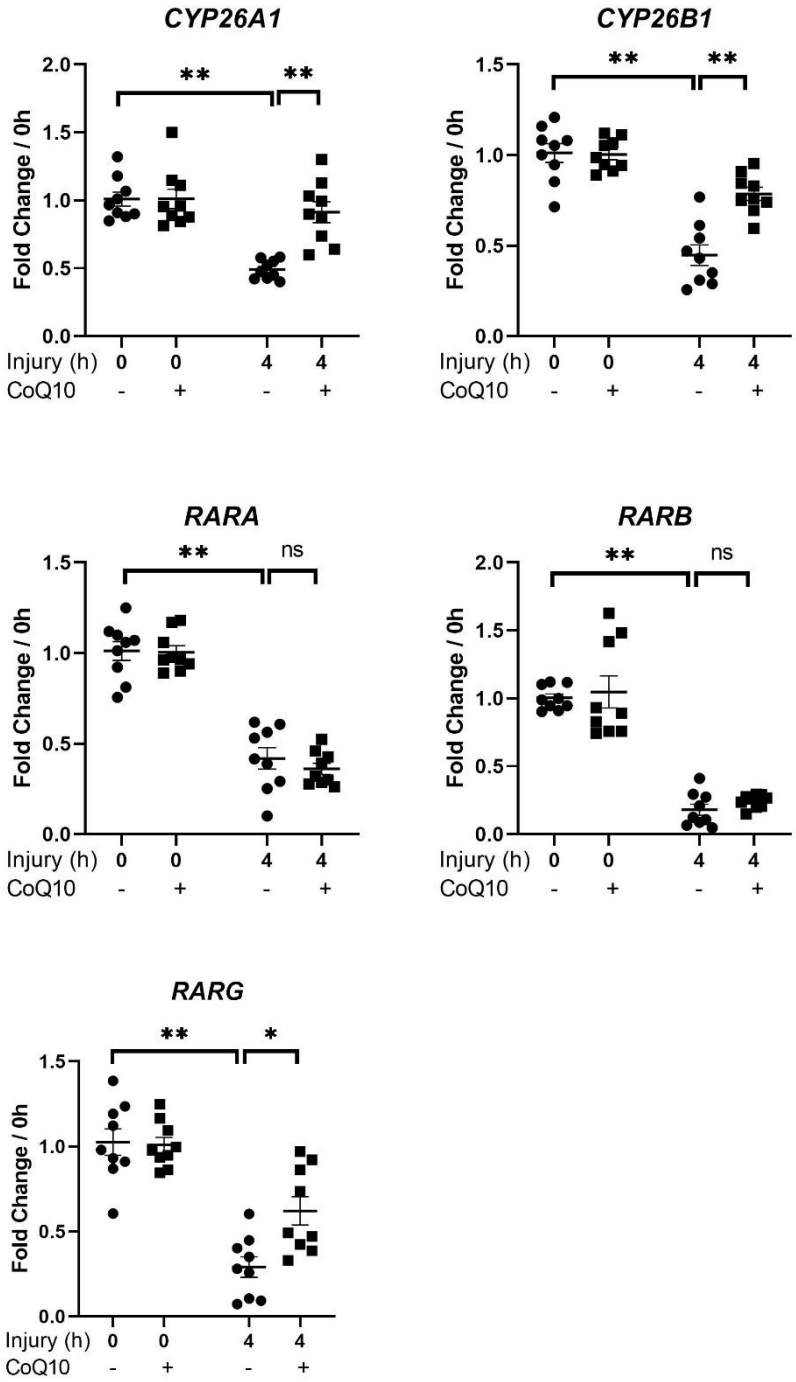
CYP26A1
**
**
Fold Change / 0h
2.0
1.5
1.0
0.5
0.0
Injury (h) 0 0 4 4
CoQ10 - + - +
CYP26B1
**
**
Fold Change / 0h
1.5
1.0
0.5
0.0
Injury (h) 0 0 4 4
CoQ10 - + - +
RARA
**
ns
Fold Change / 0h
1.5
1.0
0.5
0.0
Injury (h) 0 0 4 4
CoQ10 - + - +
RARB
**
ns
Fold Change / 0h
2.0
1.5
1.0
0.5
0.0
Injury (h) 0 0 4 4
CoQ10 - + - +
RARG
**
*
Fold Change / 0h
1.5
1.0
0.5
0.0
Injury (h) 0 0 4 4
CoQ10 - + - +

Figure 4.10: CoQ10 prevents the downregulation of atRA-responsive genes on cartilage injury.

Porcine metacarpophalangeal (MCP) joints were decontaminated in 2% Virkon for 20 minutes before being equilibrated at 37 °C, 5% CO_2 for 1 hour. MCP joints were injected with either 150 µM CoQ10 or vehicle control and incubated for another 1 hour at 37 °C. The MCP joints were opened and cartilage was rapidly explanted. Explanted cartilage was either immediately snap frozen in liquid nitrogen (zero hour time-point) or cultured in serum free DMEM with or without CoQ10 for 4 hours at 37 °C, 5% CO_2 before being snap frozen. RNA was subsequently extracted from the tissue and used in quantitative reverse transcriptase-polymerase chain reaction to measure a panel of atRA-responsive genes. Statistical significance of comparison between treatment groups was conducted using a two-way ANOVA, with post-hoc multiple comparisons corrected using Tukey's tests. Bars shows the mean ± SEM of 3 independent experiments in which each experiment was performed on 3 individual trotter joints (n= 9 separate trotters). ns = not significant, * = $P < 0.05$; ** = $P < 0.01$, by two-way ANOVA. CYP26A1 = Cytochrome P450 Family 26 Subfamily A Member 1, CYP26B1 = Cytochrome P450 Family 26 Subfamily B Member 1, RARA = Retinoic Acid Receptor Alpha, RARB = = Retinoic Acid Receptor Beta, RARG = = Retinoic Acid Receptor Gamma.

4.2.8.4 Upregulation of inflammatory genes on cartilage injury is CoQ10-sensitive

Having observed CoQ10 to prevent the downregulation of key atRA-responsive genes on cartilage injury, I next explored the effect of CoQ10 on inflammatory gene regulation. Similar to NAC, CoQ10 has been reported to exert anti-inflammatory effects in systems including the cardiovascular system and skin. However, looking at the effect of CoQ10 on injury-induced inflammatory gene regulation would give an insight into the role of mitochondrial generated ROS in the context of cartilage injury. I used the cDNA from the experiment conducted in section 4.2.8.3 to examine inflammatory gene regulation.

Cartilage injury rapidly upregulated all inflammatory genes by 4 hours ($p < 0.01$) (Fig 4.11). CoQ10 completely reversed the upregulation of *IL6* (100%, SD ± 2.21), *COX2* (100%, SD ± 1.27), *ADAMTS4* (100%, SD ± 0.425), *CCL2* (100%, SD ± 0.310), *TIMP1* (100%, SD ± 0.175) and *NGF* (100%, SD ± 2.33) (Fig 4.11). The upregulation of *CDKN1A* was only partially suppressed by 62.4% (SD ± 0.460) through the use of CoQ10. In contrast, *MMP3* expression was induced by 3.2-fold ($p < 0.01$) (SD ± 0.287) by the preinjection of trotter MCP joints with CoQ10 compared to injured vehicle-injected joints.

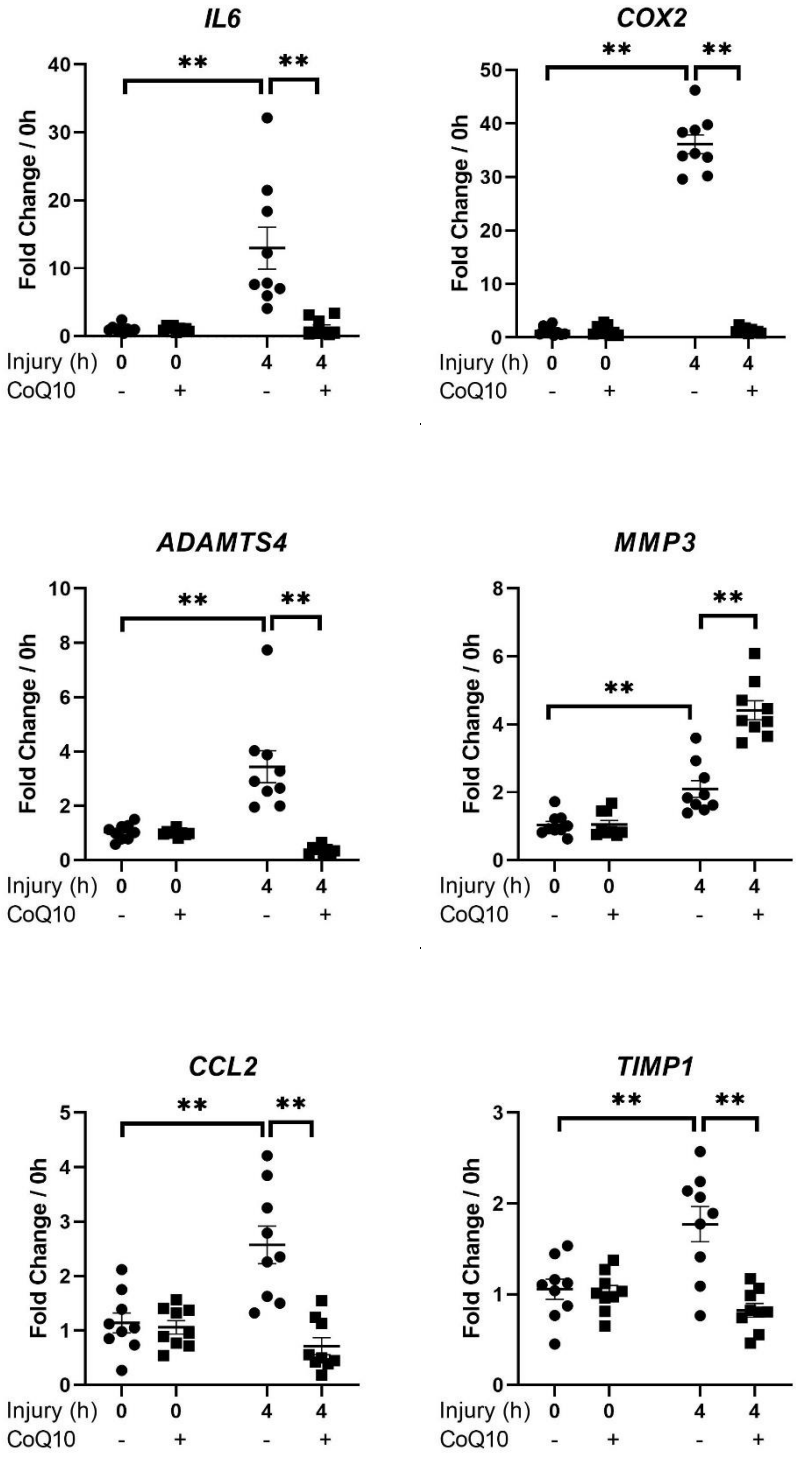
IL6
COX2
ADAMTS4
MMP3
CCL2
TIMP1
Fold Change / 0h
Injury (h) 0 0 4 4
CoQ10 - + - +
**

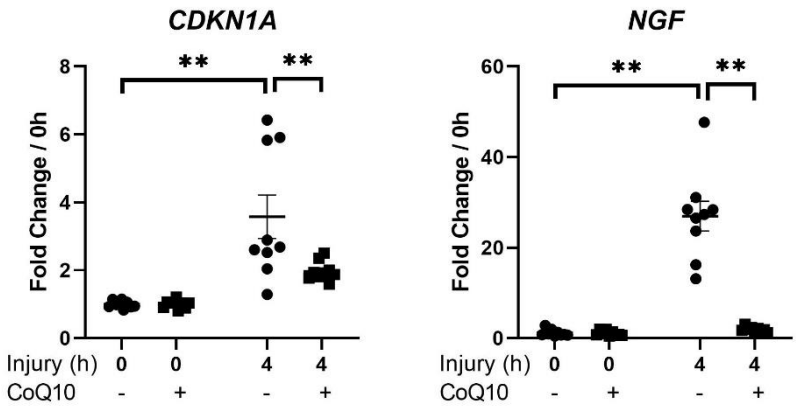

Figure 4.11: CoQ10 suppresses the upregulation of inflammatory genes on cartilage injury.

Porcine metacarpophalangeal (MCP) joints were decontaminated in 2% Virkon for 20 minutes before being equilibrated at 37 °C, 5% CO_2 for 1 hour. MCP joints were injected with either 150 µM CoQ10 or vehicle control and incubated for another 1 hour at 37 °C. The MCP joints were opened and cartilage was rapidly explanted. Explanted cartilage was either immediately snap frozen in liquid nitrogen (zero hour time point) or cultured in serum free DMEM with or without CoQ10 for four hours at 37 °C, 5% CO_2 before being snap frozen. RNA was subsequently extracted from the tissue and used in quantitative reverse transcriptase-polymerase chain reaction to measure a panel of inflammatory genes. Statistical significance of comparison between treatment groups was conducted using a two-way ANOVA, with post-hoc multiple comparisons corrected using Tukey's tests. Bars shows the mean ± SEM of 3 independent experiments in which each experiment was performed on 3 individual trotter joints (n= 9 separate trotters). ns = not significant, * = P < 0.05; ** = P < 0.01, by two-way ANOVA. . IL6 = Interleukin 6, COX2= Cyclooxygenase-2, ADAMTS4 = ADAM Metallopeptidase With Thrombospondin Type 1 Motif 4, MMP3= Matrix metalloproteinase-3, CCL2= C-C Motif Chemokine Ligand 2, TIMP1= TIMP metallopeptidase inhibitor 1, CDKN1A= Cyclin Dependent Kinase Inhibitor 1A, NGF= Nerve growth factor.

4.2.8.5 Downregulation of atRA-responsive genes on cartilage injury is NOX-sensitive

Having shown that cellular ROS (inhibited by NAC) and mitochondrial ROS (inhibited by CoQ10) prevented the downregulation of atRA-responsive genes and suppressed inflammatory gene regulation on cartilage injury, I next focused on membrane sources of ROS in chondrocytes. NADPH oxidase is a membrane-bound enzyme complex which produces ROS in chondrocytes by transferring electrons from NADPH to molecular oxygen. This accounts for approximately 40% of the ROS produced in chondrocytes [285]. I used a commercially available inhibitor to NOX, apocynin, which inhibits the release of superoxide

through the complex by preventing proper subunit assembly. From the commercially available inhibitors, apocynin was one of the most selective and specific towards NOX with an IC50 value of 10 μM.

I conducted the injury assay in the presence of 1 mM of apocynin. Injured explants were incubated for four hours in serum-free media containing either apocynin or vehicle (n = 4 separate trotters). RNA was extracted and converted to cDNA, and RT-PCR was conducted for atRA-responsive gene expression.

atRA-responsive genes were significantly downregulated on cartilage injury by four hours in injured vehicle-injected joints ($p < 0.01$) (Fig 4.12). The downregulation of *CYP26A1* was completely prevented by apocynin (100%, SD ± 0.195) ($p < 0.01$) whereas the downregulation of *CYP26B1* was prevented by 98.7% (SD ± 0.158) ($p < 0.01$). Apocynin had no statistically significant effect on the downregulation of *RAR* genes on cartilage injury compared to injured vehicle-injected MCP joints (Fig 4.12).

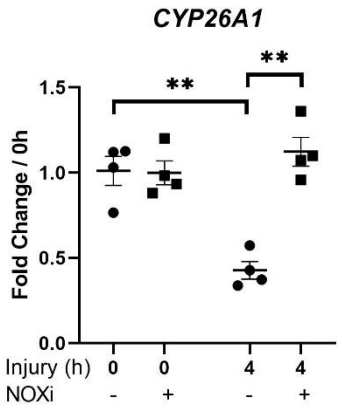
CYP26A1
**
**
Fold Change / 0h
1.5
1.0
0.5
0.0
Injury (h) 0 0 4 4
NOXi - + - +

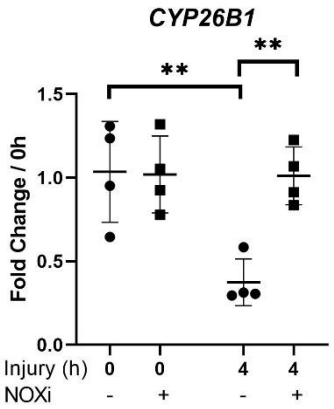
CYP26B1
**
**
Fold Change / 0h
1.5
1.0
0.5
0.0
Injury (h) 0 0 4 4
NOXi - + - +

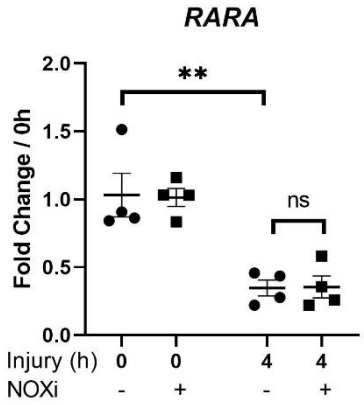
RARA
**
ns
Fold Change / 0h
2.0
1.5
1.0
0.5
0.0
Injury (h) 0 0 4 4
NOXi - + - +

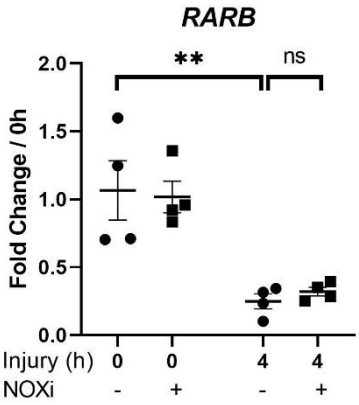
RARB
**
ns
Fold Change / 0h
2.0
1.5
1.0
0.5
0.0
Injury (h) 0 0 4 4
NOXi - + - +

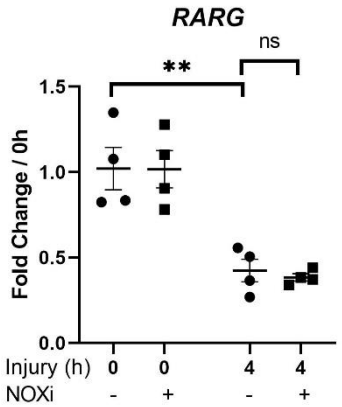
RARG
**
ns
Fold Change / 0h
1.5
1.0
0.5
0.0
Injury (h) 0 0 4 4
NOXi - + - +

Figure 4.12: NOX inhibition prevents the downregulation of atRA-responsive genes on cartilage injury.

Porcine metacarpophalangeal (MCP) joints were decontaminated in 2% Virkon for 20 minutes before being equilibrated at 37 °C, 5% CO_2 for 1 hour. MCP joints were injected with either 1mM NOXi or vehicle control and incubated for another 1 hour at 37 °C. The MCP joints were opened and cartilage was rapidly explanted. Explanted cartilage was either immediately snap frozen in liquid nitrogen (zero hour time point) or cultured in serum free DMEM with or without NOXi for 4 hours at 37 °C, 5% CO_2 before being snap frozen. RNA was subsequently extracted from the tissue and used in quantitative reverse transcriptase-polymerase chain reaction to measure a panel of atRA-responsive genes. Statistical significance of comparison between treatment groups was conducted using a two-way ANOVA, with post-hoc multiple comparisons corrected using Tukey's tests. Bars shows the mean ± SEM of 3 independent experiments in which each experiment was performed on 3 individual trotter joints (n= 9 separate trotters). ns = not significant, * = $P < 0.05$; ** = $P < 0.01$, by two-way ANOVA. . CYP26A1 = Cytochrome P450 Family 26 Subfamily A Member 1, CYP26B1 = Cytochrome P450 Family 26 Subfamily B Member 1, RARA = Retinoic Acid Receptor Alpha, RARB = = Retinoic Acid Receptor Beta, RARG = = Retinoic Acid Receptor Gamma.

4.2.8.6 Upregulation of inflammatory genes on cartilage injury is NOX-sensitive

Having showed that the downregulation of certain atRA-responsive genes was NOX-sensitive, I tested the expression of inflammatory genes on injury under the influence of apocynin. I used the same cDNA samples collected from the experiment conducted in section 4.2.8.5 and tested inflammatory gene expression.

As expected, inflammatory genes tested were all upregulated on cartilage injury at four hours (Fig 4.13). Apocynin significantly suppressed the upregulation of *IL6, COX2* an *ADAMTS4* by 49.8% (SD ± 1.36), 62% (SD ± 3.37) and 65.7% (SD ± 0.384), respectively ($p < 0.01$). Apocynin was not able to suppress the upregulation of *MMP3*, *CCL2*, *TIMP1*, *NGF* and *CDKN1A* on cartilage injury (Fig 4.13).

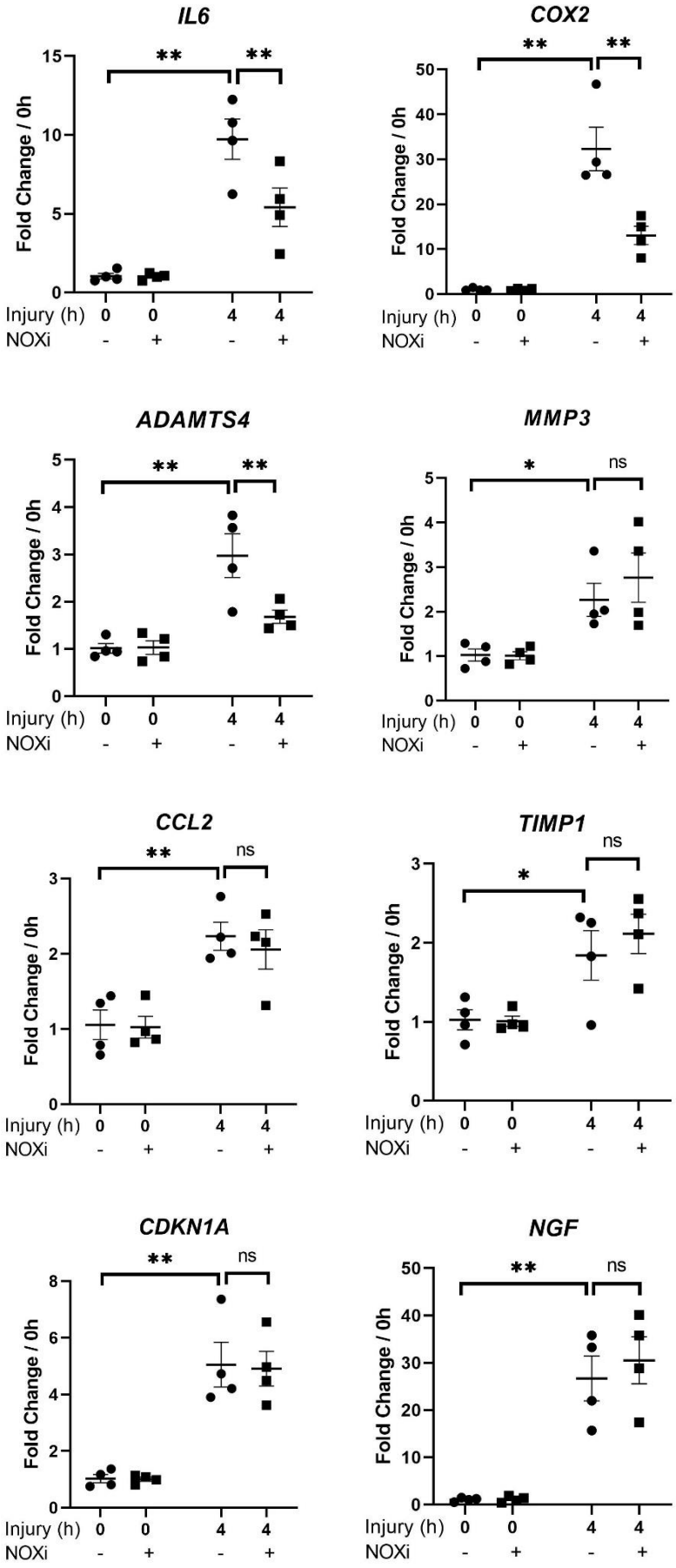
IL6
COX2
ADAMTS4
MMP3
CCL2
TIMP1
CDKN1A
NGF
Fold Change / 0h
Injury (h) 0 0 4 4
NOXi - + - +
**
*
ns

Figure 4.13: NOX inhibition suppresses the upregulation of inflammatory genes on cartilage injury.

Porcine metacarpophalangeal (MCP) joints were decontaminated in 2% Virkon for 20 minutes before being equilibrated at 37 °C, 5% CO_2 for 1 hour. MCP joints were injected with either 1mM NOXi or vehicle control and incubated for another 1 hour at 37 °C. The MCP joints were opened and cartilage was rapidly explanted. Explanted cartilage was either immediately snap frozen in liquid nitrogen (zero hour time point) or cultured in serum free DMEM with or without NOXi for 4 hours at 37 °C, 5% CO_2 before being snap frozen. RNA was subsequently extracted from the tissue and used in quantitative reverse transcriptase-polymerase chain reaction to measure a panel of inflammatory genes. Statistical significance of comparison between treatment groups was conducted using a two-way ANOVA, with post-hoc multiple comparisons corrected using Tukey's tests. Bars shows the mean ± SEM of 3 independent experiments in which each experiment was performed on 3 individual trotter joints (n= 9 separate trotters). ns = not significant, * = $P < 0.05$; ** = $P < 0.01$, by two-way ANOVA. . IL6 = Interleukin 6, COX2= Cyclooxygenase-2, ADAMTS4 = ADAM Metallopeptidase With Thrombospondin Type 1 Motif 4, MMP3= Matrix metalloproteinase-3, CCL2= C-C Motif Chemokine Ligand 2, TIMP1= TIMP metallopeptidase inhibitor 1, CDKN1A= Cyclin Dependent Kinase Inhibitor 1A, NGF= Nerve growth factor.

4.3 Discussion

4.3.1 Relationship between arachidonic acid metabolism and atRA biosynthesis

The downregulation of atRA-responsive genes and the upregulation of certain inflammatory genes on cartilage injury was cPLA2-sensitive. cPLA2 inhibition fully prevented the downregulation of *CYP26* genes and *RARA* however it only partially prevented the downregulation of *RARG*. cPLA2 inhibition was not able to prevent the downregulation *RARB*. This suggests that each atRA-responsive gene might be differentially regulated at the nuclear transcriptional level. Only *CYP26A1* and *RARA* has been reported in the literature to possess the canonical RARE-motifs in their promoter regions [376]. The others (*CYP26B1*, *RARB* and *RARG*) have been reported to be atRA-responsive (i.e. mRNA expression dependent on the concentration of cellular atRA levels) but not reported to have identifiable RARE-motifs in their promoter regions [376]. Therefore, this suggests a more complex pattern of regulation between the different atRA-responsive genes. As discussed, cPLA2 belongs to a group of enzymes responsible for the liberation of arachidonic acid from PUFAs in the lipid bilayer membrane [311]. Arachidonic acid can be further metabolised by a group of enzymes known as 12/15 LOX into lipid metabolites [311]. 12/15 LOX inhibition prevented the downregulation of *CYP26* genes, *RARB* and *RARG*. Similar to the effect of cPLA2 inhibition, 12/15 LOX inhibition fully prevented the downregulation of *CYP26A1* and *CYP26B1* on injury. However, 12/15 LOX inhibition only partially prevented the downregulation of both *RARB* and *RARG*. It might be the case that the regulation of *CYP26* genes are more representative read-outs or are more sensitive to intracellular atRA levels than *RAR* genes. Nonetheless, given that both cPLA2 inhibition and 12/15 LOX inhibition were able to prevent the downregulation of key atRA-responsive genes between them, this is strongly suggestive of the fact that arachidonic acid metabolism reduces levels of cellular atRA on cartilage injury (Figure 4.15). Evidence from the literature suggests that certain

lipid peroxidation products (produced downstream of cPLA2 and 12/15 LOX) are able to inhibit the synthesis of atRA [324]. In particular, 4-HNE has been demonstrated to inhibit the ALDH1A2 enzyme that is responsible for the rate-limiting step in the production of atRA [324]. 4-HNE is produced downstream of 12/15 LOX secondary to the radical induced inactivation of GPx, thereby diverting 12- and 15- HpETE towards lipid peroxidation products [288]. Therefore, the diversion of lipid metabolism towards lipid peroxidation products requires the presence of ROS. It is important to note that we are only inferring (from literature evidence and that obtained by my results) that 4-HNE might be the downstream factor from cPLA2 metabolism, to decrease atRA levels. In support of this, I showed that in-vitro, 4-HNE downregulated atRA-responsive genes in cultured primary porcine chondrocytes. However, further work must be done to validate this hypothesis. Such work would firstly involve measuring whether 4-HNE, or indeed other lipid metabolites, was regulated on cartilage injury by the use of ELISA or mass spectroscopy (MS). Secondly, enzymatic activity assays can be used to determine the inhibition profile of 4-HNE on the ALDH1A2 enzyme and subsequent atRA-synthesis. One study showed that 4-HNE-modified protein conjugates are increased, (by western blot analysis and MS), in chondrocyte extracts of OA patients compared to non-OA patients [377]. Morquette et al. further showed in an in-vitro study that 4-HNE is capable of promoting the degradation of COL2 through increased MMP-13 expression [316]. 4-HNE has also been associated with chondrocyte apoptosis in human OA samples [378]. However, functional in-vivo and clinical translational studies that target 4-HNE in the context of OA are still widely lacking and requires further investigation.

4.3.2 cPLA2-sensitive suppression of mechanoflammation

cPLA2 and 12/15 LOX inhibition not only prevented the downregulation of key atRA-responsive genes, but also suppressed the upregulation of certain inflammatory genes. cPLA2 inhibition suppressed the upregulation of *IL6*, *COX2*, *ADAMTS4*, *MMP3* and *TIMP1*. The pattern of suppression was very similar with 12/15 LOX inhibition except that *TIMP1* expression was not suppressed on injury by 12/15 LOX inhibition although it showed a downward trend. Although the pattern of gene expression regulation by cPLA2 and 12/15 LOX inhibition was similar, it varied slightly from that achieved by TLZ. Whereas TLZ further enhanced the expression of *MMP3* on injury, both cPLA2 and 12/15 LOX inhibition suppressed *MMP3* expression. This suggests that perhaps inhibiting arachidonic acid metabolism (and enzymes downstream) might exert an anti-inflammatory effect through mechanisms that are also independent of atRA. Various studies have shown anti-inflammatory effects being mediated through inhibiting arachidonic acid metabolism [311]. The nonsteroidal anti-inflammatory drugs inhibit prostaglandin synthesis, which is produced by the action of COX2 on arachidonic acid [372]. Therefore, the release of arachidonic acid from the phospholipid membrane is one of the rate-limiting factors for the production of eicosanoids [311]. Moreover, PLA2-dependent hydrolysis of PUFAs, liberation of arachidonic acid and subsequent catalysis by LOX enzymes produce leukotrienes [313]. Leukotrienes are potent pro-inflammatory mediators with an established pathophysiological role in asthma [314]. In addition to producing eicastanoids, cPLA2 is responsible for the initiating step in the production of PAF which is another potent inflammatory molecule [310]. Strikingly, the inflammatory genes that were suppressed by both cPLA2 and 12/15 LOX inhibition on injury were highly TAK1-sensitive. This suggested that there might be a relationship between TAK1 and cPLA2 activation on cartilage injury. I further interrogated this relationship in the subsequent chapter.

Collectively, cPLA2-dependent hydrolysis of arachidonic acid might be exerting a suppressive effect on inflammatory gene regulation predominantly through an atRA-responsive manner, but we cannot exclude other collateral mechanisms (Figure 4.15). It is also worth noting key limitations from these inhibitor studies. PACOF3 is reported to prevent the phosphorylation of selective serine residues on cPLA2 with an IC50 value of 3.8 μM, which compared to other pharmacological agents, is not very selective. Therefore, the inhibitor might also have exerted off-target actions on other PLA2 isoforms which cannot be excluded, including sPLA2 and iPLA2. As such, it is important to interpret results from these inhibitor studies cautiously. Ideally, such work should be validated with further in-vivo experiments that might, for example, involve loss-of-function knock out gene studies. I did attempt to validate this work with cPLA2 KO mice. However, due to time restrictions, I was unable to complete this work.

4.3.3 Role of cPLA2 in cartilage injury

cPLA2 was phosphorylated by 10 and 30 minutes post porcine cartilage injury, and this was suppressed by the use of a cPLA2 inhibitor. This showed cPLA2 to be mechanosensitive and regulated by cartilage injury (Figure 4.15). The early activation of cPLA2, through its phosphorylation, followed an appropriate temporal pattern that made it a good candidate for driving down atRA levels in the cartilage post injury. This hypothesis was strengthened by the finding that the downregulation of atRA-responsive genes on cartilage injury was cPLA2-sensitive (Figure 4.15).

There is emerging evidence for the role of arachidonic acid metabolism in OA. Early studies demonstrated high activity of PLA2 in the synovial fluid of OA patients [379, 380]. It was observed that deeper layers of the cartilage contained threefold more PLA2 than superficial layers. Moreover, PLA2 was shown to be released extracellularly [379]. B. Johansen et al.

further revealed that multiple cPLA2 isoforms are expressed in OA chondrocytes and resulted in increased AA release and PGE2 production [372]. More recently, and drawing parallels with my own work, in 2021, T. Wei. et al. revealed that sPLA2 (secretory PLA2) was increased in the articular cartilage of human and mouse OA cartilage [381]. This expression was mechanosensitive and enhanced by increased mechanical loading. Moreover, inhibition of sPLA2 by the use of engineered sPLA2 inhibitor-loaded micellar nanoparticles (sPLA2i-NPs) was able to mitigate OA progression in an in-vivo mouse model [381].

From my work, it was observed that the phosphorylation of cPLA2 on cartilage injury was first seen only at 10 mins and not at 5 mins, a timescale that is slower than that observed for the phosphorylation of TAK1 and the MAPKs (JNK, ERK and p38). Previous work by Ismail et al. demonstrated that TAK1 and ERK are activated within 30 seconds post injury, JNK by 2 mins and p38 by 1 minute [99]. This brought into question what was activating cPLA2 on injury and whether this might be TAK1-driven. The cPLA2-sensitive inflammatory genes mirrored those that were regulated by TAK1 on cartilage injury; therefore, it was plausible that TAK1 might be driving cPLA2. I interrogated the causes of cPLA2 activation on cartilage injury in Chapter 5.

4.3.4 Relationship between ROS and atRA metabolism

The downregulation of atRA-responsive genes on cartilage injury was highly ROS-sensitive. NAC prevented the downregulation of *CYP26* genes, *RARB* and *RARG*. Similarly, CoQ10 prevented the downregulation of *CYP26* genes and *RARG*, whilst NOX inhibition prevented only the downregulation of *CYP26* genes on cartilage injury. The commonality between all antioxidative agents was their strong preventive effect on the downregulation of *CYP26A1* and *CYP26B1*. As mentioned earlier, *CYP26A1* has an established RARE-motif in its

promoter region [376]. Although, *CYP26B1* has not been identified as having a canonical RARE-motif, it has still been reported as being an atRA-responsive gene [337]. It appears that perhaps the *CYP26* genes are far more sensitive to intracellular atRA levels than *RAR* genes and might be a more reliable surrogate marker for atRA.

Given that atRA-responsive genes are maintained on cartilage injury in the presence of redox restoring agents, ROS is likely to be involved in driving down cellular atRA levels on injury. The mechanism by which ROS does this might be related to the generation of lipid peroxidation products. The formation of lipid metabolites, in particular 4-HNE, is dependent on the presence of free radicals which saturate GPx [288]. Saturation of GPx diverts the metabolism of 12- and 15-HpETE towards the toxic 4-HNE, which has been reported to decrease atRA biosynthesis by inhibiting the ALDH1A2 enzyme [324].

4.3.5 ROS-sensitive suppression of mechanoflammation

Each of the antioxidant agents that I used (NAC, CoQ10 and NOX inhibitor) suppressed the upregulation of various inflammatory genes. CoQ10 had the strongest anti-inflammatory effect of all the antioxidative agents and suppressed the upregulation of *IL6*, *COX2*, *ADAMTS4*, *CCL2*, *TIMP1*, *CDKN1A* and *NGF*. This was very striking, especially as CoQ10 also suppressed NGF which was not atRA-responsive. Given that CoQ10 is reported to block the production of ROS from the mitochondria, this is perhaps suggestive of the stronger role the mitochondria plays in ROS production in chondrocytes compared to cytosolic or membrane-generated ROS that is inhibited by NAC and apocynin, respectively. In chondrocytes, the mitochondria is the major cellular sink for ROS reduction, and also possesses the greatest potential for ROS formation [277]. Oxidative phosphorylation occurs in the mitochondria whereas glycolysis occurs in the cytoplasm; however, only 25% of the

ATP consumption in chondrocytes is provided for by oxidative phosphorylation, the majority being generated via glycolysis [277]. Alongside ATP production, the mitochondria also play a key role in regulating redox balance and cellular Ca2+ ion concentration and mediating chondrocyte death signals [300]. Mitochondria maintain low cellular levels of ROS by housing a highly potent antioxidant system which includes SOD and GPx [277, 283]. Therefore, inhibiting the mitochondria would not only disturb the metabolic balance between glycolysis and oxidative phosphorylation, perturbing ATP production, but will also vastly increase intracellular ROS production to mediate inflammation and likely chondrocyte cell death. Collectively, this might explain why CoQ10, which restores mitochondrial balance, exerted a powerful anti-inflammatory effect on cartilage injury.

The inflammatory genes suppressed by CoQ10 did not entirely match that suppressed by TLZ. This suggests additional mechanisms, independent of atRA, by which CoQ10 suppresses inflammatory gene regulation. I investigated such mechanisms by looking at the relationship between TAK1 activation and ROS sequestration in Chapter 6. A similarity I observed was that both TLZ and CoQ10 treatment resulted in a further enhancement of *MMP3* gene expression on cartilage injury. Conversely, CoQ10 also suppressed *NGF* which was not atRA-responsive. This may highlight mitochondrial-derived ROS as a potential target for addressing OA-related pain, which has been reported to be strongly driven by NGF in OA [360, 361]. This is supported by a study conducted by Carissa Chu et al. in 2011 [382]. The authors demonstrated that NGF-induced mechanical hyperalgesia in rats was markedly suppressed by inhibiting mitochondrial proteins which in turn decreased ROS generation [382].

NAC, which is responsible for the sequestration of cellular ROS, had a weaker effect on the suppression of inflammatory genes compared to CoQ10. This might be because the effect of NAC is not as selective but predominantly works in an indirect manner by restoring

intracellular levels of GSH. However, the biologically active action of GSH is also dependent on the availability of other cofactors such as NADPH and selenium, which maintains GSH in the reduced state [286]. Therefore, the use of NAC as an antioxidant fails to account for secondary factors required to provide redox protection to a cell. This might therefore explain the weaker anti-inflammatory effects with NAC. It is worth noting that NAC was used at very high concentrations (mM) in the joint as has been reported in other systems. We cannot exclude that the non-specific action of NAC, at high concentrations, might have exerted off-target effects and influence cell viability due to the acidic nature of the drug. Future studies would therefore need to be done to validate this work by looking at chondrocyte viability and using inhibitor assay data in conjunction with robust in-vivo work. Interestingly NAC has been used in vivo and demonstrates disease modification after surgical induction of OA [375].

Apocynin was the weakest of the anti-oxidant agents in the suppression of inflammatory genes on injury. It only suppressed the upregulation of *IL6*, *COX2* and *ADAMTS4*. This might be because membrane-derived ROS do not contribute a large proportion to the overall ROS in chondrocytes [288]. Several studies have reported that although NOX is critical in the production of ROS, the vast majority comes from the mitochondria [383, 384]. In addition, the presence of low concentration of free radical species can itself initiate and propagate a chain reaction of further radical production. This would perpetuate the production of cellular ROS which would be immune to any membrane specific ROS-blockade. Another factor that might explain the reduced effectiveness of apocynin as an anti-inflammatory is the relative non-specificity of the inhibitor. The inhibitor has an IC50 of 10 μm, so a high concentration of 1 mM was used in the trotter joints. Although the apocynin is a pan NOX inhibitor, there might also be functional redundancies between the different

NOX isoforms in the production of membrane-derived ROS. Redundancies between different NOX isoforms have in fact been reported in the literature [385].

4.3.6 Role of ROS in cartilage injury

Collectively, my results demonstrated that ROS contribute to driving mechanoflammation on cartilage injury. Studies have supported this finding showing that ROS act as intracellular signalling mediators to initiate various inflammatory responses in OA. Several transcription factors have been shown to be redox sensitive including NF-κB, AP1, p53 and HIF-1α [386]. Cysteine groups in these transcription factors may constitute redox-sulfhydryl sensors which regulate gene expression [386]. There has been evidence to suggest that ROS also act as signalling mediators to cytokines and growth factors [298]. TNFα and bFGF were shown to induce NOX-dependent ROS production, which itself was shown to induce c-fos expression in bovine chondrocytes [298]. C-fos is a proto-oncogene that stimulates inflammatory gene regulation in conjunction with AP1 transcription factors. Separate studies have shown that inhibition of c-fos/AP1 provides chondroprotection [387, 388]. Moreover, treatment of chondrocytes with NO increases *MMP13* gene expression; the mechanism is thought to involve the reduction of the binding affinity of AP1 transcription factor to the promoter regions of genes secondary to direct redox modulation of cysteine residues on the AP1 binding site. My results demonstrated that CoQ10 provided an almost complete suppression of mechanoflammation whereas NAC, and apocynin provided partial suppression. Taken together, the mechanisms by which ROS from each of these sources were driving inflammation might have been through regulation of transcription factor binding and/or

acting as signalling intermediates of cytokines and growth factors over and above its role in suppressing atRA.

Although I did not directly investigate chondrocyte cell survival or measures of matrix composition, ROS have been implicated in each of these from previous studies. It has been established that NO, in a concomitant fashion with O2-, is an inducer of chondrocyte apoptosis by inducing caspase 3 activation [320]. In vitro studies have also suggested a function for ROS in cartilage degradation. Pelletier et al. demonstrated that inhibition of iNOS protected against cartilage degradation in a surgically induced model of dog OA [389]. Subsequent work revealed that the NOS inhibitor, L-NMMA, suppressed IL1-induced proteoglycan breakdown [390]. SOD has also been implicated in inhibiting proteoglycan synthesis in primary bovine chondrocytes [391]. These findings suggest that ROS not only increase inflammatory gene regulation in a mechanosensitive manner but have also been demonstrated to exert a catabolic effect on cartilage composition that is reversed by restoring the redox balance.

Consistent with my data, previous studies have also implicated ROS in the regulation of pro-inflammatory cytokines [285]. IL1β stimulation of chondrocytes increases the production of ROS which results in mitochondrial dysfunction [392]. Increased levels of intracellular ROS activates certain redox-sensitive transcription factors, such as AP1, resulting in the induction of inflammatory genes such as *IL6*, *COX2* and *INOS* [288]. Moreover, ROS has also been demonstrated to inhibit proteoglycan synthesis by activating the MAPK/ERK pathway [393].

Some studies have reported that ROS exerts anti-inflammatory effects in the joint. For example, iNOS-deficient mice demonstrated enhanced inflammation illustrated by increased leukocyte infiltration into the perivascular tissues and synovial tissues of animals

[394]. In another study, inhibiting the production of NO failed to relieve and in fact increased clinical manifestations of arthritis [395]. It is well established that ROS are important as second messengers to control a multitude of functions including apoptosis, cell proliferation and differentiation [276]. Likewise, in chondrocytes, ROS are responsible for the activation of a number of intracellular signalling cascades involved in cell growth and proliferation [285]. The deleterious actions of ROS are thought to be induced due to an imbalance in the redox state of the cell. Key cellular antioxidants such as GPx, Trx system and SOD, which normally regulate the physiological range of ROS, to drive beneficial end effects, become dysregulated in diseased cartilage [285]. SOD2 is responsible for catalysing the reaction of the superoxide anion into hydrogen peroxide and oxygen. SOD2 therefore regulates the levels of intracellular superoxide anion. Studies have demonstrated that mitochondrial dysfunction is associated with downregulation of SOD2 [283, 287]. Christos Gav et al. showed that not only was lipid peroxidation levels higher in OA cartilage, but this was associated with SOD2 depletion in chondrocytes [396]. Moreover, SOD2 depletion led to increased mtDNA strand breaks and release of excess ROS [396]. Richard Loser and his group demonstrated that the GSH and Trx antioxidant systems are also dysregulated in chondrocytes with increasing age [397]. Chondrocytes that were isolated from older donors had decreased activities of gluthathione and thioredoxin peroxidase [397]. In addition, cells treated with SIN-1 (to induce oxidative stress) in-vitro were more susceptible to cell death induced by SIN-1 due to depleted intracellular GSH levels [397].

ROS are crucial intracellular mediators under normal physiological conditions, which for chondrocytes, is typified by an avascular environment with low oxygen tension. Collectively, these studies demonstrate that pathological effects of ROS become apparent when the concentrations of either ROS or their end metabolites (lipid peroxidation products) exceed physiological levels. Moreover, the loss of protective antioxidants in the cell with

disease can perpetuate the increase in intracellular ROS and can contribute towards aberrant inflammation and consequent cartilage degradation. However, these in-vitro studies demonstrating ROS as a potential catabolic agent have, to date, only been supported by very limited in-vivo and clinical translational studies to further validate antioxidative agents as disease modifying in OA. This might be due to a number of reasons that might include drug selection, dosing and route of administration. There is therefore still a pressing need for further supportive in-vivo and clinical studies to definitively identify ROS as a driver of disease in OA.

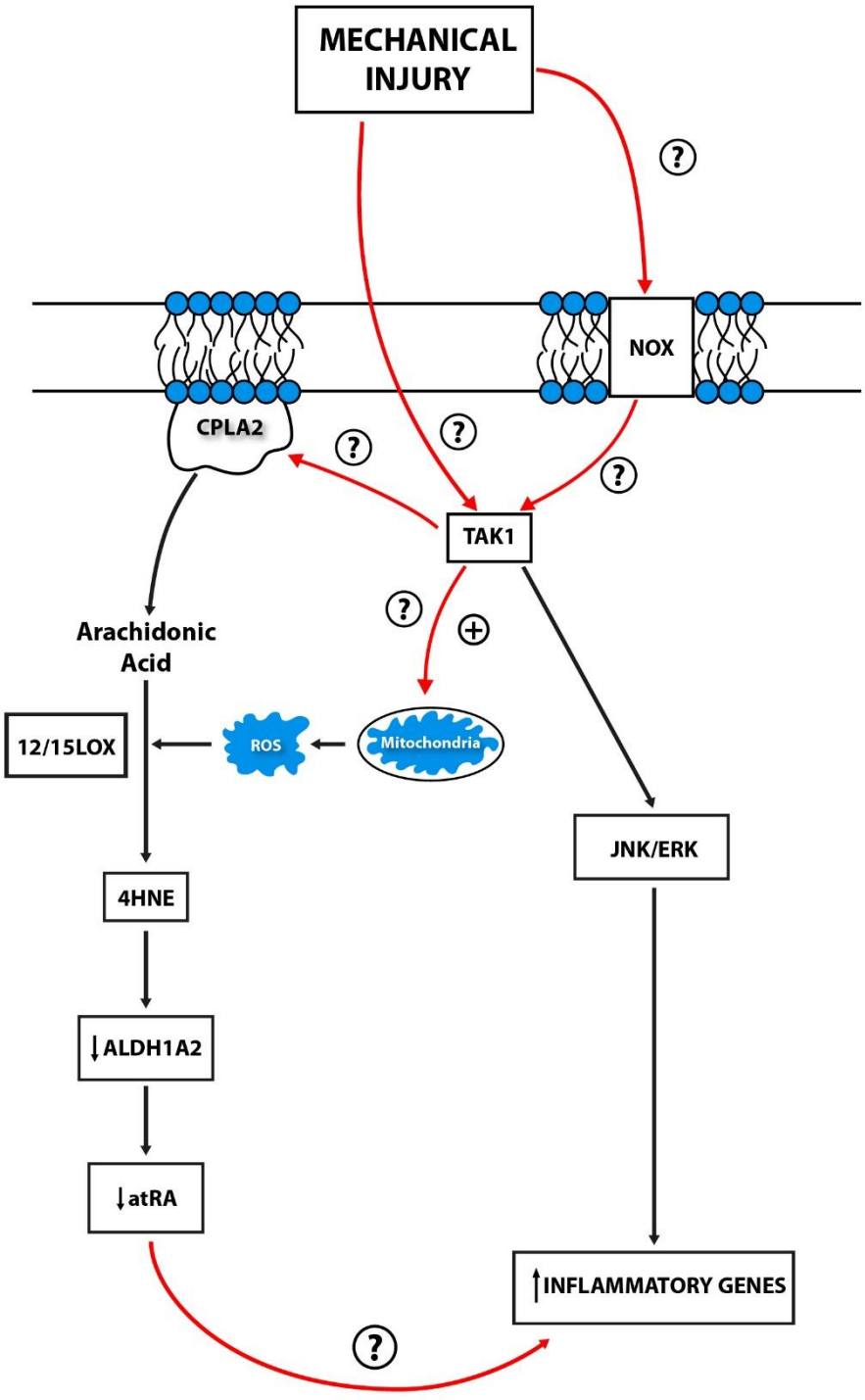
MECHANICAL INJURY
?
NOX
CPLA2
?
?
?
TAK1
?
⊕
Arachidonic Acid
12/15LOX
ROS
Mitochondria
JNK/ERK
4HNE
↓ALDH1A2
↓atRA
↑INFLAMMATORY GENES
?

Figure 4.14: Schematic representing working hypothesis achieved at the end of Chapter 4.

Mechanical injury downregulates all-trans-retinoic acid (atRA)-responsive genes in both a reactive oxygen species (ROS)-sensitive and cytosolic phospholipase A2 (cPLA2)-sensitive manner. cPLA2 and transforming growth factor activated-beta kinase 1 (TAK1) are phosphorylated on cartilage injury. However, by the end of Chapter 4 it was yet to be determined what caused the activation of both cPLA2 and TAK1 on cartilage injury. Block red line = undetermined; block black line = full activation; dotted black line = partial activation.

5 CHAPTER 5: DETERMINING THE MECHANISM BY WHICH INJURY ACTIVATES cPLA2

5.1 Introduction

In Chapter 4, I demonstrated that not only was cPLA2 activated on cartilage injury, but the downregulation of atRA-responsive genes on injury was also sensitive to cPLA2 activation. Inhibiting cPLA2 or downstream enzymes (namely 12/15 LOX) prevented the downregulation of atRA-responsive genes and also suppressed inflammatory gene regulation on cartilage injury.

Next, I determined what caused the activation of cPLA2. The enzymatic activity of cPLA2 is determined by its phosphorylation at serine 505 [307]. Doing so enables cPLA2 to hydrolyse PUFAs in the lipid bilayer to liberate arachidonic acid. Studies have long implicated MAPKs in the phosphorylation and activation of cPLA2 [398, 399]. For example, ERK1/2 has been shown to phosphorylate cPLA2 in multiple cell lines including vascular smooth muscle cells, neural glial cells and hepatocytes [307, 399, 400]. However, MAPK-independent activation of cPLA2 has also been reported, such as by protein kinase C mediated phosphorylation [401]. Our lab has previously shown that TAK1 itself is rapidly activated (within 30 seconds of injury) on cartilage injury and subsequently activates downstream MAPK signalling pathways (namely JNK, ERK and p38) and NF-κB signalling although we have not yet discovered the upstream mediator which activates TAK1 [99]. Our group has further shown that the downregulation of atRA-responsive genes on cartilage injury (and subsequent increase in inflammatory gene regulation) was highly TAK1-sensitive. I also noted that atRA-responsive genes were regulated by ROS in Chapter 4.

Based on these collective observations, I determined whether any of these factors activated cPLA2 on injury and, in doing so, further categorised the cPLA2, ROS and TAK1 pathways on cartilage injury.

5.1.1 TAK1 and MAPKs are phosphorylated on cartilage injury

Having shown that cPLA2 was phosphorylated on cartilage injury, I next investigated the mechanism by which this occurred. I hypothesised that TAK1 was a likely candidate to cause the phosphorylation of cPLA2. As discussed, our group previously showed that TAK1 is phosphorylated on injury, and this resulted in the phosphorylation of downstream MAPKs (JNK and ERK). First, I validated these previous findings and showed the activation of TAK1 and MAPKs on cartilage injury.

Porcine cartilage injury lysates were generated at 0 minutes, 5 mins, 10 mins and 30 mins post cartilage injury. Lysates were immunoblotted for pJNK, pERK and tERK. A new set of injury lysates were generated to test pTAK1.

JNK, ERK (Fig 5.1A) and TAK1 (Fig 5.1B) were not phosphorylated at zero hour but were all phosphorylated by 5 mins post cartilage injury, and this was seen up to 30 mins post injury.

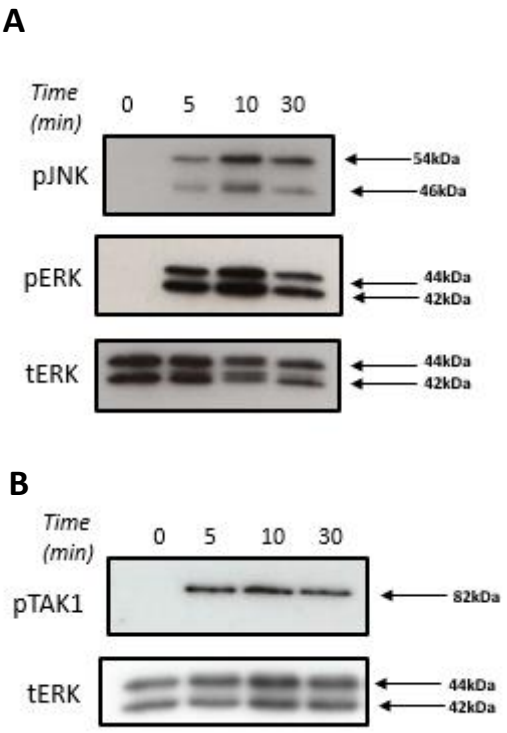

Figure 5.1: TAK1 and MAPKs are phosphorylated on cartilage injury.

Porcine metacarpophalangeal (MCP) joints were decontaminated in 2% Virkon for 20 minutes before being equilibrated at 37°C, 5% CO_2 for 1 hour. The MCP joints were opened and cartilage was rapidly explanted, as described in Materials and Methods. Explanted cartilage was either immediately cooled in ice-cold 1X RIPA Buffer nitrogen (zero hour time point) or cultured in serum free DMEM for various periods of time (5min, 10min and 30min) at 37 °C, 5% CO_2 before being transferred to ice cold, 1X RIPA buffer. Explants with 1X RIPA buffer, were mildly shaken for 45 minutes at 4°C. Lysates were run on 10% Sodium Dodecyl Sulphate-Polyacrylamide Gel (SDS PAGE) and transferred to poly (vinylidene) (PVDF) membrane. PVDF membrane was blocked in 5% milk for 1 hour at room temperature, incubated overnight in 1:1000 primary antibody (either pJNK or pERK; A). A new set of lysates were run to immunoblot pTAK1 (B). The membranes were washed 3 times in 1X TBST and incubated for a further hour in 1:2000 secondary antibody. Signal was enhanced by use of chemiluminescence and subsequently visualised using autoradiography. The blots were stripped and re-probed for total ERK.

5.1.2 The phosphorylation of MAPKs and cPLA2 on cartilage injury is TAK1-sensitive

Having shown that JNK, ERK and TAK1 were phosphorylated by 5 mins post porcine cartilage injury, I used a TAK1 inhibitor (5-Z-Oxozeanol, 5Z-7) to suppress the phosphorylation of each of these kinases. Our lab has previously shown that phosphorylation

of MAPKs are highly TAK1-sensitive [99]. I validated these results by using the same trotter injury model validated in Chapter 4.

I preinjected porcine MCP joints with either 5 μM 5Z-7 or vehicle control. Injured cartilage explants were incubated for various times in serum-free media containing either 5Z-7 or vehicle. Lysates were extracted and immunoblotted for pERK, pJNK, pTAK1 and tERK (Fig 5.2A). Quantification of three separate experiments was performed using FIJI-App, ImageJ-win64 Gel Analysis software. Results were normalised to tERK and statistical significance of comparison between groups analysed by a two-way ANOVA, with post hoc multiple comparisons corrected using Tukey's tests.

In the ex-vivo tissue (zero hour), there was no basal phosphorylation of either JNK, ERK or TAK1 (Fig 5.2A). In those injured joints injected with vehicle, there was an increase in the phosphorylation of JNK, ERK and TAK1 at 5 mins which lasted up to 30 mins post injury. The phosphorylation of JNK, ERK and TAK1 increased by 15.1-fold ($p < 0.01$) (Fig 5.2B), 4.1-fold ($p < 0.01$) (Fig 4.24C) and 14.9-fold ($p < 0.01$) (Fig 4.24A), respectively, in MCP joints treated with vehicle. In contrast, 5Z-7 markedly suppressed the phosphorylation of JNK ($p < 0.01$), ERK ($p < 0.01$) and TAK1 ($p < 0.01$) between 5 mins and 30 mins post cartilage injury compared to vehicle-injected joints (Fig 5.2B-D).

Given that TAK1 is rapidly activated on cartilage injury (prior to the phosphorylation of cPLA2) and that inhibiting both TAK1 and cPLA2 at the point injury prevented the downregulation of atRA-responsive genes, I determined whether the use of 5Z-7 suppressed the phosphorylation of cPLA2. Lysates from cartilage treated with 5Z-7 were run on new SDS-PAGE gels and immunoblotted for pcPLA2 (Fig 5.3A). Quantification of three separate experiments was performed and normalised to tERK.

Preinjection of the joints with 5Z-7 partially suppressed the phosphorylation of cPLA2 by 48.7% (SD ± 0.879) ($p < 0.01$) between 0 and 30 mins post injury compared to injured vehicle-injected joints.

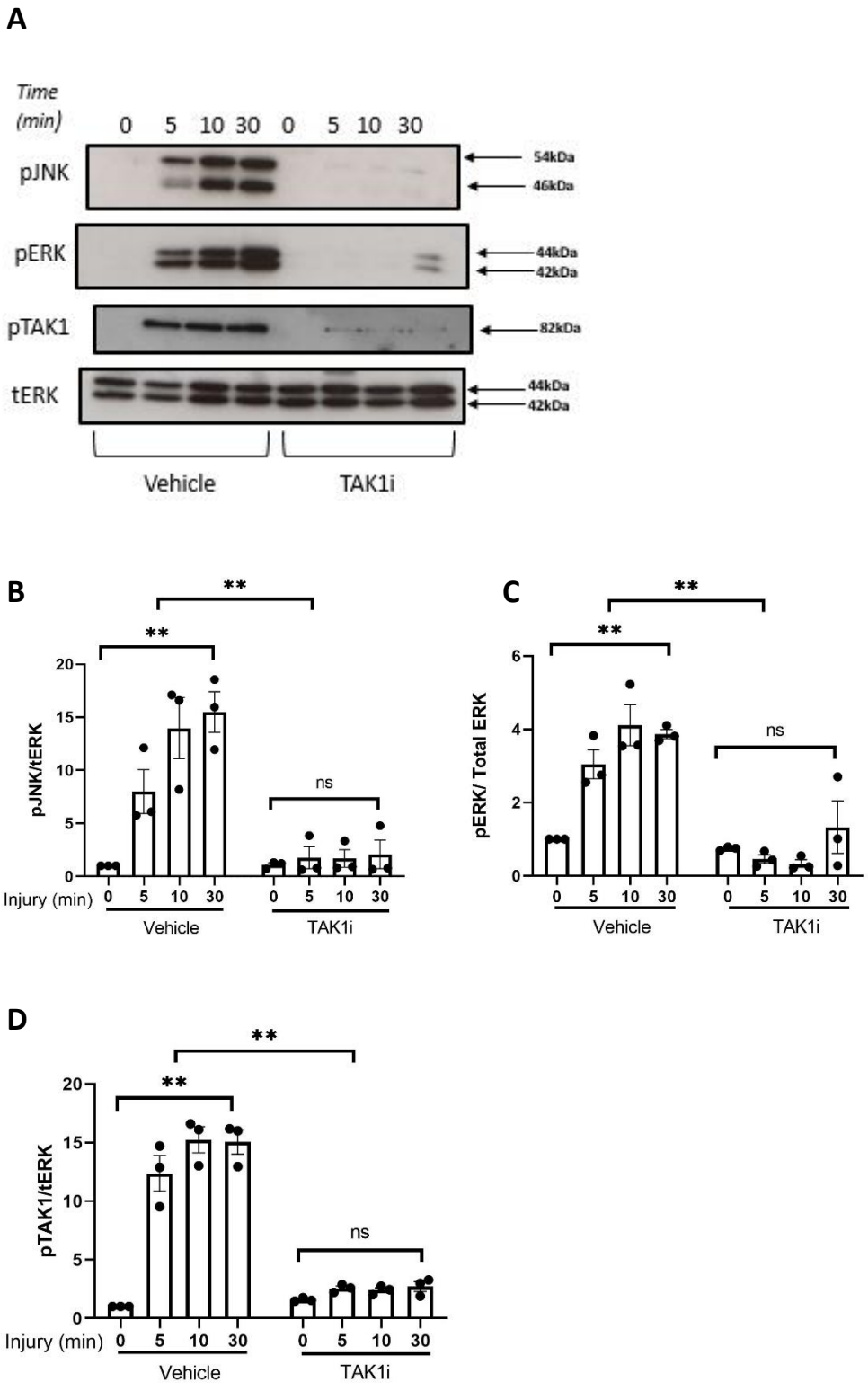

Figure 5.2: TAK1 inhibition suppresses the phosphorylation of MAPKs on cartilage injury.

Porcine metacarpophalangeal (MCP) joints were decontaminated in 2% Virkon for 20 minutes before being equilibrated at 37°C, 5% CO_2 for 1 hour. MCP joints were injected with either 5 µM TAK1i or vehicle control and incubated for another 1 hour at 37 °C. The MCP joints were opened and cartilage was rapidly explanted, as described in Materials and Methods. Explanted cartilage was either immediately cooled in ice-cold 1X RIPA Buffer nitrogen (zero hour time point) or cultured in serum free DMEM with or without TAK1i for various periods of time (5min, 10min and 30min) at 37 °C, 5% CO_2 before being transferred to ice cold, 1X RIPA buffer. Explants with 1X RIPA buffer, were mildly shaken for 45 minutes at 4°C. Lysates were run on 10% Sodium Dodecyl Sulphate-Polyacrylamide Gel (SDS PAGE) and transferred to poly (vinylidene) (PVDF) membrane. PVDF membrane was blocked in 5% milk for 1 hour at room temperature and immunoblotted for pJNK, pERK and pTAK1. Signal was enhanced by use of chemiluminescence and subsequently visualised using autoradiography. Representative blot of three repeats shown (A). The blot was stripped and re-probed for total ERK. The quantification of three separate experiments was performed using FIJI-App, ImageJ-win64 Gel Analysis software and normalised to total ERK (B-D).

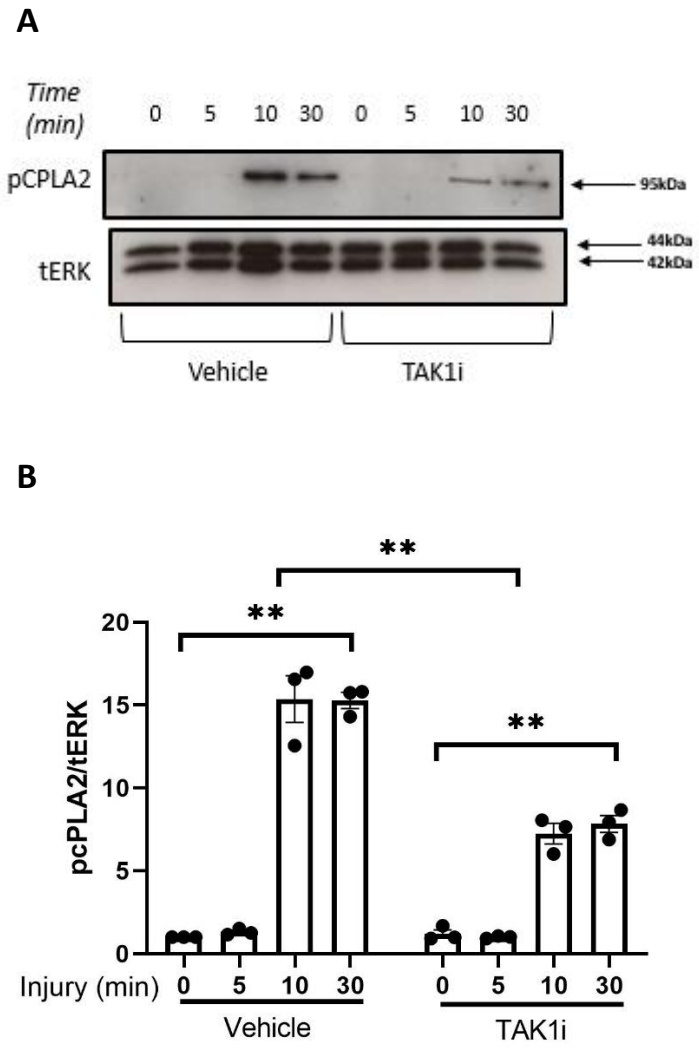

Figure 5.3: TAK1 inhibition partially suppresses the phosphorylation of cPLA2 on cartilage injury.

Porcine metacarpophalangeal (MCP) joints were decontaminated in 2% Virkon for 20 minutes before being equilibrated at 37°C, 5% CO_2 for 1 hour. MCP joints were injected with either 5 µM TAK1i inhibitor or vehicle control and incubated for another 1 hour at 37 °C. The MCP joints were opened and cartilage was rapidly explanted, as described in Materials and Methods. Explanted cartilage was either immediately cooled in ice-cold 1X RIPA Buffer nitrogen (zero hour time point) or cultured in serum free DMEM with or without TAK1i for various periods of time (5min, 10min and 30min) at 37 °C, 5% CO_2 before being transferred to ice cold, 1X RIPA buffer. Explants with 1X RIPA buffer, were mildly shaken for 45 minutes at 4°C. Lysates were run on 10% Sodium Dodecyl Sulphate-Polyacrylamide Gel (SDS PAGE) and transferred to poly (vinylidene) (PVDF) membrane. PVDF membrane was blocked in 5% milk for 1 hour at room temperature, incubated overnight in 1:1000 primary antibody (pcPLA2), washed 3 times in 1X TBST and incubated for a further hour in 1:2000 secondary antibody. pcPLA2 Signal was enhanced by use of chemiluminescence (A) and subsequently visualised using autoradiography. Representative blot of three repeats shown (A). The blot was stripped and re-probed for total ERK. The quantification of three separate experiments testing pcPLA2 was performed using FIJI-App, ImageJ-win64 Gel Analysis software and normalised to total ERK (B).

5.1.3 NAC does not affect the phosphorylation of cPLA2 on cartilage injury

At this point, I discovered that TAK1 was acting upstream of both cPLA2 and MAPK phosphorylation. I also demonstrated that the downregulation of atRA-responsive genes (and subsequent upregulation of inflammatory genes) was not only TAK1-sensitive (previously established data), but it was also cPLA2- and ROS-sensitive. Next, I determined whether ROS generation influenced atRA-responsive gene expression by acting either upstream or downstream of cPLA2 phosphorylation.

I injected serum-free media containing either vehicle or 20 mM NAC into trotter MCP joints prior to injury. Cartilage explants were cultured for various times, and lysates were immunoblotted for pcPLA2 and normalised to tERK (n = 3 separate trotters).

Preinjection of trotter MCP joints with 20 mM NAC did not have any significant effect on the phosphorylation of cPLA2 between 0 mins and 30 mins post cartilage injury compared to injured vehicle-injected joints (Fig 5.4B).

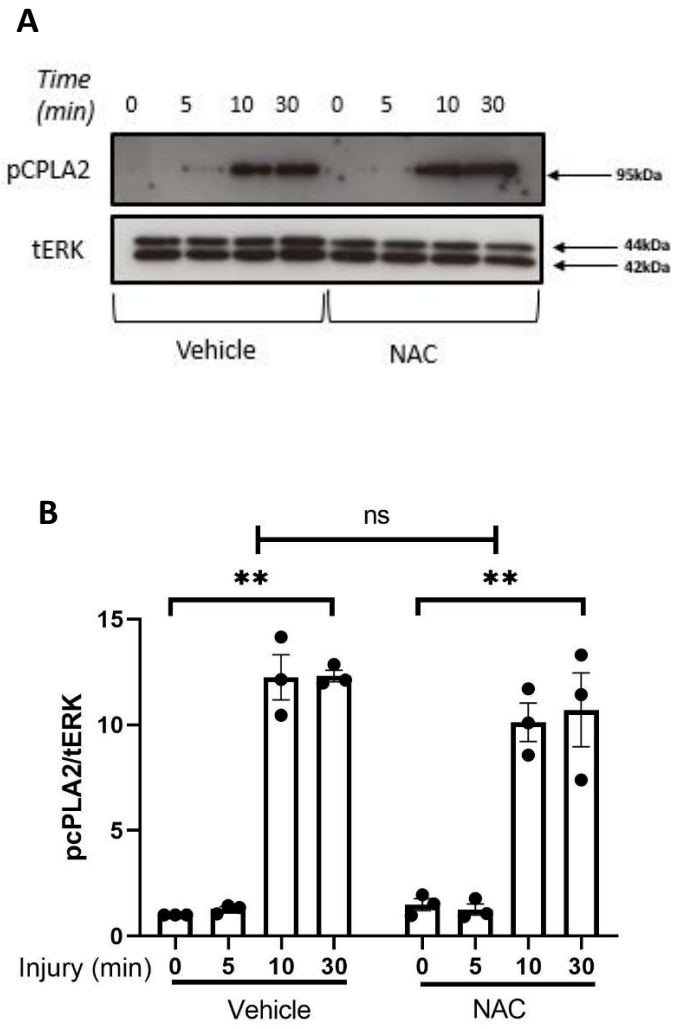

Figure 5.4: NAC does not affect the phosphorylation of cPLA2 on cartilage injury.

Porcine metacarpophalangeal (MCP) joints were decontaminated in 2% Virkon for 20 minutes before being equilibrated at 37°C, 5% CO_2 for 1 hour. MCP joints were injected with either 20mM NAC or vehicle control and incubated for another 1 hour at 37 °C. The MCP joints were opened and cartilage was rapidly explanted, as described in Materials and Methods. Explanted cartilage was either immediately cooled in ice-cold 1X RIPA Buffer nitrogen (zero hour time point) or cultured in serum free DMEM with or without NAC for various periods of time (5min, 10min and 30min) at 37 °C, 5% CO_2 before being transferred to ice cold, 1X RIPA buffer. Explants with 1X RIPA buffer, were mildly shaken for 45 minutes at 4°C. Lysates were run on 10% Sodium Dodecyl Sulphate-Polyacrylamide Gel (SDS PAGE) and transferred to poly (vinylidene) (PVDF) membrane. PVDF membrane was blocked in 5% milk for 1 hour at room temperature, incubated overnight in 1:1000 primary antibody (pcPLA2), washed 3 times in 1X TBST and incubated for a further hour in 1:2000 secondary antibody. pcPLA2 Signal was enhanced by use of chemiluminescence (A Upper) and subsequently visualised using autoradiography. Representative blot of three repeats shown (A). The blot was stripped and re-probed for total ERK. The quantification of three separate experiments testing pcPLA2 was performed using FIJI-App, ImageJ-win64 Gel Analysis software and normalised to total ERK (B).

5.1.4 CoQ10 does not affect the phosphorylation of cPLA2 on cartilage injury

Next, I determined whether mitochondrial-derived ROS influenced the phosphorylation of cPLA2 on injury. CoQ10 inhibits the production of ROS from the mitochondria, and earlier, I showed that both cPLA2 inhibitor and CoQ10 prevented the downregulation of atRA-responsive genes (and subsequent upregulation of inflammatory genes) on cartilage injury. Therefore, I investigated whether ROS-derived from the mitochondria mediated this cPLA2-sensitive downregulation of atRA-responsive genes on injury.

MCP joints were preinjected with 150 μM of CoQ10 or vehicle prior to injury. Injured cartilage were incubated in serum-free media containing either CoQ10 or vehicle for various times as mentioned above. Lysates were collected and immunoblotted for pcPLA2. Quantification of three separate experiments was performed, and results were normalised to tERK.

Like NAC, CoQ10 had no significant effect on the phosphorylation of cPLA2 between 0 mins and 30 mins post cartilage injury (Fig 5.5B). NAC and CoQ10 had significant roles in preventing the downregulation of atRA-responsive genes on cartilage injury. These results indicated that cytoplasmic and mitochondrial ROS were exerting their effects downstream of cPLA2.

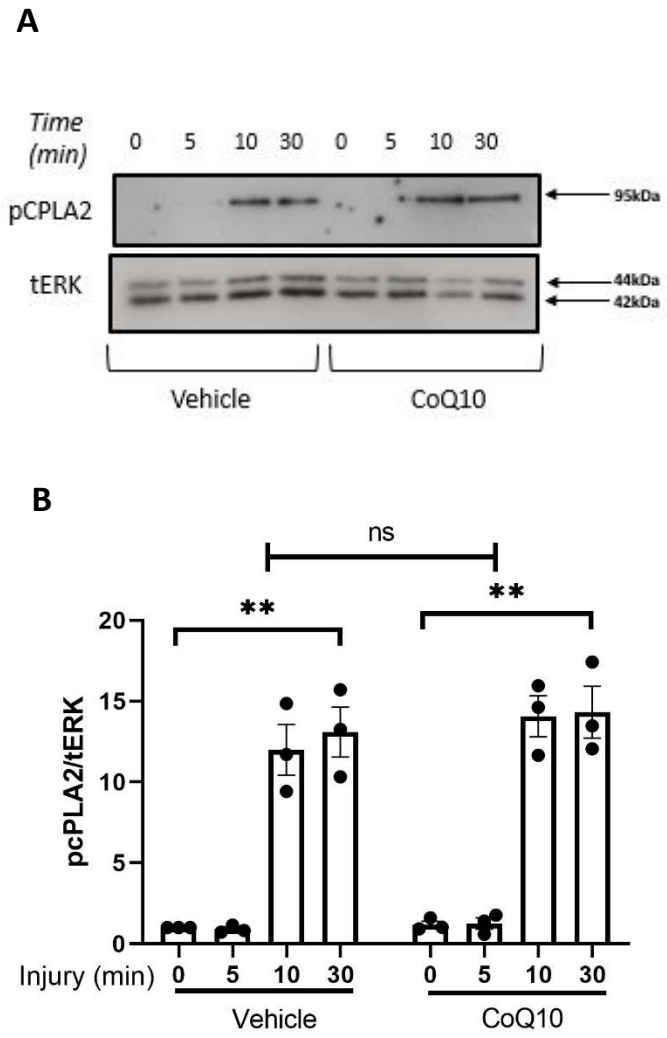

Figure 5.5: CoQ10 does not affect the phosphorylation of cPLA2 on cartilage injury.

Porcine metacarpophalangeal (MCP) joints were decontaminated in 2% Virkon for 20 minutes before being equilibrated at 37°C, 5% CO_2 for 1 hour. MCP joints were injected with either 150 µM CoQ10 or vehicle control and incubated for another 1 hour at 37 °C. The MCP joints were opened and cartilage was rapidly explanted, as described in Materials and Methods. Explanted cartilage was either immediately cooled in ice-cold 1X RIPA Buffer nitrogen (zero hour time point) or cultured in serum free DMEM with or without CoQ10 for various periods of time (5min, 10min and 30min) at 37 °C, 5% CO_2 before being transferred to ice cold, 1X RIPA buffer. Explants with 1X RIPA buffer, were mildly shaken for 45 minutes at 4°C. Lysates were run on 10% Sodium Dodecyl Sulphate-Polyacrylamide Gel (SDS PAGE) and transferred to poly (vinylidene) (PVDF) membrane. PVDF membrane was blocked in 5% milk for 1 hour at room temperature, incubated overnight in 1:1000 primary antibody (pcPLA2), washed 3 times in 1X TBST and incubated for a further hour in 1:2000 secondary antibody. pcPLA2 signal was enhanced by use of chemiluminescence (A) and subsequently visualised using autoradiography. Representative blot of three repeats shown (A). The blot was stripped and re-probed for total ERK. The quantification of three separate experiments testing pcPLA2 was performed using FIJI-App, ImageJ-win64 Gel Analysis software and normalised to total ERK (B).

5.1.5 The phosphorylation of cPLA2 on cartilage injury is partially NOX-sensitive

I next determined whether ROS derived from the membrane-bound NOX complex influenced cPLA2 phosphorylation. Earlier I showed that inhibiting NOX partially prevented the downregulation of atRA-responsive genes on injury and exerted a partial anti-inflammatory effect. I determined whether ROS derived from NOX was acting upstream of cPLA2 phosphorylation.

Trotter MCP joints preinjected with either 1 mM apocynin or vehicle control were dissected open and cartilage explanted. Explanted cartilage was incubated in serum-free media containing inhibitor or vehicle for specified times. Lysates were immunoblotted for pcPLA2. Quantification of three separate experiments was performed, and results were normalised to tERK.

Compared to injured vehicle-injected joints, apocynin partially suppressed the phosphorylation of cPLA2 by 29.4% (SD ± 0.947) ($p < 0.01$) between 0 and 30 mins post injury (Fig 5.6B).

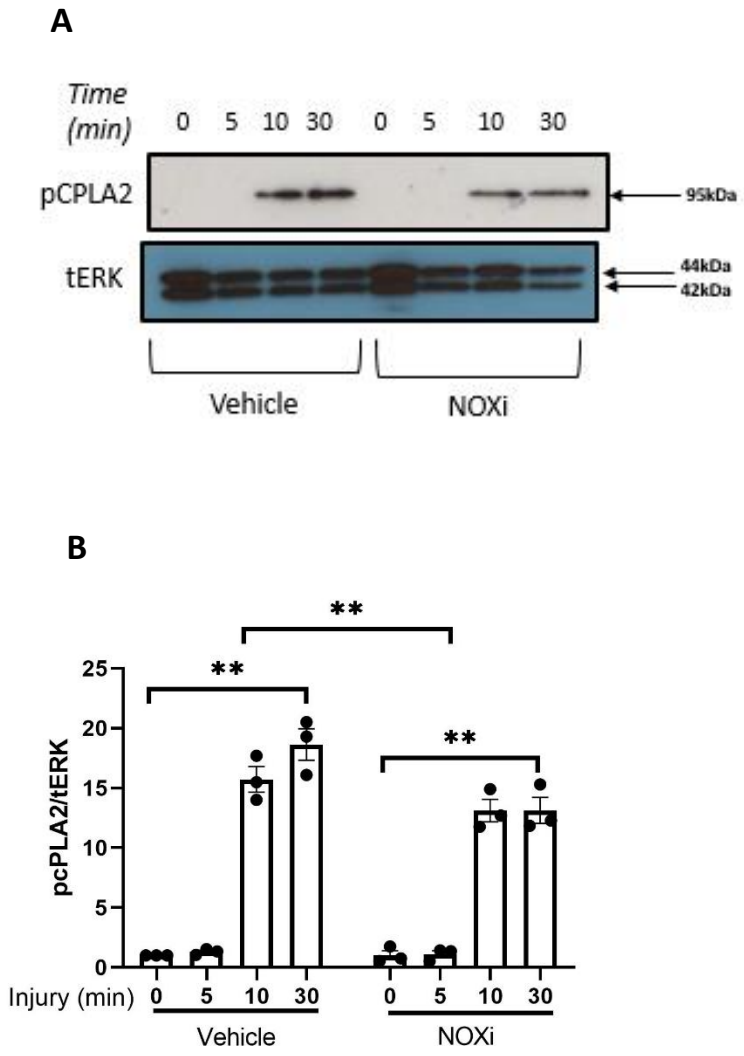

Figure 5.6: NOX inhibition partially suppresses the phosphorylation of cPLA2 on cartilage injury.

Porcine metacarpophalangeal (MCP) joints were decontaminated in 2% Virkon for 20 minutes before being equilibrated at 37°C, 5% CO_2 for 1 hour. MCP joints were injected with either 1mM NOXi inhibitor or vehicle control and incubated for another 1 hour at 37 °C. The MCP joints were opened and cartilage was rapidly explanted, as described in Materials and Methods. Explanted cartilage was either immediately cooled in ice-cold 1X RIPA Buffer nitrogen (zero hour time point) or cultured in serum free DMEM with or without NOXi for various periods of time (5min, 10min and 30min) at 37 °C, 5% CO_2 before being transferred to ice cold, 1X RIPA buffer. Explants with 1X RIPA buffer, were mildly shaken for 45 minutes at 4°C. Lysates were run on 10% Sodium Dodecyl Sulphate-Polyacrylamide Gel (SDS PAGE) and transferred to poly (vinylidene) (PVDF) membrane. PVDF membrane was blocked in 5% milk for 1 hour at room temperature, incubated overnight in 1:1000 primary antibody (pcPLA2), washed 3 times in 1X TBST and incubated for a further hour in 1:2000 secondary antibody. pcPLA2 signal was enhanced by use of chemiluminescence (A) and subsequently visualised using autoradiography. Representative blot of three repeats shown (A). The blot was stripped and re-probed for total ERK. The quantification of three separate experiments testing pcPLA2 was performed using FIJI-App, ImageJ-win64 Gel Analysis software and normalised to total ERK (B).

5.1.6 12/15 LOX inhibition does not affect the phosphorylation of cPLA2 on cartilage injury

12/15 LOX acts downstream of cPLA2 to regulate atRA-responsive genes, so it is not predicted to affect the phosphorylation of cPLA2. Trotter MCP joints were preinjected with either 1 μM 12/15 LOXi (ML351) or vehicle control prior to injury. Explants were cultured for various times in serum-free media containing either vehicle or inhibitor. Lysates were immunoblotted for pcPLA2 and normalised to tERK (n = 3 separate trotters). As expected, ML351 had no significant effect on the phosphorylation of cPLA2 between 0 mins and 30 mins post cartilage injury (Fig 5.7B).

Taken together, these data show that TAK1 was mainly responsible for the phosphorylation of cPLA2 on cartilage injury. In addition, ROS derived from the membrane-bound NOX complex is partly driving cPLA2 phosphorylation and therefore acting upstream of cPLA2. However, neither cellular ROS (inhibited by NAC) nor mitochondrial derived ROS (inhibited by CoQ10) affected the phosphorylation of cPLA2, suggesting they act downstream of cPLA2 phosphorylation to prevent the downregulation of atRA-responsive genes on cartilage injury. NOX could be exerting these effects through TAK1. In the next chapter, I explored the upstream activators of TAK1.

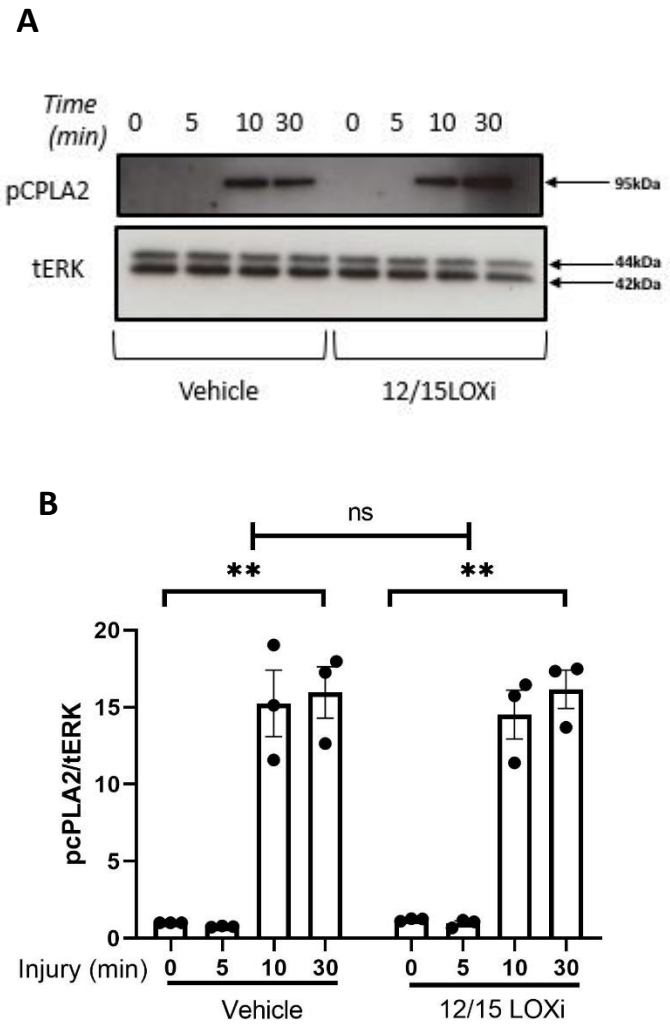

Figure 5.7: 12/15LOX inhibition does not affect the phosphorylation of cPLA2 on cartilage injury.

Porcine metacarpophalangeal (MCP) joints were decontaminated in 2% Virkon for 20 minutes before being equilibrated at 37°C, 5% CO_2 for 1 hour. MCP joints were injected with either 1 µM 12/15LOXi or vehicle control and incubated for another 1 hour at 37 °C. The MCP joints were opened and cartilage was rapidly explanted, as described in Materials and Methods. Explanted cartilage was either immediately cooled in ice-cold 1X RIPA Buffer nitrogen (zero hour time point) or cultured in serum free DMEM with or without 12/15LOXi for various periods of time (5min, 10min and 30min) at 37 °C, 5% CO_2 before being transferred to ice cold, 1X RIPA buffer. Explants with 1X RIPA buffer, were mildly shaken for 45 minutes at 4°C. Lysates were run on 10% Sodium Dodecyl Sulphate-Polyacrylamide Gel (SDS PAGE) and transferred to poly (vinylidene) (PVDF) membrane. PVDF membrane was blocked in 5% milk for 1 hour at room temperature, incubated overnight in 1:1000 primary antibody (pcPLA2), washed 3 times in 1X TBST and incubated for a further hour in 1:2000 secondary antibody. pcPLA2 signal was enhanced by use of chemiluminescence (A) and subsequently visualised using autoradiography. Representative blot of three repeats shown (A). The blot was stripped and re-probed for total ERK. The quantification of three separate experiments testing pcPLA2 was performed using FIJI-App, ImageJ-win64 Gel Analysis software and normalised to total ERK (B).

5.2 Discussion

5.2.1 TAK1 and MAPK activation on cartilage injury

TAK1 was phosphorylated rapidly by 5 mins post cartilage injury. The MAPKs, JNK and ERK were also phosphorylated by 5 mins following injury. Our lab previously showed that TAK1 is actually phosphorylated within a few seconds following injury [99]. Equally downstream MAPKs, ERK and p38 were phosphorylated within 30 seconds, whilst the earliest JNK phosphorylation was seen by 2 mins [99].

The use of a TAK1 inhibitor (5Z-7) abolished the phosphorylation of TAK1, ERK and JNK. It is well established that TAK1 is at least partially responsible for the activation of downstream MAPKs. Ismail et al. demonstrated that 5Z-7 not only suppressed TAK1 and MAPK activation, but it also suppressed the upregulation of inflammatory genes [99]. In yet unpublished data, our group further demonstrated that the downregulation of atRA-responsive genes on cartilage injury was TAK1-sensitive. Although we hypothesised that the action of atRA was downstream of both TAK1 and MAPK, I investigated this relationship in Chapter 7. In a separate study, Ismail et al. revealed that JNK2 KO mice had suppressed inflammatory gene regulation after OA induction and were partially protected from disease development [123]. Independent studies have also shown that inhibition or knockdown of ERK1 and ERK2 prevented the IL1-β-induced upregulation of *MMP3* and *MMP13* [402]. Moreover, the mRNA expression of COL2 and aggrecan was increased in the ERK1/2 knockdown chondrocytes [402].

Although I was unable to validate the phospho-p38 antibody, this has been shown to be implicated in mechanoflammation by our group [99]. P38 is rapidly phosphorylated within a few seconds following porcine and murine cartilage injury [99]. Secondly, Kurosaka et al.

further demonstrated that mechanical-stress-induced chondrocyte cell death reduced after inhibition of the p38 MAPK [403]. Another mechanism by which p38 can enhance inflammation is through increasing the mRNA stability of inflammatory genes. Clark et al. demonstrated that p38 MAPK was responsible for phosphorylating a zinc finger protein tristetraprolin (TTP) via the MAPK-activated protein kinase 2 (MAPKAPK2) [404]. This resulted in the stabilisation of the TTP mRNA. TTP is responsible for binding onto adenosine/uridine (AU) -rich elements (AREs) on the 3' region of short-lived inflammatory gene mRNA transcripts and target these for degradation [405]. However, the phosphorylation of TTP secondary to p38 MAPK activation inhibits deadenylation and thereby stabilises the mRNA transcript of inflammatory genes [405].

There has also been conflicting evidence surrounding the role of p38 MAPK pathway in cartilage biology. Prasadam et al. showed that, at an in-vivo level, the administration of a p38 MAPK inhibitor led to significant loss of proteoglycan, aggrecan and cartilage thickness [406]. More recently, Chun-Na et al. demonstrated that MAPK inhibitors protected against early-stage OA by activating autophagy [407]. Perhaps these results suggest a dual role for MAPKs in the progression of OA determined by the different stages of disease. The view around a dual role for MAPKs is supported by findings from Andy Clark et al. who showed that certain dual-specificity phosphatases (DUSPs) are activated by MAPKs, in particular ERK [408]. DUSPs are responsible for dephosphorylating and thereby inhibiting JNK and p38 activation in a negative feedback loop [408, 409]. This interaction between DUSPs and MAPKs helps to fine tune anti-inflammatory responses. An emerging consensus is that the acute mechanoinflammatory response might actually be important in initiating repair pathways, and instead it is the chronic insidious inflammation that requires pharmacological targeting and dampening in OA.

5.2.2 cPLA2 activation by TAK1

It was evident that cPLA2 was activated, at least partially, by TAK1 on cartilage injury. The TAK1 inhibitor, 5Z-7, was able to achieve a 70% suppression on the phosphorylation of cPLA2 on cartilage injury. This is strongly suggestive that TAK1 is acting upstream of cPLA2 and subsequent downregulation of atRA-responsive genes and upregulation of inflammatory genes (Figure 5.8). This is congruous with observations that atRA-responsive and inflammatory gene regulation on injury is TAK1-sensitive, and the temporal patterns of activation observed for both cPLA2 (at 10 mins) and TAK1 (within a few seconds from literature evidence). The phosphorylation of cPLA2 occurs at the serine 502 position [307], and numerous studies have reported this to be secondary to MAPKs (notably p38 and ERK) [398, 401]. However, one study reported cPLA2 phosphorylation to occur directly through TAK1 signalling [410]. In section 5.2.3, I discussed why the phosphorylation of cPLA2, in our system, is likely to be secondary to TAK1 and not the MAPKs.

The phosphorylation of cPLA2 was partially dependent on NOX but to a much lesser extent than TAK1. NOX is responsible for the production of ROS at the cellular membrane by catalysing the transfer of electrons to molecular oxygen and in the process generating superoxide anion and hydrogen peroxide. Given the weaker activation of cPLA2 by NOX in comparison to TAK1 (with further results obtained that showed the relationship between NOX and TAK1 phosphorylation on cartilage injury, discussed in Chapter 6) led us to hypothesise that NOX was perhaps acting upstream of TAK1 (Figure 5.8). The partial inhibition obtained by apocynin might also be explained by the lack of specificity of this drug towards NOX or even functional redundancies between the various different isoforms of NOX. Nonetheless, we hypothesised that NOX was acting to suppress cPLA2 phosphorylation through TAK1. To support this, one study demonstrated that ROS

generated from the NOX complex is capable of driving TAK1 signalling. Jiang et al. demonstrated that NOX4 gene silencing inhibited the TAK1-dependent SMAD2/3 phosphorylation in cardiac fibroblasts [411]. Furthermore, another group showed that TAK1-dependent SMAD2 phosphorylation is considerably reduced in NOX4-KO mice [412]. There is also evidence that NOX can promote the cPLA2 pathway and subsequent arachidonic acid metabolism. In 2016, Chung Lun et al. revealed that cPLA2 expression was enhanced via the NOX/ROS complex in human pulmonary alveolar epithelial cells [410]. The study reported that TNFα markedly stimulated NOX activity and ROS production in the form of superoxide anion, which resulted in an increase in cPLA2 gene expression [410]. Pretreatment of cells with a NOX inhibitor suppressed the TNFα-induced activation of cPLA2 [410]. However, it is important to note that I did not directly measure the activity of the NOX complex on injury. This would be important to measure if we are to further bolster evidence that NOX might be acting upstream of TAK1. Furthermore, the activity of NOX after mechanical injury must be very rapid (within seconds) and direct for it to be a regulator of TAK1. Further studies using fluorescent assays measuring NOX activity on injury would need to be conducted to determine this. In addition, the use of in-vivo NOX KO models could further validate my inhibitor assay results.

Collectively, the results strengthen the findings that both TAK1 and NOX are potential upstream regulators of cPLA2 activation (Figure 5.8). I investigated the detailed relationship between NOX and TAK1 in Chapter 6. Taken together with evidence from the literature, we hypothesised that NOX might be acting upstream of TAK1 on cartilage injury.

5.2.3 Cellular and mitochondrial-derived ROS does not activate cPLA2

Neither NAC nor CoQ10 suppressed the phosphorylation of cPLA2 on cartilage injury. Previously, I showed that both NAC and CoQ10 prevented the downregulation of atRA-

responsive genes and also suppressed the upregulation of inflammatory genes on injury. The downregulation of atRA-responsive genes on cartilage injury was also cPLA2-sensitive, which implied that ROS, inhibited by both NAC and CoQ10, was acting downstream of cPLA2 signalling (Fig. 5.8). This finding is supported by studies showing the interaction between mitochondrial ROS and cPLA2 metabolism. Mihalas et al. demonstrated that ROS-induced production of highly electrophilic aldehydes, such as 4-HNE, in oocytes was downstream of cPLA2 metabolism [413]. 4-HNE has been shown to inhibit the ALDH1A2 enzyme involved in the biosynthesis of atRA [367]. The hypothesis suggesting 4-HNE-mediated inhibition of ALDH1A2 was strengthened by our finding that mitochondrial-derived ROS did not influence cPLA2 phosphorylation.

The commonality between NAC/CoQ10 and cPLA2 inhibition was that they all prevented atRA-responsive gene downregulation. This further strengthened the hypothesis that ROS produced from the mitochondria (inhibited by CoQ10) and cytoplasmic-derived ROS (inhibited by NAC) was likely acting downstream of cPLA2 phosphorylation (Fig. 5.8). As discussed, the vast majority of ROS in chondrocytes are produced from the mitochondria (> 60%). Increased production of mitochondrial ROS has been shown to be a bigger contributor to the diversion of lipid metabolism into toxic aldehydes, such as 4-HNE, than ROS derived from other sources such NOX [288]. The involvement of mitochondrial-induced lipid peroxidation has been well documented in many neurodegenerative diseases, including Alzheimer's disease, Parkinson's disease, Huntington's disease and frontotemporal dementia [277]. Although both mitochondria and NOX have been implicated in the production of ROS in these neurodegenerative disorders, only the use of specific mitochondrial inhibitors have been shown to be effective in preventing ROS-induced lipid peroxidation in these conditions [277].

Furthermore, CoQ10 had a profound suppressive effect on inflammatory gene regulation which implied that the mitochondria might also form part of a separate pathway that is driving inflammatory gene regulation, independent of cPLA2, and likely downstream of atRA metabolism. Moreover, NOX inhibition partially suppressed cPLA2 phosphorylation whereas CoQ10 and NAC did not, suggesting that differential ROS might be produced between the NOX complex and mitochondria. In addition, it is also suggestive of the fact that cPLA2 might show differential sensitivities to different species of ROS. In support of this, studies have reported the mitochondria to produce a wide array of ROS ranging from superoxide, hydroxyl radical, peroxyl radical and singlet oxygen whereas NOX is capable of only producing hydrogen peroxide and superoxide anion [414]. The difference in function between NOX and mitochondrial-derived ROS was demonstrated by Mustapha et al. in 2010. The authors showed that NOX and not mitochondrial-derived ROS was responsible for the accelerated apoptosis of pericytes in diabetic retinopathy [414]. This varied ROS generation between the mitochondria and NOX might also be the case when chondrocytes respond to cartilage injury. However, this would need to be further investigated by the use of mass spectroscopy (MS) to determine whether ROS is released on cartilage injury. Secondly, the different species of ROS (if released by cartilage injury) would need to be determined by MS with and without the presence of inhibitors targeted against either the mitochondria or NOX complex. Therefore, from my work we can only begin to infer a role for mitochondrial ROS and NOX in mechanoflammation but this would require further quantitative and in-vivo studies to provide direct evidence and validate the hypothesis.

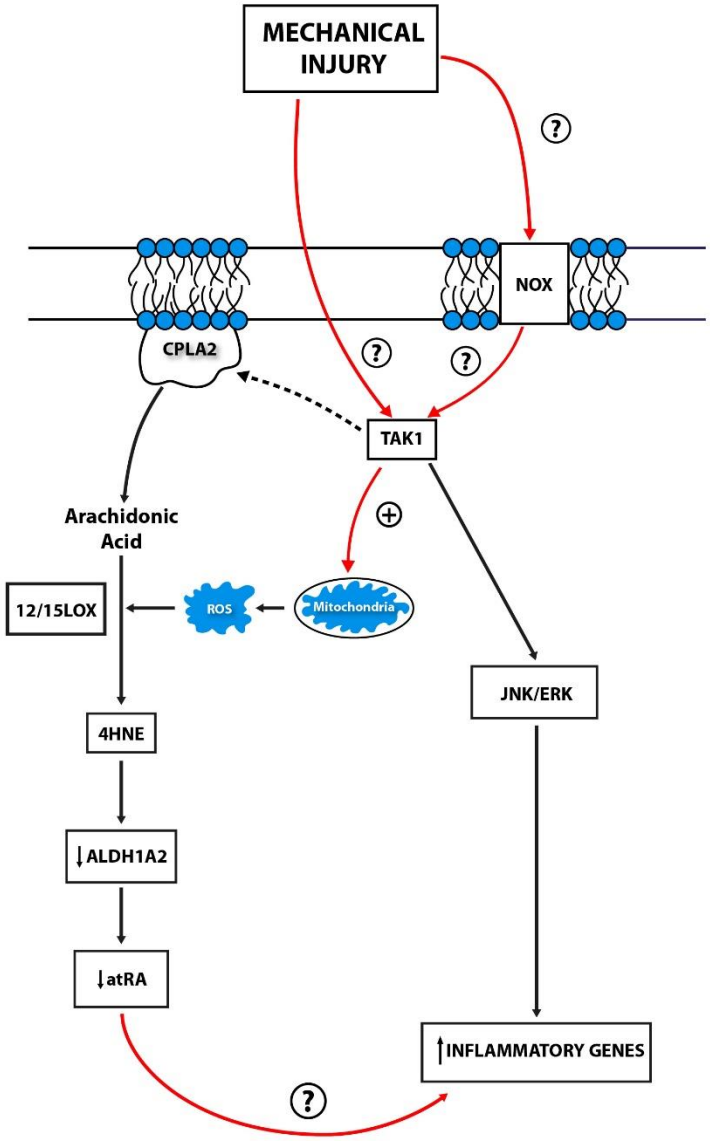

Figure 5.8: Schematic representing working hypothesis achieved at the end of Chapter 5.

Mechanical injury downregulates all-trans-retinoic acid (atRA)-responsive genes in both a reactive oxygen species (ROS)-sensitive and cytosolic phospholipase A2 (cPLA2)-sensitive manner. Transforming growth factor activated-beta kinase 1 (TAK1) is responsible for partially phosphorylating cPLA2 on cartilage injury. The phosphorylation of cPLA2 on cartilage injury is also NOX-sensitive and likely mediated via TAK1. By the end of Chapter 5 it was yet to be determined what activated TAK1 on cartilage injury and whether TAK1 was acting upstream or downstream of mitochondrial/cellular derived ROS. Block red line = undetermined; block black line = full activation; dotted black line = partial activation.

6 CHAPTER 6: DETERMING WHAT CAUSES THE ACTIVATION OF TAK1 ON CARTILAGE INJURY

6.1 Introduction

My results thus far validated the previous observations that TAK1 is rapidly activated on cartilage injury and that the activation of TAK1 on injury is responsible for driving mechanoflammation. In addition, they identify TAK1 as an important driver of cPLA2 activation. It was therefore important to identify upstream pathways that activate TAK1. Doing so would define a potential pharmacological target focused towards the suppression of mechanoflammation. Previous work from the lab had failed to find evidence of a soluble factor for the activation of TAK1 in injury. This was done by showing that explanted cartilage-conditioned medium was unable to activate TAK1 in cultured chondrocytes (unpublished data). This finding is further supported by the fact that TAK1 activation was not MyD88-dependent; the latter transduces signals from TLRs and IL1-R1 [99]. Given that both TAK1 and NOX inhibition suppressed cPLA2 activation, I hypothesised that NOX activation might be an upstream mediator of TAK1 on cartilage injury.

6.1.1 TAK1 phosphorylation on cartilage injury is ROS-sensitive

6.1.1.1 Phosphorylation of TAK1 on cartilage injury is partially NOX-sensitive

I determined whether inhibiting the membrane-bound NOX complex suppressed TAK1 and MAPK phosphorylation. The western blot membranes generated from the experiments conducted in section 5.1.5 were stripped with reblot buffer and immunoblotted for pJNK, pERK and pTAK1. Quantification of three separate experiments was performed, and results were normalised to tERK.

Apocynin partially suppressed JNK, ERK and TAK1 phosphorylation 30 mins after cartilage injury by 49.6% (SD ± 0.722), 65.4% (SD ± 0.393) and 67.8% (SD ± 1.30) respectively (Fig 6.1).

Collectively, these results showed that TAK1, ERK and JNK phosphorylation were at least partly ROS-sensitive but demonstrated distinct cellular activities. For instance, NOX appears to be partially responsible for TAK1, MAPK and cPLA2 activation whereas cytoplasmic and mitochondrial ROS appear to be key drivers of MAPKs, partial drivers of TAK1, and have no effect on cPLA2 phosphorylation.

Taken together, the partial inhibition of TAK1 on cartilage injury by NAC and CoQ10 cannot account for their full suppression on the phosphorylation of MAPKs. As such, I hypothesised that there might be another MAPKKK that is highly ROS-sensitive, responsible for the activation of the MAPKs and the subsequent increase in inflammatory gene regulation on cartilage injury. Apoptosis signal regulating kinase 1 (ASK1) is another MAPKKK, and its phosphorylation has been reported to be highly ROS-sensitive [415, 416]. Therefore, I next investigated the role of ASK1 in cartilage injury.

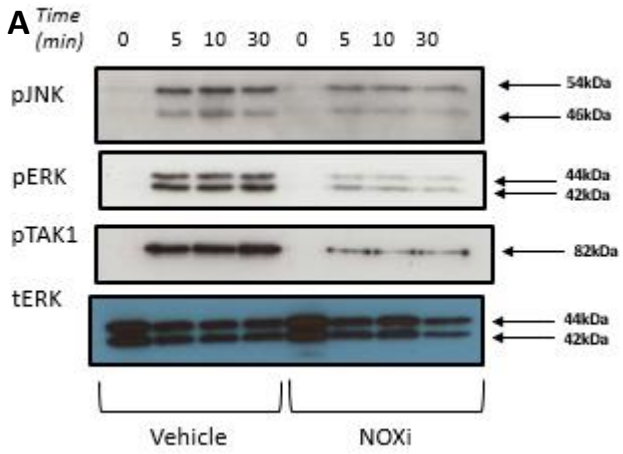
A
Time (min)
0 5 10 30 0 5 10 30
pJNK
pERK
pTAK1
tERK
54kDa
46kDa
44kDa
42kDa
82kDa
44kDa
42kDa
Vehicle
NOXi

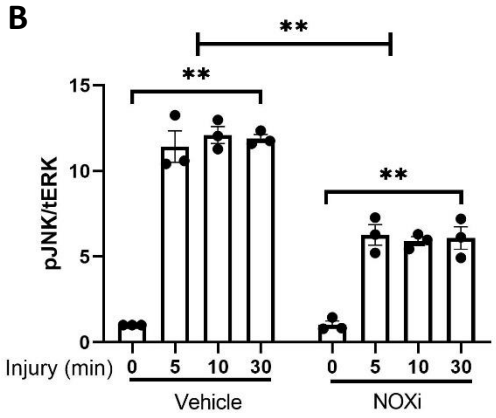
B
pJNK/tERK
Injury (min) 0 5 10 30 0 5 10 30
Vehicle
NOXi

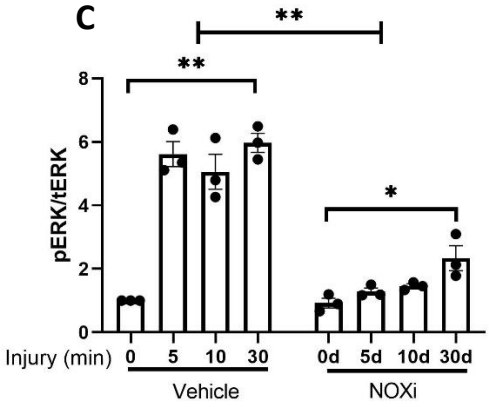
C
pERK/tERK
Injury (min) 0 5 10 30 0d 5d 10d 30d
Vehicle
NOXi

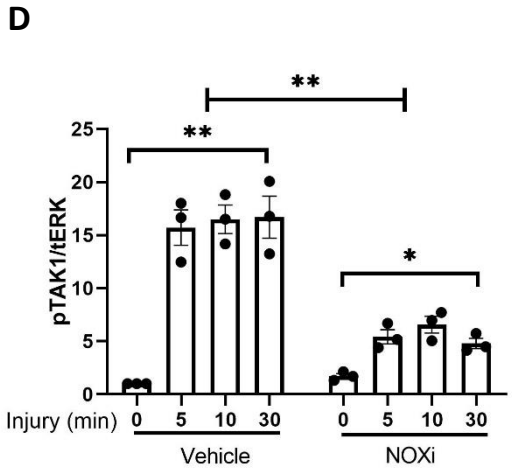
D
pTAK1/tERK
Injury (min) 0 5 10 30 0 5 10 30
Vehicle
NOXi

Figure 6.1: NOX inhibition partially suppresses the phosphorylation of TAK1 and MAPKs on cartilage injury.

Porcine metacarpophalangeal (MCP) joints were decontaminated in 2% Virkon for 20 minutes before being equilibrated at 37°C, 5% CO_2 for 1 hour. MCP joints were injected with either 1mM NOXi or vehicle control and incubated for another 1 hour at 37 °C. The MCP joints were opened and cartilage was rapidly explanted, as described in Materials and Methods. Explanted cartilage was either immediately cooled in ice-cold 1X RIPA Buffer nitrogen (zero hour time point) or cultured in serum free DMEM with or without NOXi for various periods of time (5min, 10min and 30min) at 37 °C, 5% CO_2 before being transferred to ice cold, 1X RIPA buffer. Explants with 1X RIPA buffer, were mildly shaken for 45 minutes at 4°C. Lysates were run on 10% Sodium Dodecyl Sulphate-Polyacrylamide Gel (SDS PAGE) and transferred to poly (vinylidene) (PVDF) membrane. PVDF membrane was blocked in 5% milk for 1 hour at room temperature and immunoblotted for pJNK, pERK and pTAK1. Signal was enhanced by use of chemiluminescence (A) and subsequently visualised using autoradiography. Representative blot of three repeats shown (A). The blot was stripped and re-probed for total ERK. The quantification of three separate experiments was performed using FIJI-App, ImageJ-win64 Gel Analysis software and normalised to total ERK (B-D).

6.1.1.2 NAC partially suppresses TAK1 phosphorylation but completely inhibits MAPK phosphorylation on cartilage injury

Having shown that NOX was partially responsible for the activation of TAK1, I looked to see whether TAK1 and MAPK phosphorylation were also affected by cytoplasmic ROS. Lysates generated from the experiment conducted in section 5.1.3 were run on new SDS-PAGE gels and immunoblotted for pJNK, pERK and pTAK1. Quantification of three separate experiments was performed, and results were normalised to tERK.

As previously shown, in ex-vivo zero hour time points, there was no basal phosphorylation of JNK, ERK or TAK1 (Fig 6.2A). NAC strikingly suppressed the phosphorylation of JNK (100%, SD ± 0.891) and ERK (100%, SD ± 1.05) at 30 mins ($p < 0.01$) (Fig 6.2B & C) and partially suppressed the phosphorylation of TAK1 at 30 mins post injury by 58.8% (SD ± 1.37) ($p < 0.05$) (Fig 6.2D).

A

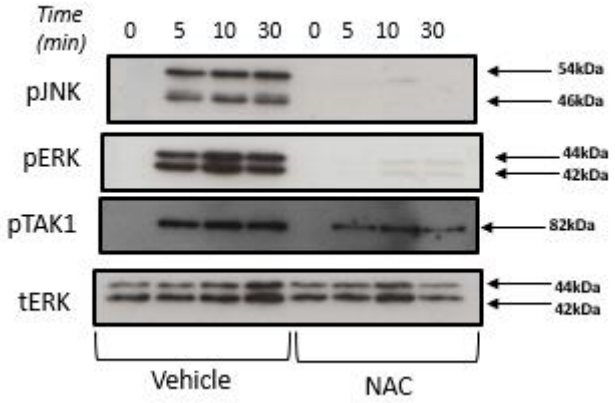
Time (min)
0 5 10 30 0 5 10 30
pJNK
pERK
pTAK1
tERK
54kDa
46kDa
44kDa
42kDa
82kDa
44kDa
42kDa
Vehicle
NAC

B

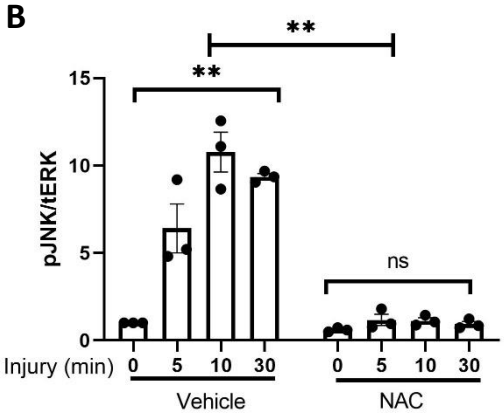
pJNK/tERK
**
**
ns
Injury (min) 0 5 10 30 0 5 10 30
Vehicle
NAC

C

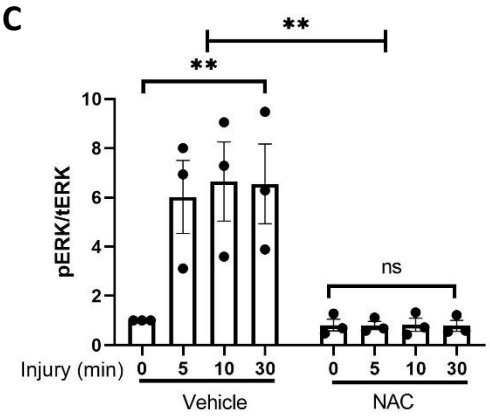
pERK/tERK
**
**
ns
Injury (min) 0 5 10 30 0 5 10 30
Vehicle
NAC

D

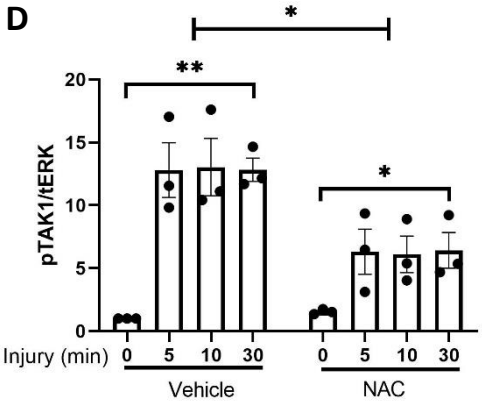
pTAK1/tERK
*
**
*
Injury (min) 0 5 10 30 0 5 10 30
Vehicle
NAC

Figure 6.2: NAC partially suppresses the phosphorylation of TAK1 and completely suppresses the phosphorylation of MAPKs on cartilage injury.

Porcine metacarpophalangeal (MCP) joints were decontaminated in 2% Virkon for 20 minutes before being equilibrated at 37°C, 5% CO_2 for 1 hour. MCP joints were injected with either 20mM NAC or vehicle control and incubated for another 1 hour at 37 °C. The MCP joints were opened and cartilage was rapidly explanted, as described in Materials and Methods. Explanted cartilage was either immediately cooled in ice-cold 1X RIPA Buffer nitrogen (zero hour time point) or cultured in serum free DMEM with or without NAC for various periods of time (5min, 10min and 30min) at 37 °C, 5% CO_2 before being transferred to ice cold, 1X RIPA buffer. Explants with 1X RIPA buffer, were mildly shaken for 45 minutes at 4°C. Lysates were run on 10% Sodium Dodecyl Sulphate-Polyacrylamide Gel (SDS PAGE) and transferred to poly (vinylidene) (PVDF) membrane. PVDF membrane was blocked in 5% milk for 1 hour at room temperature and immunoblotted for pJNK, pERK and pTAK1. Signal was enhanced by use of chemiluminescence (A) and subsequently visualised using autoradiography. Representative blot of three repeats shown (A). The blot was stripped and re-probed for total ERK. The quantification of three separate experiments was performed using FIJI-App, ImageJ-win64 Gel Analysis software and normalised to total ERK (B-D).

6.1.1.3 CoQ10 partially suppresses TAK1 phosphorylation but completely suppresses MAPK phosphorylation on cartilage injury

Having shown that NAC partially suppressed the phosphorylation of TAK1 but fully suppressed the phosphorylation of JNK and ERK on cartilage injury, I next determined whether CoQ10 had similar effects on the phosphorylation of TAK1 and MAPKs on injury.

Lysates generated from the experiment conducted in section 5.1.4 were run on new SDS-PAGE gels and immunoblotted for pJNK, pERK and pTAK1. Quantification of three separate experiments was performed, and results were normalised to tERK.

CoQ10 completely suppressed the phosphorylation of JNK (100%, SD ± 1.35) and ERK (100%, SD ± 0.870) at 30 mins post cartilage injury (Fig 6.3C & D) ($p < 0.01$) whereas TAK1 phosphorylation was suppressed by 48.7% (SD ± 1.35) (Fig 6.3E) ($p < 0.01$) in samples treated with CoQ10 compared to injured vehicle-injected joints.

A

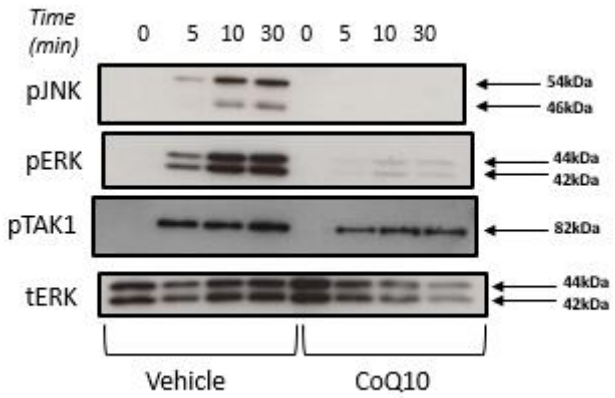
Time (min)
0 5 10 30 0 5 10 30
pJNK
pERK
pTAK1
tERK
54kDa
46kDa
44kDa
42kDa
82kDa
44kDa
42kDa
Vehicle
CoQ10

B

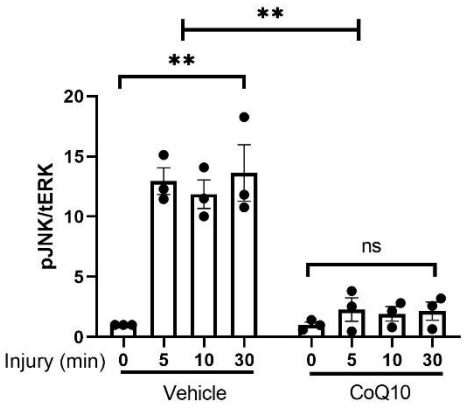
pJNK/tERK
**
**
ns
Injury (min) 0 5 10 30 0 5 10 30
Vehicle
CoQ10

C

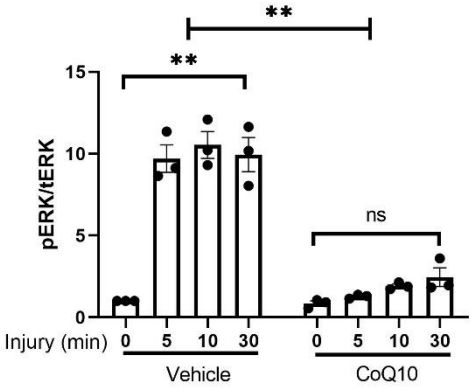
pERK/tERK
**
**
ns
Injury (min) 0 5 10 30 0 5 10 30
Vehicle
CoQ10

D

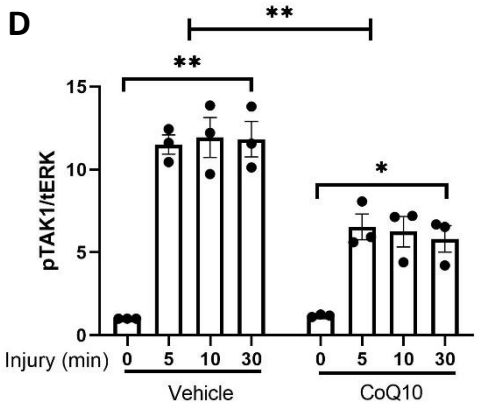
pTAK1/tERK
**
**
*
Injury (min) 0 5 10 30 0 5 10 30
Vehicle
CoQ10

Figure 6.3: CoQ10 partially suppresses the phosphorylation of TAK1 and completely suppresses the phosphorylation of MAPKs on cartilage injury.

Porcine metacarpophalangeal (MCP) joints were decontaminated in 2% Virkon for 20 minutes before being equilibrated at 37°C, 5% CO_2 for 1 hour. MCP joints were injected with either 150 µM CoQ10 or vehicle control and incubated for another 1 hour at 37 °C. The MCP joints were opened and cartilage was rapidly explanted, as described in Materials and Methods. Explanted cartilage was either immediately cooled in ice-cold 1X RIPA Buffer nitrogen (zero hour time point) or cultured in serum free DMEM with or without CoQ10 for various periods of time (5min, 10min and 30min) at 37 °C, 5% CO_2 before being transferred to ice cold, 1X RIPA buffer. Explants with 1X RIPA buffer, were mildly shaken for 45 minutes at 4°C. Lysates were run on 10% Sodium Dodecyl Sulphate-Polyacrylamide Gel (SDS PAGE) and transferred to poly (vinylidene) (PVDF) membrane. PVDF membrane was blocked in 5% milk for 1 hour at room temperature and immunoblotted for pJNK, pERK and pTAK1. Signal was enhanced by use of chemiluminescence (A) and subsequently visualised using autoradiography. Representative blot of three repeats shown (A). The blot was stripped and re-probed for total ERK. The quantification of three separate experiments was performed using FIJI-App, ImageJ-win64 Gel Analysis software and normalised to total ERK (B-D).

6.1.2 TAK1 activation on cartilage injury is not sensitive to ASK1-inhibition but MAPK activation is ASK1-sensitive

Having determined that TAK1 activation is partially ROS-sensitive and that the activation of MAPKs was fully suppressed by NAC and CoQ10. I hypothesised that the ROS-mediated activation of the MAPKs was conducted through another MAPKKK other than TAK1. The likely candidate for this was ASK1, as its phosphorylation is established to be solely ROS-sensitive. I tested whether inhibiting ASK1 affects TAK1 and MAPK signalling in the same trotter injury model.

Trotter MCP joints were preinjected with either 10 µM ASK1 inhibitor (selonsertib) or vehicle control prior to injury. Injured cartilage were incubated in either inhibitor or vehicle for various times. Lysates were immunoblotted for JNK, ERK and TAK1 (n = 3 separate trotters). Quantification of three separate experiments was performed, and results were normalised to tERK.

In the ex-vivo tissue (zero hour), there was no basal phosphorylation of JNK, ERK or TAK1 (Fig 6.4A). The phosphorylation of JNK and ERK was completely suppressed between 0 mins and 30 mins post cartilage injury in those samples treated with selonsertib (Fig 6.4B

& C) ($p < 0.01$). However, there was no statistically significant difference in the phosphorylation of TAK1 between 0 and 30 mins post cartilage injury in those samples treated with vehicle compared to those treated with selonsertib (Fig 6.4D).

This experiment revealed that ROS was likely activating MAPKs predominantly through ASK1. In addition, ASK1 activation itself was not upstream of TAK1 activation, as inhibiting ASK1 had no effect on the phosphorylation of TAK1. The partial activation of TAK1 by ROS suggested that this might be secondary to a positive feedback loop, with TAK1 activation initiating the release of ROS, perhaps from the mitochondria. Given that NOX inhibition partially suppressed TAK1 to a higher degree than either NAC or CoQ10, these results suggest that both NOX and cytoplasmic ROS contribute to the upstream activation of TAK1.

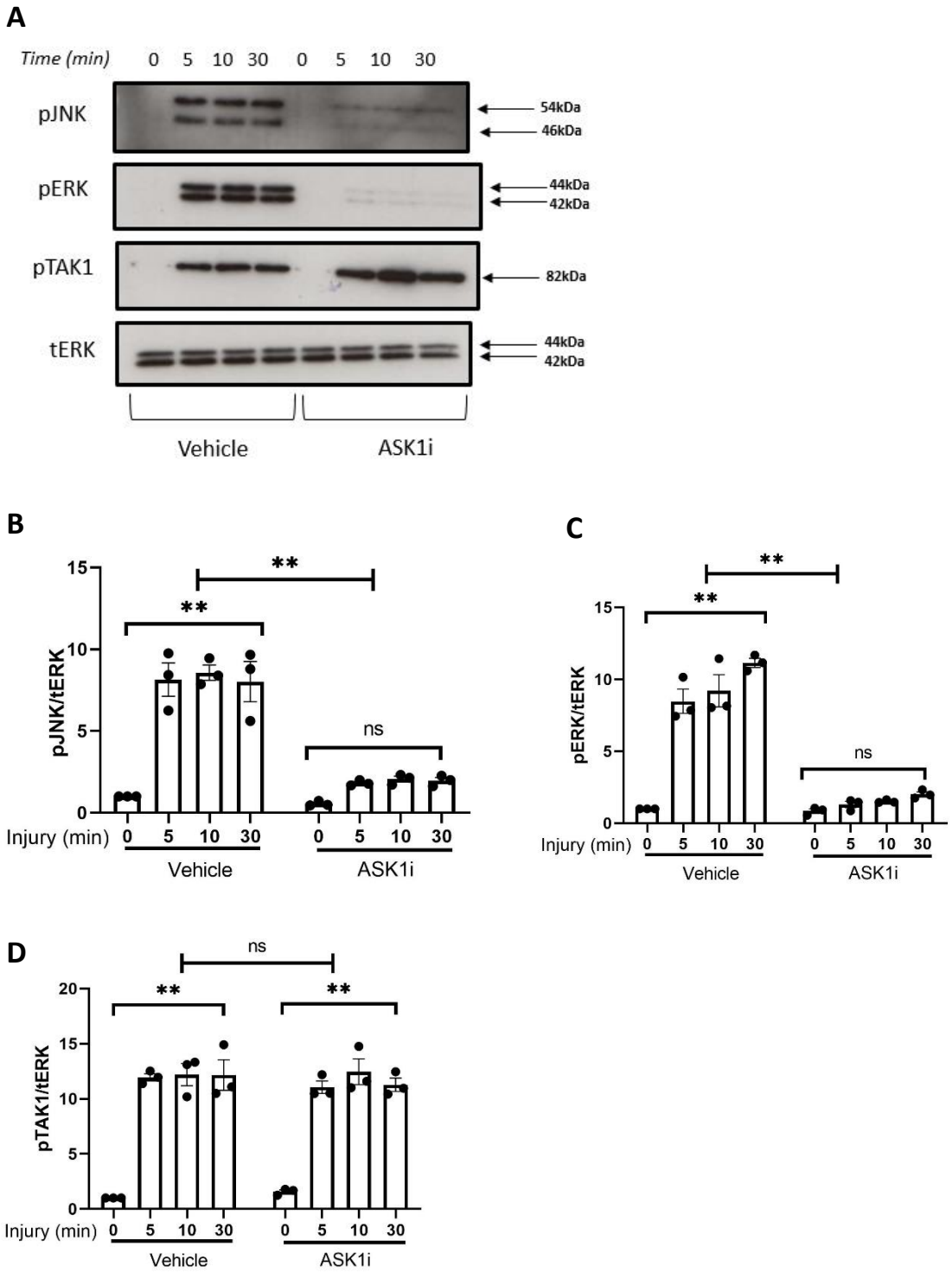
A
Time (min) 0 5 10 30 0 5 10 30
pJNK
pERK
pTAK1
tERK
54kDa
46kDa
44kDa
42kDa
82kDa
44kDa
42kDa
Vehicle
ASK1i
B
pJNK/tERK
Injury (min) 0 5 10 30 0 5 10 30
Vehicle
ASK1i
**
**
ns
C
pERK/tERK
Injury (min) 0 5 10 30 0 5 10 30
Vehicle
ASK1i
**
**
ns
D
pTAK1/tERK
Injury (min) 0 5 10 30 0 5 10 30
Vehicle
ASK1i
**
**
ns

Figure 6.4: ASK1 inhibition does not affect the phosphorylation of TAK1 but completely suppresses the phosphorylation of MAPKs on cartilage injury.

Porcine metacarpophalangeal (MCP) joints were decontaminated in 2% Virkon for 20 minutes before being equilibrated at 37°C, 5% CO_2 for 1 hour. MCP joints were injected with either 10 μM ASK1i or vehicle control and incubated for another 1 hour at 37 °C. The MCP joints were opened and cartilage was rapidly explanted, as described in Materials and Methods. Explanted cartilage was either immediately cooled in ice-cold 1X RIPA Buffer nitrogen (zero hour time point) or cultured in serum free DMEM with or without ASK1i for various periods of time (5min, 10min and 30min) at 37 °C, 5% CO_2 before being transferred to ice cold, 1X RIPA buffer. Explants with 1X RIPA buffer, were mildly shaken for 45 minutes at 4°C. Lysates were run on 10% Sodium Dodecyl Sulphate-Polyacrylamide Gel (SDS PAGE) and transferred to poly (vinylidene) (PVDF) membrane. PVDF membrane was blocked in 5% milk for 1 hour at room temperature and immunoblotted for pJNK, pERK and pTAK1. Signal was enhanced by use of chemiluminescence (A) and subsequently visualised using autoradiography. Representative blot of three repeats shown (A). The blot was stripped and re-probed for total ERK. The quantification of three separate experiments was performed using FIJI-App, ImageJ-win64 Gel Analysis software and normalised to total ERK (B-D).

6.1.3 The upregulation of inflammatory genes on cartilage injury is ASK1-sensitive

Having determined that ROS activated MAPKs on cartilage injury primarily through ASK1, I next investigated whether inhibiting ASK1 would suppress mechano-inflammatory genes on cartilage injury. I preinjected trotter MCP joints with 10 μM of selonsertib or vehicle control. Injured explants were cultured in serum-free medium containing either inhibitor or vehicle for four hours (n = 4 separate trotters). RNA was extracted and converted to cDNA and RT-PCR performed for a panel of inflammatory genes.

Inflammatory genes were significantly upregulated in injured vehicle-injected joints (Fig 6.5). Selonsertib significantly suppressed the upregulation of *IL6*, *COX2*, *ADAMTS4*, *CCL2*, *TIMP1*, *CDKN1A* and *NGF* by 85.2% (SD ± 0.545), 87.3% (SD ± 7.05), 82% (SD ± 0.536), 89% (SD ± 0.322), 98.2% (SD ± 0.238), 88.7% (SD ± 0.411) and 62.8% (SD ± 2.179), respectively. *MMP3* upregulation on cartilage injury was unaffected by the use of selonsertib.

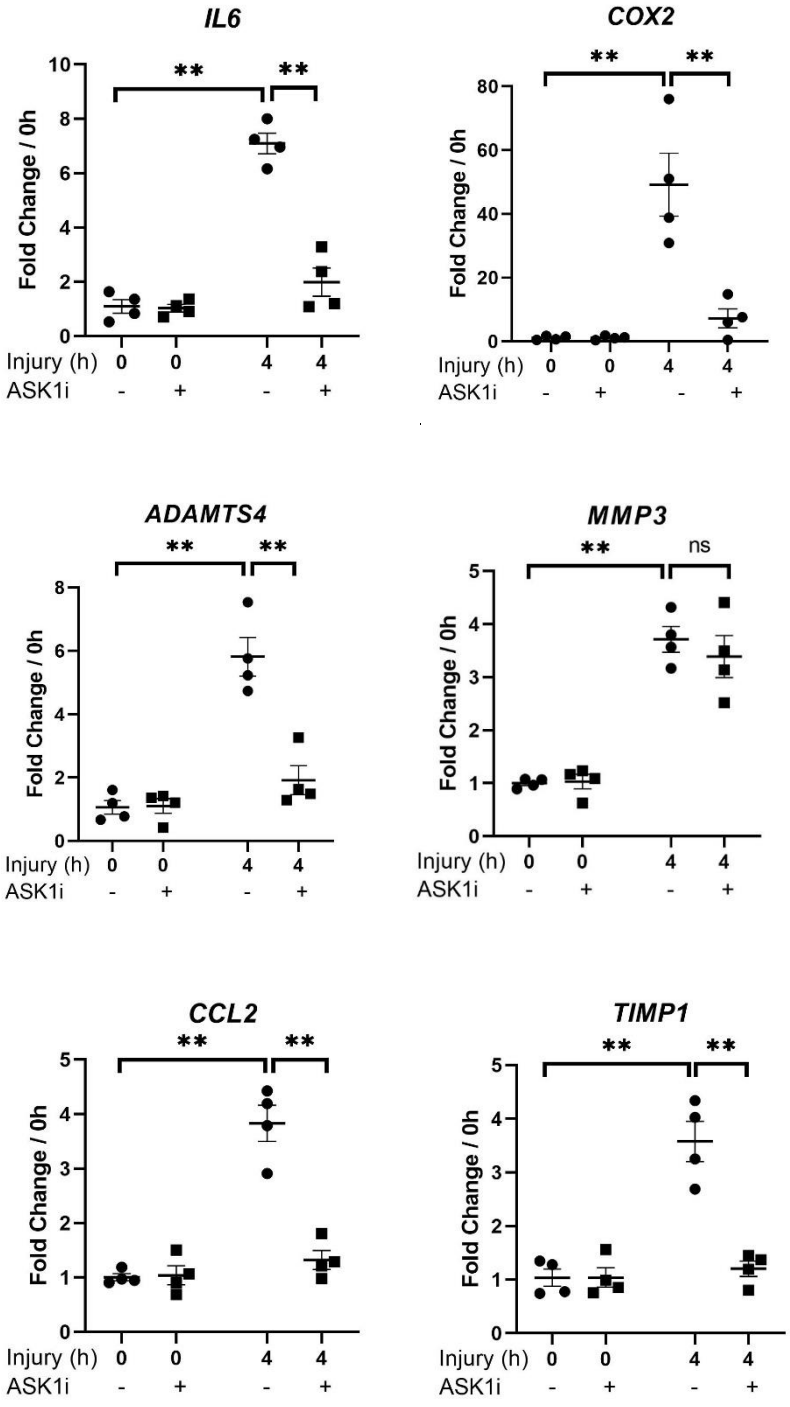
IL6
COX2
ADAMTS4
MMP3
CCL2
TIMP1
Fold Change / 0h
Injury (h) 0 0 4 4
ASK1i - + - +
**
ns

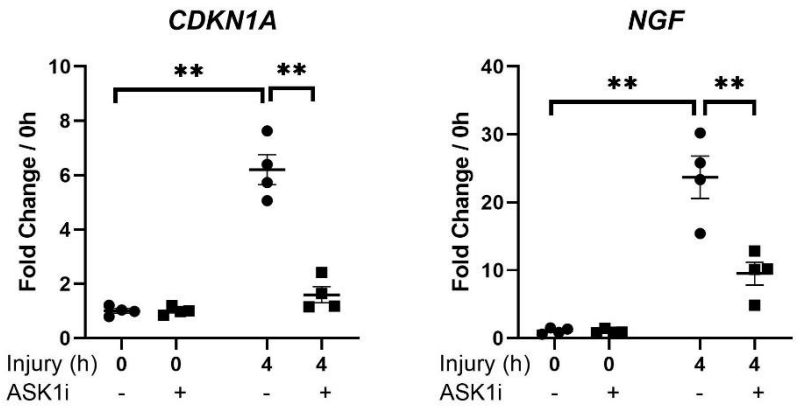

Figure 6.5: ASK1 inhibition suppresses the upregulation of inflammatory genes on cartilage injury.

Porcine metacarpophalangeal (MCP) joints were decontaminated in 2% Virkon for 20 minutes before being equilibrated at 37 °C, 5% CO_2 for 1 hour. MCP joints were injected with either 10 µM ASK1i or vehicle control and incubated for another 1 hour at 37 °C. The MCP joints were opened and cartilage was rapidly explanted. Explanted cartilage was either immediately snap frozen in liquid nitrogen (zero hour time point) or cultured in serum free DMEM with or without ASK1i for 4 hours at 37 °C, 5% CO_2 before being snap frozen. RNA was subsequently extracted from the tissue and used in quantitative reverse transcriptase-polymerase chain reaction to measure a panel of inflammatory genes. Statistical significance of comparison between treatment groups was conducted using a two-way ANOVA, with post-hoc multiple comparisons corrected using Tukey's tests. Bars shows the mean ± SEM of 3 independent experiments in which each experiment was performed on 3 individual trotter joints (n= 9 separate trotters). ns = not significant, * = P < 0.05; ** = P < 0.01, by two-way ANOVA. . IL6 = Interleukin 6, COX2= Cyclooxygenase-2, ADAMTS4 = ADAM Metallopeptidase With Thrombospondin Type 1 Motif 4, MMP3= Matrix metalloproteinase-3, CCL2= C-C Motif Chemokine Ligand 2, TIMP1= TIMP metallopeptidase inhibitor 1, CDKN1A= Cyclin Dependent Kinase Inhibitor 1A, NGF= Nerve growth factor.

6.1.4 ASK1 inhibition does not prevent the downregulation of atRA-responsive genes on cartilage injury

Next, I determined whether inhibiting ASK1 prevented the downregulation of atRA-responsive genes on cartilage injury. The cDNA samples from the experiment conducted in section 6.1.3 were used to test atRA-responsive genes.

CYP26 genes and *RAR* genes were significantly downregulated to 50% or less on cartilage injury (Fig 6.6). Selonsertib did not prevent the downregulation of any atRA-responsive genes on cartilage injury (Fig 6.6); instead, they were downregulated to a similar level to that seen in injured vehicle-injected joints.

Collectively, these results showed that although ASK1 activation does not likely contribute towards the downregulation of atRA-responsive genes on cartilage injury, it does nonetheless increase the expression of inflammatory genes. This suggested that ASK1 was activating MAPK signalling to increase inflammatory gene regulation in an atRA-independent manner. In other words, the TAK1-sensitive downregulation of atRA-responsive genes (Chapter 1, Fig. 1.8) is occurring at a level upstream of ASK1.

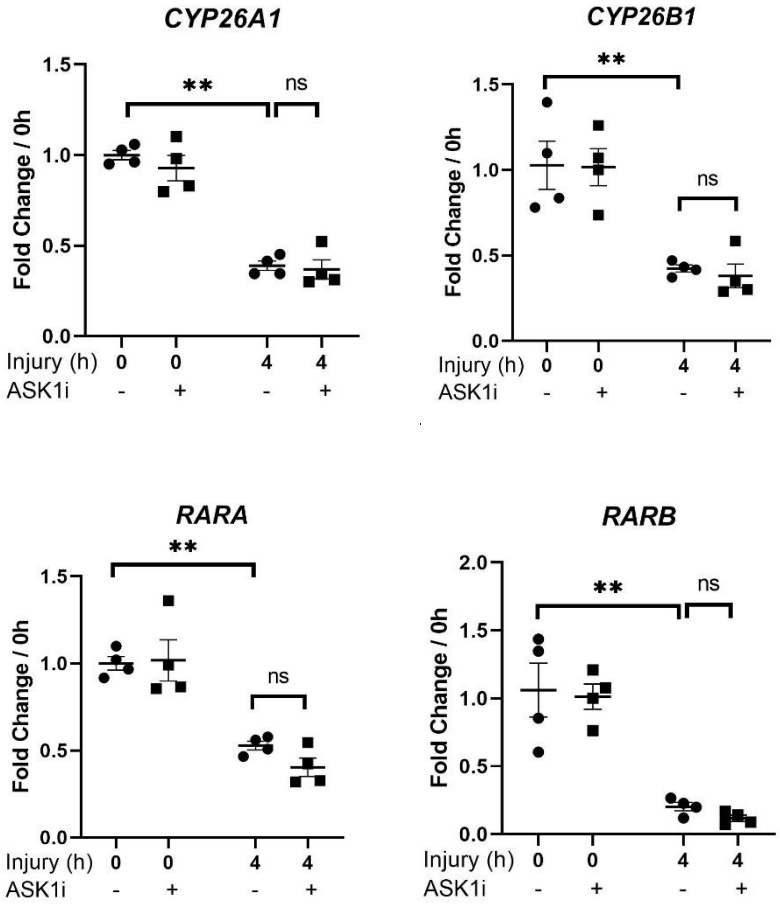

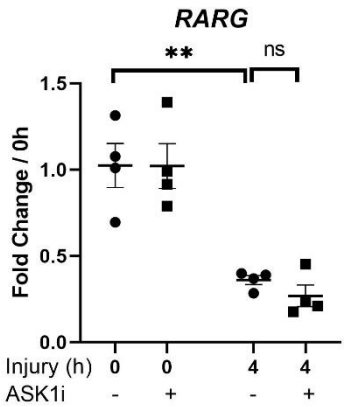

Figure 6.6: ASK1 inhibition does not prevent the downregulation of atRA-responsive genes on cartilage injury.

Porcine metacarpophalangeal (MCP) joints were decontaminated in 2% Virkon for 20 minutes before being equilibrated at 37 °C, 5% CO_2 for 1 hour. MCP joints were injected with either 10 µM ASK1i or vehicle control and incubated for another 1 hour at 37 °C. The MCP joints were opened and cartilage was rapidly explanted. Explanted cartilage was either immediately snap frozen in liquid nitrogen (zero hour time point) or cultured in serum free DMEM with or without ASK1i for 4 hours at 37 °C, 5% CO_2 before being snap frozen. RNA was subsequently extracted from the tissue and used in quantitative reverse transcriptase-polymerase chain reaction to measure a panel of atRA-responsive genes. Statistical significance of comparison between treatment groups was conducted using a two-way ANOVA, with post-hoc multiple comparisons corrected using Tukey's tests. Bars shows the mean ± SEM of 3 independent experiments in which each experiment was performed on 3 individual trotter joints (n= 9 separate trotters). ns = not significant, * = $P < 0.05$; ** = $P < 0.01$, by two-way ANOVA. . CYP26A1 = Cytochrome P450 Family 26 Subfamily A Member 1, CYP26B1 = Cytochrome P450 Family 26 Subfamily B Member 1, RARA = Retinoic Acid Receptor Alpha, RARB = = Retinoic Acid Receptor Beta, RARG = = Retinoic Acid Receptor Gamma

6.1.5 ASK1 inhibition does not affect cPLA2 phosphorylation on cartilage injury

I further determined whether ASK1 inhibition affected the phosphorylation of cPLA2 on injury. The downregulation of atRA-responsive genes on cartilage injury was cPLA2-sensitive; however, ASK1 inhibition did not affect the downregulation of atRA-responsive genes on cartilage injury despite suppressing the increase in inflammatory gene regulation. Given that cPLA2 inhibition was likely exerting an anti-inflammatory effect through preventing the downregulation of atRA-responsive genes, I therefore hypothesised ASK1 inhibition to not affect the phosphorylation of cPLA2. The PVDF membranes generated from the experiments conducted in section 6.1.2 were stripped with reblot buffer and

immunoblotted for pJNK, pERK and pTAK1. Quantification of the three separate experiments was conducted, and results normalised to tERK. Preinjection of joints with selonsertib prior to cartilage injury had no significant effect on the phosphorylation of cPLA2 between 0 mins and 30 mins (Fig 6.7B).

As hypothesised, the activation of ASK1 on cartilage injury appeared to be independent of cPLA2 activation, which itself was upstream of atRA-responsive gene regulation on injury. This further strengthened the hypothesis that inhibition of ASK1 was likely mediating an anti-inflammatory effect on cartilage injury via the suppression of MAPKs, and this was independent of cPLA2 activation and atRA-responsive gene regulation.

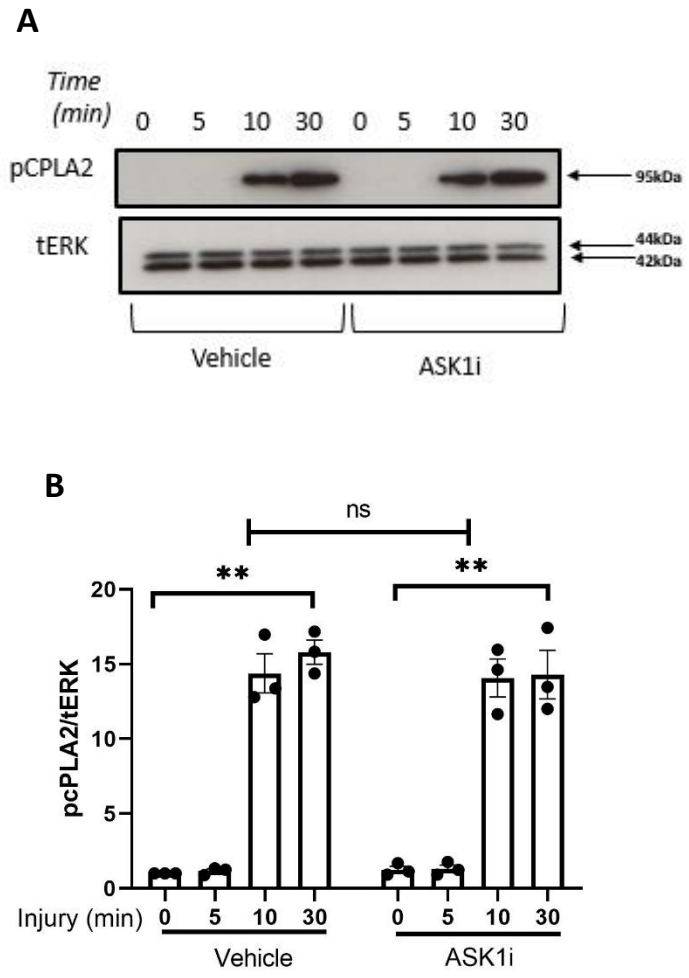

Figure 6.7: ASK1 inhibition does not affect the phosphorylation of cPLA2 on cartilage injury.

Porcine metacarpophalangeal (MCP) joints were decontaminated in 2% Virkon for 20 minutes before being equilibrated at 37°C, 5% CO_2 for 1 hour. MCP joints were injected with either 10 μM ASK1i or vehicle control and incubated for another 1 hour at 37 °C. The MCP joints were opened and cartilage was rapidly explanted, as described in Materials and Methods. Explanted cartilage was either immediately cooled in ice-cold 1X RIPA Buffer nitrogen (zero hour time point) or cultured in serum free DMEM with or without ASK1i for various periods of time (5min, 10min and 30min) at 37 °C, 5% CO_2 before being transferred to ice cold, 1X RIPA buffer. Explants with 1X RIPA buffer, were mildly shaken for 45 minutes at 4°C. Lysates were run on 10% Sodium Dodecyl Sulphate-Polyacrylamide Gel (SDS PAGE) and transferred to poly (vinylidene) (PVDF) membrane. PVDF membrane was blocked in 5% milk for 1 hour at room temperature, incubated overnight in 1:1000 primary antibody (pcPLA2), washed 3 times in 1X TBST and incubated for a further hour in 1:2000 secondary antibody. pcPLA2 signal was enhanced by use of chemiluminescence (A) and subsequently visualised using autoradiography. Representative blot of three repeats shown (A). The blot was stripped and re-probed for total ERK. The quantification of three separate experiments testing pcPLA2 was performed using FIJI-App, ImageJ-win64 Gel Analysis software and normalised to total ERK (B).

6.1.6 cPLA2 inhibition does not affect TAK1 and MAPK phosphorylation on cartilage injury

To further support the findings that cPLA2 phosphorylation was independent of MAPK activation, which was shown to be driven through ASK1, I determined whether inhibiting cPLA2 affected MAPK phosphorylation. In Chapter 4, I demonstrated that TAK1 inhibition partially suppressed the phosphorylation of cPLA2; therefore, I predicted the inhibition of cPLA2 to not affect TAK1 phosphorylation on injury.

Lysates from cartilage explants treated with 10 μM cPLA2 inhibitor (PACOCF3) from the experiment conducted in section 4.2.3 were run on new SDS-PAGE gels and immunoblotted for pJNK, pERK and pTAK1. Quantification of the three separate experiments were conducted and results normalised to tERK.

Preinjection of trotter MCP joints with PACOOF3 did not affect the phosphorylation of JNK, ERK and TAK1 between 0 and 30 mins post injury compared to injured vehicle-injected joints (Fig 6.8B–D).

A

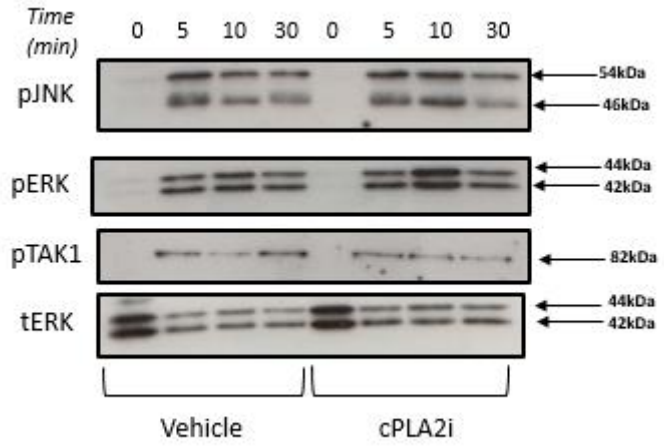
Time (min)
0 5 10 30 0 5 10 30
pJNK
54kDa
46kDa
pERK
44kDa
42kDa
pTAK1
82kDa
tERK
44kDa
42kDa
Vehicle
cPLA2i

B

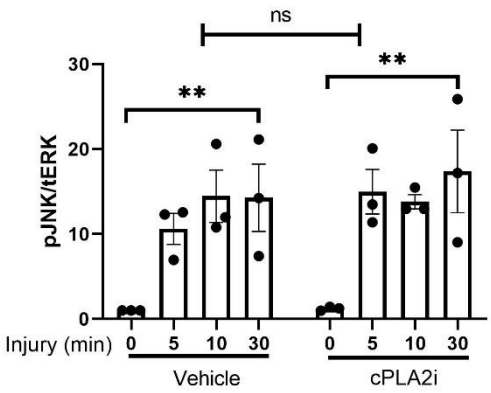
ns
**
**
pJNK/tERK
30
20
10
0
Injury (min) 0 5 10 30 0 5 10 30
Vehicle
cPLA2i

C

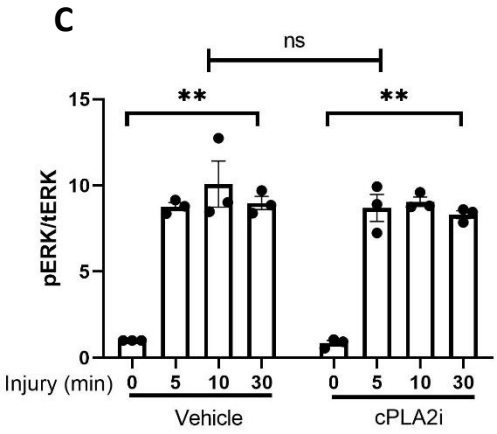
ns
**
**
pERK/tERK
15
10
5
0
Injury (min) 0 5 10 30 0 5 10 30
Vehicle
cPLA2i

D

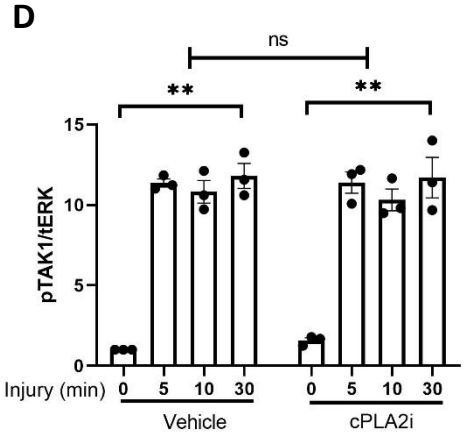
ns
**
**
pTAK1/tERK
15
10
5
0
Injury (min) 0 5 10 30 0 5 10 30
Vehicle
cPLA2i

Figure 6.8: cPLA2 inhibition does not affect TAK1 and MAPK phosphorylation on cartilage injury.

Porcine metacarpophalangeal (MCP) joints were decontaminated in 2% Virkon for 20 minutes before being equilibrated at 37°C, 5% CO_2 for 1 hour. MCP joints were injected with either 10 µM cPLA2i or vehicle control and incubated for another 1 hour at 37 °C. The MCP joints were opened and cartilage was rapidly explanted, as described in Materials and Methods. Explanted cartilage was either immediately cooled in ice-cold 1X RIPA Buffer nitrogen (zero hour time point) or cultured in serum free DMEM with or without cPLA2i for various periods of time (5min, 10min and 30min) at 37 °C, 5% CO_2 before being transferred to ice cold, 1X RIPA buffer. Explants with 1X RIPA buffer, were mildly shaken for 45 minutes at 4°C. Lysates were run on 10% Sodium Dodecyl Sulphate-Polyacrylamide Gel (SDS PAGE) and transferred to poly (vinylidene) (PVDF) membrane. PVDF membrane was blocked in 5% milk for 1 hour at room temperature and immunoblotted for pJNK, pERK and pTAK1. Signal was enhanced by use of chemiluminescence (A) and subsequently visualised using autoradiography. Representative blot of three repeats shown (A). The blot was stripped and re-probed for total ERK. The quantification of three separate experiments was performed using FIJI-App, ImageJ-win64 Gel Analysis software and normalised to total ERK (B-D).

6.1.7 12/15 LOX inhibition does not affect TAK1 and MAPK phosphorylation on cartilage injury

Given that 12/15 LOX acts downstream of cPLA2, inhibition of 12/15 LOX was not predicted to affect either TAK1 or MAPK phosphorylation. Lysates generated from 1 µM 12/15 LOX inhibitor (ML351) treated cartilage explants from the experiment conducted in section 5.1.6 were run on new SDS-PAGE gels and immunoblotted for pJNK, pERK and pTAK1. Quantification of the three separate experiments were conducted and results normalised to tERK.

ML351 had no significant effect on the phosphorylation of JNK, ERK or TAK1 on cartilage injury by 30 mins compared to injured vehicle-injected joints (Fig 6.9B–D)

Collectively, these set of results confirmed that the cPLA2-sensitive pathway downregulating atRA-responsive genes was independent of the ASK1-sensitive pathway driving MAPKs and subsequent inflammatory gene regulation on cartilage injury.

A

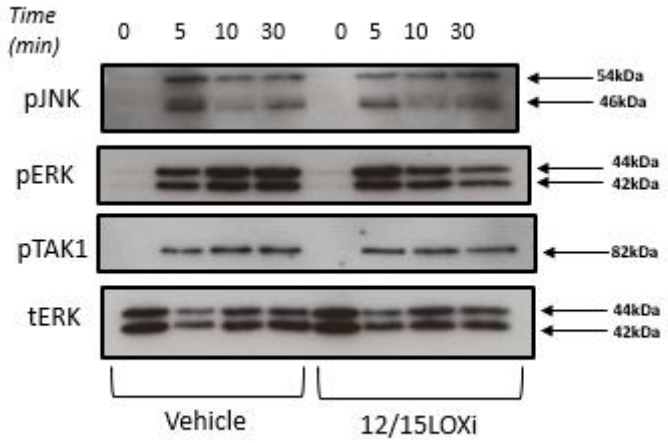
Time (min)
0 5 10 30 0 5 10 30
pJNK
pERK
pTAK1
tERK
54kDa
46kDa
44kDa
42kDa
82kDa
44kDa
42kDa
Vehicle
12/15LOXi

B

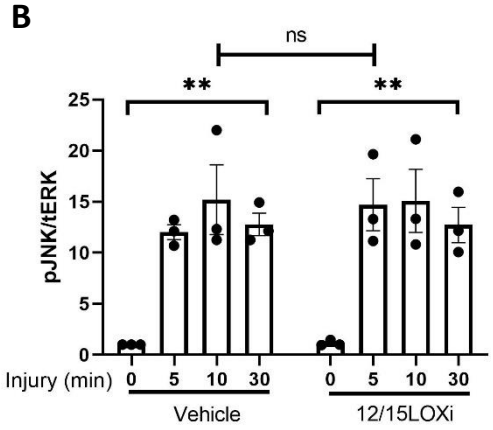
ns
**
**
pJNK/tERK
Injury (min) 0 5 10 30 0 5 10 30
Vehicle
12/15LOXi

C

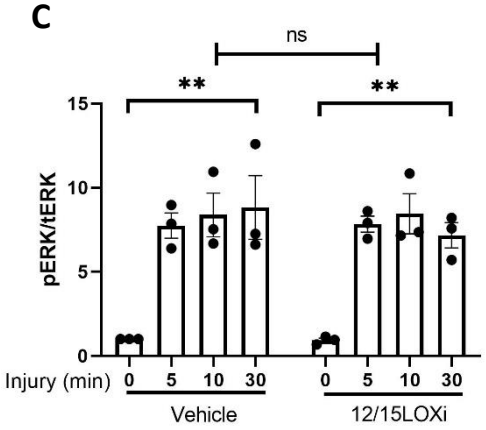
ns
**
**
pERK/tERK
Injury (min) 0 5 10 30 0 5 10 30
Vehicle
12/15LOXi

D

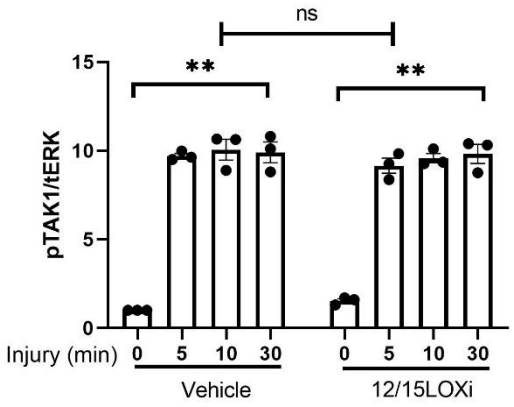
ns
**
**
pTAK1/tERK
Injury (min) 0 5 10 30 0 5 10 30
Vehicle
12/15LOXi

Figure 6.9: 12/15 LOX inhibition does not affect TAK1 and MAPK phosphorylation on cartilage injury.

Porcine metacarpophalangeal (MCP) joints were decontaminated in 2% Virkon for 20 minutes before being equilibrated at 37°C, 5% CO_2 for 1 hour. MCP joints were injected with either 1 µM 12/15LOXi or vehicle control and incubated for another 1 hour at 37 °C. The MCP joints were opened and cartilage was rapidly explanted, as described in Materials and Methods. Explanted cartilage was either immediately cooled in ice-cold 1X RIPA Buffer nitrogen (zero hour time point) or cultured in serum free DMEM with or without 12/15LOXi for various periods of time (5min, 10min and 30min) at 37 °C, 5% CO_2 before being transferred to ice cold, 1X RIPA buffer. Explants with 1X RIPA buffer, were mildly shaken for 45 minutes at 4°C. Lysates were run on 10% Sodium Dodecyl Sulphate-Polyacrylamide Gel (SDS PAGE) and transferred to poly (vinylidene) (PVDF) membrane. PVDF membrane was blocked in 5% milk for 1 hour at room temperature and immunoblotted for pJNK, pERK and pTAK1. Signal was enhanced by use of chemiluminescence (A) and subsequently visualised using autoradiography. Representative blot of three repeats shown (A). The blot was stripped and re-probed for total ERK. The quantification of three separate experiments was performed using FIJI-App, ImageJ-win64 Gel Analysis software and normalised to total ERK (B-D).

6.1.8 Varying oxygen tension does not affect the phosphorylation of JNK, ERK or TAK1 on cartilage injury

Lastly, I determined whether ambient oxygen tension was affecting the phosphorylation of TAK1 and MAPKs. I saw this as an important control, as dissected cartilage explants are immediately exposed to higher ambient levels of oxygen in comparison to their in-situ environment in the joint, where chondrocytes are harboured in a hypoxic environment at 2%–4% O_2.

I conducted the trotter injury assay in either a hypoxic chamber (2% O_2) or a normal tissue culture hood (21% O_2). Cartilage was explanted and incubated for various times in its respective oxygen tension (either 21% O_2 or 2% O_2). Lysates were generated from injured cartilage explants and immunoblotted for JNK, ERK and TAK1. Quantification of three separate experiments was performed, and results were normalised to tERK.

Varying oxygen tension did not affect the phosphorylation of either JNK, ERK or TAK1 between 0 and 30 mins post cartilage injury (Fig 6.10B–D).

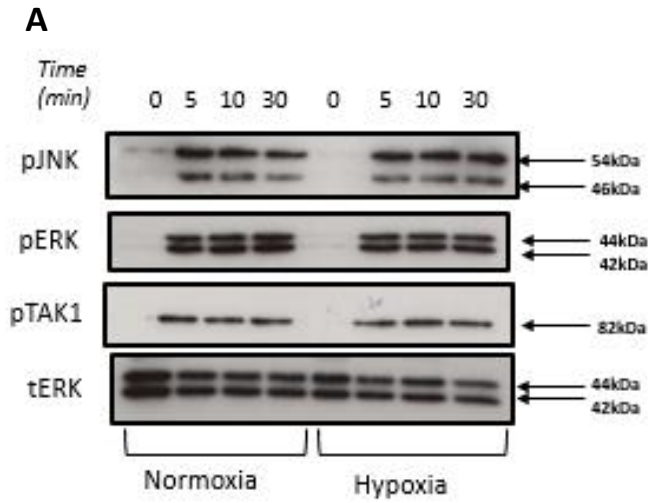
A
Time (min)
0 5 10 30 0 5 10 30
pJNK
pERK
pTAK1
tERK
54kDa
46kDa
44kDa
42kDa
82kDa
44kDa
42kDa
Normoxia
Hypoxia

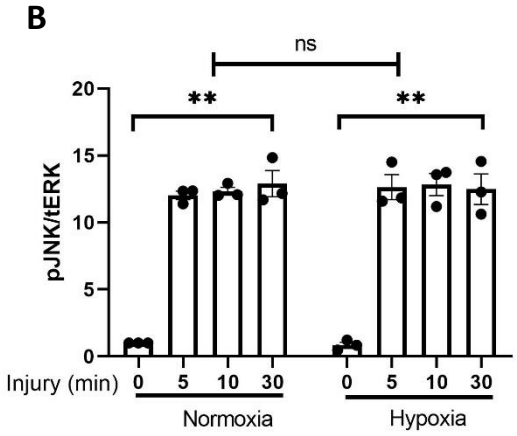
B
ns
**
**
pJNK/tERK
20
15
10
5
0
Injury (min) 0 5 10 30 0 5 10 30
Normoxia
Hypoxia

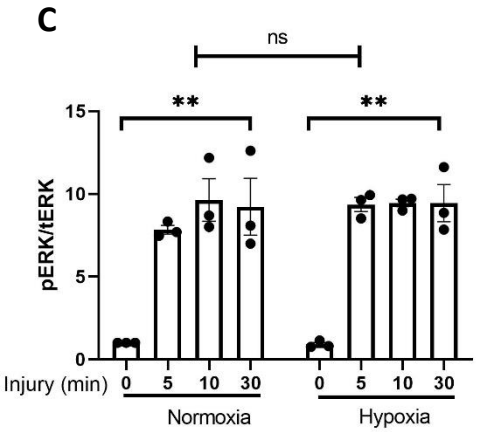
C
ns
**
**
pERK/tERK
15
10
5
0
Injury (min) 0 5 10 30 0 5 10 30
Normoxia
Hypoxia

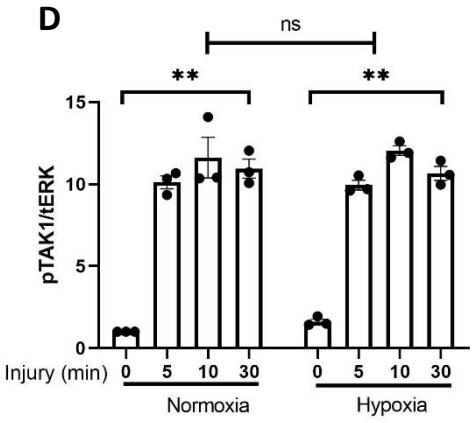
D
ns
**
**
pTAK1/tERK
15
10
5
0
Injury (min) 0 5 10 30 0 5 10 30
Normoxia
Hypoxia

Figure 6.10: Varying oxygen tension does not affect the phosphorylation of MAPKs.

Porcine metacarpophalangeal (MCP) joints were decontaminated in 2% Virkon for 20 minutes before being equilibrated at 37°C, 5% CO_2 for 1 hour. The MCP joints were opened and cartilage was rapidly explanted, in either normoxic (21% O_2) or hypoxic (2% O_2) conditions, as described in Materials and Methods. All reagents and media were equilibrated at their respective oxygen tension for 1 hour prior to the experiment. Explanted cartilage was either immediately cooled in ice-cold 1X RIPA Buffer nitrogen (zero hour time point) or cultured in serum free DMEM various periods of time (5min, 10min and 30min) at 37 °C, 5% CO_2 at their respective oxygen tensions (normoxic or hypoxic conditions) before being transferred to ice cold, 1X RIPA buffer. Explants with 1X RIPA buffer, were mildly shaken for 45 minutes at 4°C. Lysates were run on 10% Sodium Dodecyl Sulphate-Polyacrylamide Gel (SDS PAGE) and transferred to poly (vinylidene) (PVDF) membrane. PVDF membrane was blocked in 5% milk for 1 hour at room temperature and immunoblotted for pJNK, pERK and pTAK1. Signal was enhanced by use of chemiluminescence (A) and subsequently visualised using autoradiography. Representative blot of three repeats shown (A). The blot was stripped and re-probed for total ERK. The quantification of three separate experiments was performed using FIJI-App, ImageJ-win64 Gel Analysis software and normalised to total ERK (B-D).

6.2 Discussion

6.2.1 ROS-mediated activation of TAK1

NAC and CoQ10 partially suppressed the phosphorylation of TAK1. This suggested that cellular and mitochondrial ROS are involved in driving the activation of TAK1. This was consistent with previous findings from Onodera et al. in 2015 which showed that hydrogen peroxide mediated the phosphorylation of TAK1 in synovial fibroblasts [417]. However, the authors also demonstrated that inhibition of TAK1 during H2O2 treatment, blocked the gene expression of *COX2* and synthesis of PGE_2. This suggested the existence of a dual relationship between mitochondrial-derived ROS and TAK1 signalling. Therefore, in combination with evidence from my work, that is, given the partial reduction in TAK1 phosphorylation by CoQ10 and NAC, we hypothesised that TAK1 is likely the driver of mitochondrial ROS, which in turn perpetuates TAK1 signalling in a positive feedback loop (Fig. 6.11). This inference is supported by other studies that showed TAK1 regulating mitochondrial permeability. Suzuki et al. in 2020 used cefotaxime (CTX), an antibacterial agent that increases mitochondrial ROS, and showed TAK-1-deficient macrophages exhibit strong resistance to mitochondrial-induced oxidative stress stimulated by CTX [418]. Moreover, microscopic analysis revealed that mitochondrial induced ROS production was obliterated by TAK1 KO or inhibition [418]. Another study conducted by Zeng et al. revealed that TAK1 increased both cytosolic ROS and mitochondrial ROS in cardiomyocytes [419]. The authors further noted that TAK1 caused the loss of mitochondrial membrane potential, and this was markedly inhibited by the ROS scavenges NAC and BHA [419]. This regulatory loop between TAK1 and mitochondria also exists in cancer cells, where TAK1 regulates mitochondrial ROS whilst dysregulating antioxidative enzyme expression [420].

Apocynin (a NOX inhibitor) was able to suppress the phosphorylation of TAK1 to a greater degree than either NAC or CoQ10. This suggested that TAK1 was more sensitive to NOX-derived ROS than it was to mitochondrial or cellular-derived ROS. This is supported by findings that NOX4-derived ROS has been implicated in TAK1-induced pancreatic cancer cell chemotaxis [421]. Moreover, I demonstrated that both apocynin and 5Z-7 were able to suppress the phosphorylation of cPLA2 on injury. Therefore, we proposed that NOX was acting upstream of TAK1 which in turn phosphorylated cPLA2 whereas ROS derived from the mitochondria was acting in a regulatory positive feedback loop with TAK1. It is worth noting again that the IC50 value of apocynin to NOX is 10 μM. Therefore, the non-specificity of apocynin to NOX might also explain the partial suppression of TAK1 on cartilage injury in response to apocynin. Future studies with a more specific NOX inhibitor or supportive functional studies would be required to further investigate and confirm the relationship between NOX and TAK1 phosphorylation on cartilage injury.

Unlike its effect on TAK1 phosphorylation, CoQ10 and NAC were powerful and completely suppressed MAPK phosphorylation (namely JNK and ERK phosphorylation on injury). It is well established that TAK1 is an activator of the downstream MAPKs even within the injured cartilage model [99, 103]. Therefore, the partial reduction in pTAK1 by both CoQ10 and NAC does not account for their full suppression of MAPKs on cartilage injury. Although TAK1 might be responsible for the generation of mitochondrial ROS, it appeared that there was probably another MAPKK or MAPKKK which was responsible for the phosphorylation of the MAPKs on cartilage injury. The strong sensitivity of JNK and ERK to both NAC and CoQ10 suggested that the alternative MAPKKK driver of these MAPKs should also be highly ROS-sensitive. We proposed that ASK1 was the likely ROS-sensitive, MAPKKK that was responsible for the activation of MAPKs. It is established that ASK1 activation is sensitive to the presence of ROS [422]. Thioredoxin (Trx), a redox-

sensitive protein, is present within the catalytic domain of the ASK1 protein. Whilst the reduced Trx binds onto the catalytic domain to inhibit ASK1's kinase activity, this oxidised form of Trx dissociates from the catalytic domain in the presence of ROS [422]. This ROS-mediated activation of ASK1 has been demonstrated to phosphorylate downstream ERK, JNK and p38 and also influence NF-κB signalling in multiple systems [422, 423].

6.2.2 ASK1 drives mechanoflammation in a TAK1-sensitive manner

ASK1 inhibition with selonsertib completely suppressed MAPK phosphorylation, notably JNK and ERK phosphorylation. The sequestration of mitochondrial and cellular ROS with CoQ10 and NAC, respectively, only partially suppressed TAK1 phosphorylation and suggests that ROS-mediated ASK1 activation might be the key driver of MAPK signalling on cartilage injury. Studies have demonstrated that ROS can promote the dissociation of ASK1 and Trx and thereby render it to become active and phosphorylate downstream MAPKs [422]. Selonsertib did not affect TAK1 phosphorylation, suggesting that ASK1 was downstream of TAK1. Therefore, it is possible that the regulatory loop between TAK1 and ROS production from the mitochondria increases the kinase activity of ASK1. Although there has been no direct literature evidence for the activation of ASK1 by TAK1, my data suggest that mitochondrial ROS production acts as the intermediate between the two MAPKKKs. TRAF6 has been shown to activate ASK1 in a similar manner to that of TAK1 [424]. TRAF 6 is a ubiquitin E3 ligase, responsible for the transduction of surface receptor–mediated signals to TAK1. Matsuzawa et al. demonstrated that ROS-dependent TRAF6-ASK1 signalling is also crucial for toll-like receptor 4 (TLR4)-mediated mammalian innate immunity [424]. As such, there is some, although circumstantial, evidence to suggest ASK1 might lie on the injury-induced signalling axis as that seen for TAK1, even though, it is commonly viewed that TAK1 and ASK1 are independently activated MAPKKKs. The

relationship between TAK1 and ASK1 activation via mitochondrial ROS production requires further investigation. As a first step it would be important to demonstrate direct phosphorylation of ASK1 on cartilage injury and the TAK1 and ROS-sensitive nature of this. The use of the ASK1 inhibitor, serlonsertib, to demonstrate a role for ASK1 relies on its selectivity at the dose used. We again cannot exclude that the inhibitor might have non-specific actions on other MAPKKKs. Therefore such work requires further validation by measuring ASK1 phosphorylation on injury in combination with in-vivo knock out gene studies. ASK1 inhibition did not prevent the downregulation of atRA-responsive genes on cartilage injury, nor did it suppress the phosphorylation of cPLA2 on injury. This suggests that the cPLA2-atRA signalling axis is independent of the ASK1-MAPK axis activated on injury (Fig. 6.11), even though both of these signalling pathways appear to have TAK1 activation as a common upstream kinase. Several pieces of evidence support this. First, I have demonstrated that TAK1 inhibition suppresses the phosphorylation of cPLA2 and also prevents the downregulation of atRA-responsive genes (unpublished data). Second, the inhibition of TAK1 markedly suppressed MAPK phosphorylation. Lastly, inflammatory gene regulation on cartilage injury is highly TAK-1-sensitive [99]. Therefore, collectively, TAK1 is a likely central regulator in driving not only cPLA2 activation but also ROS-sensitive ASK1 activation and subsequent MAPK signalling (Fig. 6.11). Importantly, the ROS-sensitive suppression of MAPKs on injury was mediated predominantly through ASK1. Therefore, ASK1 might be an important driver of MAPK-mediated mechanoflammation in the joint. This is supported by the observation that selonsertib had an extremely strong effect on the suppression of inflammatory gene regulation on cartilage injury. It was noted that the effect of selonsertib on inflammatory gene regulation was very similar to that achieved by CoQ10. This further supports the mitochondrial-ROS dependence of ASK1 activation in driving MAPKs and subsequent inflammatory genes

(Fig. 6.11). These findings are supported by evidence implicating ASK1 in OA. Zhang et al. demonstrated that cartilage samples from patients with OA showed increased ASK1 expression [425]. The authors further demonstrated that ASK1 KO mice were protected against OA progression in both surgically induced model and aging mice [425]. It was also noted that ASK1 KO mice showed an absence of phosphorylation of downstream JNK and p38. More recently, Jiyuan Yan et al. showed that selonsertib alleviated the progression of rat OA in both in-vitro and in-vivo studies [426]. It was shown that selonsertib markedly alleviated IL1β-induced inflammatory gene regulation, cartilage degradation and cell apoptosis in rat chondrocytes [426]. Collectively, these results suggest that the absence or inhibition of ASK1 suppresses MAPK signalling, which might contribute towards preventing the release of proteolytic enzymes involved in cartilage destruction and chondrocyte death. Although, this requires further in-vivo work and clinical translational work to confirm, our work provides insights into the therapeutic potential of ASK1 inhibition as a potential avenue in OA treatment and its mechanism of action.

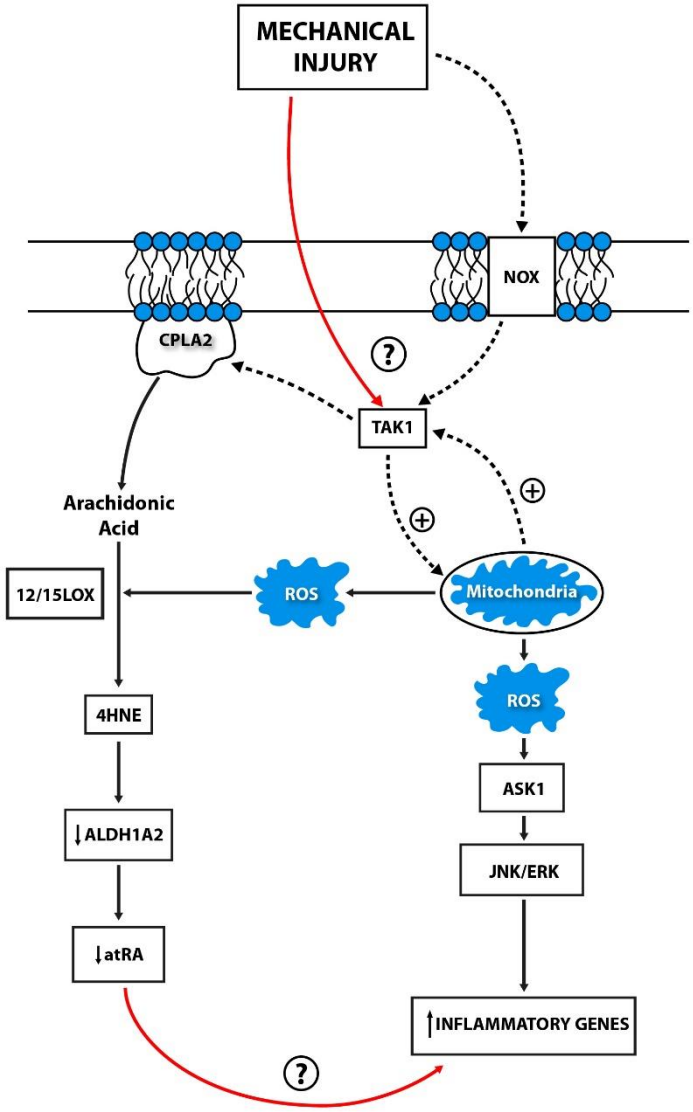

Figure 6.11: Schematic representing working hypothesis achieved at the end of Chapter 6.

Mechanical injury downregulates all-trans-retinoic acid (atRA)-responsive genes in both reactive oxygen species (ROS)-sensitive and cytosolic phospholipase A2 (cPLA2)-sensitive manner. Transforming growth factor activated-beta kinase 1 (TAK1) is partially phosphorylated on cartilage injury in a NADPH oxidase (NOX)-sensitive manner. TAK1 is responsible for partially phosphorylating cPLA2 on injury and likely acts in an auto-regulatory cycle with mitochondrial ROS. Apoptosis signal-regulating kinase 1 (ASK1) activation, secondary to ROS production from the mitochondria, likely drives the phosphorylation of the mitogen activated protein kinases (MAPKs) (Jun N-terminal kinase (JNK) and extracellular signal-regulated kinase (ERK)) on cartilage which subsequently increases inflammatory gene regulation. Block red line = undetermined; block black line = full activation; dotted black line = partial activation.

7 CHAPTER 7: DETERMINING THE MECHANISM BY WHICH TALARAZOLE SUPPRESSES MECHANOFLAMMATION

7.1 Introduction

In Chapter 3, I showed that maintaining levels of atRA in the cartilage, using TLZ, prevented the downregulation of atRA-responsive genes on cartilage injury, and, by doing so, it also suppressed the upregulation of inflammatory genes. As previously discussed, mechanical injury is one of the principal risk factors in the development of OA. By suppressing the upregulation inflammatory genes on cartilage injury, TLZ (or RAMBAs) can lend itself as a potential therapeutic agent in the cartilage, acting as an anti-inflammatory by offsetting mechanoflammation.

In order to explore how atRA might be acting to suppress mechanoflammation, I focused on reported mechanisms of how atRA acts as an anti-inflammatory in other systems. (i) Through suppression of inflammatory signalling. Specifically, atRA has been shown to interfere with inflammatory signalling in other systems [273]. (ii) Through suppression of mechano-inflammatory genes through the oestrogen nuclear receptors. RAR is capable of forming a heterodimer with the oestrogen receptor (ER) on the promoter regions of genes [227]. Oestrogen is a known anti-inflammatory molecule which has been implicated in anti-inflammatory actions through a number of different mechanisms. Tissue availability of oestrogen is determined by aromatase (CYP19A) activity. Of note, previously the group identified that *CYP19A* was strongly downregulated on cartilage injury (data not shown) and was a known atRA-responsive gene (unpublished data from our lab). This was also attractive because there is high prevalence of hand OA in perimenopausal women [427], a state characterised by low tissue oestrogen levels. (iii) Suppression of mechano-inflammatory

genes through atRA binding to the RXR-PPAR heterodimeric complex. PPARG in particular has been shown to suppress inflammation in multiple systems, including lung, brain tissue and bowel [428, 429]. In addition, PPARG KO mice showed accelerated OA, suggesting a protective role for PPARG in the development of OA [430].

7.2 Results

7.2.1 Talarozole does not affect TAK1 or MAPK phosphorylation on cartilage injury

Having validated previously observed results in our lab, I next investigated whether TLZ was able to suppress the MAPK signalling pathway. In Chapter 4, I showed that TLZ suppressed the upregulation of inflammatory genes on cartilage injury, and so I tested whether the mechanism by which it does so was through the suppression of TAK1, JNK or ERK.

MCP joints were preinjected with either 1 ml serum-free DMEM containing either 5 μM TLZ or vehicle control prior to cartilage explantation. Cartilage explants were snap-frozen or incubated for short time points post injury in either vehicle or TLZ. Cartilage lysates were generated and western-blotted for pJNK, pERK, pTAK1 and tERK. Quantification of three separate experiments was performed using FIJI-App, ImageJ-win64 Gel Analysis software. Results were normalised to total ERK1/2 and statistical significance of comparison between groups analysed by a two-way ANOVA, with post hoc multiple comparisons corrected using Tukey's tests.

TAK1 (Fig 7.1A), JNK (Fig 7.1B) and ERK (Fig 7.1C) was phosphorylated by 5 mins post cartilage injury, and this lasted up to 30 mins. The phosphorylation of TAK1, JNK and ERK on cartilage injury was unaffected by TLZ (Fig 7.1C–E).

These results revealed that the mechanism by which TLZ suppressed mechano-inflammatory genes on cartilage injury was not directly through the inhibition of either TAK1 or MAPK signalling pathway.

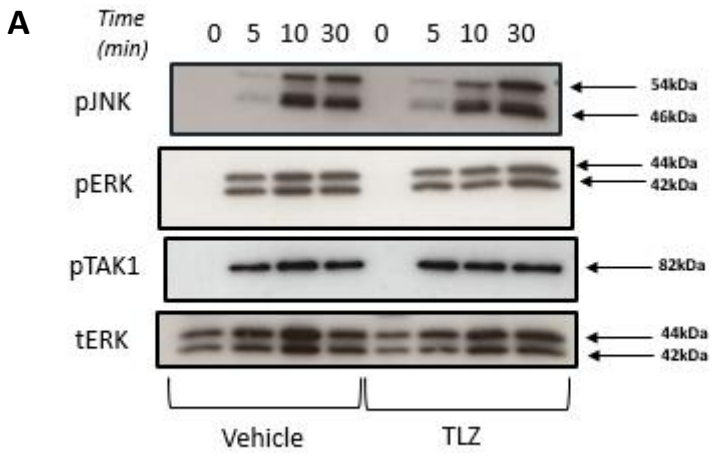
A
Time (min)
0 5 10 30 0 5 10 30
pJNK
pERK
pTAK1
tERK
54kDa
46kDa
44kDa
42kDa
82kDa
44kDa
42kDa
Vehicle
TLZ

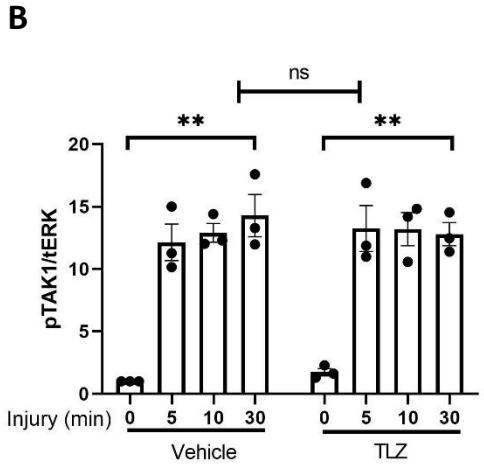
B
ns
**
**
pTAK1/tERK
Injury (min) 0 5 10 30 0 5 10 30
Vehicle
TLZ

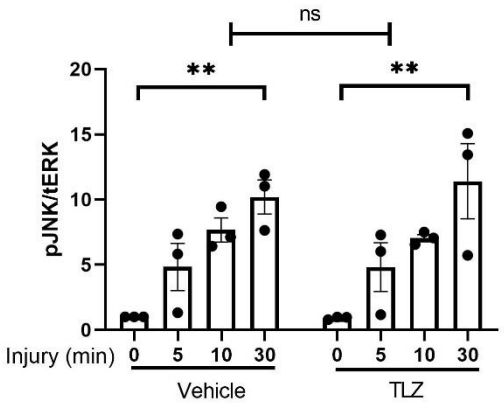
C
ns
**
**
pJNK/tERK
Injury (min) 0 5 10 30 0 5 10 30
Vehicle
TLZ

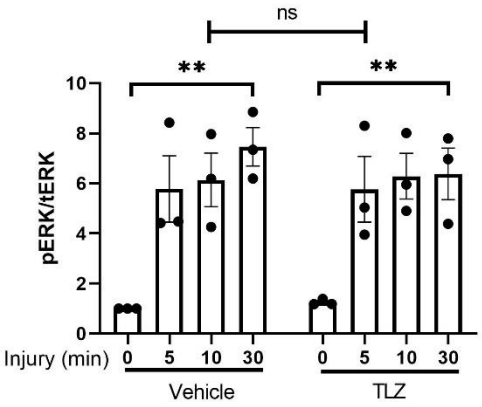
D
ns
**
**
pERK/tERK
Injury (min) 0 5 10 30 0 5 10 30
Vehicle
TLZ

Figure 7.1: Talarozole does not affect the phosphorylation of TAK1 or MAPKs on cartilage injury.

Porcine metacarpophalangeal (MCP) joints were decontaminated in 2% Virkon for 20 minutes before being equilibrated at 37°C, 5% CO_2 for 1 hour. MCP joints were injected with either 5 μM talarozole or vehicle control and incubated for another 1 hour at 37 °C. The MCP joints were opened and cartilage was rapidly explanted, as described in Materials and Methods. Explanted cartilage was either immediately cooled in ice-cold 1X RIPA Buffer nitrogen (zero hour time point) or cultured in serum free DMEM with or without talarozole for various periods of time (5min, 10min and 30min) at 37 °C, 5% CO_2 before being transferred to ice cold, 1X RIPA buffer. Explants with 1X RIPA buffer, were mildly shaken for 45 minutes at 4°C. Lysates were run on 10% Sodium Dodecyl Sulphate-Polyacrylamide Gel (SDS PAGE) and transferred to poly (vinylidene) (PVDF) membrane. PVDF membrane was blocked in 5% milk for 1 hour at room temperature and immunoblotted for pJNK, pERK and pTAK1. Signal was enhanced by use of chemiluminescence (A) and subsequently visualised using autoradiography. Representative blot of three repeats (A). The blot was stripped and re-probed for total ERK. The quantification of three separate experiments was performed using FIJI-App, ImageJ-win64 Gel Analysis software and normalised to total ERK (B-D).

7.2.2 Talarozole does not prevent the downregulation of atRA-responsive genes on cartilage injury through oestrogen metabolism

Having shown that TLZ does not suppress the upregulation of inflammatory genes on cartilage injury through affecting MAPK signalling, I next focused on the nuclear receptors through which atRA signals. One possible mechanism by which atRA can supress mechanoflammation is through oestrogen because CYP19A (aromatase, the enzyme which converts androgens to oestrogen in the tissue) is highly atRA-responsive and downregulated on cartilage injury. I determined whether inhibiting the production of oestrogen through the use of an aromatase inhibitor (letrozole, LTZ) would first reverse the effect of TLZ on atRA-responsive genes on cartilage injury and then looked at inflammatory gene regulation.

I performed the same trotter injury assay described above. MCP joints were preinjected with serum-free DMEM containing either vehicle (DMSO), TLZ (5 μM), LTZ (5 μM) or combined treatment with TLZ and LTZ. After incubation, the MCP joints were opened, cartilage rapidly dissected, cut into smaller pieces and either snap-frozen or cultured in serum-free medium containing drug or vehicle for four hours. The expression of each atRA-

responsive gene was normalised to 18S and further expressed relative to its normalised zero hour time points (n = 9 separate trotters). Statistical significance of the comparison between treatment groups was conducted using a two-way ANOVA, with multiple comparisons corrected using post hoc Tukey's tests.

Cartilage injury resulted in a significant downregulation of atRA-responsive genes in vehicle-injected joints ($p < 0.01$ for all atRA-responsive genes). TLZ completely reversed the downregulation of *CYP26A1* (100% SD ± 0.013, $p < 0.01$), *CYP26B1* (100% SD ± 0.053, $p < 0.01$) and *RARA* (100% SD ± 0.124, $p < 0.01$) on cartilage injury. *RARB* and *RARG* downregulation on cartilage injury was prevented, in the presence of TLZ, by 90% (SD ± 0.076, $p < 0.01$) and 75% (SD ± 0.077, $p < 0.01$), respectively. There was no significant difference in the expression of atRA-responsive genes at four hours post cartilage injury between TLZ-treated joints and TLZ/LTZ-cotreated joints. Therefore, the use of LTZ (an anastrazole inhibitor) did not reverse the effect of TLZ on any atRA-responsive gene expression at four hours post cartilage injury.

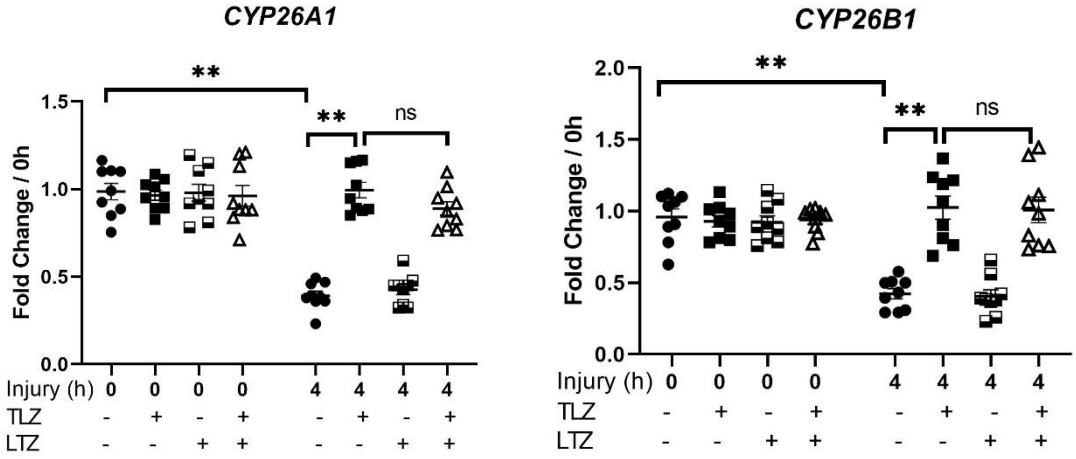

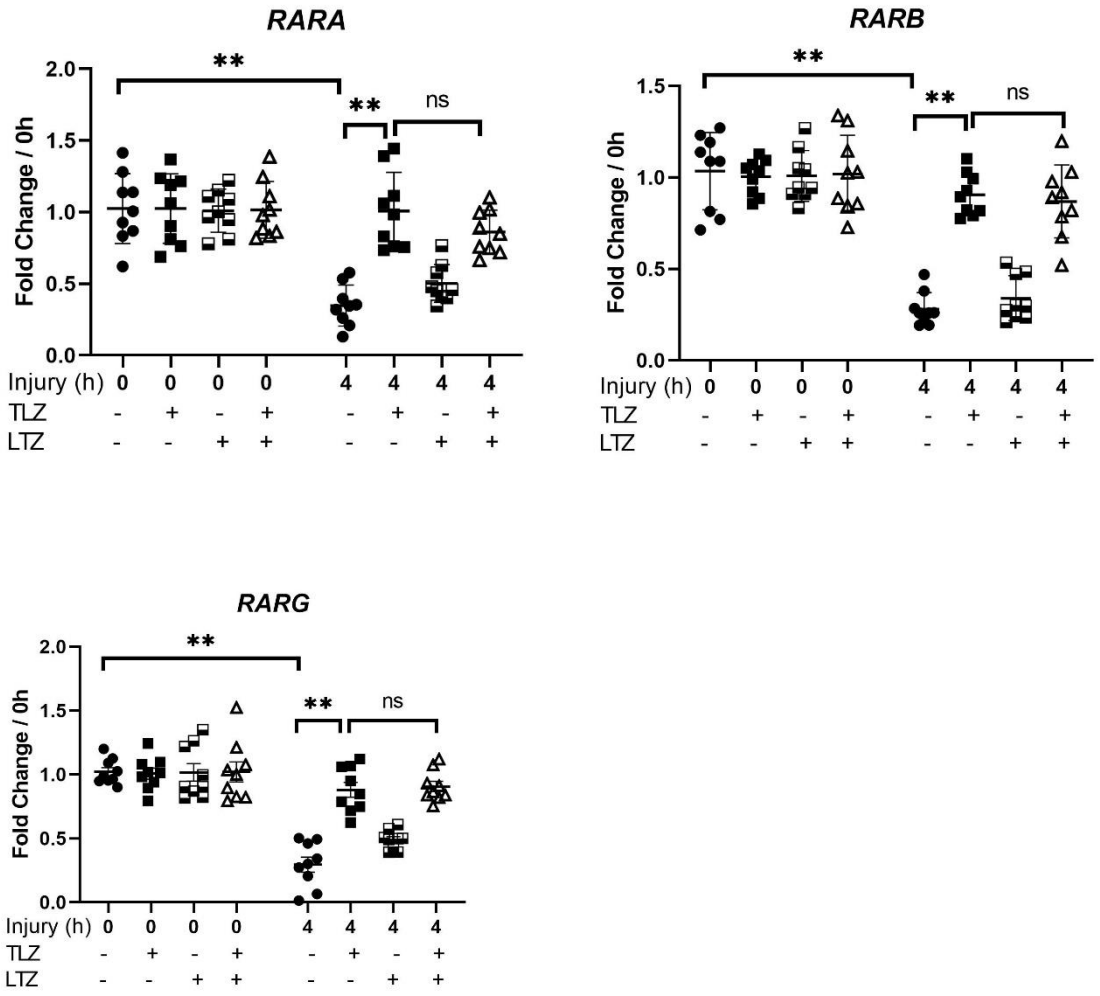

Figure 7.2: Letrozole does not reverse the effect of talarozole on atRA-responsive gene regulation on cartilage injury.

Porcine metacarpophalangeal (MCP) joints were decontaminated in 2% Virkon for 20 minutes before being equilibrated at 37 °C, 5% CO_2 for 1 hour. MCP joints were injected with either 5µM letrozole (LTZ), 5µM talarozole (TLZ), co-treated with LTZ/TLZ or vehicle control and incubated for another 1 hour at 37 °C. The MCP joints were opened and cartilage was rapidly explanted as described in Materials and Methods. Explanted cartilage was either immediately snap frozen in liquid nitrogen (zero hour time-point) or cultured in serum free DMEM with afore mentioned drug or vehicle for 4 hours at 37 °C, 5% CO_2 before being snap frozen. RNA was subsequently extracted from the tissue and used in quantitative reverse transcriptase-polymerase chain reaction to measure a panel of atRA- responsive genes. Statistical significance of comparison between treatment groups was conducted using a two-way ANOVA, with post-hoc multiple comparisons corrected using Tukey's tests. Bars shows the mean ± SEM of 3 independent experiments, in which each experiment was performed on 3 individual trotter joints (n=9 separate trotters). ns = not significant, * = $P < 0.05$; ** = $P < 0.01$, by two-way ANOVA. CYP26A1 = Cytochrome P450 Family 26 Subfamily A Member 1, CYP26B1 = Cytochrome P450 Family 26 Subfamily B Member 1, RARA = Retinoic Acid Receptor Alpha, RARB = = Retinoic Acid Receptor Beta, RARG = = Retinoic Acid Receptor Gamma.

7.2.3 Talarozole does not suppress the upregulation of inflammatory genes on cartilage injury through oestrogen metabolism.

Having shown that the effect of TLZ on the regulation of atRA-responsive gene on cartilage injury was not dependent on oestrogen signalling, I next measured the expression of inflammatory genes using the cDNA samples collected from the experiment conducted in section 7.2.2. I investigated whether inhibiting the production of oestrogen through the use of an aromatase inhibitor (letrozole/LTZ) would reverse the anti-inflammatory effects of TLZ.

Each inflammatory gene was significantly upregulated on cartilage injury ($p < 0.01$). TLZ, as expected, suppressed the upregulation of *IL6* (87% suppression, SD ± 1.474, $p < 0.01$), *COX2* (71% suppression, SD ± 1.302, $p < 0.01$), *ADAMTS4* (100% suppression, SD ± 0.268, $p < 0.01$), *CCL2* (70% suppression, SD ± 0.358, $p < 0.01$), *TIMP1* (79% suppression, SD ± 0.194, $p < 0.01$) and *CDKN1A* (53% suppression, SD ± 0.171, $p < 0.01$). *MMP3* regulation was induced further on injury by 1.73-fold (SD ± 0.179, $p < 0.01$) by TLZ at 4 hours compared to injured vehicle control joints. TLZ had no effect on the upregulation of *NGF* on cartilage injury, as previously seen. LTZ suppressed the upregulation of *IL6* (71.1% suppression, SD ± 1.474, $p < 0.01$), *COX2* (58.5% suppression, SD ± 1.302, $p < 0.01$), *ADAMTS4* (67.8% suppression, SD ± 0.268, $p < 0.01$), *MMP3* (52.9% suppression, SD ± 0.179, $p < 0.01$), *CDKN1A* (32.3% suppression, SD ± 0.171, $p < 0.01$) and *TIMP1* (51.7% suppression, SD ± 0.194, $p < 0.01$) on cartilage injury.

In cotreated joints, LTZ was able to reverse the effect of TLZ on *MMP3* such that *MMP3* was downregulated significantly in cotreated joints compared to TLZ-only-treated joints or injured vehicle control joints ($p < 0.01$). On the other hand, LTZ augmented the effect of

TLZ on *CDKN1A* on injury by supressing the upregulation of *CDKN1A* even further at four hours ($p < 0.01$).

Collectively, these results showed that rather suprsingly, LTZ exerted an anti-inflammatory effect in the joint. This was largely unexpected and perhaps suggested a separate mechanism by which LTZ suppresses inflammation. This observation, however, was in conflict with clinical findings which purport higher oestrogen levels to be protective against the development of OA.

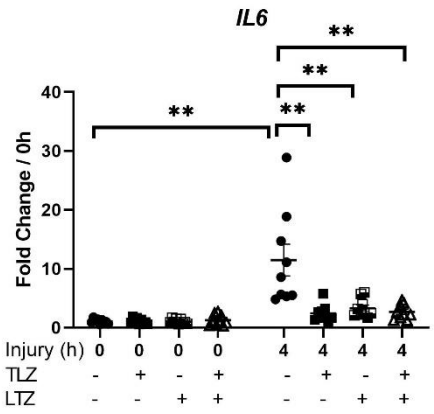
IL6
Fold Change / 0h
Injury (h) 0 0 0 0 4 4 4 4
TLZ - + - + - + - +
LTZ - - + + - - + +

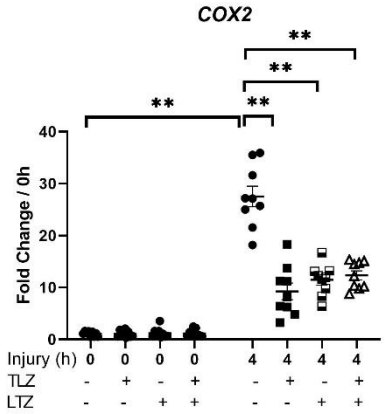
COX2
Fold Change / 0h
Injury (h) 0 0 0 0 4 4 4 4
TLZ - + - + - + - +
LTZ - - + + - - + +

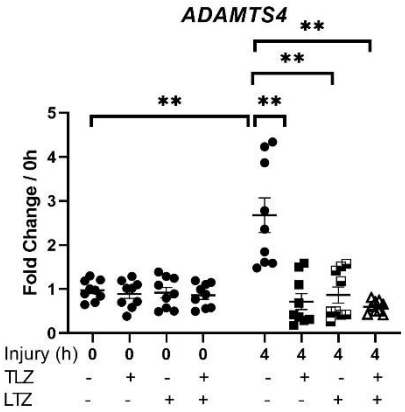
ADAMTS4
Fold Change / 0h
Injury (h) 0 0 0 0 4 4 4 4
TLZ - + - + - + - +
LTZ - - + + - - + +

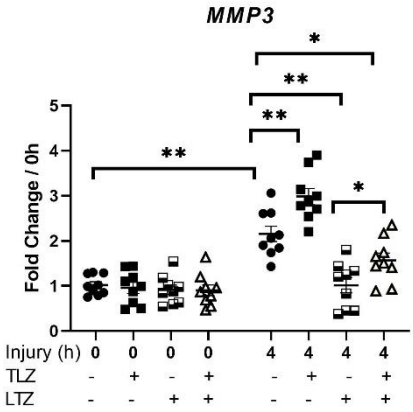
MMP3
Fold Change / 0h
Injury (h) 0 0 0 0 4 4 4 4
TLZ - + - + - + - +
LTZ - - + + - - + +

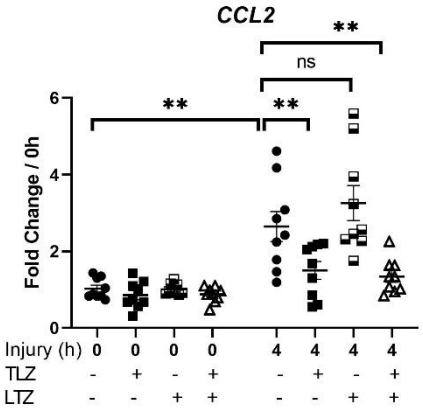
CCL2
ns
Fold Change / 0h
Injury (h) 0 0 0 0 4 4 4 4
TLZ - + - + - + - +
LTZ - - + + - - + +

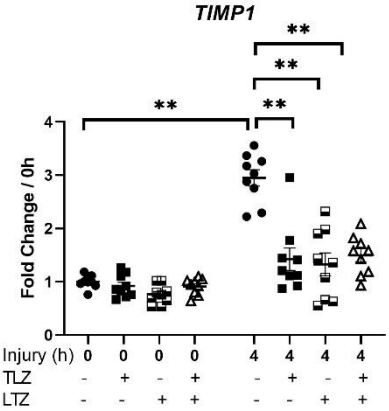
TIMP1
Fold Change / 0h
Injury (h) 0 0 0 0 4 4 4 4
TLZ - + - + - + - +
LTZ - - + + - - + +

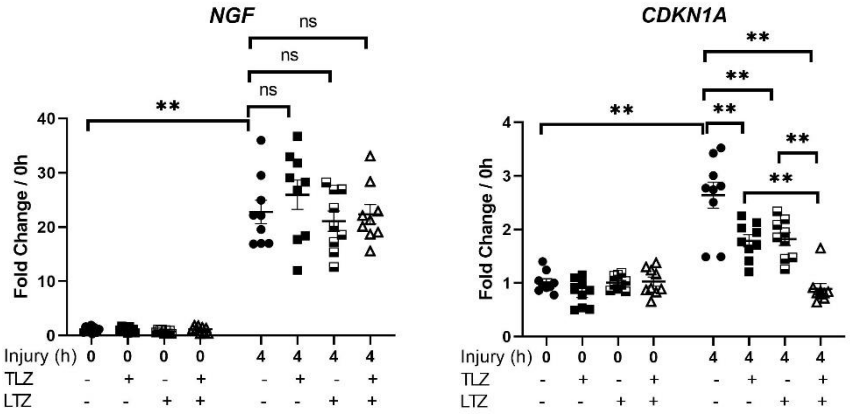

Figure 7.3: Letrozole does not reverse the effect of talarozole on inflammatory gene regulation on cartilage injury.

Porcine metacarpophalangeal (MCP) joints were decontaminated in 2% Virkon for 20 minutes before being equilibrated at 37 °C, 5% CO_2 for 1 hour. MCP joints were injected with either 5µM letrozole (LTZ), 5µM talarozole (TLZ), co-treated with LTZ/TLZ or vehicle control and incubated for another 1 hour at 37 °C. The MCP joints were opened and cartilage was rapidly explanted as described in Materials and Methods. Explanted cartilage was either immediately snap frozen in liquid nitrogen (zero hour time-point) or cultured in serum free DMEM with afore mentioned drug or vehicle for 4 hours at 37 °C, 5% CO_2 before being snap frozen. RNA was subsequently extracted from the tissue and used in quantitative reverse transcriptase-polymerase chain reaction to measure a panel of inflammatory genes. Statistical significance of comparison between treatment groups was conducted using a two-way ANOVA, with post-hoc multiple comparisons corrected using Tukey's tests. Bars shows the mean ± SEM of 3 independent experiments, in which each experiment was performed on 3 individual trotter joints (n=9 separate trotters). ns = not significant, * = P < 0.05; ** = P < 0.01, by two-way ANOVA. IL6 = Interleukin 6, COX2= Cyclooxygenase-2, ADAMTS4 = ADAM Metallopeptidase With Thrombospondin Type 1 Motif 4, MMP3= Matrix metalloproteinase-3, CCL2= C-C Motif Chemokine Ligand 2, TIMP1= TIMP metallopeptidase inhibitor 1, CDKN1A= Cyclin Dependent Kinase Inhibitor 1A, NGF= Nerve growth factor.

7.2.4 Downregulation of atRA-responsive genes on cartilage injury is talarozole-sensitive but not affected by PPARG-inhibition

Having ruled out MAPK signalling and oestrogen metabolism as potential mechanims by which TLZ suppresses mechanoflammation, I focused on the nuclear signalling receptors which atRA-binds onto. atRA influences gene transcription by binding onto one of two DNA-motifs: RARE or PPRE. RAREs are characterised by a heterodimeric complex of RARs and RXRs whereas PPREs are characterised by a heterodimeric complex of PPARs

and RXRs. PPARG has been extensively described in the literature for its anti-inflammatory role at a nuclear level. PPARG KO mice have been further shown to be protected from developing OA. Therefore, I tested the hypothesis that TLZ was preventing the drop of atRA-responsive genes and suppressed mechano-inflammatory genes on cartilage injury in a PPARG-sensitive manner.

The trotter injury assay was performed as previously described. MCP joints were preinjected with serum-free DMEM containing either vehicle (DMSO), TLZ (5 μM) or PPARG inhibitor (GW9662) (10 μM). Following 1 hour incubation, MCP joints were opened, cartilage rapidly dissected, cut into smaller pieces and either snap-frozen or cultured in serum-free medium containing drug or vehicle for four hours. The expression of each atRA-responsive gene was normalised to 18S and further expressed relative to its normalised zero hour time points (n = 9 separate trotters). Statistical significance of comparison between treatment groups was conducted using a two-way ANOVA, with multiple comparisons corrected using post hoc Tukey's tests.

All atRA-responsive genes were significantly downregulated on cartilage injury ($p < 0.01$). The use of TLZ significantly reversed the downregulation of each atRA-responsive gene (*CYP26A1* 89.1% reversal, SD ± 0.522, $p < 0.01$; *CYP26B1* 100% reversal, SD ± 0.371, $p < 0.01$; *RARA*, 84.4% reversal, SD ± 0.213, $p < 0.01$; *RARB*, 79.2% reversal, SD ± 0.521, $p < 0.01$; *RARG*, 100% reversal, SD ± 0.234, $p < 0.01$). The use of GW9662 did not inhibit TLZ from preventing the downregulation of atRA-responsive genes on cartilage injury. Following these observations, I concluded that the downregulation of atRA-responsive genes on cartilage injury was TLZ-sensitive but not sensitive to PPARG inhibiton.

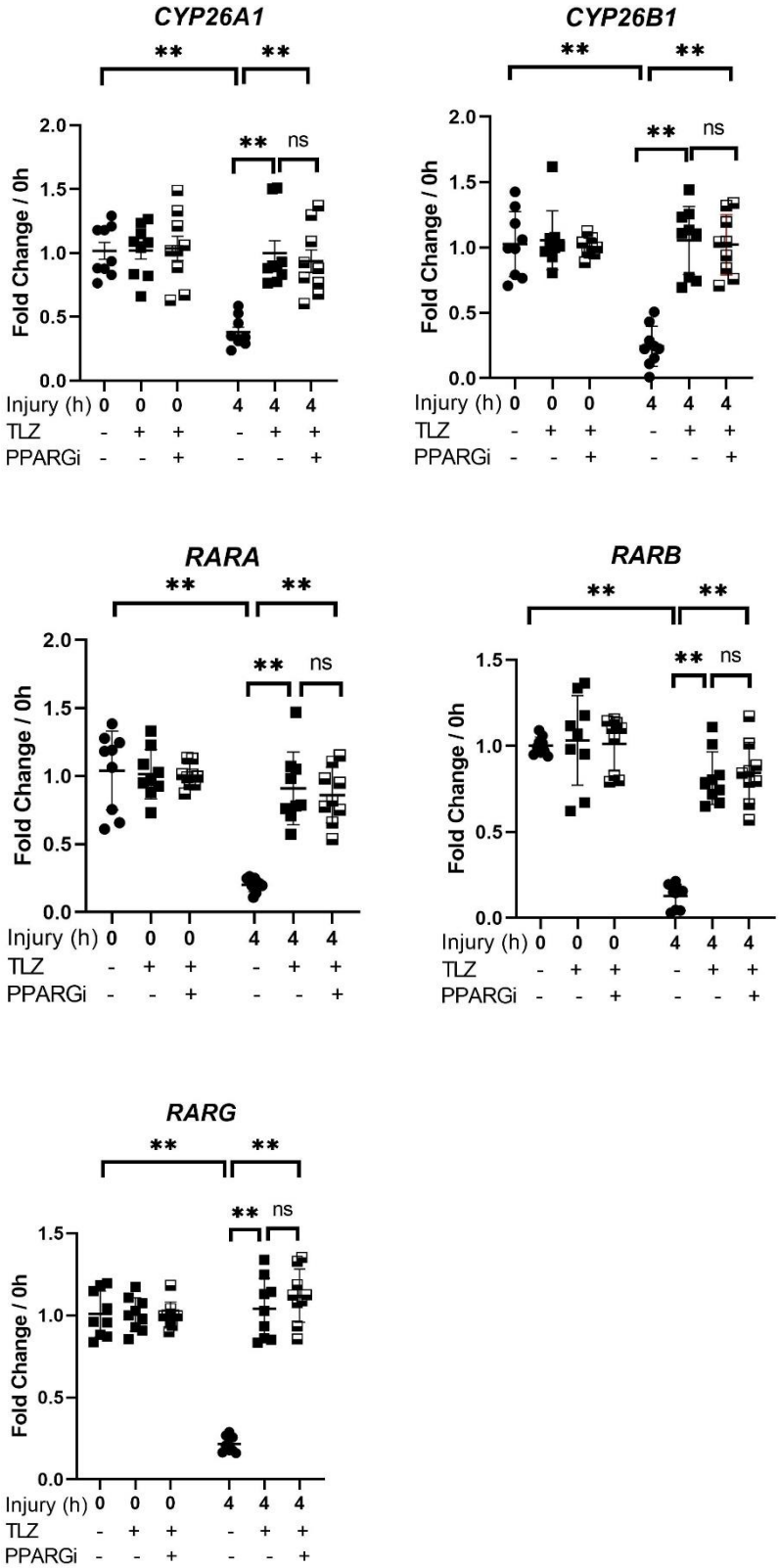
CYP26A1
CYP26B1
RARA
RARB
RARG
Fold Change / 0h
Injury (h)
TLZ
PPARGi
**
ns

Figure 7.4: The downregulation of atRA-responsive genes on cartilage injury is talarozole-sensitive but not affected by PPARG-inhibition.

Porcine metacarpophalangeal (MCP) joints were decontaminated in 2% Virkon for 20 minutes before being equilibrated at 37 °C, 5% CO_2 for 1 hour. MCP joints were injected with either 10 µM PPARGi (GW9662), 5 µM talarozole (TLZ), co-treated with PPARGi/TLZ or vehicle control and incubated for another 1 hour at 37 °C. The MCP joints were opened and cartilage was rapidly explanted as described in Materials and Methods. Explanted cartilage was either immediately snap frozen in liquid nitrogen (zero hour time-point) or cultured in serum free DMEM with afore mentioned drug or vehicle for 4 hours at 37 °C, 5% CO_2 before being snap frozen. RNA was subsequently extracted from the tissue and used in quantitative reverse transcriptase-polymerase chain reaction to measure a panel of inflammatory genes. Statistical significance of comparison between treatment groups was conducted using a two-way ANOVA, with post-hoc multiple comparisons corrected using Tukey's tests. Bars shows the mean ± SEM of 3 independent experiments, in which each experiment was performed on 3 individual trotter joints (n=9 separate trotters). ns = not significant, * = $P < 0.05$; ** = $P < 0.01$, by two-way ANOVA. CYP26A1 = Cytochrome P450 Family 26 Subfamily A Member 1, CYP26B1 = Cytochrome P450 Family 26 Subfamily B Member 1, RARA = Retinoic Acid Receptor Alpha, RARB = Retinoic Acid Receptor Beta, RARG = = Retinoic Acid Receptor Gamma.

7.2.5 The upregulation of some inflammatory genes on cartilage injury is talarozole-sensitive and PPARG-sensitive

After having observed that the downregulation of atRA-responsive genes on cartilage injury was TLZ-sensitive but not affected by PPARG-inhibition, I tested the expression of inflammatory genes in those joints that were injected with TLZ, GW9662 or vehicle control. The same cDNA samples were used from the experiment conducted in section 7.2.4.

IL6, *COX2*, *ADAMTS4* and *TIMP1* were all significantly upregulated on cartilage injury ($p < 0.01$). TLZ, as expected, suppressed the upregulation of *IL6* (100% suppression, SD ± 3.41, $p < 0.01$), *COX2* (87.2% suppression, SD ± 3.21, $p < 0.01$), *ADAMTS4* (98.8% suppression, SD ± 0.523, $p < 0.01$) and *TIMP1* (47.4% suppression, SD ± 0.391, $p < 0.01$) on cartilage injury. GW9662 significantly reversed the effects of TLZ on *IL6*, *COX2*, *ADAMTS4* and *TIMP1* on cartilage injury at 4 hours. GW9662 reversed the suppressive action of TLZ on *IL6* by 39.8% (SD ± 3.71, $p < 0.01$), *COX2* by 55.8 % (SD ± 4.83, p <

0.01), *ADAMTS4* by 36.4 % (SD ± 0.901, $p < 0.01$) and *TIMP1* by 100% (SD ± 0.331, $p < 0.01$).

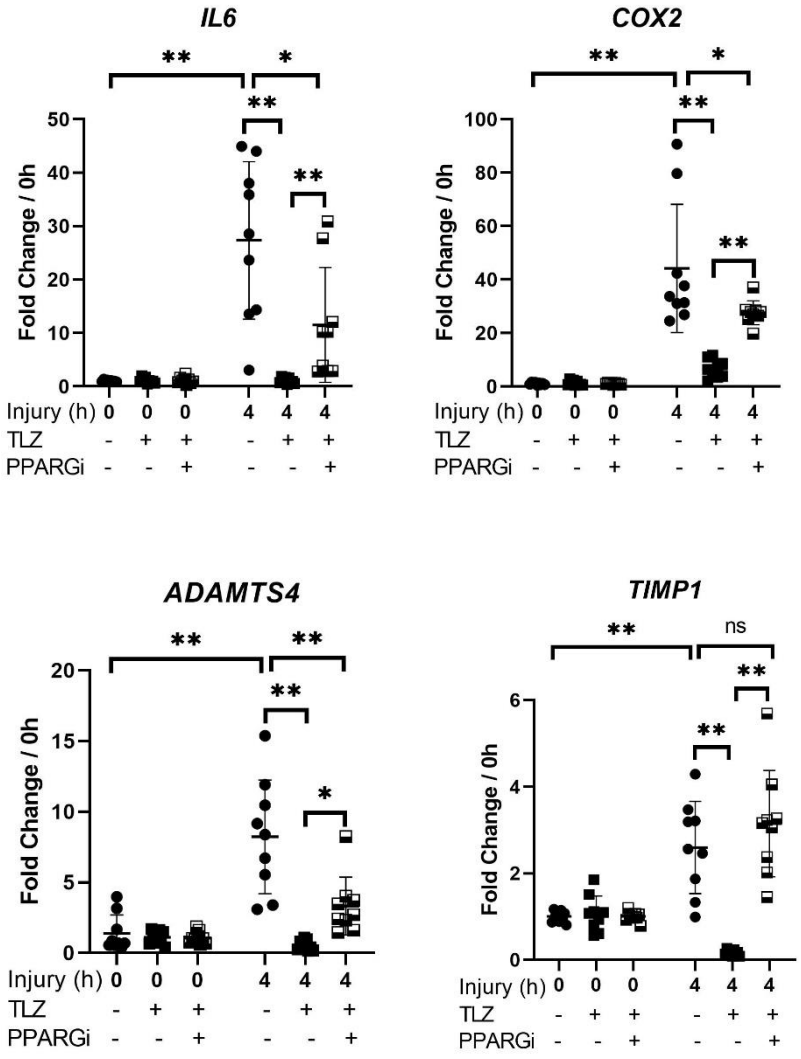

Figure 7.5: The upregulation of inflammatory genes on cartilage injury is talarozole-sensitive and PPARG-sensitive.

Porcine metacarpophalangeal (MCP) joints were decontaminated in 2% Virkon for 20 minutes before being equilibrated at 37 °C, 5% CO_2 for 1 hour. MCP joints were injected with either 10 µM PPARGi (GW9662), 5 µM talarozole (TLZ), co-treated with PPARGi/TLZ or vehicle control and incubated for another 1 hour at 37 °C. The MCP joints were opened and cartilage was rapidly explanted as described in Materials and Methods. Explanted cartilage was either immediately snap frozen in liquid nitrogen (zero hour time-point) or cultured in serum free DMEM with afore mentioned drug or vehicle for 4 hours at 37 °C, 5% CO_2 before being snap frozen. RNA was subsequently extracted from the tissue and used in quantitative reverse transcriptase-polymerase chain reaction to measure a panel of inflammatory genes. Statistical significance of comparison between treatment groups was conducted using a two-way ANOVA, with post-hoc multiple comparisons corrected using Tukey's tests. Bars shows the mean ± SEM of 3 independent experiments, in which each experiment was performed on 3 individual trotter joints (n=9 separate trotters). ns = not significant, * = P < 0.05; ** = P < 0.01, by two-way ANOVA. . IL6 = Interleukin 6, COX2= Cyclooxygenase-2, ADAMTS4 = ADAM Metallopeptidase With Thrombospondin Type 1 Motif 4, TIMP1= TIMP metallopeptidase inhibitor 1.

7.2.6 The upregulation of MMP3 on cartilage injury is talarozole-sensitive but not affected by PPARG-inhibition

I measured the expression of *MMP3* on the cDNA samples generated from the experiment conducted in section 7.2.4. *MMP3* ($p < 0.01$) expression was significantly upregulated on cartilage injury. The use of TLZ, as previously seen, further enhanced the expression of *MMP3* by 3.4-fold on cartilage injury ($p < 0.01$). Interestingly, GW9662 reversed the effect of TLZ on *MMP3*, suppressing the action of TLZ by 79.2% (SD ± 0.810, $p < 0.01$).

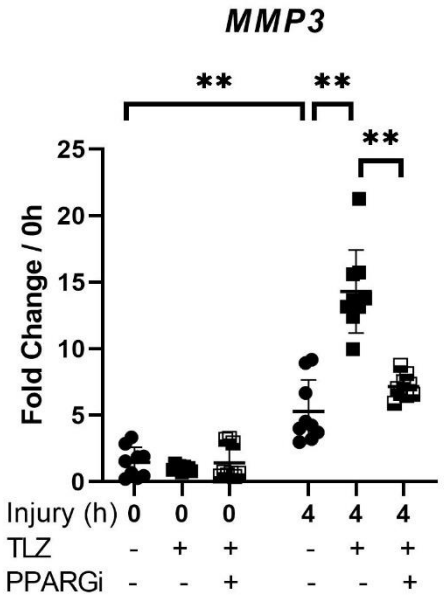

Figure 7.6: The upregulation of MMP3 on cartilage injury is talarozole-sensitive but not affected by PPARG-inhibition.

Porcine metacarpophalangeal (MCP) joints were decontaminated in 2% Virkon for 20 minutes before being equilibrated at 37 °C, 5% CO_2 for 1 hour. MCP joints were injected with either 10 µM PPARGi (GW9662), 5 µM talarozole (TLZ), co-treated with PPARGi/TLZ or vehicle control and incubated for another 1 hour at 37 °C. The MCP joints were opened and cartilage was rapidly explanted as described in Materials and Methods. Explanted cartilage was either immediately snap frozen in liquid nitrogen (zero hour time point) or cultured in serum free DMEM with afore mentioned drug or vehicle for 4 hours at 37 °C, 5% CO_2 before being snap frozen. RNA was subsequently extracted from the tissue and used in quantitative reverse transcriptase-polymerase chain reaction to measure the expression of MMP3. Statistical significance of comparison between treatment groups was conducted using a two-way ANOVA, with post-hoc multiple comparisons corrected using Tukey's tests. Bars shows the mean ± SEM of 3 independent experiments, in which each experiment was performed on 3 individual trotter joints (n=9 separate trotters). ns = not significant, * = P < 0.05; ** = P < 0.01, by two-way ANOVA. MMP3= Matrix metalloproteinase-3.

7.2.7 The upregulation of NGF and CDKN1A on cartilage injury is not affected by talarozole but PPARG-sensitive

Next, I measured the expression of *NGF* and *CDKN1A* in the same cDNA samples extracted from the injured MCP joints that were injected with either vehicle, TLZ or a combination of TLZ and GW9662. Both *NGF* and *CDKN1A* were upregulated on cartilage injury ($p < 0.05$). Although, there was a downward trend in the gene expression of *CDKN1A* on cartilage injury in those joints injected with TLZ compared to injured, vehicle-injected joints, this did

not quite reach statistical significance as compared to previous experiments. The use of combined GW9662 and TLZ significantly increased the upregulation of *CDKN1A* at 4 hours compared to injured, vehicle-injected joints ($p < 0.01$). Similarly, preinjection of MCP joints with a combination of GW9662 and TLZ significantly increased *NGF* expression by 20.2-fold ($p < 0.01$) compared to injured, vehicle-injected joints at 4 hours post injury.

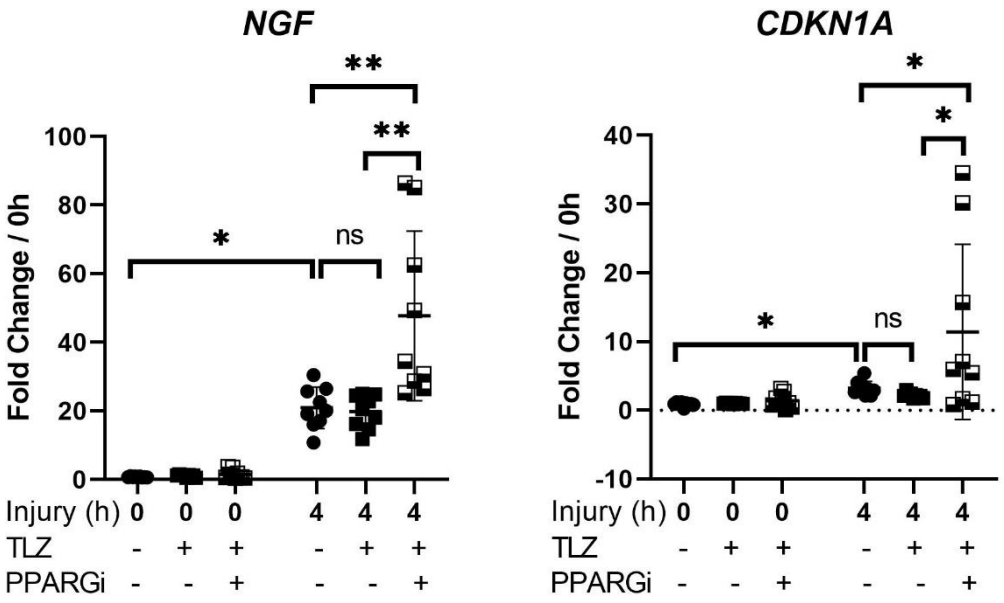

Figure 7.7: The upregulation of NGF and CDKN1A on cartilage injury is not affected by talarozole but PPARG-sensitive.

Porcine metacarpophalangeal (MCP) joints were decontaminated in 2% Virkon for 20 minutes before being equilibrated at 37 °C, 5% CO_2 for 1 hour. MCP joints were injected with either 10 µM PPARGi (GW9662), 5 µM talarozole (TLZ), co-treated with PPARGi/TLZ or vehicle control and incubated for another 1 hour at 37 °C. The MCP joints were opened and cartilage was rapidly explanted as described in Materials and Methods. Explanted cartilage was either immediately snap frozen in liquid nitrogen (zero hour time-point) or cultured in serum free DMEM with afore mentioned drug or vehicle for 4 hours at 37 °C, 5% CO_2 before being snap frozen. RNA was subsequently extracted from the tissue and used in quantitative reverse transcriptase-polymerase chain reaction to measure the expression of NGF and CDKN1A. Statistical significance of comparison between treatment groups was conducted using a two-way ANOVA, with post-hoc multiple comparisons corrected using Tukey's tests. Bars shows the mean ± SEM of 3 independent experiments, in which each experiment was performed on 3 individual trotter joints (n=9 separate trotters). ns = not significant, * = P < 0.05; ** = P < 0.01, ns= not significant, by two-way ANOVA. CDKN1A= Cyclin Dependent Kinase Inhibitor 1A, NGF= Nerve growth factor.

7.2.8 The upregulation of CCL2 on cartilage injury is not sensitive to talarozole or PPARG-inhibition

Lastly, I measured the expression of *CCL2* in the cDNA samples from the experiment conducted in section 7.2.4. *CCL2* was significantly upregulated on cartilage injury ($p < 0.01$). Although the use of TLZ resulted in a downward trend in the regulation of *CCL2* on cartilage injury by four hours, this did not reach statistical significance in this experimental set. There was no statistically significant difference in the expression of *CCL2* between those injured joints preinjected with TLZ or with a combination of TLZ and GW9662.

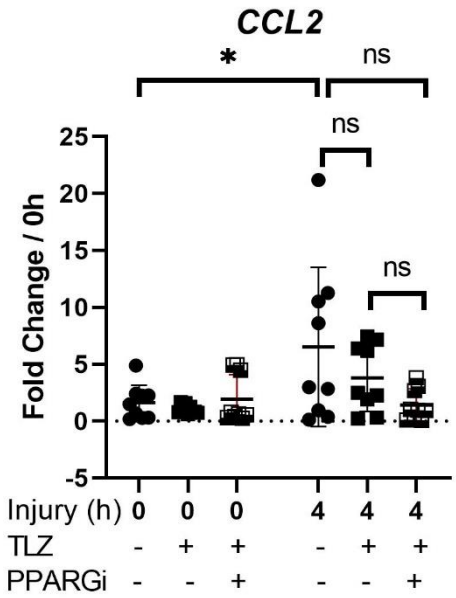

Figure 7.8: The upregulation of CCL2 on cartilage injury is not sensitive to talarozole or PPARG-inhibition.

Porcine metacarpophalangeal (MCP) joints were decontaminated in 2% Virkon for 20 minutes before being equilibrated at 37 °C, 5% CO_2 for 1 hour. MCP joints were injected with either 10 µM PPARGi (GW9662), 5 µM talarozole (TLZ), co-treated with PPARGi/TLZ or vehicle control and incubated for another 1 hour at 37 °C. The MCP joints were opened and cartilage was rapidly explanted as described in Materials and Methods. Explanted cartilage was either immediately snap frozen in liquid nitrogen (zero hour time-point) or cultured in serum free DMEM with afore mentioned drug or vehicle for 4 hours at 37 °C, 5% CO_2 before being snap frozen. RNA was subsequently extracted from the tissue and used in quantitative reverse transcriptase-polymerase chain reaction to measure the expression of CCL2. Statistical significance of comparison between treatment groups was conducted using a two-way ANOVA, with post-hoc multiple comparisons corrected using Tukey's tests. Bars shows the mean ± SEM of 3 independent experiments, in which each experiment was performed on 3 individual trotter joints (n=9 separate trotters). ns = not significant, * = $P < 0.05$; ** = $P < 0.01$, ns= not significant, by two-way ANOVA. CCL2= C-C Motif Chemokine Ligand 2.

7.2.9 The presence of atRA-binding sites in the promoter regions of ALDH1A2-dependent and talarozole-sensitive genes

Having shown that atRA-responsive genes are not regulated differentially on cartilage injury by the presence of PPARGi (GW9662), I determined whether the classical atRA-responsive genes (i.e. CYP genes and RAR genes) had a RARE-motif in their promoter regions which would not be influenced by the presence of GW9662. RARE consists of a direct repeat (DR)

of a combination of two motifs separated by less than eight nucleotides or no gap. The literature has reported *CYP26A1* and *RARB* as the two genes that have a consensus RARE-motif. I validated whether this and the other atRA-responsive genes also had any RARE-motifs. To achieve this, I used the ensemble genome database and searched for the promoter sequence of each atRA-responsive genes (*CYP26A1*, *CYP26B1*, *RARA*, *RARB* and *RARG*), 2000 kilobases (kb) upstream of the 5' region. This was performed for both the forward and reverse strand. Clustal Omega software was used to align the different sequences of potential RARE-motifs to the imported promoter sequence from ensemble. All searches were conducted in the pig species (sus scrofa). The results are summarised in Table 7.1.

CYP26A1, *RARA*, *RARB* and *RARG* had a double palindromic sequence that depicted a RARE-motif up to 2000 kb upstream of the 5' region of the promoter sequence. The palindromic sequences for each of these genes were spaced by fewer than eight nucleotides. *CYP2B1* had two singlet RARE-motifs present at -890kb and -846kb, respectively, from the 5' region. As such, the RARE-motifs for *CYP26B1* were separated by 44 bases, which is not characteristic for typical RARE-dependent genes, as described in the literature.

Following this, I looked at potential atRA-binding sites in the promoter regions of other ALDH1A2-dependent and TLZ -sensitive genes. I found that *ADAMTS4* and *MMP3* contained a typical RARE-motif in their promoter regions. This was found at -1710 base pairs (bp) upstream from the forward strand 5' site of the promoter region of *ADAMTS4* and -1040 bp from the 5' upstream from the forward strand 5' site of the promoter region of *MMP3*.

The other inflammatory genes did not contain the typical double-palindromic sequence that is characteristic for RARE-binding sites. Instead, they contained one atRA-binding motif in either their forward or reverse strand. Interestingly, according to the literature, the PPARG

binding site, shared the same homology to one of the atRA-binding motifs: AGGTCA. However, the literature around the general consensus sequence for the PPRE-motif is limited and not explored in detail.

Table 7.1: The presence of retinoic acid binding sites in the promoter regions of ALDH1A2-dependent and talarozole-sensitive genes.

GENE	Forward Strand	Reverse Strand
CYP26A1	**Y Double Sequence** (-1559)	N
CYP26B1	N	**Y Double Sequence** (-890, -846)
RARA	N	**Y Double Sequence** (-386)
RARB	**Y Double Sequence** (-20)	N
RARG	**Y Double Sequence** (-1149)	N
HOXA1	N	**Y Double Sequence** (-980)
IL6	Y (-1457,-907, -369)	Y (-1099, -548)
COX2	Y (-1570, -1271, -730)	Y (-1983, -1277, -739, -436)
ADAMTS4	**Y Double Sequence** (-1710, -1681, -1452 -1579, -509)	Y (-1495, -554, -284, -267)
CCL2	Y (-1825, -1603, -1198, -1161)	Y (-839, -802, -175)
MMP3	**Y Double Sequence** (-1040)	N
TIMP1	Y (-1531, -1330, -1120, -976, -483)	Y (-1030, -860, -676, -463)
NGF	Y (-1152, -672, -515, -212)	Y(-1820, -1362, -1298, -935, -928)
HAND2	Y (-1397)	Y (-610, -61)
MGAM	Y (-587, -694)	Y (-1936)
SMAD3	Y (-1586, -1500, -658, -2)	(-1942, -1342, -785, -500, -408)
CAMK2B	Y (-1764, -1712, -1277, -258, -142)	Y (-1158, -914, -863, -811, -682, -214)
FGFR3	Y (-1752, -1638, -1630, -1134, -1069, -532)	Y (-1462, -1153, -925, -861, -712, -557, -376, -368)
CDKN1A	Y (-1576**,** -1519, -1162, -924, -318)	Y (-1458, -1063, -976)
SMAD2	Y (-1052, -499)	Y (-766)
MYC	Y (-1511, -1301, -1214, -1106, -441)	Y (-1816, -1514, -924)
MMP1	Y (-1670, -1516, -1334, -1162, -316 -151, -47)	N
MMP13	Y (-1451, -665, -611, -412)	Y (-1834, -822, -752, -545)
CXCL5	Y (-1456, -1132, -731)	Y (-1433, -721, -614, -531, -111)

7.3 Discussion

7.3.1 atRA does not suppress mechanoflammation through MAPK signalling

Maintaining atRA-levels, by the use of TLZ, does not affect TAK1 or MAPK (JNK and ERK) phosphorylation. This indicates that atRA is modulating inflammatory gene regulation but is not the primary driver of inflammatory signalling on cartilage injury. This is in contrast to one study which demonstrated atRA influences MAPK signalling in retinal pigment epithelial cells. Yo-Chen Chang et al. demonstrated that pretreatment with atRA blunted the early phosphorylation of Akt and MAPK signalling mediators including p38, JNK1/2 and ERK1/2 [431]. However, the study used micromolar concentrations of atRA which are not physiologically relevant. Work from our group suggests that TLZ is most unlikely to increase atRA levels beyond nM levels (data not shown). Moreover, the direct application of atRA onto cells also promotes the process of autoinduction, inducing CYP26 enzymes to break down atRA. Meanwhile, another study showed that pretreatment with nanomolar concentrations of atRA was able to suppress IL1 and IL6 receptor upregulation in natural regulatory T cells (nTregs) [432]. The authors further demonstrated that atRA reduced the levels of phosphorylated p38 MAPK, downstream of IL1 and IL6 stimulation [432]. However, again the study did not account for autoinduction of CYP26 enzymes. Despite these contrasting findings in the literature, we discovered that in our system, atRA did not exert any influence on early TAK1 and MAPK signalling. We did not look at whether MAPK activity might have been altered at later time points. This might be relevant, as another nuclear receptor complex mediated by the glucocorticoid receptor, exerts anti-inflammatory actions, at least in part, by inducing the phosphatase DUSP1 which switches off MAPK activation [408].

From a therapeutic perspective, this might actually be beneficial. TAK1 and downstream MAPK and NF-κB signalling appear to be critical pathways involved in normal physiological functions including cell survival, cell proliferation and regulation of the innate and adaptive immune responses [420]. In fact, post-natal pan tissue deletion of TAK1 is lethal in mice (our group's unpublished data) and would not be conducive to clinical translation. Moreover, there is a growing consensus that the acute inflammatory signalling that ensues from the initial mechanical insult is important in promoting initial cartilage repair responses such as FGF2 and TGF-β signalling. Instead, it is the chronic, repetitive inflammatory drive that is deemed to be catabolic to the cartilage. Since atRA is unlikely to be the driver of the acute inflammatory signalling (either through TAK1 or MAPKs) it does not interfere with this potentially protective initial tissue repair responses. Rather atRA has the potential to act as a dampener of inflammation, making it an attractive putative candidate drug target in OA patients, with reduced adverse effects.

7.3.2 atRA suppresses mechanoflammation at the nuclear level through PPARG

The atRA-responsive genes that we measured can be broadly categorised into two groups; those that are induced by TLZ and those that are suppressed by TLZ. Those genes that were induced by TLZ on cartilage injury include *CYP26* genes and *RAR* genes. Both *CYP26* genes and *RAR* genes were noted to have classical RARE-motifs in their promoter regions. Therefore, the mechanism by which *CYP26* genes and *RAR* genes were maintained by TLZ on injury likely involved the binding of available ligand (atRA) to heterodimers of RAR-RXR, which then bind onto classical RARE-motifs in the promoter regions of these genes.

This was supported showing that, the use of a PPARG inhibitor did not influence the action of TLZ on either *CYP26* or *RAR* genes. The group of atRA-responsive genes which were

suppressed by TLZ, notably *IL6*, *COX2*, *ADAMTS4* and *TIMP1*, were highly TLZ- and PPARG-dependent. This suggested that the anti-inflammatory action of atRA was mediated in large part via the RXR-PPARG heterodimer that is somehow able to suppress inflammatory gene transcriptions. However, it is important to note that further studies need to be done to understand the detailed mechanisms by which the RXR-PPAR heterodimer suppresses transcription of inflammatory genes in the presence of atRA. Specifically, it will be important to determine whether the heterodimeric complex binds directly to the DNA to suppress transcription or whether it interferes with the binding and activation of a pro-inflammatory transcriptional regulator. One possibility would be to use chromatin immunoprecipitation (ChIP) analysis to immunoprecipitate PPARG from injury lysates treated with either vehicle or TLZ. Doing so, would help us to identify and confirm whether the promoter regions of the inflammatory genes that are PPARG-dependent do indeed have a PPAR-RXR heterodimeric complex. ChIP and sequencing would help to determine whether direct chromatin binding was occurring and what the binding sequence was. Site directed mutagenesis could then be used to confirm essential determinants of binding. Further investigation involving reporter assays would then be warranted to explore the mechanism by which mRNA transcription of these inflammatory genes are repressed in the presence of atRA.

The anti-inflammatory action of PPARG has been extensively described with mechanisms involving epigenetic changes, e.g. histone modification and direct gene transcriptional changes (promoting activation or repression) through direct binding to the PPRE-motif [428, 429]. Interestingly, the literature describes the PPAR- binding site to be identical to one of the motifs of the atRA-binding site (both heterodimers have a common RXR so this may account for the shared reported single motif binding site). Further exploration to characterise better PPRE-motifs on the promoter regions of genes is needed. In any case, our results

indicate that the inflammatory genes are suppressed in a PPARG-dependent manner and this is predicted to be beneficial in the cartilage injury response (Fig. 7.9). This finding is supported by a study conducted in 2016 by Kapoor et al. The group demonstrated that the deletion (KO) of PPARG in surgically induced OA in mice caused increased OA [433]. This was associated with by an upregulation of inflammatory gene regulation in the PPARG KO mice compared to wild type. Interestingly, a separate study showed that a PPARG agonist did not modify disease progression (unpublished data from Kapoor et al.). This suggests that atRA levels in the joint after injury might be the rate-limiting factor in modulating inflammation through the RXR-PPARG heterodimeric complex rather than levels of the PPARG-ligand. Therefore, increasing PPARG ligands further renders no beneficial effect. This underpins the importance of restoring atRA levels in the cartilage following injury in order to suppress the inflammatory gene regulation that drives chronic mechano-inflammatory disease.

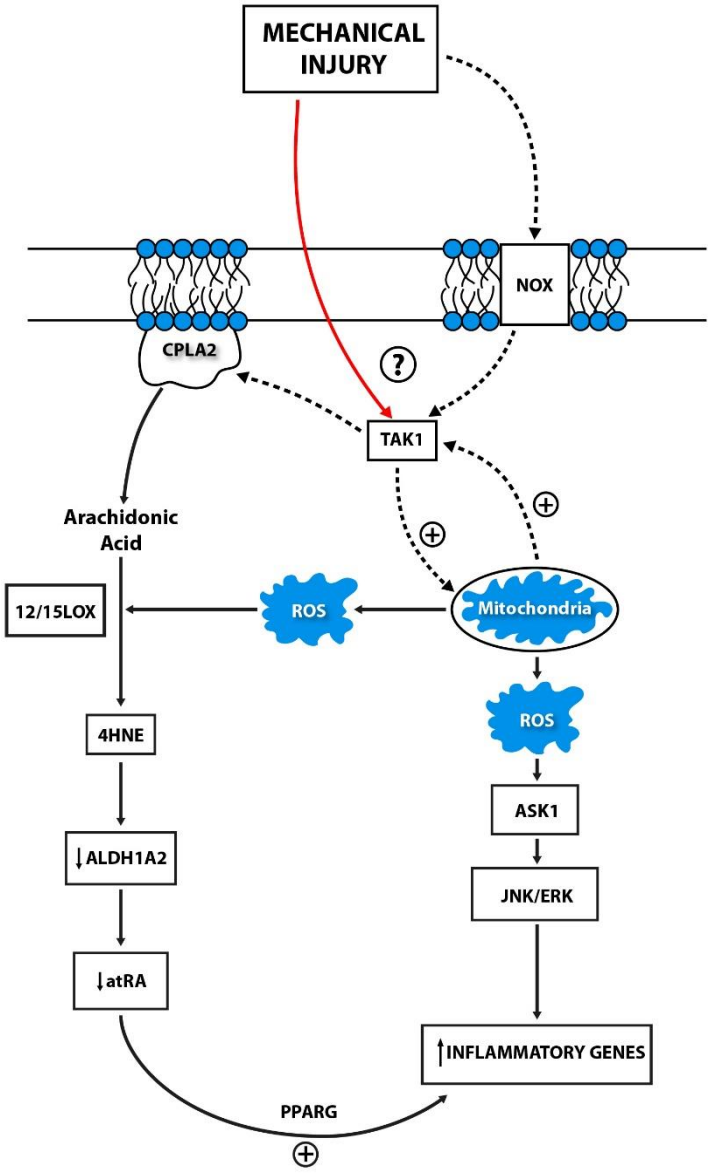

Figure 7.9: Final schematic proposing the mechanism by which atRA is both downregulated on cartilage injury and how it suppresses mechanoflammation.

Mechanical injury downregulates all-trans-retinoic acid (atRA)-responsive genes in both reactive oxygen species (ROS)-sensitive and cytosolic phospholipase A2 (cPLA2)-sensitive manner. Transforming growth factor activated-beta kinase 1 (TAK1) is partially phosphorylated on cartilage injury in a NADPH oxidase (NOX)-sensitive manner. TAK1 is responsible for partially phosphorylating cPLA2 on injury and likely acts in an auto-regulatory cycle with mitochondrial ROS. Apoptosis signal-regulating kinase 1 (ASK1) activation, secondary to ROS production from the mitochondria, likely drives the phosphorylation of the mitogen activated protein kinases (MAPKs) (Jun N-terminal kinase (JNK) and extracellular signal-regulated kinase (ERK)) on cartilage which subsequently increases inflammatory gene regulation. atRA suppresses inflammatory gene regulation in a peroxisome proliferator activated receptor gamma (PPARG)-sensitive manner. Block red line = undetermined; block black line = full activation; dotted black line = partial activation.

8 CHAPTER 8: FINAL DISCUSSION

Stemming from the initial GWAS study that identified a link between polymorphic variants in *ALDH1A2* and severe hand OA [200], we have revealed that atRA is a highly mechanosensitive pleiotropic factor regulated by cartilage injury. This is perhaps unsurprising given the impact that varying endogenous atRA concentrations have on forelimb, axial and digital formation. During development, atRA acts as a morphogenic factor driven by its temporo-spatial patterning in developing limbs. Deficiency in *ALDH1A2* results in failure of forelimb sprouting, reduced cartilage condensations and complete agenesis of the radius and ulna [248, 253, 254]. Post development, exogenous atRA has been shown to exert catabolic effects on cartilage formation [262, 263, 265]. However, these studies used very high concentrations of atRA which are not regarded as physiologically irrelevant. In this work, I highlight a novel and important postnatal role for atRA in cartilage biology.

atRA is extremely difficult to directly measure as it is highly photosensitive and rapidly degraded [335]. Therefore, I measured atRA-responsive genes (those genes that are upregulated by atRA through direct binding to RARE motifs) as a surrogate marker of atRA levels in the cartilage. We discovered that atRA-responsive genes were rapidly downregulated by four hours on cartilage injury, at the same time that inflammatory genes were upregulated. The upregulation of inflammatory genes on cartilage injury is part of a process that Vincent has termed mechanoflammation [2]. This describes the TAK-1-dependent activation of MAPKs (JNK, ERK and p38) and NF-κB signalling to drive inflammatory gene regulation resulting in the production of degradative enzymes, control of protease activity and production of NGF, a key mediator of pain in OA. The use of a CYP26 inhibitor, to maintain levels of atRA, at the point of injury prevented the downregulation of

atRA-responsive genes and importantly suppressed inflammatory gene expression. atRA was therefore acting as an anti-inflammatory agent in the joint. We discovered that atRA was likely acting to suppress mechanoflammation at the nuclear level through the PPARG-RXR heterodimeric complex rather than by directly influencing TAK1 or MAPK signalling.

The use of TLZ therefore lends itself as a potentially attractive disease-modifying agent for OA. TLZ has been previously used in acne and psoriasis patients in phase II and III clinical trials with an acceptable safety profile indicating that the route to clinical testing in OA could be relatively rapid [334]. Our group tested TLZ in murine OA. Due to its rapid clearance, we needed to deliver the drug through subcutaneous osmotic mini-pumps. In doing so we were able to show that TLZ was able to suppress cartilage degradation and osteophyte formation i.e. was structure modifying (Zhu, Kamalathevan et al., in revision). In my study, although TLZ was capable of suppressing key catabolic genes, it did not affect *NGF* gene expression. As NGF is a key mediator of pain in OA we don't yet know whether TLZ will also been symptom modifying [361]. This might limit licensing of such a treatment for OA.

We investigated the mechanisms of the downregulation of atRA-responsive genes, potentially identifying other pathways that could modify OA. We discovered that the expression of atRA-responsive and inflammatory genes on cartilage injury were both cPLA2- , 12/15-LOX- and ROS-sensitive.

cPLA2 is responsible for the liberation of arachidonic acid from PUFAs in the lipid bilayer to generate arachidonic acid [311]. The sequential metabolism of arachidonic acid by 12/15 LOX enzymes, in the presence of ROS, produces toxic lipid metabolites [311]. The most commonly produced lipid peroxidation product that has also been implicated in OA, 4-HNE, has been shown to inhibit ALDH1A2 post-translationally in retinal pigment epithelial cells, to reduce atRA levels [324]. Since I started my DPhil, PLA2 has been further implicated in

OA. In 2021, Wei et al. demonstrated that the secretory PLA2 (sPLA2) has disease-modifying effects in surgically induced OA [381]. The authors first showed that sPLA2 was elevated in OA cartilage of mice after surgical induction of OA. Administration of an inhibitor to sPLA2 within nanoparticles into the articular cartilage ameliorated aggrecan degradation and decreased inflammatory gene regulation after surgically induced OA. Moreover, osteophytes were seen to be markedly reduced in the sPLA2i-NP-treated group compared to control-treated groups [381]. A striking reduction in osteophytes was also observed in our lab in TLZ-treated OA mice, providing further evidence for a close relationship between PLA2 and atRA metabolism in the joint. Data supporting the involvement of dysregulated arachidonic acid metabolism was further provided by Kaizhe Chen et al. Their study demonstrated that silencing 15-LOX by siRNA alleviated mechanically induced cartilage degradation and decreased the gene expression of *MMP13* and *MMP1* [434]. Taken together, these studies and my findings demonstrate the importance of the arachidonic acid pathway in the regulation of inflammation after cartilage injury and might reveal an alternative therapeutic target. Inhibitors to cPLA2 have been used in hypoxic brain insults and have been shown to provide neuroprotection [435]. Inhibition of cPLA2 is thought to suppress the production of prostaglandins, leukotrienes, thromboxanes and platelet-activating factor [311]. The production of these mediators has been shown to promote atherosclerotic plaque development in cerebrovascular and coronary artery disease through the accumulation of toxic aldehyde metabolites [435]. PLA2 inhibitors have been used successfully in phase II and III clinical trials for patients with atherosclerotic vascular disease. The Stabilisation of Atherosclerotic Plaque by Initiation of Darapladib Therapy (STABILITY) [436] and the Stabilisation of Plaque Using Darapladib – Thrombolysis in Myocardial Infarction 52 (SOLID-TIMI 52) [437] studies are both phase III, randomised, clinical trials that were conducted to investigate the efficacy and safety profile of darapladib

(a PLA2 inhibitor) versus conventional medical therapy in patients with stable CHD and acute coronary syndrome. However, in both studies, darapladib failed to reduce the risk of coronary events compared to placebo. Moreover, the studies demonstrated that darapladib had high discontinuation rates due to adverse side effects that included gastrointestinal side effects and malodorous faeces, urine and skin [436, 437]. This is likely due to the ubiquitous expression and fundamental function of PLA2 in multiple tissues. Nonspecific targeting of cPLA2 in OA might therefore pose a problem because of the likelihood of systemic adverse effects. In which case, selective delivery of the drug into the joint would probably be necessary to mitigate such effects. It is also important to note that normal cPLA2 function is crucial in thermoregulation, innate immune responses, gastrointestinal protection and liver function [310]. Therefore, such risks need to be weighed up and tested before clinical translation.

I demonstrated that ROS-sequestering drugs are also implicated in mechanoflammation. Not only was the downregulation of atRA-responsive genes sensitive to ROS, but so too was the phosphorylation of TAK1 and downstream MAPKs. NAC was able to suppress, partially, upregulation of inflammatory genes on cartilage injury including NGF. NAC has been used in murine OA to suppress disease progression [375]. In 2019, Kaneko et al. demonstrated that oral administration of NAC-protected rats from developing OA in a surgically induced model by suppressing *MMP13* expression and increasing the expression of COL2 [375]. Human data was provided by Mustafa et al. who demonstrated that patients administered NAC, by intra-articular injection, had significant reductions in total antioxidant status and *MMP3* expression [438]. However, it is important to note that neither the participant nor the observer were blinded to injections. Further, to this there was no report on structural change, pain or joint function. In addition, there was no placebo-control arm in the study. To date, there have been no reported double-blinded, randomised, placebo-controlled trials with

NAC in patients with OA. However, the challenges with NAC administration have been described from other non-OA-related human studies. Most recently, the effect of NAC was investigated in a phase II clinical trial for treatment of severe acute respiratory syndrome caused by COVID-19 [439]. Patients were randomised to receive NAC 21 g for 20 hours or dextrose 5% in a double-blind, randomised, placebo-controlled trial. The administration of NAC at high doses did not affect the evolution of severe COVID-19. Importantly, the authors concluded that the dosage and choice of NAC as an antioxidant therapy might not have been optimal to restore redox balance [439]. The recommended dose of NAC was 300 mg/kg, yet this was not efficacious in the study [439]. Failure may have been due to the relative non-specificity of NAC as an antioxidant and the need for an even higher dose to restore redox balance secondary to replenishing intracellular GSH. Given these reasons, it is difficult to envision NAC as a treatment option in patients with OA. The need for continuous infusions and extremely high doses to achieve bioactive effects is not realistic for a chronic disorder such as OA.

CoQ10, an inhibitor of mitochondrial ROS, was a more potent inhibitor of inflammatory genes on cartilage injury, suggesting that pharmacological agents targeted at inhibiting the mitochondria might prove to be more efficacious in suppressing mechanoflammation. As discussed earlier, oral treatment with CoQ10 ameliorated pain and cartilage degradation in a rat model of OA with associated downregulation of *MMP13*, *IL6*, *IL15* and *INOS* [440]. This was consistent with my results that showed CoQ10 also suppressed *NGF* gene expression on cartilage injury. Given that pain is the leading cause of disability in OA, drugs targeting the mitochondria might seem like an attractive therapeutic in OA. There have been no reported randomised, placebo controlled clinical trials with mitochondrial inhibitors in patients with OA. CoQ10 has, however, been used in a phase III randomised, placebo-controlled, double-blinded clinical trial in patients with Parkinson's disease [441]. Patients

were given a high dose of CoQ10 (1.4 g to 2.4 g/day); the study reported no adverse effects, and treatment was well tolerated [441]. Although this study did not demonstrate any significant therapeutic effect provided by CoQ10, it highlighted the ease of administration (orally) and a good safety profile that could be translated to patients with OA. However, global inhibition of mitochondrial function can be extremely harmful. The mitochondria is vital for oxidative phosphorylation and ATP generation [277]. Even in chondrocytes, normal mitochondrial function is important to maintain calcium homeostasis [292]. For such reasons, more selective and bioavailable mitochondrial inhibitors have been developed. These include Idebenone (Raxone), which is a short synthetic chain of CoQ10 but with improved solubility and pharmacokinetics [442]. Idebenone transfers electrons from respiratory complex II to III and has been shown to have a good safety profile and antioxidant properties in several clinical trials [442]. Another compound for targeting mitochondrial ROS is anethole trithione (Sulfarlem). Studies have demonstrated that it inhibits 80% of superoxide production from complex I but without disrupting oxidative phosphorylation [443]. Although there have been no clinical trials to date with this drug, the good safety profile established in human studies provides a good platform for its use in future clinical trials.

Our previous work has identified TAK1 as a central mediator in injury-induced mechanoflammation [99]. My work has further demonstrated that ROS, likely derived from the mitochondria, is in an autoregulatory loop with TAK1. TAK1, at least partly, drives cPLA2 activation on injury and is itself partly induced by NOX. Taken together, TAK1 appears to be acting as a central orchestrator in mediating mechanoflammation and therefore represents a central target in OA. However, TAK1 also has important functions in cartilage development and bone growth [104, 107]. Gunnell et al. demonstrated that genetic deletion of TAK1 in chondrocytes resulted in embryonic developmental cartilage defects due to

decreased chondrocyte proliferation and survival [444]. The authors further showed that loss of TAK1 impaired downstream MAPK, bone morphogenetic protein (BMP)/SMAD signalling. Collectively, this suggests that TAK1 plays a vital role in cartilage and bone development. Postnatally, TAK1 also has a critical role in cell survival in multiple systems over and above its influence on downstream MAPK signalling pathways [104]. Inhibition of TAK1 is followed by caspase 8 and caspase 3 activation secondary to TNFα induction [445]. This suggests that TAK1 inhibits caspase activation and blocks cell death. The mechanisms by which TAK1 inhibits cell death has been confirmed by several studies [420]. Consistent with this, unpublished results from our group show that pan tissue, post natal deletion of TAK1 results in death within 48h. Collectively, these suggest that TAK1 has indispensable roles in normal physiology which go beyond its effects on mechanoflammation. The fundamental role of TAK1 in development is further demonstrated by the fact that global deletion of TAK1 in mice renders them unviable, with death being a consequence of cardiac and vascular pathology [446]. Therefore, it would be important to manipulate mechanoflammation in OA down stream of TAK1.

My data revealed that ASK1, another MAPKKK, was the key driver of MAPKs (JNK and ERK) on cartilage injury. The activation of ASK1 is known to be ROS-sensitive [422], and in our system, this appears to be driven by the mitochondria. Given that TAK1 is not a viable target because of its important physiological functions, ASK1 lends itself as a better target to suppress mechanoflammation. My data has already demonstrated that inhibiting ASK1 has a profound effect on suppressing inflammatory gene regulation. In addition, inhibiting ASK1 has no effect on TAK1. Therefore, inhibiting ASK1 has the potential to maintain the activity of TAK1 for normal cellular function whilst suppressing mechanoflammation. As previously mentioned, ASK1 KO mice are protected from developing OA [425]. A supporting study showed that selonsertib alleviated the progression of rat OA [426].

Selonsertib has been used in a few non-OA-related randomised clinical trials. Rohit Loomba et al. used selonsertib in a phase II randomised clinical trial in patients with nonalcoholic steatohepatitis (NASH) [447]. Selonsertib was administered to patients orally once a day. There were a higher proportion of adverse events in the selonsertib group which included headache, nausea, fatigue, parasthesiae and elevated liver enzymes. However, only one patient had to discontinue study treatment. Selonsertib appeared to improve the primary study endpoint (liver fibrosis), and the authors concluded an overall good safety profile [447]. Two other clinical trials using selonsertib for NASH are now in progress. One is a phase II clinical trial NASH-induced bridging fibrosis **(***NCT03449446)* whilst the second is a phase II trial which combines selonsertib with a nonsteroidal FXR agonist and firsocostat for NASH-induced fibrosis **(***NCT03053050)***.** Collectively, these studies support the clinical translation of selonsertib as a potential clinical trial drug for patients with OA.

Although mechanoflammation is largely regarded as exerting a catabolic effect on cartilage and ECM homeostasis, the initial acute inflammatory response may be important to initiate certain repair responses by the cartilage. Cartilage injury activates several other injury response including the release of the growth factors TGF-β and FGF2 [16, 94, 100]. TGF-β is one of the growth factors present in the PCM, and it becomes less abundant with age. The release of TGF-β on cartilage injury may contributes towards mechanoadaptation over the course of a person's life [94]. FGF2 is another growth factor that is released from the PCM on injury and is strongly chondroprotective in vivo [16]. Recently, other cell surface mechanosensors have been discovered, namely, PIEZO1 and TRPV4 [30]. The activation of these receptors has been shown to drive anabolic responses that involve proteoglycan synthesis and cartilage repair [86, 448]. How these protective injury responses interact with mechanoflammation is unknown, but it is likely that some degree of inflammation/protease activity is important in the early stages of tissue repair. We speculate that it is the chronic

activation of TAK1 and downstream inflammatory genes which is detrimental to cartilage homeostasis, switching the balance towards a pro-denegerative phenotype. Therefore, it may be better to use an agent that is a modulator of inflammation rather than switch it off entirely.

The mechanism of action of TLZ was demonstrated to be PPARG-sensitive. This suggested that atRA may be modulating inflammation by binding onto the RXR-PPARG heterodimeric complex on the promoter regions of target inflammatory genes. Therefore atRA, could be regarded as a mechano-inflammatory 'dampener' rather than inhibitor. By dampening mechanoflammation, TLZ is an ideal candidate drug to suppress the chronic inflammation without interfering with other acute mechano-inflammatory responses.

8.1 Limitations

The vast majority of my work involved the use of commercial inhibitors to various targets. Although the use of inhibitors can give mechanistic insights into signalling pathways, they can be relatively crude and carry certain disadvantages. Firstly, commercially available inhibitors might not be entirely specific to its target and exert off-target actions towards other signalling components especially at high concentrations. Secondly, in some cases, the inhibitors need to be used at a very high concentration to be efficacious towards inhibiting its target. The latter was the case for both NAC and apocynin which were used in mM concentrations. Using such high concentrations can pose problems for clinically translating these agents into patients, where supraphysiological doses would not be clinically relevant or safe. Drug inhibitor studies can be strengthened by loss-of-function studies such as with KO animal models. The mechanistic insights that drug inhibitor studies provide, build a platform from which more robust experiments can be built. For example, our lab has generated a pan tissue inducible conditional cPLA2-KO mouse. Ongoing work includes conducting hip avulsion (injury) experiments in cPLA2-KO and WT-mice to look for

changes in gene regulation, and looking at disease progression in surgically-induced OA. I attempted to harvest tissue from the hip of cPLA2-KO mice post hip avulsion, however, due to time constraints I was not able to complete this.

In the case of ASK1 activation, I relied on the selectivity of the inhibitor, selonsertib, to its target, in order to conclude that ASK1 was likely the main driver of MAPK activation on injury. However, we cannot exclude non-selective actions of selonsertib towards other MAPKs in our experimental set-up (although reassuringly it did not affect TAK1 phosphorylation). It would be important to establish the direct activation of ASK1 on cartilage injury by phospho-western blot and to further disentangle its relationship with TAK1 activation on injury. This use of an in-vivo ASK1 KO mice model would further help to validate our working hypothesis.

Lastly, we suggested a role for ROS and lipid peroxidation products, such as 4-HNE, in mechanoflammation by using anti-oxidative agents in the injury assay. As a next step, it would be important to directly measure whether ROS or indeed lipid peroxidation products, are regulated by mechanical injury by reporter assay or mass spectroscopy.

8.2 Conclusion

OA is highly prevalent condition that significantly affects the elderly population resulting in pain, disability and loss of joint function. There is currently an unmet need for a DMOAD for the treatment of OA. My work has helped to identify two potential targets for such disease modifying therapy in OA. The first, TLZ, (a CYP26 inhibitor which increases cellular atRA levels), has been identified as a modulator of chronic inflammation by dampening mechanoflammation in a PPARG-sensitive manner. ASK1, has been identified as the key driver of MAPK activation on cartilage injury in a ROS-sensitive manner to

activate mechanoflammation. ASK1 inhibition using selonsertib, in particular, suppresses *NGF* expression, which has been strongly associated with pain in OA. Although the work requires further supporting in-vivo and clinical translational studies, the use of TLZ and selonsertib present themselves as potential disease modifying agents to combat pain, joint function and disability in OA.

9 REFERENCES

1. Martel-Pelletier, J., et al., *Osteoarthritis.* Nature Reviews Disease Primers, 2016. **2**(1): p. 16072.
2. Vincent, T.L., *Mechanoflammation in osteoarthritis pathogenesis.* Semin Arthritis Rheum, 2019. **49**(3s): p. S36-s38.
3. Vincent, T.L., *Of mice and men: converging on a common molecular understanding of osteoarthritis.* The Lancet. Rheumatology, 2020. **2**(10): p. e633-e645.
4. Berenbaum, F., *Osteoarthritis as an inflammatory disease (osteoarthritis is not osteoarthrosis!).* Osteoarthritis Cartilage, 2013. **21**(1): p. 16-21.
5. Bitton, R., *The economic burden of osteoarthritis.* Am J Manag Care, 2009. **15**(8 Suppl): p. S230-5.
6. Decker, R.S., *Articular cartilage and joint development from embryogenesis to adulthood.* Seminars in cell & developmental biology, 2017. **62**: p. 50-56.
7. Mansfield, J.C., J.S. Bell, and C.P. Winlove, *The micromechanics of the superficial zone of articular cartilage.* Osteoarthritis and Cartilage, 2015. **23**(10): p. 1806-1816.
8. Lee, Y., J. Choi, and N.S. Hwang, *Regulation of lubricin for functional cartilage tissue regeneration: a review.* Biomaterials Research, 2018. **22**(1): p. 9.
9. Sophia Fox, A.J., A. Bedi, and S.A. Rodeo, *The basic science of articular cartilage: structure, composition, and function.* Sports health, 2009. **1**(6): p. 461-468.
10. James, C.B. and T.L. Uhl, *A review of articular cartilage pathology and the use of glucosamine sulfate.* Journal of athletic training, 2001. **36**(4): p. 413-419.
11. Eyre, D.R., et al., *Covalent cross-linking of the NC1 domain of collagen type IX to collagen type II in cartilage.* J Biol Chem, 2004. **279**(4): p. 2568-74.
12. Aigner, T., et al., *Type X collagen expression in osteoarthritic and rheumatoid articular cartilage.* Virchows Arch B Cell Pathol Incl Mol Pathol, 1993. **63**(4): p. 205-11.
13. Gilbert, S.J., C.S. Bonnet, and E.J. Blain, *Mechanical Cues: Bidirectional Reciprocity in the Extracellular Matrix Drives Mechano-Signalling in Articular Cartilage.* International journal of molecular sciences, 2021. **22**(24): p. 13595.
14. Keppie, S.J., et al., *Matrix-Bound Growth Factors are Released upon Cartilage Compression by an Aggrecan-Dependent Sodium Flux that is Lost in Osteoarthritis.* Function, 2021. **2**(5): p. zqab037.
15. Vincent, T.L., et al., *FGF-2 is bound to perlecan in the pericellular matrix of articular cartilage, where it acts as a chondrocyte mechanotransducer.* Osteoarthritis and Cartilage, 2007. **15**(7): p. 752-763.
16. Vincent, T., et al., *Basic FGF mediates an immediate response of articular cartilage to mechanical injury.* Proceedings of the National Academy of Sciences of the United States of America, 2002. **99**(12): p. 8259-8264.
17. Palukuru, U.P., C.M. McGoverin, and N. Pleshko, *Assessment of hyaline cartilage matrix composition using near infrared spectroscopy.* Matrix Biology, 2014. **38**: p. 3-11.
18. Huang, Y.-F., S. Mizumoto, and M. Fujita, *Novel Insight Into Glycosaminoglycan Biosynthesis Based on Gene Expression Profiles.* Frontiers in Cell and Developmental Biology, 2021. **9**.
19. Chandran, P.L. and F. Horkay, *Aggrecan, an unusual polyelectrolyte: review of solution behavior and physiological implications.* Acta biomaterialia, 2012. **8**(1): p. 3-12.
20. Grodzinsky, A.J., et al., *Cartilage Tissue Remodeling in Response to Mechanical Forces.* Annual Review of Biomedical Engineering, 2000. **2**(1): p. 691-713.
21. Guilak, F., et al., *The pericellular matrix as a transducer of biomechanical and biochemical signals in articular cartilage.* Ann N Y Acad Sci, 2006. **1068**: p. 498-512.
22. Zhao, Z., et al., *Mechanotransduction pathways in the regulation of cartilage chondrocyte homoeostasis.* Journal of cellular and molecular medicine, 2020. **24**(10): p. 5408-5419.

23. Boraschi-Diaz, I., et al., *Collagen Type I as a Ligand for Receptor-Mediated Signaling.* Frontiers in Physics, 2017. **5**.
24. Ocken, A.R., et al., *Perlecan Knockdown Significantly Alters Extracellular Matrix Composition and Organization During Cartilage Development.* Mol Cell Proteomics, 2020. **19**(7): p. 1220-1235.
25. Nam, J., et al., *Biomechanical thresholds regulate inflammation through the NF-kappaB pathway: experiments and modeling.* PLoS One, 2009. **4**(4): p. e5262.
26. Trompeter, N., et al., *Extracellular Matrix Stiffness Alters TRPV4 Regulation in Chondrocytes.* bioRxiv, 2021: p. 2021.09.14.460172.
27. Millward-Sadler, S.J., et al., *Mechanotransduction via integrins and interleukin-4 results in altered aggrecan and matrix metalloproteinase 3 gene expression in normal, but not osteoarthritic, human articular chondrocytes.* Arthritis & Rheumatism, 2000. **43**(9): p. 2091-2099.
28. Nims, R.J., L. Pferdehirt, and F. Guilak, *Mechanogenetics: harnessing mechanobiology for cellular engineering.* Curr Opin Biotechnol, 2022. **73**: p. 374-379.
29. Lee, W., F. Guilak, and W. Liedtke, *Chapter Ten - Role of Piezo Channels in Joint Health and Injury*, in *Current Topics in Membranes*, P.A. Gottlieb, Editor. 2017, Academic Press. p. 263-273.
30. Zhang, M., et al., *TRPV4 and PIEZO Channels Mediate the Mechanosensing of Chondrocytes to the Biomechanical Microenvironment.* Membranes, 2022. **12**(2).
31. Fitzgerald, J.B., et al., *Shear- and Compression-induced Chondrocyte Transcription Requires MAPK Activation in Cartilage Explants*.* Journal of Biological Chemistry, 2008. **283**(11): p. 6735-6743.
32. Hoon, J.L., M.H. Tan, and C.-G. Koh, *The Regulation of Cellular Responses to Mechanical Cues by Rho GTPases.* Cells, 2016. **5**(2): p. 17.
33. Henrotin, Y., B. Kurz, and T. Aigner, *Oxygen and reactive oxygen species in cartilage degradation: friends or foes?* Osteoarthritis and Cartilage, 2005. **13**(8): p. 643-654.
34. Lafont, J.E., *Lack of oxygen in articular cartilage: consequences for chondrocyte biology.* International journal of experimental pathology, 2010. **91**(2): p. 99-106.
35. Coyle, C.H., N.J. Izzo, and C.R. Chu, *Sustained hypoxia enhances chondrocyte matrix synthesis.* Journal of orthopaedic research : official publication of the Orthopaedic Research Society, 2009. **27**(6): p. 793-799.
36. Bae, H.C., et al., *Hypoxic condition enhances chondrogenesis in synovium-derived mesenchymal stem cells.* Biomaterials research, 2018. **22**: p. 28-28.
37. Kong, P., et al., *HIF-1α repairs degenerative chondrocyte glycolytic metabolism by the transcriptional regulation of Runx2.* Eur Rev Med Pharmacol Sci, 2021. **25**(3): p. 1206-1214.
38. Sartori-Cintra, A.R., et al., *Regulation of hypoxia-inducible factor-1α (HIF-1α) expression by interleukin-1β (IL-1 β), insulin-like growth factors I (IGF-I) and II (IGF-II) in human osteoarthritic chondrocytes.* Clinics (Sao Paulo, Brazil), 2012. **67**(1): p. 35-40.
39. Grimshaw, M.J. and R.M. Mason, *Modulation of bovine articular chondrocyte gene expression in vitro by oxygen tension.* Osteoarthritis Cartilage, 2001. **9**(4): p. 357-64.
40. Maldonado, M. and J. Nam, *The role of changes in extracellular matrix of cartilage in the presence of inflammation on the pathology of osteoarthritis.* BioMed research international, 2013. **2013**: p. 284873-284873.
41. Tortorella, M.D., et al., *Sites of Aggrecan Cleavage by Recombinant Human Aggrecanase-1 (ADAMTS-4)*.* Journal of Biological Chemistry, 2000. **275**(24): p. 18566-18573.
42. Durigova, M., et al., *Characterization of an ADAMTS-5-mediated cleavage site in aggrecan in OSM-stimulated bovine cartilage.* Osteoarthritis and Cartilage, 2008. **16**(10): p. 1245-1252.

43. Verma, P. and K. Dalal, *ADAMTS-4 and ADAMTS-5: key enzymes in osteoarthritis.* J Cell Biochem, 2011. **112**(12): p. 3507-14.
44. Koshy, P.J., et al., *The modulation of matrix metalloproteinase and ADAM gene expression in human chondrocytes by interleukin-1 and oncostatin M: a time-course study using real-time quantitative reverse transcription-polymerase chain reaction.* Arthritis Rheum, 2002. **46**(4): p. 961-7.
45. Glasson, S.S., et al., *Characterization of and osteoarthritis susceptibility in ADAMTS-4-knockout mice.* Arthritis Rheum, 2004. **50**(8): p. 2547-58.
46. Glasson, S.S., et al., *Deletion of active ADAMTS5 prevents cartilage degradation in a murine model of osteoarthritis.* Nature, 2005. **434**(7033): p. 644-8.
47. Cooke, M.E., et al., *Matrix degradation in osteoarthritis primes the superficial region of cartilage for mechanical damage.* Acta Biomaterialia, 2018. **78**: p. 320-328.
48. Williams, K.E. and D.R. Olsen, *Matrix metalloproteinase-1 cleavage site recognition and binding in full-length human type III collagen.* Matrix Biol, 2009. **28**(6): p. 373-9.
49. Jabłońska-Trypuć, A., M. Matejczyk, and S. Rosochacki, *Matrix metalloproteinases (MMPs), the main extracellular matrix (ECM) enzymes in collagen degradation, as a target for anticancer drugs.* J Enzyme Inhib Med Chem, 2016. **31**(sup1): p. 177-183.
50. Malemud, C.J., *Matrix metalloproteinases (MMPs) in health and disease: an overview.* Front Biosci, 2006. **11**: p. 1696-701.
51. Kaspiris, A., et al., *Subchondral cyst development and MMP-1 expression during progression of osteoarthritis: an immunohistochemical study.* Orthop Traumatol Surg Res, 2013. **99**(5): p. 523-9.
52. Van Doren, S.R., *Matrix metalloproteinase interactions with collagen and elastin.* Matrix biology : journal of the International Society for Matrix Biology, 2015. **44-46**: p. 224-231.
53. Hu, Q. and M. Ecker, *Overview of MMP-13 as a Promising Target for the Treatment of Osteoarthritis.* International journal of molecular sciences, 2021. **22**(4): p. 1742.
54. Yamamoto, K., et al., *MMP-13 is constitutively produced in human chondrocytes and co-endocytosed with ADAMTS-5 and TIMP-3 by the endocytic receptor LRP1.* Matrix Biology, 2016. **56**: p. 57-73.
55. Neuhold, L.A., et al., *Postnatal expression in hyaline cartilage of constitutively active human collagenase-3 (MMP-13) induces osteoarthritis in mice.* The Journal of clinical investigation, 2001. **107**(1): p. 35-44.
56. Wang, M., et al., *MMP13 is a critical target gene during the progression of osteoarthritis.* Arthritis Research & Therapy, 2013. **15**(1): p. R5.
57. Little, C.B., et al., *Matrix metalloproteinase 13-deficient mice are resistant to osteoarthritic cartilage erosion but not chondrocyte hypertrophy or osteophyte development.* Arthritis and rheumatism, 2009. **60**(12): p. 3723-3733.
58. Zeng, G.Q., et al., *High MMP-1, MMP-2, and MMP-9 protein levels in osteoarthritis.* Genet Mol Res, 2015. **14**(4): p. 14811-22.
59. Lin, P.M., C.T. Chen, and P.A. Torzilli, *Increased stromelysin-1 (MMP-3), proteoglycan degradation (3B3- and 7D4) and collagen damage in cyclically load-injured articular cartilage.* Osteoarthritis Cartilage, 2004. **12**(6): p. 485-96.
60. Woessner, J.F., Jr., *MMPs and TIMPs--an historical perspective.* Mol Biotechnol, 2002. **22**(1): p. 33-49.
61. Arpino, V., M. Brock, and S.E. Gill, *The role of TIMPs in regulation of extracellular matrix proteolysis.* Matrix Biology, 2015. **44-46**: p. 247-254.
62. Chevalier, X., et al., *Tissue inhibitor of metalloprotease-1 (TIMP-1) serum level may predict progression of hip osteoarthritis.* Osteoarthritis Cartilage, 2001. **9**(4): p. 300-7.
63. Nakamura, H., et al., *Aggrecanase-selective tissue inhibitor of metalloproteinase-3 (TIMP3) protects articular cartilage in a surgical mouse model of osteoarthritis.* Scientific Reports, 2020. **10**(1): p. 9288.

64. Yamamoto, K., et al., *Inhibition of Shedding of Low-Density Lipoprotein Receptor-Related Protein 1 Reverses Cartilage Matrix Degradation in Osteoarthritis.* Arthritis Rheumatol, 2017. **69**(6): p. 1246-1256.
65. Liu, Z., et al., *A novel rabbit model of early osteoarthritis exhibits gradual cartilage degeneration after medial collateral ligament transection outside the joint capsule.* Scientific Reports, 2016. **6**(1): p. 34423.
66. Ganz, R., et al., *The etiology of osteoarthritis of the hip: an integrated mechanical concept.* Clinical orthopaedics and related research, 2008. **466**(2): p. 264-272.
67. van Valburg, A.A., et al., *Joint distraction in treatment of osteoarthritis (II): effects on cartilage in a canine model.* Osteoarthritis Cartilage, 2000. **8**(1): p. 1-8.
68. Goh, E.L., et al., *The role of joint distraction in the treatment of knee osteoarthritis: a systematic review and quantitative analysis.* Orthopedic research and reviews, 2019. **11**: p. 79-92.
69. van Valburg, A.A., et al., *Joint distraction in treatment of osteoarthritis: a two-year follow-up of the ankle.* Osteoarthritis Cartilage, 1999. **7**(5): p. 474-9.
70. Sun, Y., et al., *Histological examination of collagen and proteoglycan changes in osteoarthritic menisci.* Open Rheumatol J, 2012. **6**: p. 24-32.
71. Silver, F.H., G. Bradica, and A. Tria, *Elastic energy storage in human articular cartilage: estimation of the elastic modulus for type II collagen and changes associated with osteoarthritis.* Matrix Biol, 2002. **21**(2): p. 129-37.
72. Fleming, B.C., et al., *Ligament Injury, Reconstruction and Osteoarthritis.* Current opinion in orthopaedics, 2005. **16**(5): p. 354-362.
73. Papalia, R., et al., *Meniscectomy as a risk factor for knee osteoarthritis: a systematic review.* Br Med Bull, 2011. **99**: p. 89-106.
74. Donell, S., *Subchondral bone remodelling in osteoarthritis.* EFORT open reviews, 2019. **4**(6): p. 221-229.
75. Goldring, M.B. and S.R. Goldring, *Articular cartilage and subchondral bone in the pathogenesis of osteoarthritis.* Ann N Y Acad Sci, 2010. **1192**: p. 230-7.
76. Khoshgoftar, M., P.A. Torzilli, and S.A. Maher, *Influence of the pericellular and extracellular matrix structural properties on chondrocyte mechanics.* Journal of orthopaedic research : official publication of the Orthopaedic Research Society, 2018. **36**(2): p. 721-729.
77. Wilusz, R.E., S. Zauscher, and F. Guilak, *Micromechanical mapping of early osteoarthritic changes in the pericellular matrix of human articular cartilage.* Osteoarthritis Cartilage, 2013. **21**(12): p. 1895-903.
78. Choi, J.B., et al., *Zonal changes in the three-dimensional morphology of the chondron under compression: the relationship among cellular, pericellular, and extracellular deformation in articular cartilage.* J Biomech, 2007. **40**(12): p. 2596-603.
79. Poole, C.A., et al., *Immunolocalization of type IX collagen in normal and spontaneously osteoarthritic canine tibial cartilage and isolated chondrons.* Osteoarthritis Cartilage, 1997. **5**(3): p. 191-204.
80. Poole, C.A., A. Matsuoka, and J.R. Schofield, *Chondrons from articular cartilage. III. Morphologic changes in the cellular microenvironment of chondrons isolated from osteoarthritic cartilage.* Arthritis Rheum, 1991. **34**(1): p. 22-35.
81. Lee, G.M., et al., *The incidence of enlarged chondrons in normal and osteoarthritic human cartilage and their relative matrix density.* Osteoarthritis Cartilage, 2000. **8**(1): p. 44-52.
82. Ross, J.M., A.F. Sherwin, and C.A. Poole, *In vitro culture of enzymatically isolated chondrons: a possible model for the initiation of osteoarthritis.* Journal of anatomy, 2006. **209**(6): p. 793-806.

83. Mrosek, E.H., et al., *Subchondral bone trauma causes cartilage matrix degeneration: an immunohistochemical analysis in a canine model.* Osteoarthritis Cartilage, 2006. **14**(2): p. 171-8.
84. Nguyen, A.M. and C.R. Jacobs, *Emerging role of primary cilia as mechanosensors in osteocytes.* Bone, 2013. **54**(2): p. 196-204.
85. Ruhlen, R. and K. Marberry, *The chondrocyte primary cilium.* Osteoarthritis and Cartilage, 2014. **22**(8): p. 1071-1076.
86. Phan, M.N., et al., *Functional characterization of TRPV4 as an osmotically sensitive ion channel in porcine articular chondrocytes.* Arthritis Rheum, 2009. **60**(10): p. 3028-37.
87. Tao, F., et al., *Primary cilia: Versatile regulator in cartilage development.* Cell Proliferation, 2020. **53**(3): p. e12765.
88. Chia, S.L., et al., *Fibroblast growth factor 2 is an intrinsic chondroprotective agent that suppresses ADAMTS-5 and delays cartilage degradation in murine osteoarthritis.* Arthritis Rheum, 2009. **60**(7): p. 2019-27.
89. Tang, J., et al., *Fibroblast Growth Factor Receptor 3 Inhibits Osteoarthritis Progression in the Knee Joints of Adult Mice.* Arthritis Rheumatol, 2016. **68**(10): p. 2432-43.
90. Yan, D., et al., *Fibroblast growth factor receptor 1 is principally responsible for fibroblast growth factor 2-induced catabolic activities in human articular chondrocytes.* Arthritis Res Ther, 2011. **13**(4): p. R130.
91. Xie, Y., et al., *Fibroblast growth factor signalling in osteoarthritis and cartilage repair.* Nature Reviews Rheumatology, 2020. **16**(10): p. 547-564.
92. Duchesne, L., et al., *Transport of fibroblast growth factor 2 in the pericellular matrix is controlled by the spatial distribution of its binding sites in heparan sulfate.* PLoS biology, 2012. **10**(7): p. e1001361-e1001361.
93. Blaney Davidson, E.N., et al., *TGF β-induced cartilage repair is maintained but fibrosis is blocked in the presence of Smad7.* Arthritis Research & Therapy, 2006. **8**(3): p. R65.
94. Tang, X., et al., *Connective tissue growth factor contributes to joint homeostasis and osteoarthritis severity by controlling the matrix sequestration and activation of latent TGFβ.* Annals of the Rheumatic Diseases, 2018. **77**(9): p. 1372-1380.
95. Shen, J., et al., *Deletion of the transforming growth factor β receptor type II gene in articular chondrocytes leads to a progressive osteoarthritis-like phenotype in mice.* Arthritis Rheum, 2013. **65**(12): p. 3107-19.
96. Serra, R., et al., *Expression of a truncated, kinase-defective TGF-beta type II receptor in mouse skeletal tissue promotes terminal chondrocyte differentiation and osteoarthritis.* J Cell Biol, 1997. **139**(2): p. 541-52.
97. Hata, A. and Y.-G. Chen, *TGF-β Signaling from Receptors to Smads.* Cold Spring Harbor perspectives in biology, 2016. **8**(9): p. a022061.
98. Li, T.-F., et al., *Aberrant hypertrophy in Smad3-deficient murine chondrocytes is rescued by restoring transforming growth factor beta-activated kinase 1/activating transcription factor 2 signaling: a potential clinical implication for osteoarthritis.* Arthritis and rheumatism, 2010. **62**(8): p. 2359-2369.
99. Ismail, H.M., et al., *Rapid Activation of Transforming Growth Factor β-Activated Kinase 1 in Chondrocytes by Phosphorylation and K(63) -Linked Polyubiquitination Upon Injury to Animal Articular Cartilage.* Arthritis & rheumatology (Hoboken, N.J.), 2017. **69**(3): p. 565-575.
100. Burleigh, A., et al., *Joint immobilization prevents murine osteoarthritis and reveals the highly mechanosensitive nature of protease expression in vivo.* Arthritis Rheum, 2012. **64**(7): p. 2278-88.
101. Loeser, R.F., et al., *Osteoarthritis: a disease of the joint as an organ.* Arthritis and rheumatism, 2012. **64**(6): p. 1697-1707.

102. Dell'Accio, F., et al., *Activation of WNT and BMP signaling in adult human articular cartilage following mechanical injury.* Arthritis Res Ther, 2006. **8**(5): p. R139.
103. Xu, Y.-R. and C.-Q. Lei, *TAK1-TABs Complex: A Central Signalosome in Inflammatory Responses.* Frontiers in Immunology, 2021. **11**.
104. Dai, L., et al., *TAK1, more than just innate immunity.* IUBMB Life, 2012. **64**(10): p. 825-834.
105. Sylvain-Prévost, S., et al., *Activation of TAK1 by Chemotactic and Growth Factors, and Its Impact on Human Neutrophil Signaling and Functional Responses.* J Immunol, 2015. **195**(11): p. 5393-403.
106. Hirata, Y., et al., *Post-Translational Modifications of the TAK1-TAB Complex.* International journal of molecular sciences, 2017. **18**(1): p. 205.
107. Shim, J.-H., et al., *TAK1 is an essential regulator of BMP signalling in cartilage.* The EMBO journal, 2009. **28**(14): p. 2028-2041.
108. Klatt, A.R., et al., *TAK1 downregulation reduces IL-1beta induced expression of MMP13, MMP1 and TNF-alpha.* Biomed Pharmacother, 2006. **60**(2): p. 55-61.
109. Cheng, J., et al., *Inhibition of transforming growth factor β-activated kinase 1 prevents inflammation-related cartilage degradation in osteoarthritis.* Scientific Reports, 2016. **6**(1): p. 34497.
110. Cargnello, M. and P.P. Roux, *Activation and function of the MAPKs and their substrates, the MAPK-activated protein kinases.* Microbiology and molecular biology reviews : MMBR, 2011. **75**(1): p. 50-83.
111. Cuenda, A., *Mitogen-Activated Protein Kinases (MAPK) in Cancer*, in *Encyclopedia of Cancer (Third Edition)*, P. Boffetta and P. Hainaut, Editors. 2019, Academic Press: Oxford. p. 472-480.
112. Sabio, G. and R.J. Davis, *TNF and MAP kinase signalling pathways.* Seminars in immunology, 2014. **26**(3): p. 237-245.
113. Wang, X., H. Wu, and A.H. Miller, *Interleukin 1alpha (IL-1alpha) induced activation of p38 mitogen-activated protein kinase inhibits glucocorticoid receptor function.* Mol Psychiatry, 2004. **9**(1): p. 65-75.
114. Kogkopoulou, O., et al., *Conditional up-regulation of IL-2 production by p38 MAPK inactivation is mediated by increased Erk1/2 activity.* J Leukoc Biol, 2006. **79**(5): p. 1052-60.
115. Nishikai-Yan Shen, T., et al., *Interleukin-6 stimulates Akt and p38 MAPK phosphorylation and fibroblast migration in non-diabetic but not diabetic mice.* PloS one, 2017. **12**(5): p. e0178232-e0178232.
116. Boileau, C., et al., *PD-0200347, an alpha2delta ligand of the voltage gated calcium channel, inhibits in vivo activation of the Erk1/2 pathway in osteoarthritic chondrocytes: a PKCalpha dependent effect.* Ann Rheum Dis, 2006. **65**(5): p. 573-80.
117. Starkman, B.G., et al., *IGF-I stimulation of proteoglycan synthesis by chondrocytes requires activation of the PI 3-kinase pathway but not ERK MAPK.* The Biochemical journal, 2005. **389**(Pt 3): p. 723-729.
118. Lin, A., *Activation of the JNK signaling pathway: breaking the brake on apoptosis.* Bioessays, 2003. **25**(1): p. 17-24.
119. Yang, P., et al., *Expression profile of cytokines and chemokines in osteoarthritis patients: Proinflammatory roles for CXCL8 and CXCL11 to chondrocytes.* Int Immunopharmacol, 2016. **40**: p. 16-23.
120. Deng, Y., et al., *Reciprocal inhibition of YAP/TAZ and NF-κB regulates osteoarthritic cartilage degradation.* Nature Communications, 2018. **9**(1): p. 4564.
121. Zhang, P., et al., *SP600125, a JNK-Specific Inhibitor, Regulates in vitro Auricular Cartilage Regeneration by Promoting Cell Proliferation and Inhibiting Extracellular Matrix Metabolism.* Front Cell Dev Biol, 2021. **9**: p. 630678.

122. Vincenti, M.P. and C.E. Brinckerhoff, *Transcriptional regulation of collagenase (MMP-1, MMP-13) genes in arthritis: integration of complex signaling pathways for the recruitment of gene-specific transcription factors.* Arthritis Research & Therapy, 2002. **4**(3): p. 157.
123. Ismail, H.M., et al., *Brief Report: JNK-2 Controls Aggrecan Degradation in Murine Articular Cartilage and the Development of Experimental Osteoarthritis.* Arthritis Rheumatol, 2016. **68**(5): p. 1165-71.
124. Dean, J.L., et al., *The involvement of AU-rich element-binding proteins in p38 mitogen-activated protein kinase pathway-mediated mRNA stabilisation.* Cell Signal, 2004. **16**(10): p. 1113-21.
125. Winzen, R., et al., *Distinct domains of AU-rich elements exert different functions in mRNA destabilization and stabilization by p38 mitogen-activated protein kinase or HuR.* Molecular and cellular biology, 2004. **24**(11): p. 4835-4847.
126. Sun, H.Y., K.Z. Hu, and Z.S. Yin, *Inhibition of the p38-MAPK signaling pathway suppresses the apoptosis and expression of proinflammatory cytokines in human osteoarthritis chondrocytes.* Cytokine, 2017. **90**: p. 135-143.
127. Brown, K.K., et al., *P38 MAP kinase inhibitors as potential therapeutics for the treatment of joint degeneration and pain associated with osteoarthritis.* Journal of inflammation (London, England), 2008. **5**: p. 22-22.
128. Zhang, H., et al., *Effects of Notch/p38MAPK signaling pathway on articular cartilage defect recovery by BMSCs tissue based on the rabbit articular cartilage defect models.* Saudi J Biol Sci, 2020. **27**(3): p. 859-864.
129. Wada, Y., et al., *Novel p38 mitogen-activated protein kinase inhibitor R-130823 protects cartilage by down-regulating matrix metalloproteinase-1,-13 and prostaglandin E2 production in human chondrocytes.* Int Immunopharmacol, 2006. **6**(2): p. 144-55.
130. Roux, P.P. and J. Blenis, *ERK and p38 MAPK-activated protein kinases: a family of protein kinases with diverse biological functions.* Microbiology and molecular biology reviews : MMBR, 2004. **68**(2): p. 320-344.
131. Pelletier, J.P., et al., *In vivo selective inhibition of mitogen-activated protein kinase kinase 1/2 in rabbit experimental osteoarthritis is associated with a reduction in the development of structural changes.* Arthritis Rheum, 2003. **48**(6): p. 1582-93.
132. Liu, T., et al., *NF-κB signaling in inflammation.* Signal Transduction and Targeted Therapy, 2017. **2**(1): p. 17023.
133. Oeckinghaus, A. and S. Ghosh, *The NF-kappaB family of transcription factors and its regulation.* Cold Spring Harbor perspectives in biology, 2009. **1**(4): p. a000034-a000034.
134. Roman-Blas, J.A. and S.A. Jimenez, *NF-κB as a potential therapeutic target in osteoarthritis and rheumatoid arthritis.* Osteoarthritis and Cartilage, 2006. **14**(9): p. 839-848.
135. Choi, M.-C., et al., *NF-κB Signaling Pathways in Osteoarthritic Cartilage Destruction.* Cells, 2019. **8**(7): p. 734.
136. Kobayashi, H., et al., *Biphasic regulation of chondrocytes by Rela through induction of anti-apoptotic and catabolic target genes.* Nature Communications, 2016. **7**(1): p. 13336.
137. Murahashi, Y., et al., *Intra-articular administration of IκBα kinase inhibitor suppresses mouse knee osteoarthritis via downregulation of the NF-κB/HIF-2α axis.* Scientific reports, 2018. **8**(1): p. 16475-16475.
138. Ryu, J.H., et al., *Hypoxia-inducible factor-2α regulates Fas-mediated chondrocyte apoptosis during osteoarthritic cartilage destruction.* Cell Death Differ, 2012. **19**(3): p. 440-50.
139. Wondimu, E.B., et al., *Elf3 Contributes to Cartilage Degradation in vivo in a Surgical Model of Post-Traumatic Osteoarthritis.* Scientific Reports, 2018. **8**(1): p. 6438.

140. Ding, F., et al., *Osteopontin stimulates matrix metalloproteinase expression through the nuclear factor-κB signaling pathway in rat temporomandibular joint and condylar chondrocytes.* American journal of translational research, 2017. **9**(2): p. 316-329.
141. Liu, Q., et al., *Osteopontin inhibits osteoarthritis progression via the OPN/CD44/PI3K signal axis.* Genes & Diseases, 2022. **9**(1): p. 128-139.
142. Conde, J., et al., *IL-36α: a novel cytokine involved in the catabolic and inflammatory response in chondrocytes.* Sci Rep, 2015. **5**: p. 16674.
143. Vincent, T.L., *Fibroblast growth factor 2: good or bad guy in the joint?* Arthritis Research & Therapy, 2011. **13**(5): p. 127.
144. Su, N., M. Jin, and L. Chen, *Role of FGF/FGFR signaling in skeletal development and homeostasis: learning from mouse models.* Bone Research, 2014. **2**(1): p. 14003.
145. Nummenmaa, E., et al., *Effects of FGF-2 and FGF receptor antagonists on MMP enzymes, aggrecan, and type II collagen in primary human OA chondrocytes.* Scand J Rheumatol, 2015. **44**(4): p. 321-30.
146. Ji, Q., et al., *miR-105/Runx2 axis mediates FGF2-induced ADAMTS expression in osteoarthritis cartilage.* J Mol Med (Berl), 2016. **94**(6): p. 681-94.
147. Zhu, L., et al., *TSG-6 Is Weakly Chondroprotective in Murine OA but Does not Account for FGF2-Mediated Joint Protection.* ACR Open Rheumatol, 2020. **2**(10): p. 605-615.
148. Li, X., et al., *Exogenous bFGF promotes articular cartilage repair via up-regulation of multiple growth factors.* Osteoarthritis and Cartilage, 2013. **21**(10): p. 1567-1575.
149. Davidson, D., et al., *Fibroblast growth factor (FGF) 18 signals through FGF receptor 3 to promote chondrogenesis.* J Biol Chem, 2005. **280**(21): p. 20509-15.
150. Johnson, A.N. and S.J. Newfeld, *The TGF-beta family: signaling pathways, developmental roles, and tumor suppressor activities.* ScientificWorldJournal, 2002. **2**: p. 892-925.
151. van der Kraan, P.M., et al., *Age-dependent alteration of TGF-β signalling in osteoarthritis.* Cell and tissue research, 2012. **347**(1): p. 257-265.
152. Wang, G., et al., *TGFβ attenuates cartilage extracellular matrix degradation via enhancing FBXO6-mediated MMP14 ubiquitination.* Annals of the Rheumatic Diseases, 2020. **79**(8): p. 1111-1120.
153. Tabeian, H., et al., *IL-1β Damages Fibrocartilage and Upregulates MMP-13 Expression in Fibrochondrocytes in the Condyle of the Temporomandibular Joint.* International journal of molecular sciences, 2019. **20**(9): p. 2260.
154. Clements, K.M., et al., *Gene deletion of either interleukin-1beta, interleukin-1beta-converting enzyme, inducible nitric oxide synthase, or stromelysin 1 accelerates the development of knee osteoarthritis in mice after surgical transection of the medial collateral ligament and partial medial meniscectomy.* Arthritis Rheum, 2003. **48**(12): p. 3452-63.
155. Fukai, A., et al., *Lack of a chondroprotective effect of cyclooxygenase 2 inhibition in a surgically induced model of osteoarthritis in mice.* Arthritis Rheum, 2012. **64**(1): p. 198-203.
156. Kloppenburg, M., et al., *Phase IIa, placebo-controlled, randomised study of lutikizumab, an anti-interleukin-1α and anti-interleukin-1β dual variable domain immunoglobulin, in patients with erosive hand osteoarthritis.* Ann Rheum Dis, 2019. **78**(3): p. 413-420.
157. Fleischmann, R.M., et al., *A Phase II Trial of Lutikizumab, an Anti-Interleukin-1α/β Dual Variable Domain Immunoglobulin, in Knee Osteoarthritis Patients With Synovitis.* Arthritis Rheumatol, 2019. **71**(7): p. 1056-1069.
158. Chevalier, X., et al., *Intraarticular injection of anakinra in osteoarthritis of the knee: a multicenter, randomized, double-blind, placebo-controlled study.* Arthritis Rheum, 2009. **61**(3): p. 344-52.

159. Tsuchida, A.I., et al., *Interleukin-6 is elevated in synovial fluid of patients with focal cartilage defects and stimulates cartilage matrix production in an in vitro regeneration model.* Arthritis Res Ther, 2012. **14**(6): p. R262.
160. Zanotti, S. and E. Canalis, *Interleukin 6 mediates selected effects of Notch in chondrocytes.* Osteoarthritis and cartilage, 2013. **21**(11): p. 1766-1773.
161. Sahu, N., H.J. Viljoen, and A. Subramanian, *Continuous low-intensity ultrasound attenuates IL-6 and TNFα-induced catabolic effects and repairs chondral fissures in bovine osteochondral explants.* BMC Musculoskeletal Disorders, 2019. **20**(1): p. 193.
162. Navarro-Millán, I. and J.R. Curtis, *Newest clinical trial results with antitumor necrosis factor and nonantitumor necrosis factor biologics for rheumatoid arthritis.* Current opinion in rheumatology, 2013. **25**(3): p. 384-390.
163. Aitken, D., et al., *A randomised double-blind placebo-controlled crossover trial of HUMira (adalimumab) for erosive hand OsteoaRthritis - the HUMOR trial.* Osteoarthritis Cartilage, 2018. **26**(7): p. 880-887.
164. Wang, J., *Efficacy and safety of adalimumab by intra-articular injection for moderate to severe knee osteoarthritis: An open-label randomized controlled trial.* J Int Med Res, 2018. **46**(1): p. 326-334.
165. Punzi, L., et al., *Inflammatory osteoarthritis of the hand.* Best Pract Res Clin Rheumatol, 2010. **24**(3): p. 301-12.
166. Haar, D., et al., *A double-blind comparative study of hydroxychloroquine and dapsone, alone and in combination, in rheumatoid arthritis.* Scand J Rheumatol, 1993. **22**(3): p. 113-8.
167. Clark, P., et al., *Hydroxychloroquine compared with placebo in rheumatoid arthritis. A randomized controlled trial.* Ann Intern Med, 1993. **119**(11): p. 1067-71.
168. Kingsbury, S.R., et al., *Hydroxychloroquine Effectiveness in Reducing Symptoms of Hand Osteoarthritis.* Annals of Internal Medicine, 2018. **168**(6): p. 385-395.
169. Yu, L.P., Jr., et al., *Reduction of the severity of canine osteoarthritis by prophylactic treatment with oral doxycycline.* Arthritis Rheum, 1992. **35**(10): p. 1150-9.
170. Smith, G.N., Jr., et al., *Oral administration of doxycycline reduces collagenase and gelatinase activities in extracts of human osteoarthritic cartilage.* J Rheumatol, 1998. **25**(3): p. 532-5.
171. Brandt, K.D., et al., *Effects of doxycycline on progression of osteoarthritis: results of a randomized, placebo-controlled, double-blind trial.* Arthritis Rheum, 2005. **52**(7): p. 2015-25.
172. Snijders, G.F., et al., *The effects of doxycycline on reducing symptoms in knee osteoarthritis: results from a triple-blinded randomised controlled trial.* Ann Rheum Dis, 2011. **70**(7): p. 1191-6.
173. Burt, P.M., et al., *Ablation of low-molecular-weight FGF2 isoform accelerates murine osteoarthritis while loss of high-molecular-weight FGF2 isoforms offers protection.* J Cell Physiol, 2019. **234**(4): p. 4418-4431.
174. Moore, E.E., et al., *Fibroblast growth factor-18 stimulates chondrogenesis and cartilage repair in a rat model of injury-induced osteoarthritis.* Osteoarthritis Cartilage, 2005. **13**(7): p. 623-31.
175. Mori, Y., et al., *Identification of fibroblast growth factor-18 as a molecule to protect adult articular cartilage by gene expression profiling.* The Journal of biological chemistry, 2014. **289**(14): p. 10192-10200.
176. Ladel, C.H., et al., *Tissue distribution of sprifermin (recombinant human fibroblast growth factor 18) in the rat following intravenous and intra-articular injection.* Osteoarthritis and Cartilage Open, 2020. **2**(3): p. 100068.

177. Hochberg, M.C., et al., *Effect of Intra-Articular Sprifermin vs Placebo on Femorotibial Joint Cartilage Thickness in Patients With Osteoarthritis: The FORWARD Randomized Clinical Trial.* Jama, 2019. **322**(14): p. 1360-1370.
178. Tuan, R.S., A.F. Chen, and B.A. Klatt, *Cartilage regeneration.* The Journal of the American Academy of Orthopaedic Surgeons, 2013. **21**(5): p. 303-311.
179. Hollander, A.P., S.C. Dickinson, and W. Kafienah, *Stem cells and cartilage development: complexities of a simple tissue.* Stem cells (Dayton, Ohio), 2010. **28**(11): p. 1992-1996.
180. Dowthwaite, G.P., et al., *The surface of articular cartilage contains a progenitor cell population.* J Cell Sci, 2004. **117**(Pt 6): p. 889-97.
181. Hattori, S., C. Oxford, and A.H. Reddi, *Identification of superficial zone articular chondrocyte stem/progenitor cells.* Biochem Biophys Res Commun, 2007. **358**(1): p. 99-103.
182. Xia, P., et al., *TGF-β1-induced chondrogenesis of bone marrow mesenchymal stem cells is promoted by low-intensity pulsed ultrasound through the integrin-mTOR signaling pathway.* Stem cell research & therapy, 2017. **8**(1): p. 281-281.
183. Ahn, J., et al., *AIMP1 downregulation restores chondrogenic characteristics of dedifferentiated/degenerated chondrocytes by enhancing TGF-β signal.* Cell Death & Disease, 2016. **7**(2): p. e2099-e2099.
184. Shen, J., S. Li, and D. Chen, *TGF-β signaling and the development of osteoarthritis.* Bone Research, 2014. **2**(1): p. 14002.
185. Toyoda, E., et al., *Candidates for Intra-Articular Administration Therapeutics and Therapies of Osteoarthritis.* International journal of molecular sciences, 2021. **22**(7): p. 3594.
186. Prodromos, C., et al., *Autologous Mesenchymal Stem Cell Treatment is Consistently Effective for the Treatment of Knee Osteoarthritis: The Results of a Systematic Review of Treatment and Comparison to a Placebo Group.* Medicines (Basel, Switzerland), 2020. **7**(8): p. 42.
187. Pers, Y.M., et al., *Adipose Mesenchymal Stromal Cell-Based Therapy for Severe Osteoarthritis of the Knee: A Phase I Dose-Escalation Trial.* Stem Cells Transl Med, 2016. **5**(7): p. 847-56.
188. Jiang, L., et al., *RNA Sequencing Reveals LINC00167 as a Potential Diagnosis Biomarker for Primary Osteoarthritis: A Multi-Stage Study.* Frontiers in genetics, 2021. **11**: p. 539489-539489.
189. Coutinho de Almeida, R., et al., *RNA sequencing data integration reveals an miRNA interactome of osteoarthritis cartilage.* Ann Rheum Dis, 2019. **78**(2): p. 270-277.
190. Sebastian, A., et al., *Single-Cell RNA-Seq Reveals Transcriptomic Heterogeneity and Post-Traumatic Osteoarthritis-Associated Early Molecular Changes in Mouse Articular Chondrocytes.* Cells, 2021. **10**(6): p. 1462.
191. Ji, Q., et al., *Single-cell RNA-seq analysis reveals the progression of human osteoarthritis.* Annals of the Rheumatic Diseases, 2019. **78**(1): p. 100.
192. Aki, T., et al., *A whole-genome transcriptome analysis of articular chondrocytes in secondary osteoarthritis of the hip.* PloS one, 2018. **13**(6): p. e0199734-e0199734.
193. Gao, X., et al., *KLF2 Protects against Osteoarthritis by Repressing Oxidative Response through Activation of Nrf2/ARE Signaling In Vitro and In Vivo.* Oxid Med Cell Longev, 2019. **2019**: p. 8564681.
194. Li, Z., et al., *Single-cell transcriptome analyses reveal novel targets modulating cardiac neovascularization by resident endothelial cells following myocardial infarction.* Eur Heart J, 2019. **40**(30): p. 2507-2520.
195. Uffelmann, E., et al., *Genome-wide association studies.* Nature Reviews Methods Primers, 2021. **1**(1): p. 59.

196. arc, O.C., et al., *Identification of new susceptibility loci for osteoarthritis (arcOGEN): a genome-wide association study.* Lancet (London, England), 2012. **380**(9844): p. 815-823.
197. Valdes, A.M., et al., *The GDF5 rs143383 polymorphism is associated with osteoarthritis of the knee with genome-wide statistical significance.* Ann Rheum Dis, 2011. **70**(5): p. 873-5.
198. Day-Williams, A.G., et al., *A variant in MCF2L is associated with osteoarthritis.* American journal of human genetics, 2011. **89**(3): p. 446-450.
199. Day-Williams, A.G., et al., *A variant in MCF2L is associated with osteoarthritis.* Am J Hum Genet, 2011. **89**(3): p. 446-50.
200. Styrkarsdottir, U., et al., *Severe osteoarthritis of the hand associates with common variants within the ALDH1A2 gene and with rare variants at 1p31.* Nat Genet, 2014. **46**(5): p. 498-502.
201. Shepherd, C., et al., *Functional Characterization of the Osteoarthritis Genetic Risk Residing at ALDH1A2 Identifies rs12915901 as a Key Target Variant.* Arthritis Rheumatol, 2018. **70**(10): p. 1577-1587.
202. Unguryte, A., et al., *Human articular chondrocytes with higher aldehyde dehydrogenase activity have stronger expression of COL2A1 and SOX9.* Osteoarthritis Cartilage, 2016. **24**(5): p. 873-82.
203. Steinberg, J., et al., *Widespread epigenomic, transcriptomic and proteomic differences between hip osteophytic and articular chondrocytes in osteoarthritis.* Rheumatology (Oxford), 2018. **57**(8): p. 1481-1489.
204. Gelse, K., et al., *Molecular differentiation between osteophytic and articular cartilage--clues for a transient and permanent chondrocyte phenotype.* Osteoarthritis Cartilage, 2012. **20**(2): p. 162-71.
205. Chu, M., et al., *The rs4238326 polymorphism in ALDH1A2 gene potentially associated with non-post traumatic knee osteoarthritis susceptibility: a two-stage population-based study.* Osteoarthritis Cartilage, 2017. **25**(7): p. 1062-1067.
206. Napoli, J.L., *Physiological insights into all-trans-retinoic acid biosynthesis.* Biochim Biophys Acta, 2012. **1821**(1): p. 152-67.
207. Molotkov, A., et al., *Stimulation of retinoic acid production and growth by ubiquitously expressed alcohol dehydrogenase Adh3.* Proceedings of the National Academy of Sciences of the United States of America, 2002. **99**(8): p. 5337-5342.
208. Xie, Y., et al., *A spectral-domain optical coherence tomographic analysis of Rdh5-/- mice retina.* PloS one, 2020. **15**(4): p. e0231220-e0231220.
209. Sandell, L.L., et al., *RDH10 is essential for synthesis of embryonic retinoic acid and is required for limb, craniofacial, and organ development.* Genes & development, 2007. **21**(9): p. 1113-1124.
210. Chrispell, J.D., et al., *Rdh12 activity and effects on retinoid processing in the murine retina.* The Journal of biological chemistry, 2009. **284**(32): p. 21468-21477.
211. Cunningham, T.J. and G. Duester, *Mechanisms of retinoic acid signalling and its roles in organ and limb development.* Nature reviews. Molecular cell biology, 2015. **16**(2): p. 110-123.
212. Niederreither, K., et al., *Embryonic retinoic acid synthesis is essential for early mouse post-implantation development.* Nat Genet, 1999. **21**(4): p. 444-8.
213. Chu, M., et al., *The rs4238326 polymorphism in ALDH1A2 gene potentially associated with non-post traumatic knee osteoarthritis susceptibility: a two-stage population-based study.* Osteoarthritis and Cartilage, 2017. **25**(7): p. 1062-1067.
214. Niederreither, K. and P. Dollé, *Retinoic acid in development: towards an integrated view.* Nature Reviews Genetics, 2008. **9**(7): p. 541-553.
215. Donovan, M., et al., *The cellular retinoic acid binding proteins.* J Steroid Biochem Mol Biol, 1995. **53**(1-6): p. 459-65.

216. Cai, A.Q., et al., *Cellular retinoic acid-binding proteins are essential for hindbrain patterning and signal robustness in zebrafish.* Development (Cambridge, England), 2012. **139**(12): p. 2150-2155.
217. Napoli, J.L., *Cellular retinoid binding-proteins, CRBP, CRABP, FABP5: Effects on retinoid metabolism, function and related diseases.* Pharmacol Ther, 2017. **173**: p. 19-33.
218. Ghyselinck, N.B. and G. Duester, *Retinoic acid signaling pathways.* Development, 2019. **146**(13).
219. Zhang, R., et al., *Transcriptional Factors Mediating Retinoic Acid Signals in the Control of Energy Metabolism.* International journal of molecular sciences, 2015. **16**(6): p. 14210-14244.
220. Chandra, V., et al., *Structure of the intact PPAR-gamma-RXR- nuclear receptor complex on DNA.* Nature, 2008. **456**(7220): p. 350-356.
221. So, E.N. and D.L. Crowe, *Characterization of a retinoic acid responsive element in the human ets-1 promoter.* IUBMB Life, 2000. **50**(6): p. 365-70.
222. Delacroix, L., et al., *Cell-Specific Interaction of Retinoic Acid Receptors with Target Genes in Mouse Embryonic Fibroblasts and Embryonic Stem Cells.* Molecular and Cellular Biology, 2010. **30**(1): p. 231.
223. Savory, J.G.A., et al., *Identification of novel retinoic acid target genes.* Developmental Biology, 2014. **395**(2): p. 199-208.
224. Zhu, L., et al., *Cartilage injury regulates inflammatory gene expression in part by suppressing cellular retinoic acid signaling.* Osteoarthritis and Cartilage, 2017. **25**: p. S168.
225. Balmer, J.E. and R. Blomhoff, *Gene expression regulation by retinoic acid.* J Lipid Res, 2002. **43**(11): p. 1773-808.
226. Balmer, J.E. and R. Blomhoff, *A robust characterization of retinoic acid response elements based on a comparison of sites in three species.* J Steroid Biochem Mol Biol, 2005. **96**(5): p. 347-54.
227. Ross-Innes, C.S., et al., *Cooperative interaction between retinoic acid receptor-alpha and estrogen receptor in breast cancer.* Genes Dev, 2010. **24**(2): p. 171-82.
228. Sun, G., W. Porter, and S. Safe, *Estrogen-Induced Retinoic Acid Receptor α1 Gene Expression: Role of Estrogen Receptor-Sp1 Complex.* Molecular Endocrinology, 1998. **12**(6): p. 882-890.
229. Stoll, B.A., *Linkage between retinoid and fatty acid receptors: implications for breast cancer prevention.* Eur J Cancer Prev, 2002. **11**(4): p. 319-25.
230. Watt, F.E., *Hand osteoarthritis, menopause and menopausal hormone therapy.* Maturitas, 2016. **83**: p. 13-8.
231. Marcantonio, P., et al., *Synergic effect of retinoic acid and extremely low frequency magnetic field exposure on human neuroblastoma cell line BE(2)C.* Bioelectromagnetics, 2010. **31**(6): p. 425-33.
232. Thatcher, J.E. and N. Isoherranen, *The role of CYP26 enzymes in retinoic acid clearance.* Expert opinion on drug metabolism & toxicology, 2009. **5**(8): p. 875-886.
233. White, J.A., et al., *Identification of the retinoic acid-inducible all-trans-retinoic acid 4-hydroxylase.* J Biol Chem, 1996. **271**(47): p. 29922-7.
234. Fujii, H., et al., *Metabolic inactivation of retinoic acid by a novel P450 differentially expressed in developing mouse embryos.* The EMBO journal, 1997. **16**(14): p. 4163-4173.
235. Ray, W.J., et al., *CYP26, a novel mammalian cytochrome P450, is induced by retinoic acid and defines a new family.* J Biol Chem, 1997. **272**(30): p. 18702-8.
236. Niederreither, K., et al., *Genetic evidence that oxidative derivatives of retinoic acid are not involved in retinoid signaling during mouse development.* Nature Genetics, 2002. **31**(1): p. 84-88.
237. Krivospitskaya, O., et al., *A CYP26B1 polymorphism enhances retinoic acid catabolism and may aggravate atherosclerosis.* Mol Med, 2012. **18**: p. 712-8.

238. Taimi, M., et al., *A novel human cytochrome P450, CYP26C1, involved in metabolism of 9-cis and all-trans isomers of retinoic acid.* J Biol Chem, 2004. **279**(1): p. 77-85.
239. Topletz, A.R., et al., *Comparison of the function and expression of CYP26A1 and CYP26B1, the two retinoic acid hydroxylases.* Biochem Pharmacol, 2012. **83**(1): p. 149-63.
240. Thatcher, J.E., A. Zelter, and N. Isoherranen, *The relative importance of CYP26A1 in hepatic clearance of all-trans retinoic acid.* Biochem Pharmacol, 2010. **80**(6): p. 903-12.
241. Shirakami, Y., et al., *Hepatic metabolism of retinoids and disease associations.* Biochimica et biophysica acta, 2012. **1821**(1): p. 124-136.
242. Nelson, C.H., B.R. Buttrick, and N. Isoherranen, *Therapeutic potential of the inhibition of the retinoic acid hydroxylases CYP26A1 and CYP26B1 by xenobiotics.* Current topics in medicinal chemistry, 2013. **13**(12): p. 1402-1428.
243. Dersch, H. and M.H. Zile, *Induction of normal cardiovascular development in the vitamin A-deprived quail embryo by natural retinoids.* Dev Biol, 1993. **160**(2): p. 424-33.
244. Dickman, E.D., C. Thaller, and S.M. Smith, *Temporally-regulated retinoic acid depletion produces specific neural crest, ocular and nervous system defects.* Development, 1997. **124**(16): p. 3111-21.
245. Lohnes, D., et al., *Function of the retinoic acid receptors (RARs) during development (I). Craniofacial and skeletal abnormalities in RAR double mutants.* Development, 1994. **120**(10): p. 2723-48.
246. Williams, J.A., et al., *Retinoic acid receptors are required for skeletal growth, matrix homeostasis and growth plate function in postnatal mouse.* Dev Biol, 2009. **328**(2): p. 315-27.
247. De Luca, F., et al., *Retinoic Acid is a Potent Regulator of Linear Growth • 413.* Pediatric Research, 1998. **43**(4): p. 73-73.
248. Mic, F.A., I.O. Sirbu, and G. Duester, *Retinoic acid synthesis controlled by Raldh2 is required early for limb bud initiation and then later as a proximodistal signal during apical ectodermal ridge formation.* J Biol Chem, 2004. **279**(25): p. 26698-706.
249. Mercader, N., et al., *Opposing RA and FGF signals control proximodistal vertebrate limb development through regulation of Meis genes.* Development, 2000. **127**(18): p. 3961-70.
250. Yashiro, K., et al., *Regulation of retinoic acid distribution is required for proximodistal patterning and outgrowth of the developing mouse limb.* Dev Cell, 2004. **6**(3): p. 411-22.
251. Helms, J.A., et al., *Retinoic acid signaling is required during early chick limb development.* Development, 1996. **122**(5): p. 1385-94.
252. Stratford, T., C. Horton, and M. Maden, *Retinoic acid is required for the initiation of outgrowth in the chick limb bud.* Curr Biol, 1996. **6**(9): p. 1124-33.
253. Niederreither, K., et al., *Embryonic retinoic acid synthesis is required for forelimb growth and anteroposterior patterning in the mouse.* Development, 2002. **129**(15): p. 3563-74.
254. McEwan, J., J. Lynch, and C.W. Beck, *Expression of key retinoic acid modulating genes suggests active regulation during development and regeneration of the amphibian limb.* Dev Dyn, 2011. **240**(5): p. 1259-70.
255. Cunningham, T.J., et al., *Rdh10 mutants deficient in limb field retinoic acid signaling exhibit normal limb patterning but display interdigital webbing.* Developmental dynamics : an official publication of the American Association of Anatomists, 2011. **240**(5): p. 1142-1150.
256. Kudoh, T., S.W. Wilson, and I.B. Dawid, *Distinct roles for Fgf, Wnt and retinoic acid in posteriorizing the neural ectoderm.* Development, 2002. **129**(18): p. 4335-4346.
257. White, R.J. and T.F. Schilling, *How degrading: Cyp26s in hindbrain development.* Dev Dyn, 2008. **237**(10): p. 2775-90.
258. Zhao, X., et al., *Retinoic acid controls expression of tissue remodeling genes Hmgn1 and Fgf18 at the digit-interdigit junction.* Developmental dynamics : an official publication of the American Association of Anatomists, 2010. **239**(2): p. 665-671.

259. Williams, J.A., et al., *Retinoic acid receptors are required for skeletal growth, matrix homeostasis and growth plate function in postnatal mouse.* Developmental biology, 2009. **328**(2): p. 315-327.
260. Rossant, J., et al., *Expression of a retinoic acid response element-hsplacZ transgene defines specific domains of transcriptional activity during mouse embryogenesis.* Genes Dev, 1991. **5**(8): p. 1333-44.
261. Eichele, G. and C. Thaller, *Characterization of concentration gradients of a morphogenetically active retinoid in the chick limb bud.* J Cell Biol, 1987. **105**(4): p. 1917-23.
262. Buttle, D.J., et al., *Inhibition of cartilage proteoglycan release by a specific inactivator of cathepsin B and an inhibitor of matrix metalloproteinases. Evidence for two converging pathways of chondrocyte-mediated proteoglycan degradation.* Arthritis Rheum, 1993. **36**(12): p. 1709-17.
263. Morales, T.I. and A.B. Roberts, *The interaction between retinoic acid and the transforming growth factors-beta in calf articular cartilage organ cultures.* Arch Biochem Biophys, 1992. **293**(1): p. 79-84.
264. Dietz, U., et al., *Alterations of collagen mRNA expression during retinoic acid induced chondrocyte modulation: absence of untranslated alpha 1(I) mRNA in hyaline chondrocytes.* J Cell Biochem, 1993. **52**(1): p. 57-68.
265. Yasui, N., P.D. Benya, and M.E. Nimni, *Coordinate regulation of type IX and type II collagen synthesis during growth of chick chondrocytes in retinoic acid or 5-bromo-2'-deoxyuridine.* J Biol Chem, 1986. **261**(17): p. 7997-8001.
266. Davies, M.R., et al., *Ligands for retinoic acid receptors are elevated in osteoarthritis and may contribute to pathologic processes in the osteoarthritic joint.* Arthritis Rheum, 2009. **60**(6): p. 1722-32.
267. Shingleton, W.D., et al., *Retinoic acid and oncostatin M combine to promote cartilage degradation via matrix metalloproteinase-13 expression in bovine but not human chondrocytes.* Rheumatology (Oxford), 2006. **45**(8): p. 958-65.
268. Flannery, C.R., et al., *Effects of culture conditions and exposure to catabolic stimulators (IL-1 and retinoic acid) on the expression of matrix metalloproteinases (MMPs) and disintegrin metalloproteinases (ADAMs) by articular cartilage chondrocytes.* Matrix Biol, 1999. **18**(3): p. 225-37.
269. Sztrolovics, R., et al., *The mechanism of aggrecan release from cartilage differs with tissue origin and the agent used to stimulate catabolism.* Biochem J, 2002. **362**(Pt 2): p. 465-72.
270. Lay, E., et al., *Short- and long-term exposure of articular cartilage to curcumin or quercetin inhibits aggrecan loss.* The Journal of Nutritional Biochemistry, 2012. **23**(2): p. 106-112.
271. Freyria, A.M., et al., *Effect of retinoic acid on protein synthesis by foetal bovine chondrocytes in high-density culture: down-regulation of the glucose-regulated protein, GRP-78, and type II collagen.* The Biochemical journal, 1995. **305 (Pt 2)**: p. 391-396.
272. Napoli, J.L., *Quantification of physiological levels of retinoic acid.* Methods Enzymol, 1986. **123**: p. 112-24.
273. Zeng, X., et al., *[Prophylactic administration of all-trans retinoic acid alleviates inflammation in rats with collagen-induced arthritis].* Nan Fang Yi Ke Da Xue Xue Bao, 2016. **37**(2): p. 172-177.
274. Nozaki, Y., et al., *Anti-inflammatory effect of all-trans-retinoic acid in inflammatory arthritis.* Clin Immunol, 2006. **119**(3): p. 272-9.
275. Watanabe, H., et al., *A synthetic retinoic acid receptor agonist Am80 ameliorates renal fibrosis via inducing the production of alpha-1-acid glycoprotein.* Scientific reports, 2020. **10**(1): p. 11424-11424.

276. Sies, H. and D.P. Jones, *Reactive oxygen species (ROS) as pleiotropic physiological signalling agents.* Nature Reviews Molecular Cell Biology, 2020. **21**(7): p. 363-383.
277. Zorov, D.B., M. Juhaszova, and S.J. Sollott, *Mitochondrial reactive oxygen species (ROS) and ROS-induced ROS release.* Physiological reviews, 2014. **94**(3): p. 909-950.
278. Panday, A., et al., *NADPH oxidases: an overview from structure to innate immunity-associated pathologies.* Cellular & Molecular Immunology, 2015. **12**(1): p. 5-23.
279. He, L., et al., *Antioxidants Maintain Cellular Redox Homeostasis by Elimination of Reactive Oxygen Species.* Cellular Physiology and Biochemistry, 2017. **44**(2): p. 532-553.
280. Saini, R., *Coenzyme Q10: The essential nutrient.* Journal of pharmacy & bioallied sciences, 2011. **3**(3): p. 466-467.
281. Zhitkovich, A., *N-Acetylcysteine: Antioxidant, Aldehyde Scavenger, and More.* Chemical Research in Toxicology, 2019. **32**(7): p. 1318-1319.
282. Walayat, S., et al., *Role of N-acetylcysteine in non-acetaminophen-related acute liver failure: an updated meta-analysis and systematic review.* Annals of gastroenterology, 2021. **34**(2): p. 235-240.
283. Fukai, T. and M. Ushio-Fukai, *Superoxide dismutases: role in redox signaling, vascular function, and diseases.* Antioxidants & redox signaling, 2011. **15**(6): p. 1583-1606.
284. Sha, Y. and H.E. Marshall, *S-nitrosylation in the regulation of gene transcription.* Biochimica et biophysica acta, 2012. **1820**(6): p. 701-711.
285. Zahan, O.-M., et al., *The evaluation of oxidative stress in osteoarthritis.* Medicine and pharmacy reports, 2020. **93**(1): p. 12-22.
286. Setti, T., et al., *The protective role of glutathione in osteoarthritis.* Journal of clinical orthopaedics and trauma, 2020. **15**: p. 145-151.
287. Scott, J.L., et al., *Superoxide dismutase downregulation in osteoarthritis progression and end-stage disease.* Annals of the rheumatic diseases, 2010. **69**(8): p. 1502-1510.
288. Lepetsos, P. and A.G. Papavassiliou, *ROS/oxidative stress signaling in osteoarthritis.* Biochimica et Biophysica Acta (BBA) - Molecular Basis of Disease, 2016. **1862**(4): p. 576-591.
289. Ahmad, N., M.Y. Ansari, and T.M. Haqqi, *Role of iNOS in osteoarthritis: Pathological and therapeutic aspects.* Journal of cellular physiology, 2020. **235**(10): p. 6366-6376.
290. Blanco, F.J., M.J. López-Armada, and E. Maneiro, *Mitochondrial dysfunction in osteoarthritis.* Mitochondrion, 2004. **4**(5-6): p. 715-28.
291. Cillero-Pastor, B., et al., *Dimethylarginine dimethylaminohydrolase 2, a newly identified mitochondrial protein modulating nitric oxide synthesis in normal human chondrocytes.* Arthritis Rheum, 2012. **64**(1): p. 204-12.
292. Mao, X., et al., *Mitochondria: Potential Targets for Osteoarthritis.* Frontiers in medicine, 2020. **7**: p. 581402-581402.
293. Farnaghi, S., et al., *Protective effects of mitochondria-targeted antioxidants and statins on cholesterol-induced osteoarthritis.* Faseb j, 2017. **31**(1): p. 356-367.
294. Cao, M., et al., *Nitric oxide inhibits the synthesis of type-II collagen without altering Col2A1 mRNA abundance: prolyl hydroxylase as a possible target.* Biochem J, 1997. **324 (Pt 1)**(Pt 1): p. 305-10.
295. Wong, A.D.-S., S.: Gasic-Milenkovic, J.: Schinzel, R.: Wiesinger, H.: Riederer, P.: Munch, G., *Anti-inflammatory antioxidants attenuate the expression of inducible nitric oxide synthase mediated by advanced glycation endproducts in murine microglia.* Eur J Neurosci, 2001. **14**(12): p. 1961-7.
296. Martel-Pelletier, J., et al., *Mitogen-activated protein kinase and nuclear factor kappaB together regulate interleukin-17-induced nitric oxide production in human osteoarthritic chondrocytes: possible role of transactivating factor mitogen-activated protein kinase-activated proten kinase (MAPKAPK).* Arthritis Rheum, 1999. **42**(11): p. 2399-409.

297. Lo, Y.Y., J.M. Wong, and T.F. Cruz, *Reactive oxygen species mediate cytokine activation of c-Jun NH2-terminal kinases.* J Biol Chem, 1996. **271**(26): p. 15703-7.
298. Lo, Y.Y.C. and T.F. Cruz, *Involvement of Reactive Oxygen Species in Cytokine and Growth Factor Induction of c-fos Expression in Chondrocytes*.* Journal of Biological Chemistry, 1995. **270**(20): p. 11727-11730.
299. Aikawa, R., et al., *Reactive oxygen species in mechanical stress-induced cardiac hypertrophy.* Biochem Biophys Res Commun, 2001. **289**(4): p. 901-7.
300. Wolff, K.J., et al., *Mechanical stress and ATP synthesis are coupled by mitochondrial oxidants in articular cartilage.* J Orthop Res, 2013. **31**(2): p. 191-6.
301. Huie, R.E. and S. Padmaja, *The reaction of no with superoxide.* Free Radic Res Commun, 1993. **18**(4): p. 195-9.
302. Ma, Y., et al., *Knockdown of peroxiredoxin 5 inhibits the growth of osteoarthritic chondrocytes via upregulating Wnt/²-catenin signaling.* Free radical biology & medicine, 2014. **76**: p. 251-60.
303. Cai, D., et al., *Histone deacetylase inhibition activates Nrf2 and protects against osteoarthritis.* Arthritis Research & Therapy, 2015. **17**(1): p. 269.
304. Uozumi, N., Y. Kita, and T. Shimizu, *Modulation of lipid and protein mediators of inflammation by cytosolic phospholipase A2alpha during experimental sepsis.* J Immunol, 2008. **181**(5): p. 3558-66.
305. Moens, U., S. Kostenko, and B. Sveinbjørnsson, *The Role of Mitogen-Activated Protein Kinase-Activated Protein Kinases (MAPKAPKs) in Inflammation.* Genes, 2013. **4**(2): p. 101-133.
306. Su, H., et al., *Activation of Raf/MEK/ERK/cPLA2 signaling pathway is essential for chlamydial acquisition of host glycerophospholipids.* J Biol Chem, 2004. **279**(10): p. 9409-16.
307. Pavicevic, Z., C.C. Leslie, and K.U. Malik, *cPLA2 phosphorylation at serine-515 and serine-505 is required for arachidonic acid release in vascular smooth muscle cells.* J Lipid Res, 2008. **49**(4): p. 724-37.
308. Lee, C.W., et al., *Activation and induction of cytosolic phospholipase A2 by TNF-α mediated through Nox2, MAPKs, NF-κB, and p300 in human tracheal smooth muscle cells.* J Cell Physiol, 2011. **226**(8): p. 2103-14.
309. Petry, C., et al., *Hypoxia Increases Group IIA Phospholipase A₂ Expression under Inflammatory Conditions in Rat Renal Mesangial Cells.* Journal of the American Society of Nephrology, 2005. **16**(10): p. 2897.
310. Leslie, C.C., *Cytosolic phospholipase A2: physiological function and role in disease.* Journal of Lipid Research, 2015. **56**(8): p. 1386-1402.
311. Wang, B., et al., *Metabolism pathways of arachidonic acids: mechanisms and potential therapeutic targets.* Signal Transduction and Targeted Therapy, 2021. **6**(1): p. 94.
312. Lane, N.E., *Pain management in osteoarthritis: the role of COX-2 inhibitors.* J Rheumatol Suppl, 1997. **49**: p. 20-4.
313. Henderson, W.R., Jr., *The role of leukotrienes in inflammation.* Ann Intern Med, 1994. **121**(9): p. 684-97.
314. Jo-Watanabe, A., T. Okuno, and T. Yokomizo, *The Role of Leukotrienes as Potential Therapeutic Targets in Allergic Disorders.* International journal of molecular sciences, 2019. **20**(14): p. 3580.
315. Shi, Q., et al., *Alterations of metabolic activity in human osteoarthritic osteoblasts by lipid peroxidation end product 4-hydroxynonenal.* Arthritis research & therapy, 2006. **8**(6): p. R159-R159.
316. Morquette, B., et al., *Production of lipid peroxidation products in osteoarthritic tissues: new evidence linking 4-hydroxynonenal to cartilage degradation.* Arthritis Rheum, 2006. **54**(1): p. 271-81.

317. Schrimpe-Rutledge, A.C., K.Y. Fong, and D.W. Wright, *Impact of 4-hydroxynonenal on matrix metalloproteinase-9 regulation in lipopolysaccharide-stimulated RAW 264.7 cells.* Cell Biochem Funct, 2015. **33**(2): p. 59-66.
318. Lee, S.J., et al., *4-Hydroxynonenal enhances MMP-9 production in murine macrophages via 5-lipoxygenase-mediated activation of ERK and p38 MAPK.* Toxicol Appl Pharmacol, 2010. **242**(2): p. 191-8.
319. Vaillancourt, F., et al., *Differential regulation of cyclooxygenase-2 and inducible nitric oxide synthase by 4-hydroxynonenal in human osteoarthritic chondrocytes through ATF-2/CREB-1 transactivation and concomitant inhibition of NF-kappaB signaling cascade.* J Cell Biochem, 2007. **100**(5): p. 1217-31.
320. Blanco, F.J., et al., *Chondrocyte apoptosis induced by nitric oxide.* Am J Pathol, 1995. **146**(1): p. 75-85.
321. Brazil, D.P. and B.A. Hemmings, *Ten years of protein kinase B signalling: a hard Akt to follow.* Trends Biochem Sci, 2001. **26**(11): p. 657-64.
322. Abusarah, J., et al., *An overview of the role of lipid peroxidation-derived 4-hydroxynonenal in osteoarthritis.* Inflammation Research, 2017. **66**(8): p. 637-651.
323. El-Bikai, R., et al., *Perturbation of adhesion molecule-mediated chondrocyte-matrix interactions by 4-hydroxynonenal binding: implication in osteoarthritis pathogenesis.* Arthritis research & therapy, 2010. **12**(5): p. R201-R201.
324. Lee, S.A., O.V. Belyaeva, and N.Y. Kedishvili, *Effect of lipid peroxidation products on the activity of human retinol dehydrogenase 12 (RDH12) and retinoid metabolism.* Biochim Biophys Acta, 2008. **1782**(6): p. 421-5.
325. Singh, S., et al., *Aldehyde dehydrogenases in cellular responses to oxidative/electrophilic stress.* Free radical biology & medicine, 2013. **56**: p. 89-101.
326. Duester, G., *Families of retinoid dehydrogenases regulating vitamin A function: production of visual pigment and retinoic acid.* Eur J Biochem, 2000. **267**(14): p. 4315-24.
327. Gruber, J., et al., *Induction of interleukin-1 in articular cartilage by explantation and cutting.* Arthritis Rheum, 2004. **50**(8): p. 2539-46.
328. Watt, F.E., et al., *Src and fibroblast growth factor 2 independently regulate signaling and gene expression induced by experimental injury to intact articular cartilage.* Arthritis Rheum, 2013. **65**(2): p. 397-407.
329. Brandt, K.D., P. Dieppe, and E.L. Radin, *Commentary: Is It Useful to Subset "Primary" Osteoarthritis? A Critique Based on Evidence Regarding the Etiopathogenesis of Osteoarthritis.* Seminars in Arthritis and Rheumatism, 2009. **39**(2): p. 81-95.
330. Vincent, T.L. and A.K.T. Wann, *Mechanoadaptation: articular cartilage through thick and thin.* J Physiol, 2019. **597**(5): p. 1271-1281.
331. Levi, L., et al., *Saturated fatty acids regulate retinoic acid signalling and suppress tumorigenesis by targeting fatty acid-binding protein 5.* Nature Communications, 2015. **6**(1): p. 8794.
332. Huynh, C.K., A.M.H. Brodie, and V.C.O. Njar, *Inhibitory effects of retinoic acid metabolism blocking agents (RAMBAs) on the growth of human prostate cancer cells and LNCaP prostate tumour xenografts in SCID mice.* British journal of cancer, 2006. **94**(4): p. 513-523.
333. Bilip, M., et al., *Liposomal delivery of hydrophobic RAMBAs provides good bioavailability and significant enhancement of retinoic acid signalling in neuroblastoma tumour cells.* Journal of Drug Targeting, 2020. **28**(6): p. 643-654.
334. Geria, A.N. and N.S. Scheinfeld, *Talarozole, a selective inhibitor of P450-mediated all-trans retinoic acid for the treatment of psoriasis and acne.* Curr Opin Investig Drugs, 2008. **9**(11): p. 1228-37.
335. Tashtoush, B.M., E.L. Jacobson, and M.K. Jacobson, *UVA is the major contributor to the photodegradation of tretinoin and isotretinoin: Implications for development of improved*

pharmaceutical formulations. International journal of pharmaceutics, 2008. **352**(1-2): p. 123-128.
336. Zolfaghari, R., et al., *CYP26A1 gene promoter is a useful tool for reporting RAR-mediated retinoid activity.* Analytical biochemistry, 2019. **577**: p. 98-109.
337. Takeuchi, H., et al., *Cyp26b1 regulates retinoic acid-dependent signals in T cells and its expression is inhibited by transforming growth factor-β.* PloS one, 2011. **6**(1): p. e16089-e16089.
338. Hauksdottir, H., B. Farboud, and M.L. Privalsky, *Retinoic Acid Receptors β and γ Do Not Repress, But Instead Activate Target Gene Transcription in Both the Absence and Presence of Hormone Ligand.* Molecular Endocrinology, 2003. **17**(3): p. 373-385.
339. Marill, J., et al., *Retinoic acid metabolism and mechanism of action: a review.* Curr Drug Metab, 2003. **4**(1): p. 1-10.
340. Fu, P.P., et al., *Photodecomposition of Vitamin A and Photobiological Implications for the Skin†.* Photochemistry and Photobiology, 2007. **83**(2): p. 409-424.
341. Ihara, H., et al., *Esterification makes retinol more labile to photolysis.* J Nutr Sci Vitaminol (Tokyo), 1999. **45**(3): p. 353-8.
342. Sieber, S., et al., *Importance of Osmolarity and Oxygen Tension for Cartilage Tissue Engineering.* BioResearch Open Access, 2020. **9**(1): p. 106-115.
343. Ioele, G., et al., *Accelerated photostability study of tretinoin and isotretinoin in liposome formulations.* Int J Pharm, 2005. **293**(1-2): p. 251-60.
344. Edge, R. and T.G. Truscott, *Singlet Oxygen and Free Radical Reactions of Retinoids and Carotenoids-A Review.* Antioxidants (Basel, Switzerland), 2018. **7**(1): p. 5.
345. Conte da Frota, M.L., Jr., et al., *All-trans retinoic acid induces free radical generation and modulate antioxidant enzyme activities in rat sertoli cells.* Mol Cell Biochem, 2006. **285**(1-2): p. 173-9.
346. Lim, J.W., H. Kim, and K.H. Kim, *Nuclear factor-kappaB regulates cyclooxygenase-2 expression and cell proliferation in human gastric cancer cells.* Lab Invest, 2001. **81**(3): p. 349-60.
347. Lokau, J., et al., *Jak-Stat Signaling Induced by Interleukin-6 Family Cytokines in Hepatocellular Carcinoma.* Cancers, 2019. **11**(11): p. 1704.
348. Gupta, R., et al., *There is an Association of Synovial Interleukin-6 Levels With Chondral Damage in Anterior Cruciate Ligament–Deficient Knees.* HSS Journal®, 2021. **17**(2): p. 145-149.
349. Doss, F., et al., *Elevated IL-6 levels in the synovial fluid of osteoarthritis patients stem from plasma cells.* Scand J Rheumatol, 2007. **36**(2): p. 136-9.
350. Murphy, G. and M.H. Lee, *What are the roles of metalloproteinases in cartilage and bone damage?* Annals of the Rheumatic Diseases, 2005. **64**(suppl 4): p. iv44.
351. Li, W., et al., *Increased serum ADAMTS-4 in knee osteoarthritis: a potential indicator for the diagnosis of osteoarthritis in early stages.* Genet Mol Res, 2014. **13**(4): p. 9642-9.
352. Powell, A.J., C.B. Little, and C.E. Hughes, *Low molecular weight isoforms of the aggrecanases are responsible for the cytokine-induced proteolysis of aggrecan in a porcine chondrocyte culture system.* Arthritis Rheum, 2007. **56**(9): p. 3010-9.
353. Tortorella, M.D., et al., *The role of ADAM-TS4 (aggrecanase-1) and ADAM-TS5 (aggrecanase-2) in a model of cartilage degradation.* Osteoarthritis Cartilage, 2001. **9**(6): p. 539-52.
354. Kihara, S., et al., *Cyclin-Dependent Kinase Inhibitor-1-Deficient Mice are Susceptible to Osteoarthritis Associated with Enhanced Inflammation.* J Bone Miner Res, 2017. **32**(5): p. 991-1001.
355. Kreis, N.-N., F. Louwen, and J. Yuan, *The Multifaceted p21 (Cip1/Waf1/CDKN1A) in Cell Differentiation, Migration and Cancer Therapy.* Cancers, 2019. **11**(9): p. 1220.

356. Jeon, O.H., et al., *Local clearance of senescent cells attenuates the development of post-traumatic osteoarthritis and creates a pro-regenerative environment.* Nature Medicine, 2017. **23**(6): p. 775-781.
357. Yang, C.-C., et al., *Matrix metalloproteases and tissue inhibitors of metalloproteinases in medial plica and pannus-like tissue contribute to knee osteoarthritis progression.* PloS one, 2013. **8**(11): p. e79662-e79662.
358. Raghu, H., et al., *CCL2/CCR2, but not CCL5/CCR5, mediates monocyte recruitment, inflammation and cartilage destruction in osteoarthritis.* Ann Rheum Dis, 2017. **76**(5): p. 914-922.
359. Miotla Zarebska, J., et al., *CCL2 and CCR2 regulate pain-related behaviour and early gene expression in post-traumatic murine osteoarthritis but contribute little to chondropathy.* Osteoarthritis and cartilage, 2017. **25**(3): p. 406-412.
360. Collison, J., *Anti-NGF therapy improves osteoarthritis pain.* Nature Reviews Rheumatology, 2019. **15**(8): p. 450-450.
361. von Loga, I.S., et al., *Active immunisation targeting nerve growth factor attenuates chronic pain behaviour in murine osteoarthritis.* Annals of the Rheumatic Diseases, 2019. **78**(5): p. 672.
362. Ashraf, S., et al., *Augmented pain behavioural responses to intra-articular injection of nerve growth factor in two animal models of osteoarthritis.* Annals of the Rheumatic Diseases, 2014. **73**(9): p. 1710.
363. Njar, V.C., et al., *Retinoic acid metabolism blocking agents (RAMBAs) for treatment of cancer and dermatological diseases.* Bioorg Med Chem, 2006. **14**(13): p. 4323-40.
364. Eagling, V.A., J.F. Tjia, and D.J. Back, *Differential selectivity of cytochrome P450 inhibitors against probe substrates in human and rat liver microsomes.* Br J Clin Pharmacol, 1998. **45**(2): p. 107-14.
365. Debruyne, F.J., et al., *Liarozole--a novel treatment approach for advanced prostate cancer: results of a large randomized trial versus cyproterone acetate. Liarozole Study Group.* Urology, 1998. **52**(1): p. 72-81.
366. Bhushan, M., et al., *Oral liarozole in the treatment of palmoplantar pustular psoriasis: a randomized, double-blind, placebo-controlled study.* Br J Dermatol, 2001. **145**(4): p. 546-53.
367. Lee, S.-A., O.V. Belyaeva, and N.Y. Kedishvili, *Effect of lipid peroxidation products on the activity of human retinol dehydrogenase 12 (RDH12) and retinoid metabolism.* Biochimica et biophysica acta, 2008. **1782**(6): p. 421-425.
368. Bromfield, E.G., et al., *Inhibition of arachidonate 15-lipoxygenase prevents 4-hydroxynonenal-induced protein damage in male germ cells.* Biol Reprod, 2017. **96**(3): p. 598-609.
369. Shoeb, M., et al., *4-Hydroxynonenal in the pathogenesis and progression of human diseases.* Current medicinal chemistry, 2014. **21**(2): p. 230-237.
370. Farooqui, A.A. and L.A. Horrocks, *Phospholipase A_2-Generated Lipid Mediators in the Brain: The Good, the Bad, and the Ugly.* The Neuroscientist, 2006. **12**(3): p. 245-260.
371. Last, V., A. Williams, and D. Werling, *Inhibition of cytosolic Phospholipase A2 prevents prion peptide-induced neuronal damage and co-localisation with Beta III Tubulin.* BMC Neurosci, 2012. **13**: p. 106.
372. Leistad, L., et al., *Multiple phospholipase A2 enzymes participate in the inflammatory process in osteoarthritic cartilage.* Scand J Rheumatol, 2011. **40**(4): p. 308-16.
373. Singh, N.K. and G.N. Rao, *Emerging role of 12/15-Lipoxygenase (ALOX15) in human pathologies.* Progress in lipid research, 2019. **73**: p. 28-45.
374. Negre-Salvayre, A., et al., *Pathological aspects of lipid peroxidation.* Free Radic Res, 2010. **44**(10): p. 1125-71.

375. Kaneko, Y., et al., *Oral administration of N-acetyl cysteine prevents osteoarthritis development and progression in a rat model.* Scientific Reports, 2019. **9**(1): p. 18741.
376. Lalevée, S., et al., *Genome-wide in silico identification of new conserved and functional retinoic acid receptor response elements (direct repeats separated by 5 bp).* J Biol Chem, 2011. **286**(38): p. 33322-34.
377. Geib, T., et al., *Identification of 4-hydroxynonenal-modified proteins in human osteoarthritic chondrocytes.* Journal of Proteomics, 2021. **232**: p. 104024.
378. Vaillancourt, F., et al., *4-Hydroxynonenal induces apoptosis in human osteoarthritic chondrocytes: the protective role of glutathione-S-transferase.* Arthritis research & therapy, 2008. **10**(5): p. R107-R107.
379. Pruzanski, W., et al., *The role of phospholipase A2 in the physiopathology of osteoarthritis.* J Rheumatol Suppl, 1991. **27**: p. 117-9.
380. Vignon, E., et al., *Metalloprotease activity, phospholipase A2 activity and cytokine concentration in osteoarthritis synovial fluids.* Osteoarthritis Cartilage, 1993. **1**(2): p. 115-20.
381. Wei, Y., et al., *Phospholipase A(2) inhibitor-loaded micellar nanoparticles attenuate inflammation and mitigate osteoarthritis progression.* Sci Adv, 2021. **7**(15).
382. Chu, C., et al., *Mitochondrial dependence of nerve growth factor-induced mechanical hyperalgesia.* Pain, 2011. **152**(8): p. 1832-1837.
383. Milner, P.I., R.J. Wilkins, and J.S. Gibson, *The role of mitochondrial reactive oxygen species in pH regulation in articular chondrocytes.* Osteoarthritis and Cartilage, 2007. **15**(7): p. 735-742.
384. Kan, S., et al., *Role of Mitochondria in Physiology of Chondrocytes and Diseases of Osteoarthritis and Rheumatoid Arthritis.* CARTILAGE, 2021. **13**(2_suppl): p. 1102S-1121S.
385. Lambeth, J.D., K.H. Krause, and R.A. Clark, *NOX enzymes as novel targets for drug development.* Semin Immunopathol, 2008. **30**(3): p. 339-63.
386. Hentze, M.W., et al., *Oxidation-reduction and the molecular mechanism of a regulatory RNA-protein interaction.* Science, 1989. **244**(4902): p. 357-9.
387. Makino, H., et al., *A selective inhibition of c-Fos/activator protein-1 as a potential therapeutic target for intervertebral disc degeneration and associated pain.* Scientific Reports, 2017. **7**(1): p. 16983.
388. Yokoyama, K., et al., *C-Fos Regulation by the MAPK and PKC Pathways in Intervertebral Disc Cells.* PLOS ONE, 2013. **8**(9): p. e73210.
389. Pelletier, J.P., et al., *Selective inhibition of inducible nitric oxide synthase reduces progression of experimental osteoarthritis in vivo: possible link with the reduction in chondrocyte apoptosis and caspase 3 level.* Arthritis Rheum, 2000. **43**(6): p. 1290-9.
390. Sasaki, K., et al., *Nitric oxide mediates interleukin-1-induced gene expression of matrix metalloproteinases and basic fibroblast growth factor in cultured rabbit articular chondrocytes.* J Biochem, 1998. **123**(3): p. 431-9.
391. Oh, M., et al., *Concurrent generation of nitric oxide and superoxide inhibits proteoglycan synthesis in bovine articular chondrocytes: involvement of peroxynitrite.* J Rheumatol, 1998. **25**(11): p. 2169-74.
392. Rousset, F., et al., *IL-1beta mediates MMP secretion and IL-1beta neosynthesis via upregulation of p22(phox) and NOX4 activity in human articular chondrocytes.* Osteoarthritis Cartilage, 2015. **23**(11): p. 1972-80.
393. Yin, W., J.-I. Park, and R.F. Loeser, *Oxidative Stress Inhibits Insulin-like Growth Factor-I Induction of Chondrocyte Proteoglycan Synthesis through Differential Regulation of Phosphatidylinositol 3-Kinase-Akt and MEK-ERK MAPK Signaling Pathways*.* Journal of Biological Chemistry, 2009. **284**(46): p. 31972-31981.

394. Veihelmann, A., et al., *ANTI-INFLAMMATORY EFFECTS OF NITRIC OXIDE IN ANTIGEN-INDUCED ARTHRITIS: A STUDY ON INOS-DEFICIENT MICE.* Orthopaedic Proceedings, 2002. **84-B**(SUPP_I): p. 21-b-21.
395. Abramson, S.B., *Nitric oxide in inflammation and pain associated with osteoarthritis.* Arthritis Research & Therapy, 2008. **10**(2): p. S2.
396. Gavriilidis, C., et al., *Mitochondrial dysfunction in osteoarthritis is associated with down-regulation of superoxide dismutase 2.* Arthritis Rheum, 2013. **65**(2): p. 378-87.
397. Carlo, M.D., Jr. and R.F. Loeser, *Increased oxidative stress with aging reduces chondrocyte survival: correlation with intracellular glutathione levels.* Arthritis Rheum, 2003. **48**(12): p. 3419-30.
398. Lin, L.L., et al., *cPLA2 is phosphorylated and activated by MAP kinase.* Cell, 1993. **72**(2): p. 269-78.
399. Zhou, H., S. Das, and K.S. Murthy, *Erk1/2- and p38 MAP kinase-dependent phosphorylation and activation of cPLA2 by m3 and m2 receptors.* Am J Physiol Gastrointest Liver Physiol, 2003. **284**(3): p. G472-80.
400. Zhang, W. and H.T. Liu, *MAPK signal pathways in the regulation of cell proliferation in mammalian cells.* Cell Research, 2002. **12**(1): p. 9-18.
401. Xu, J., et al., *Role of PKC and MAPK in cytosolic PLA2 phosphorylation and arachadonic acid release in primary murine astrocytes.* J Neurochem, 2002. **83**(2): p. 259-70.
402. Wang, X., et al., *Effects and relationship of ERK1 and ERK2 in interleukin-1β-induced alterations in MMP3, MMP13, type II collagen and aggrecan expression in human chondrocytes.* Int J Mol Med, 2011. **27**(4): p. 583-9.
403. Takebe, K., et al., *Regulation of p38 MAPK phosphorylation inhibits chondrocyte apoptosis in response to heat stress or mechanical stress.* Int J Mol Med, 2011. **27**(3): p. 329-35.
404. Mahtani, K.R., et al., *Mitogen-activated protein kinase p38 controls the expression and posttranslational modification of tristetraprolin, a regulator of tumor necrosis factor alpha mRNA stability.* Molecular and cellular biology, 2001. **21**(19): p. 6461-6469.
405. Tchen, C.R., et al., *The stability of tristetraprolin mRNA is regulated by mitogen-activated protein kinase p38 and by tristetraprolin itself.* J Biol Chem, 2004. **279**(31): p. 32393-400.
406. Prasadam, I., et al., *Inhibition of p38 pathway leads to OA-like changes in a rat animal model.* Rheumatology (Oxford), 2012. **51**(5): p. 813-23.
407. Lan, C.N., et al., *MAPK inhibitors protect against early-stage osteoarthritis by activating autophagy.* Mol Med Rep, 2021. **24**(6).
408. Smallie, T., et al., *Dual-Specificity Phosphatase 1 and Tristetraprolin Cooperate To Regulate Macrophage Responses to Lipopolysaccharide.* Journal of immunology (Baltimore, Md. : 1950), 2015. **195**(1): p. 277-288.
409. Clark, A.R., J.R.S. Martins, and C.R. Tchen, *Role of dual specificity phosphatases in biological responses to glucocorticoids.* The Journal of biological chemistry, 2008. **283**(38): p. 25765-25769.
410. Lin, C.-C., et al., *TNF-α-Induced cPLA(2) Expression via NADPH Oxidase/Reactive Oxygen Species-Dependent NF-κB Cascade on Human Pulmonary Alveolar Epithelial Cells.* Frontiers in pharmacology, 2016. **7**: p. 447-447.
411. Jiang, F., et al., *NADPH oxidase-dependent redox signaling in TGF-β-mediated fibrotic responses.* Redox biology, 2014. **2**: p. 267-272.
412. Carnesecchi, S., et al., *A key role for NOX4 in epithelial cell death during development of lung fibrosis.* Antioxidants & redox signaling, 2011. **15**(3): p. 607-619.
413. Mihalas, B.P., et al., *The lipid peroxidation product 4-hydroxynonenal contributes to oxidative stress-mediated deterioration of the ageing oocyte.* Sci Rep, 2017. **7**(1): p. 6247.
414. Mustapha, N.M., et al., *NADPH Oxidase versus Mitochondria-Derived ROS in Glucose-Induced Apoptosis of Pericytes in Early Diabetic Retinopathy.* J Ophthalmol, 2010. **2010**: p. 746978.

415. Soga, M., A. Matsuzawa, and H. Ichijo, *Oxidative Stress-Induced Diseases via the ASK1 Signaling Pathway.* International journal of cell biology, 2012. **2012**: p. 439587-439587.
416. Pan, J., et al., *Reactive oxygen species-activated Akt/ASK1/p38 signaling pathway in nickel compound-induced apoptosis in BEAS 2B cells.* Chemical research in toxicology, 2010. **23**(3): p. 568-577.
417. Onodera, Y., et al., *Reactive oxygen species induce Cox-2 expression via TAK1 activation in synovial fibroblast cells.* FEBS Open Bio, 2015. **5**: p. 492-501.
418. Suzuki, M., et al., *TAK1 Mediates ROS Generation Triggered by the Specific Cephalosporins through Noncanonical Mechanisms.* International journal of molecular sciences, 2020. **21**(24): p. 9497.
419. Zeng, J., et al., *Inhibition of TGFβ-activated protein kinase 1 ameliorates myocardial ischaemia/reperfusion injury via endoplasmic reticulum stress suppression.* Journal of Cellular and Molecular Medicine, 2020. **24**(12): p. 6846-6859.
420. Mihaly, S.R., J. Ninomiya-Tsuji, and S. Morioka, *TAK1 control of cell death.* Cell Death Differ, 2014. **21**(11): p. 1667-76.
421. Hiraga, R., et al., *Nox4-derived ROS signaling contributes to TGF-β-induced epithelial-mesenchymal transition in pancreatic cancer cells.* Anticancer Res, 2013. **33**(10): p. 4431-8.
422. Noguchi, T., *ROS-dependent Activation of ASKI in Inflammatory Signaling.* Journal of Oral Biosciences, 2008. **50**(2): p. 107-114.
423. Tsou, H.K., et al., *Apoptosis signal-regulating kinase 1 is mediated in TNF-α-induced CCL2 expression in human synovial fibroblasts.* J Cell Biochem, 2012. **113**(11): p. 3509-19.
424. Matsuzawa, A., et al., *ROS-dependent activation of the TRAF6-ASK1-p38 pathway is selectively required for TLR4-mediated innate immunity.* Nature Immunology, 2005. **6**(6): p. 587-592.
425. Zhang, Q.S., et al., *Stress-Induced Activation of Apoptosis Signal-Regulating Kinase 1 Promotes Osteoarthritis.* J Cell Physiol, 2016. **231**(4): p. 944-53.
426. Yan, J., et al., *Selonsertib Alleviates the Progression of Rat Osteoarthritis: An in vitro and in vivo Study.* Frontiers in Pharmacology, 2021. **12**.
427. Mahajan, A. and R. Patni, *Menopause and Osteoarthritis: Any Association ?* Journal of mid-life health, 2018. **9**(4): p. 171-172.
428. Heming, M., et al., *Peroxisome Proliferator-Activated Receptor-γ Modulates the Response of Macrophages to Lipopolysaccharide and Glucocorticoids.* Frontiers in Immunology, 2018. **9**.
429. Zhang, Q.H., W.: Meng, B.: Tang, T., *PPARgamma agonist rosiglitazone is neuroprotective after traumatic spinal cord injury via anti-inflammatory in adult rats.* Neurol Res, 2010. **32**(8): p. 852-9.
430. Vasheghani, F., et al., *PPARγ deficiency results in severe, accelerated osteoarthritis associated with aberrant mTOR signalling in the articular cartilage.* Annals of the rheumatic diseases, 2015. **74**(3): p. 569-578.
431. Chang, Y.-C., et al., *All-trans retinoic acid suppresses the adhering ability of ARPE-19 cells via mitogen-activated protein kinase and focal adhesion kinase.* Journal of Pharmacological Sciences, 2016. **132**(4): p. 262-270.
432. Lu, L., et al., *Critical role of all-trans retinoic acid in stabilizing human natural regulatory T cells under inflammatory conditions.* Proceedings of the National Academy of Sciences of the United States of America, 2014. **111**(33): p. E3432-E3440.
433. Vasheghani, F., et al., *PPARγ deficiency results in severe, accelerated osteoarthritis associated with aberrant mTOR signalling in the articular cartilage.* Ann Rheum Dis, 2015. **74**(3): p. 569-78.
434. Chen, K., et al., *Increased 15-lipoxygenase-1 expression in chondrocytes contributes to the pathogenesis of osteoarthritis.* Cell Death & Disease, 2017. **8**(10): p. e3109-e3109.

435. Farooqui, A.A., W.Y. Ong, and L.A. Horrocks, *Neuroprotection abilities of cytosolic phospholipase A2 inhibitors in kainic acid-induced neurodegeneration.* Curr Drug Targets Cardiovasc Haematol Disord, 2004. **4**(1): p. 85-96.
436. White, H., et al., *Study design and rationale for the clinical outcomes of the STABILITY Trial (STabilization of Atherosclerotic plaque By Initiation of darapLadIb TherapY) comparing darapladib versus placebo in patients with coronary heart disease.* Am Heart J, 2010. **160**(4): p. 655-61.
437. O'Donoghue, M.L., et al., *Effect of Darapladib on Major Coronary Events After an Acute Coronary Syndrome: The SOLID-TIMI 52 Randomized Clinical Trial.* JAMA, 2014. **312**(10): p. 1006-1015.
438. Ozcamdalli, M., et al., *Comparison of Intra-articular Injection of Hyaluronic Acid and N-Acetyl Cysteine in the Treatment of Knee Osteoarthritis: A Pilot Study.* Cartilage, 2017. **8**(4): p. 384-390.
439. de Alencar, J.C.G., et al., *Double-blind, Randomized, Placebo-controlled Trial With N-acetylcysteine for Treatment of Severe Acute Respiratory Syndrome Caused by Coronavirus Disease 2019 (COVID-19).* Clin Infect Dis, 2021. **72**(11): p. e736-e741.
440. Lee, J., et al., *Coenzyme Q10 Ameliorates Pain and Cartilage Degradation in a Rat Model of Osteoarthritis by Regulating Nitric Oxide and Inflammatory Cytokines.* PLOS ONE, 2013. **8**(7): p. e69362.
441. The Parkinson Study Group, Q.E.I., *A Randomized Clinical Trial of High-Dosage Coenzyme Q10 in Early Parkinson Disease: No Evidence of Benefit.* JAMA Neurology, 2014. **71**(5): p. 543-552.
442. Montenegro, L., et al., *Idebenone: Novel Strategies to Improve Its Systemic and Local Efficacy.* Nanomaterials (Basel, Switzerland), 2018. **8**(2): p. 87.
443. Detaille, D., et al., *An old medicine as a new drug to prevent mitochondrial complex I from producing oxygen radicals.* PloS one, 2019. **14**(5): p. e0216385-e0216385.
444. Gunnell, L.M., et al., *TAK1 regulates cartilage and joint development via the MAPK and BMP signaling pathways.* Journal of bone and mineral research : the official journal of the American Society for Bone and Mineral Research, 2010. **25**(8): p. 1784-1797.
445. Guo, X., et al., *TAK1 regulates caspase 8 activation and necroptotic signaling via multiple cell death checkpoints.* Cell Death & Disease, 2016. **7**(9): p. e2381-e2381.
446. Li, L., et al., *Transforming growth factor β-activated kinase 1 signaling pathway critically regulates myocardial survival and remodeling*. Circulation, 2014. **130**(24): p. 2162-2172.
447. Loomba, R., et al., *The ASK1 inhibitor selonsertib in patients with nonalcoholic steatohepatitis: A randomized, phase 2 trial.* Hepatology, 2018. **67**(2): p. 549-559.
448. Corrigan, M.A., et al., *TRPV4-mediates oscillatory fluid shear mechanotransduction in mesenchymal stem cells in part via the primary cilium.* Scientific Reports, 2018. **8**(1): p. 3824.